Fine Mapping of Nematode Resistance Genes *Rlnn1* and *Cre8* in Wheat (*Triticum aestivum*)

A thesis submitted in fulfillment of the requirements for the degree of the Doctor of Philosophy at the University of Adelaide

By

Dimanthi Vihanga Jayatilake

School of Agriculture, Food and Wine

Faculty of Sciences

The University of Adelaide

September, 2014

List of Abbreviations

7AL - long arm of chromosome 7A

6BL - long arm of chromosome 6B

RLN - root lesion nematodes

CCN - cereal cyst nematodes

QTL - quantitative trait loci

MAS - marker-assisted selection

AFLP - amplified fragment length polymorphism

DH - doubled haploid

RFLP - restriction fragment length polymorphism

STS - sequence tagged site

SSR - simple sequence repeat

BAC - bacterial artificial chromosome

NBS - nucleotide-binding-site

LRR - leucine-rich-repeat

DAI - days after inoculation

qPCR - quantitative real-time polymerase chain reaction

DArT™ - Diversity Arrays Technology

SNP - single nucleotide polymorphism

ISBP - insertion site based polymorphism

KASP™ - Kompetitive allele-specific polymerase chain reaction

GBS - genotyping-by-sequencing

PCR - polymerase chain reaction

LOD - likelihood of odds

SM - single marker analysis

SIM - simple interval mapping

CIM - composite interval mapping

MIM - multiple interval mapping

WGAIM - whole genome average interval mapping

LRS - likelihood ratio statistics

EST - expressed sequence tags

Pt - *Puccinia triticina*

Pgt - *Puccinia graminis*

BLUPs - best linear unbiased predictions

RI - recombinant inbred

HRM - high resolution melting technology

BLUEs - best linear unbiased estimates

FISH - fluorescent *in-situ* hybridisation

BS - bootstrap support

TILLING - targeting induced local lesions in genomes

FISHIS - fluorescent *in-situ* hybridization in suspension

Table of contents

List of Tables

List of Figures

List of Appendices

Abstract

The root lesion nematode *Pratylenchus neglectus* and the cereal cyst nematode *Heterodera avenae* cause significant yield damage to wheat (*Triticum aestivum* L.) and crops that are grown in rotation with wheat. The focus of this thesis is on two loci in wheat, *Rlnn1*and *Cre8,* which confer resistance against *P. neglectus* and *H. avenae,* respectively, with an overall scientific goal of characterizing these two resistance loci as an initiative towards isolation of the causal gene(s) and identification of diagnostic molecular markers for the use in marker-assisted selection in wheat breeding programmes.

The thesis presents improvements to an existing Excalibur/Kukri linkage map of chromosome 7A by adding *Lr20* (a gene for resistance against leaf rust caused by *Puccinia triticina*), *Sr15* (a gene for resistance against stem rust caused by *P. graminis*), *Psy-A1* (a phytoene synthase gene), *Cat3-A1* (a catalase gene) and 59 new molecular markers. The genomic location of the *Rlnn1* quantitative trait locus (QTL) was confirmed as the distal end of long arm of chromosome 7A (7AL). It coincides with the position of *Lr20/Sr15*, *Psy-A1*, *Cat3-A1* and 34 molecular markers.

Based on the findings that 1) some markers that collocate with the resistance genes *Lr20/Sr15* and *Rlnn1* are widely separated in mapping populations that do not segregate for these genes; 2) when anchored to a chromosome 7A syntenic build, these markers spanned a 0.9-Mb region; and 3) no recombinants were found in a large population of recombinant inbred lines, it is suggested that the clustering of molecular markers/genes/QTL at the distal end of 7AL is due to suppressed recombination. The suppressed recombination in Excalibur may be a result of a translocation. This suggestion is based on 1) phylogenetic analysis of *Psy-A1* alleles; 2) marker amplification patterns that suggested that sequences at the distal end of 7AL in Excalibur are very different from those in Kukri and Chinese

Spring; 3) amplicons observed for a normally 7B-specific marker that collocates with *Rlnn1* on 7AL, and 4) FISH images that revealed an unknown putative translocation in Excalibur that is absent in Kukri. It seems likely that the *Rlnn1*-containing segment of 7AL may have been translocated from a 7B-like chromosome arm with an unknown ancestry. Such a translocation could have pre-dated hexaploidisation and occurred in a tetraploid or diploid ancestor.

The thesis also presents a high-resolution genetic linkage map for a Trident/Molineux population. This map was used to confirm the locations of three previously reported QTL for *H. avenae,* including the *Cre8* locus mapped as a large-effect QTL at the distal end of the long arm of chromosome 6B (6BL), with an estimated position 0.9 cM from the closest markers. A cross was designed and made to develop a population for future use in fine mapping. With these materials and with the closely-linked molecular markers developed here, *Cre8* seems amenable to positional cloning.

In the research conducted for this thesis, the *Rlnn1* and *Cre8* resistance loci were mapped at the distal ends of 7AL and 6BL, respectively and diagnostic markers were identified for the use in marker-assisted selection. A suppressed recombination at the end of 7AL impedes the prospects of cloning *Rlnn1,* while the research reported here have identified suitable markers and genetic resources for cloning the *Cre8* gene with a forward genetics approach.

Thesis declaration

I certify that this work contains no material which has been accepted for the award of any other degree or diploma in my name, in any university or other tertiary institution and, to the best of my knowledge and belief, contains no material previously published or written by another person, except where due reference has been made in the text. In addition, I certify that no part of this work will, in the future, be used in a submission in my name, for any other degree or diploma in any university or other tertiary institution without the prior approval of the University of Adelaide and where applicable, any partner institution responsible for the joint-award of this degree.

I give consent to this copy of my thesis when deposited in the University Library, being made available for loan and photocopying, subject to the provisions of the Copyright Act 1968.

The author acknowledges that copyright of published works contained within this thesis resides with the copyright holder(s) of those works.

I also give permission for the digital version of my thesis to be made available on the web, via the University's digital research repository, the Library Search and also through web search engines, unless permission has been granted by the University to restrict access for a period of time.

……. ……..

Signature Date

Acknowledgements

I extend my sincere gratitude to my supervisors Prof Diane Mather and Associate Prof Ken Chalmers for their guidance, support and encouragement throughout my PhD candidature. I am extremely grateful for their advice, lengthy discussions and 'open door' policy which allowed me to meet them whenever I needed guidance. I especially thank Prof Diane Mather for her comments and suggestions on thesis and manuscripts and for the fast turn-around time between drafts despite her busy schedule. I thank my postgraduate coordinator Dr Matthew Denton and my external advisor Dr Klaus Oldach for their support. With much appreciation, I thank collaborators: Ms Elise Tucker, Dr Harbans Bariana, Dr Peng Zhang, Dr Melissa Garcia, Mr John Toubia, Mr John Lewis, Dr Alan McKay, Dr James Edwards, Dr Haydn Kuchel, Mr Paul Eckermann, Dr Julia Brueggemann, Dr Susanne Dreisigacker, Dr Matthew Hayden, Mr Gabriel Keeble-Gagnère and Dr Simen Rød Sandve for their contribution and valuable advice. I also wish to thank Prof Peter Langridge for providing the plasmid DNA for the AWBMA20 clone. A big thank you goes to Ms Danuta Pounsett for helping out with the *P. neglectus* phenotyping, Dr Matthew Tucker, Ms Jessika Aditya and Dr Marilyn Henderson for helping me with the microscopy work, Ms Margaret Pallotta for providing primers and for valuable advice, Dr Julian Taylor for providing custom scripts in R for statistical work. I am very thankful to Dr Kelvin Khoo, Mr Greg Lott, Dr Ming Li and Dr Beata Sznajder for their valuable advice and support given to me though out my research. A special thank you to Mr Andreas Stahl and Mr James Lee for helping me out in DNA extraction and marker assays. I thank the other members of the molecular marker lab, past lab members and colleagues from ACPFG for their support and encouragement. I wish to acknowledge the Grains Research and Development Corporation, Australia for funding the research project and the University of

Adelaide, Australia for the Adelaide Scholarship International. I thank the Australian Grain Technologies and the Australian Centre for Plant Functional Genomics for development of the Excalibur/Kukri populations and providing seeds. Last but not least, to my husband Kanishka Ukuwela for helping me with the phylogenetics analysis and for being there for me at all times. I thank my family and friends for supporting and encouraging me in all I do.

Chapter 1

Introduction

Some plant parasitic nematodes are harmful pests of cultivated crops. For cereals, root lesion nematodes (*Pratylenchus* spp.) and cereal cyst nematodes (*Heterodera* spp.) are particularly problematic. These nematodes are widely distributed and are known to attack important cereal crops such as wheat (*Triticum aestivum* L.), barley (*Hordeum vulgare* L.), maize (*Zea mays* L.), oat (*Avena sativa* L.) and rye (*Secale cereale* L.). For major wheat producing countries such as China, India, the USA and Australia, these nematodes already pose a major threat [116].

In Australia, growers lose considerable grain yield annually due to root lesion nematodes and cereal cyst nematodes. However, due to the use of cultivars with moderate resistance and/or tolerance, along with other disease management practices, the yield loss figures have dropped considerably over the years [111, 179]. Regardless of the positive advancements over the past few decades, Australian wheat growers still incur a substantial crop loss due to root lesion nematodes and cereal cyst nematodes [111]. In the absence of proper control measures and when susceptible cultivars are used in rotations, soil numbers of these nematodes increase rapidly, which could subsequently lead to major yield losses. Therefore, development of new cultivars with resistance is an important aspect in wheat breeding programs.

Three of the predominant nematode pest species affecting wheat production in Australia are: the root lesion nematodes *Pratylenchus neglectus* (Rensch) Filip. & S. Stekho. and *P. thornei* L. and the cereal cyst nematode *Heterodera avenae* Woll. Several studies have

been conducted to map the loci responsible for delivering resistance against these nematodes in wheat: these loci either originated in wheat or were introgressed in to wheat to improve nematode resistance [33, 39, 40, 75, 76, 118, 145, 151, 164, 197-200, 208, 209].

The *Rlnn1* resistance locus on the long arm of chromosome 7A (7AL) and the *Cre8* locus on the long arm of chromosome 6B (6BL), are two of the main loci conferring resistance against root lesion nematode (RLN) *P. neglectus* and cereal cyst nematode (CCN) *H. avenae* respectively [197, 199, 200]. Screening of plant material for resistance against nematodes using phenotypic assays is expensive, labour intensive and time consuming. Diagnostic molecular marker assays could provide cost-effective high-throughput alternatives to phenotypic assays. Even though several molecular markers linked with the *Rlnn1* and *Cre8* quantitative trait loci (QTL) have been identified, none of these markers are ideal for marker-assisted selection (MAS); they are not suitable for high-throughput screening and may not be linked closely enough with the resistance loci. The advent of new molecular marker technologies [6, 16, 132] and publicly available sequence resources developed through the International Wheat Genome Sequencing Consortium [22], have made it possible to construct high-resolution genetic linkage maps for wheat that are saturated with markers that can be used for high-throughput screening.

The overall scientific goal of the thesis was to characterize two nematode resistance loci (*Rlnn1* and *Cre8*) in wheat as an initiative towards isolation of the causal gene(s) and to identify diagnostic molecular markers for the use in marker-assisted selection in wheat breeding programmes. Accordingly, the specific objectives of the research conducted for this thesis were: 1) to fine map the RLN *P. neglectus* resistance locus *Rlnn1*; 2) to improve the Trident/Molineux genetic linkage map with special emphasis on the *Cre8* QTL region

of 6BL; 3) to identify or develop diagnostic molecular markers for *Rlnn1* and *Cre8* to be used in MAS; and 4) to develop a large mapping population for fine mapping of *Cre8*.

The thesis consists of eight chapters, as follows:

Chapter 1 (Introduction): A general background to the research topic, briefly identifying the research gaps and stating the specific objectives of the thesis research.

Chapter 2 (Literature review): A comprehensive literature review setting the background to the research topic, pointing out the research gaps and giving an overview about some of the techniques used in the thesis research.

Chapter 3 (Genetic mapping and marker development for resistance of wheat against the root lesion nematode *Pratylenchus neglectus*): A report on research that confirmed the location of the *Rlnn1* QTL on the distal end of 7AL, identified and developed diagnostic markers to be used in MAS and provided evidence of suppressed recombination at the distal end of 7AL in the cultivar Excalibur. This chapter has been published in the journal *BMC Plant Biology* (Jayatilake et al. 2013).

Chapter 4 (Suppressed recombination in a region of wheat chromosome 7A that carries loci affecting resistance against a root lesion nematode and fungal pathogens): This chapter will be prepared as a manuscript for submission to *BMC Genomics*. We plan to augment it soon with results of additional work still being undertaken by collaborators.

Chapter 5 (Genetic mapping of the *Cre8* locus for resistance against cereal cyst nematode (*Heterodera avenae* Woll.) in wheat): A report on research that improved the Trident/Molineux linkage map through the addition and ordering of

hundreds of new molecular markers, clarified the position of *Cre8* on that map and developed assays for diagnostic molecular markers for MAS and for fine mapping. This chapter has been submitted to the journal *Molecular Breeding* and is currently under review.

Chapter 6 (Development of materials for fine mapping *Cre8*): A report on the development of a large mapping population, as a genetic resource for future fine mapping of *Cre8*.

Chapter 7 (General discussion): A discussion on the significance of the research reported in this thesis, identification of drawbacks, suggestions for improvements and future research directions.

Chapter 8 (Contributions to knowledge): A list of the significant contributions to scientific knowledge arising from this research. For research conducted in collaboration with others, this list specifies my personal contributions.

The thesis also has four appendices:

Appendix 1: Supplementary material of Chapter 3

Appendix 2: Supplementary material of Chapter 4

Appendix 3: Supplementary material of Chapter 5

Appendix 4: A first look at the infection of cereal cyst nematode (*Heterodera avenae* Woll.) and establishment of syncytia in wheat carrying the *Cre8* resistance allele

In the manuscript-style chapters (3 and 5), minor changes have been made to provide a consistent format throughout the thesis. These include the renumbering of tables and figures and the consolidation of all references into a single list at the end of the thesis.

Chapter 2

Literature review

2.1 Root lesion nematodes

Root lesion nematodes are migratory endoparasites [78]. Several root lesion nematode species (*Pratylenchus neglectus, P. thornei, P. penetrans, P. crenatus* and *P. teres*) are agronomically important for cereal crops, as they cause yield damage in wheat (*Triticum aestivum* L.), barley (*Hordeum vulgare* L.), maize (*Zea mays* subsp. *mays* L.), oat (*Avena sativa* L.) and rye (*Secale cereale* L.) [116, 142, 193]. Among these, *P. neglectus* and *P. thornei* are often associated with yield losses in wheat [165]. According to a review by Nicol and Rivoal [115], these two species are widely distributed in Australia, Europe, the Indian sub-continent, the Mediterranean basin, the Middle East, West Asia, North Africa, and North America. Surveys done in the USA [166] and Australia [36, 140, 179, 182] have revealed the presence of one or both of these species at levels sufficient to cause considerable yield losses. These nematode species have been estimated to be responsible for wheat yield losses up to 37% (*P. neglectus*) and 85% (*P. thornei*) respectively [165]. In Australia, both species have been reported in almost all wheat growing agro-ecological zones [111], and they have been estimated to cause average annual losses of A$ 73 million (*P. neglectus*) and A$ 50 million (*P. thornei*)[111].

Generally, the life cycle of root lesion nematodes lasts for 45 to 65 d depending on the species and the environmental conditions [1, 165]. The lifecycle begins with mature females laying eggs, either inside plant cells or in soil. The first moult happens before the eggs hatch and J_2 juveniles emerge from the eggs [78]. They undergo two more moults (J_3

and J_4) before morphing into adults. All juvenile stages and the adult have a vermiform body shape [1, 165]. They are parasitic and are not confined to one plant [1, 165]. The nematodes puncture the root tissues as they enter and then migrate towards the cortical tissues [165]. Considerable damage is done by the nematodes that settle in for longer feeding hours, than those that exit the root sooner. Furthermore, the free-entry and exit behaviour of these nematodes, creates entry points for secondary infection by fungi and bacteria [1, 115, 116].

The above-ground symptoms of root lesion nematodes are non-specific: yellowed leaves, premature death of lower leaves, reduced tillers, stunted growth, and reduced grain yield and quality [165]. In contrast, the below-ground symptoms are very distinct: brown/black lesions that girdle the roots [116]. These necrotic lesions are formed as a result of tissue damage, due to feeding and migration of the nematodes within the roots [78, 116]. These lesions spread and cover large areas on the roots, leading to root die-off [1, 193]. Infected plants can also exhibit secondary symptoms such as 'witches broom', irregular root swelling and reduction of the root zone [38]. These conditions impair water and nutrient uptake, reducing vegetative growth and yield [1].

Most developmental stages of root lesion nematodes (all except the egg-producing females) can overwinter in infected soil/plant material [1]. When conditions become favourable, they break dormancy and infect host plants [175]. As *Pratylenchus* spp. are polyphagous, a control strategy *via* an integrative approach of crop rotation with non-hosts (some cultivars of barley, safflower (*Carthamus tinctorius* L.), triticale (× *Triticosecale Wittmack*), flax (*Linum usitatissimum* L.), field pea (*Pisum sativum* L.) and faba beans (*Vicia faba* L.), field sanitation, removal of alternative hosts from the fields, application of chemical nematicides and most importantly, the use of resistant and tolerant cultivars are suitable for the disease prone regions [116, 165, 177]. A cultivar that is tolerant may not be

resistant to root lesion nematodes and *vice versa* [165]. Combining both resistance and tolerance would limit nematode multiplication and lower the yield damage [182]. As a result, the cropping frequency of important cereal crops could be increased, with less risk of nematode build-up in soil and subsequent yield losses [182]. Often, *P. neglectus* and *P. thornei* are both present in fields, therefore, cultivars with resistance and tolerance to both species would be ideal. However, resistance to *P. neglectus* is not necessarily effective against *P. thornei* and *vice versa* [165]. The research conducted for this thesis addressed resistance against *P. neglectus,* but not resistance against *P. thornei.*

2.1.1 Resistance against *Pratylenchus neglectus* in wheat

Controlling *P. neglectus* through crop rotation is challenging because the polyphagous feeding behaviour of the nematode limits the crops that can be used in rotations. Genetic resistance in wheat has been looked upon as a sustainable approach to control this pest [165]. To my knowledge, no commercial wheat cultivar with complete resistance to *P. neglectus* is available. Some of the varieties that are known to be at least moderately resistant to *P. neglectus* in Australia include Bowie, Wyalkatchem, Cascades, Krichauff, Worrakatta, Vectis, Bindawarra, Tatiara, Thew, Aroona, Orion, and Excalibur ([177]; NVT Online [120]). In contrast, other Australian varieties including Correll, Kukri, Sunbri, Sunlin, Sunvale, Sunstate, AGT Scythe, Annuello, Babbler, Calingiri, Chara, Hartog, Gladius, Yitpi, Machete, Janz and Buckley are at least moderately susceptible to *P. neglectus* ([177, 186]; NVT Online [120]).

Several major and minor QTL affecting resistance against *P. neglectus* have been identified in wheat and in synthetic hexaploids [200, 208]. Using a consensus mapping approach, Williams et al. [200] mapped a major resistance locus for *P. neglectus* in wheat on 7AL (designated as *Rlnn1*). The wheat cultivars Excalibur and Krichauff carried the

allele conveying resistance at the *Rlnn1* locus. Five other QTL associated with *P. neglectus* resistance have been mapped to the chromosomes 2B, 3D, 4B, 4D and 6D using a CPI133872/Janz population [207, 208]. However, only *QRlnn.lrc-2B.1* and *QRlnn.lrc-6D.1* were consistently detected as significant QTL [207]. The *QRlnn.lrc-6D.1* QTL for *P. neglectus* resistance from Janz and the *QRlnt.lrc-6D.1* for *P. thornei* from synthetic wheat CPI133872 were found to be collocating [207, 208]. In barley, QTL conferring resistance against *P. neglectus* have been reported in chromosomes 3H, 5H, 6H and 7H [159].

2.1.2 *Pratylenchus neglectus* resistance locus *Rlnn1*

Having determined that the resistance locus *Rlnn1* was linked with the amplified fragment length polymorphism (AFLP) marker *AGC/CCT179* [200] on chromosome 7A, Williams et al. [200] constructed a consensus map of chromosome 7A using small subsets of lines from three biparental doubled haploid (DH) populations (25 from Tammin/Excalibur, 30 from RAC860/Excalibur and 31 from Trident/Krichauff), in which Excalibur and Krichauff were the sources of resistance against *P. neglectus*. In the consensus map [200], the leaf rust (*Puccinia triticina*) resistance locus *Lr20* collocated with the restriction fragment length polymorphism (RFLP) markers *cdo347*, *psr121* and *psr680*, the AFLP marker *AGC/CCT179* and the sequence tagged site (STS) marker *schfc3*. The *Rlnn1* locus was estimated to be 9.1 cM distal to *Lr20* and 13.6 cM proximal to the simple sequence repeat (SSR) marker *gwm344*. Based on these estimated map distances, the most closely linked markers were too far away from *Rlnn1* to be effectively used in MAS. Further, most of them were not suitable for high-throughput screening. Given the importance of resistance to combat the multiplication of *P. neglectus* in the field, there was a need to more precisely map the large-effect *Rlnn1* resistance QTL and to identify or develop diagnostic markers that could be used in MAS.

2.1.3. Other important genes mapped near *Rlnn1*

The region of 7AL in which the *Rlnn1* has been mapped, is known to have several other important genes including a phytoene synthase gene *Psy-A1*, a catalase gene *Cat3-A1*, the rust resistance genes *Lr20* (leaf rust, *Puccinia triticina*) and *Sr15* (stem rust, *Puccinia graminis* f.sp. *tritici*) and the powdery mildew (*Blumeria graminis* f. sp. *tritici*) resistance gene *Pm1*. As discussed before, *Lr20* has been mapped proximal to *Rlnn1* [200]. Both *Sr15* and *Pm1* have been mapped at the same position as *Lr20* and it is possible that *Sr15* and *Lr20* both represent a single pleiotropic gene [99, 114, 178]. The *Psy-A1* and *Cat3-A1* genes are linked with each other [23], but their positions relative to the *Rlnn1*, *Pm1* and *Lr20*/*Sr15* were not known.

2.1.3a Phytoene synthase gene *Psy-A1* and the catalase gene *Cat3-A1*

Yellowness in wheat endosperm is an important factor that decides the end use of the flour. Bread wheat cultivars with yellow flour are preferred in making Cantonese noodles, while white flour is preferred for bread making and Japanese noodles. For pasta, durum wheat semolina with high yellow pigment is preferred [106]. The yellowness of flour or semolina is highly correlated with the yellow pigment concentration, and both measurements can be used to grade cultivars and decide which type of an end product it is suited for [106].

While many QTL related to flour colour have been mapped, it is well established that the major QTL affecting the yellowness in bread wheat flour and in durum wheat semolina are on chromosome 7A and 7B [10, 24, 70, 83, 97, 125, 134, 139, 204, 206]. No flour colour QTL has been detected on chromosome 7D to date. The candidate genes associated with the flour/semolina yellowness QTL on group 7 are the phytoene synthase homoeologs *Psy-A1* and *Psy-B1* [24, 57, 58, 134, 139, 160] and the catalase gene *Cat3-A1* [23].

The first rate-limiting step in the carotenoid biosynthesis pathway of flowering plants is catalyzed by phytoene synthase (*PSY*) enzymes, which are considered to be key regulators of the yellow pigment concentration [64, 94]. In the carotenoid bio-synthesis pathway, *PSY* enzymes convert two molecules of geranylgeranyl diphosphate (GGDP), into a phytoene molecule (Figure 2.1).

The *Psy1* genes of cereals are well characterised. Three paralogs of phytoene synthase occur in wheat, rice and maize: *Psy1*, *Psy2* and *Psy3* [34, 48, 59, 89, 134, 192]. The expression of these genes is tissue specific: *PSY1* enzymes are mostly important for endosperm carotenoid accumulation and *PSY2* enzymes for carotenoid accumulation in photosynthetic tissues [34, 48]. The *PSY3* enzymes are mostly associated with carotenoid accumulation in root tissues and their expression is up-regulated when plants are subjected to abiotic stresses [34, 89]. Multiple alleles of *Psy1* genes have been isolated and sequenced from *Triticum* and related species. In previous studies [24, 187], the phylogeny of *Psy1* alleles was reconstructed.

Another 7AL gene that may affect flour colour is a catalase gene (*Cat3-A1*). In general catalase enzymes have antioxidant properties and thus, act upon endogenous hydrogen peroxide (which has a colour bleaching effect), reducing it to water and oxygen. Crawford et al. [23], suggested that it is likely that the *Psy-A1* alleles and the *Cat3-A1* alleles from 7AL are two of the main regulators of flour colour.

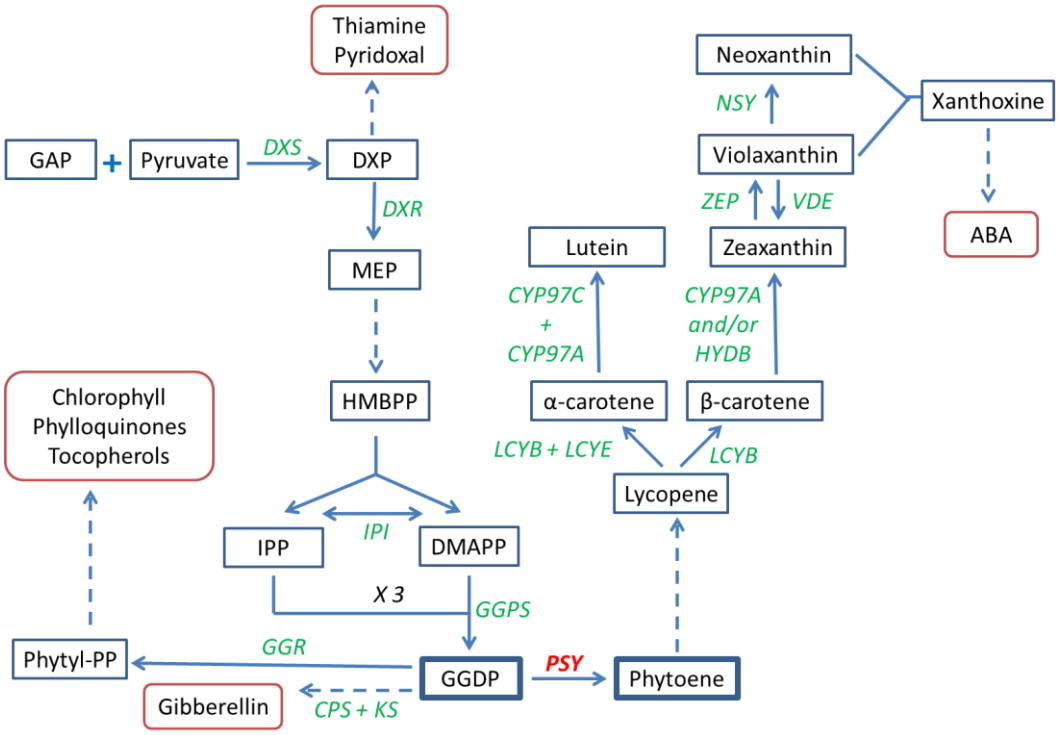

Figure 2.1: A schematic representation of the carotenoid biosynthesis pathway of plants (based on Lu and Li [94]).

GAP - glyceraldehyde-3-phosphate, DXS - 1-deoxy-D-xylulose 5-phosphate synthase, DXP - 1-deoxy-D-xylulose 5-phosphate, DXR - 1-deoxy-D-xylulose 5-phosphate reductoisomerase, MEP - 2-C-methyl-D-erythritol 4-phosphate, HMBPP - 1-hydroxy-2-methyl-2-butenyl 4-diphosphate, IPP - isopentenyl diphosphate, IPI - isopentenyl diphosphate isomerase, DMAPP - dimethylallyl diphosphate, GGPS - geranylgeranyl diphosphate synthase, GGDP - geranylgeranyl diphosphate, GGR - geranylgeranyl diphosphate reductase, CPS - ent-copalyl diphosphate synthase, KS - ent-kaurene synthase, PSY - phytoene synthase, LCYE - lycopene ε-cyclase, LCYB - lycopene β-cyclase, CYP97C - carotene ε-hydroxylase (cytochrome P450 type), CYP97A - carotene β-hydroxylase (cytochrome P450 type), HYDB - carotene β-hydroxylase (nonheme di-iron type), ZEP - zeaxanthin epoxidase, NSY - neoxanthin synthase, NCED - 9-cis-epoxycarotenoid dioxygenase, VDE – violaxanthin de-epoxidase and ABA - abscisic acid.

2.1.3b Rust resistance genes on 7AL

Leaf rust caused by *Puccinia graminis* f. sp. *tritici* and stem rust caused by *P. triticina* f. sp. *tritici* are two of the major fungal diseases that affect bread wheat. Under warm and humid weather conditions, leaf and stem rust are responsible for widespread yield damage in many wheat growing regions. The characteristic symptoms of leaf rust are the orange-brown pustules with a circular to oval shape, confined to the upper leaf sheath. Stem rust is characterized by much darker reddish-brown, oblong pustules with torn margins that are usually present in leaf sheath and in stems [73]. Resistance to rust is affected by many genes. Here, only the leaf rust resistance gene *Lr20* [13, 190] and the stem rust resistance gene *Sr15* [191] will be reviewed, due to their map position near *Rlnn1*on 7AL. The rust resistance genes *Lr20* and *Sr15* have limited agricultural use due to environmental sensitivity and development of virulent strains [101]. One such virulent strain against leaf rust resistance gene *Lr20* found in Australia is Pt 104-1,2,3,(6),(7),11 [124].

The rust resistance genes *Lr20* and *Sr15* are generally accepted to be in complete coupling phase linkage with each other and with the powdery mildew resistance gene *Pm1* [114, 178]. Although Watson and Luig [191] did report two recombinants among 116 F_2 plants and suggested that the genes are not in complete linkage, no follow up experiments were conducted to validate these lines. McIntosh [99] reported that heritable mutations that affected the powdery mildew reaction did not affect the rust reaction, indicating that *Pm1* may not be the same gene as *Lr20* and *Sr15*. However, changes in leaf rust reaction were always associated with changes in stem rust reaction, indicating that the actions of *Sr15* and *Lr20* could be pleiotropic.

Neu et al. [114] mapped the resistance genes *Lr20* and *Pm1* to 7AL. However, their attempt to isolate this gene complex through a forward genetics approach was impaired by the clustering of the two resistance genes with molecular markers at the distal end of 7AL. In a linkage map constructed by de la Pena et al. [31] for another population, some of these

markers were 30 cM apart. Further, no evidence of physical linkage was reported when a bacterial artificial chromosome (BAC) library of *Triticum monococcum* was screened with probes for these clustered markers, indicating that they are at least 100 kb apart. Thus, Neu et al. [114] suggested that the *Lr20* and *Pm1* resistance loci are in a chromosome region in which recombination is suppressed, possibly due to an alien intogression or a chromosomal rearrangement.

2.2 Cereal cyst nematodes

Cereal cyst nematodes are a group of cyst-forming plant parasitic nematodes [115]. The major species of cereal cyst nematodes that cause yield damage to cereals are *Heterodera avenae*, *H. latipons* and *H. filipjevi* [115, 116, 165]. These species are typically found in temperate, Mediterranean and continental climatic regions respectively [116]. Important cereal crops such as wheat, barley, rye and oat are known hosts for *H. avenae* [103]. As reviewed by Nicol et al. [116], *H. avenae* has been reported in many countries including Canada, Australia, China, Japan, India, Pakistan, South Africa, Morocco, Tunisia, Libya, Iran, Israel, Saudi Arabia, Turkey, Algeria and most European countries. In Australia, cereal cyst nematodes are widely distributed in almost all wheat cultivating areas, except in the northern agro-ecological zones [111]. As reviewed by Nicol and Rivoal [115], the damage caused by cereal cyst nematodes can range from 15% up to 96% when proper control is not in place. In Australia, the damage is now low due to widespread implementation of effective management practices [115], however, if uncontrolled, these nematodes could cause about A$ 572 million annual loss to the wheat industry [111].

Plants that are infested with cereal cyst nematodes show non-specific aboveground symptoms such as chlorotic older leaves, stunted growth and low tillering, and therefore, appear as pale green patches early in the cropping season [115]. These symptoms can

easily get confused with those of water and/or nutrient deficiencies. The roots of infected plants proliferate excessively, forming a 'bushy-knotted' root system. The characteristic symptom of cereal cyst nematode infection is the presence of white cysts (egg bearing females) on root surfaces. Upon the death of the female nematodes, these cysts eventually turn brown. These cysts can remain in soil for a longer period, in a dormant state, until a suitable host is found [115, 116, 165]. Cultural practices such as crop rotation with non-hosts, irrigation, early sowing, trap and mixed cropping, use of inorganic amendments and fertilizers have been used to control cereal cyst nematodes [14, 115]. Use of chemical nematicides is effective, but is not considered feasible, due to environmental concerns and high cost [115]. Crop rotation with non-cereals that do not act as hosts and maintaining a clean fallow were reviewed as effective control strategies by Smiley and Nicol [165], however, Lilley at al. [91] argued that crop rotation is not a feasible alternative, as there are few non-host crops that can be grown profitably. Cultivation of resistant and tolerant varieties can reduce the losses due to cereal cyst nematode and reduce the multiplication of nematodes in the soil [103] and thus is considered as the best approach for controlling the cereal cyst nematode.

2.2.1 Resistance against *Heterodera avenae* in wheat

Similar to the case of *P. neglectus,* much work has been done on improving genetic resistance of wheat against *H. avenae*. Among cultivars grown in South Australia, Catalina and Scout have been rated as resistant to *H. avenae*, Correll, Estoc, Grenade CL Plus, Kord CL Plus, Wallup and Yitpi as moderately resistant and Axe, Bolac, Emu Rock, Forrest, Impala, Naparoo, Orion, Sentinel, SQP Revenue and Wyalkatchem as susceptible [186].

Three resistance loci have been mapped in bread wheat and six others have been introgressed into bread wheat from related *Aegilops* species. The resistance loci from bread

wheat are *Cre1* [164, 198], *Cre8* [197, 199] and *Qcre.srd-1B* [197]. Slootmaker et al. [164] first reported a locus on chromosome 2B that confers resistance to *H. avenae* in the variety Loros. The resistance locus was designated as *Cre*, but later was renamed as *Cre1* [102]. Williams et al. [198] mapped the *Cre1* resistance gene to the chromosome 2BL and identified linked RFLP markers. Later, as a result of a cloning attempt, a diagnostic marker haplotype was identified for *Cre1* resistance gene [32]. The *Cre8* resistance locus against *H. avenae* was mapped to 6BL in wheat using Trident/Molineux DH lines [197, 199]. A more detailed review on *Cre8* will be given in a separate section. Williams et al. [197], mapped a novel *H. avenae* resistance locus on chromosome 1B and designated the locus as *QCre.srd-1B.*

The introgressed resistance loci include *Cre2* [33], *Cre5* (*CreX*) [75, 76] and *Cre6* [118] from *Aegilops ventricosa*; *Cre3* (*Ccn-D1*) and *Cre4* (*Ccn-D2*) from *Aegilops tauschii* [40]; and *Cre7* (*CreAet*) resistance locus from *Aegilops triuncialis* [145]. The *Cre3* resistance locus was found to be homeologous to *Cre1* in wheat [32]. The resistance locus *Cre5* is on chromosome 2AS [75] and *Cre3* and *Cre4* are on chromosome 2DL [40]. The chromosomal locations of resistance loci *Cre2, Cre6* and *Cre7* are not known.

2.2.2 *Heterodera avenae* resistance locus *Cre8*

An RFLP marker *cdo347* was reported to be associated with *H. avenae* resistance in the cultivar Festiguay and in the Festiguay-derived cultivars Molineux, Barunga and Frame [127]. Based on the associations of this resistance with the RFLP markers *cdo347* and *bcd1* in a Trident/Molineux population and the use of 6B nullisomic-tetrasomic aneuploid lines, Williams et al. [199] ascertained that the *Cre8* resistance locus (*CreF*) is on 6BL. At the *Cre8* locus, Molineux and Barunga would have inherited their resistance alleles from their

common ancestor Festiguay, while Frame would have inherited its resistance allele from Molineux.

Later, by using a Trident/Molineux 6B chromosome linkage map with RFLP markers and SSR markers, Williams et al. [197] mapped the *Cre8* locus distal to the collocating markers *cdo347*/*awbma20* and proximal to the marker *gdm147*. Their genetic map shows a distance of 14.7 cM between these two marker positions and their QTL analysis indicated that marker *gdm147* was the most closely linked marker to *Cre8*.

Montes et al. [107] and Safari et al. [147] attempted to assess the relative impact of the CCN resistance loci *Cre1*, *Cre3*, *Cre4*, *Cre7* and *Cre8*. In both cases, it was concluded that the *Cre8* resistance is less effective than that of *Cre1* and *Cre3*, but that *Cre8* in combination with other resistance loci (e.g., *Cre1* and *Cre3*) could have a significant impact on reducing the nematode multiplication and build-up in soil. However, the conclusion of Montes et al. [107] was based on only the cultivar Frame, and thereby was not a direct measurement of *Cre8*. The conclusions of Safari et al. [147] were based on the use of the RFLP marker *cdo347* to classify Frame/Silverstar DH lines and the use of pedigree information to classify cultivars and breeding lines. Without closely linked markers, these classifications would have been subject to error.

The resistance mechanisms exerted by the known CCN resistance genes are poorly understood. Attempts have been made to clone the homoelogous genes *Cre1* and *Cre3* [32, 84]. This led to the isolation of (1) a gene expressed in the root tissues that encodes a polypeptide containing a nucleotide-binding-site (NBS) and a leucine-rich-repeat (LRR), and (2) a pseudogene (due to a frame-shift as a result of a deletion) also with a NBS-LRR domain. However, successful confirmation experiments were not discussed and it is also not known whether these sequences are related to the causal genes. So far, no attempts have been made to clone the *H. avenae* resistance gene *Cre8*.

2.2.3. Plant defence responses to cereal cyst nematode infection

When nematodes infect plants, resistance and/or tolerance responses in plants get activated. Resistance to nematodes in plants refers to the ability of the plants to suppress nematode multiplication within the root system, whereas tolerance can be defined as the ability of the plants to grow and produce a good yield despite a heavy nematode infestation [11, 138]. Plants exert various types of responses such as secretion of chemical exudates (repellents, nematotoxins, anti-hatching agents and anti-feedants), histological changes (syncytia development and extensive vacuolation) and physiological changes (accelerated growth, root proliferation) that define the level of resistance and tolerance of a plant variety against nematodes [9, 154].

Heterodera avenae completes only one life cycle with in a crop season [167]. The life cycle begins when eggs encapsulated in cysts (dead females bearing eggs) hatch and J_2 stage vermiform nematodes are released into the soil [91]. These juveniles migrate toward the roots of a suitable host and penetrate the root tissue by thrusting their stylets against the root surface [60, 91]. Once inside, the nematodes migrate towards the vascular tissue, across the root cortex [91]. Near the vascular tissues, the nematodes penetrate a selected target cell and releases secretions to trigger the development of syncytia [60, 91]. A syncytium is a multinucleate structure that is acquired by dissolution of the cell walls of parenchyma cells and the subsequent fusion of the protoplasm to form one large feeding unit [51, 60, 154]. An active syncytium has a densely packed and metabolically active cytoplasm, with cell organelles such as mitochondria, plastids, endoplasmic reticulum, free ribosomes and small vacuoles [196]. Upon successful initiation of syncytia, the J_2 juveniles become sedentary [60]. Syncytia act as nutrient sinks for the developing juveniles and the depleting nutrients gets continuously replenished by the host plant [60].

By the end of the J_2 stage, sexual dimorphism becomes evident and the J_2 stage nematodes undergo two more moults (J_3 and J_4; each stage lasting 3 to 4 d) and reach the adult stage, [60, 91]. Under favourable conditions, most of the juveniles will morph into adult females, while under unfavourable conditions they are more likely to morph into adult males [91]. At the end of the J_4 stage, the male nematodes stop feeding and moult into a vermiform adult that is mobile, while the females remain immobile and develop lemon shaped bodies that bear eggs at maturity [91]. In time, the female will rupture the root surface and protrudes itself and expose its vulva for fertilization [91]. After fertilization the cuticle of female nematodes gets gradually tanned by a polyphenol oxidase, forming a shell around the body protecting the eggs from outside adversities, until conditions are suitable to begin the next cycle [91].

Plant responses of the resistance loci *Cre1* (wheat), *Cre3* (*Ae. tauschii*), *Rha2* (barley) and *Rha4* (barley) have been studied with respect to initial penetration, establishment and development of nematodes and the initiation and development of syncytia [51, 117, 154, 196]. In a field experiment O'Brien and Fisher [117] noted that at 22 d after sowing, there was no significant difference in the total number of nematodes between the roots of resistant (carrying *Cre1*) and susceptible lines. However, during the period between 39 and 63 d after sowing, the total numbers of nematodes increased in the susceptible line but remained constant in the resistant line. In a glasshouse experiment, Williams and Fisher [196] also noticed that both a resistant line and a susceptible line allowed successful root penetration. No differences were observed in the development of the nematodes between the resistant line and the susceptible line until 17 d after inoculation (DAI). By 20 DAI, females in the susceptible wheat cultivar grew rapidly in body size, but the females in the resistant line hardly grew at all. In the resistant line, fewer females matured into egg-bearing mature adults, leading to an unequal final sex ratio [196].

Development of syncytia is a key plant response to the *H. avenae* nematode infection and the histological changes associated with it has been investigated in wheat and barley [51, 154, 196]. Syncytia can be initiated as early as 2 DAI [154] and be fully differentiated by 4 or 5 DAI [51, 154, 196]. Grymaszewska and Golinowski [51] reported that syncytia were initiated much earlier (4 DAI) in a susceptible line than in a resistant line (around 14 DAI). In contrast, Seah et al. [154] reported accelerated syncytia initiation in resistant lines compared to susceptible lines at 2 DAI. Both Williams and Fisher [196] and Seah et al. [154] observed that syncytium development was similar between resistant and susceptible lines of wheat until 13 or 15 DAI. Beyond this period, the syncytial cytoplasm of resistant lines was highly vacuolated and seemed to be metabolically less active than that of susceptible wheat lines. Seah et al. [154] also reported that the syncytia of susceptible cultivars had dense, well stained cytoplasm with many organelles, small vacuoles and amorphous matter, indicating metabolically active cytoplasm.

When compared between resistant lines carrying *Cre1* (wheat) and *Cre3* (*Ae. tauschii*) resistance loci (based on the appearance of the syncytia at 13 DAI), it was found that the responses of *Cre1* were less advanced compared to *Cre3* [154]. However, no study has been conducted to look in to nematode penetration, establishment and development and the histological changes associated with syncytia, as a response to *H. avenae* resistance locus *Cre8*.

2.3 Evaluation of resistance against *H. avenae* and *P. neglectus*

Evaluation of resistance against nematodes requires quantification of nematode populations in roots and soil. This can be labour intensive and therefore costly, especially if it involves manual counting of nematodes [119].

For quantification of *P. neglectus*, a mist chamber method involving nematode counting and a DNA-based quantification method are both in use in Australia. In the mist chamber method, nematodes are extracted from seedlings (pre-inoculated with a known inoculum concentration) by misting and counted under a dissection microscope [200]. In the DNA-based method, a *Taqman* quantitative real-time polymerase chain reaction (qPCR) assay [121] is used. The qPCR assay is designed to target a diagnostic site on the nematode genome and therefore can be used to identify nematodes at species level. This enables quantifying mixed populations of *P. neglectus* and *P. thornei* fairly easily and accurately. This assay has a fast turnaround time and is highly sensitive. The method also facilitates handling of larger sample sizes and thus, more biological replicates can be included to increase the precision [121]. Nevertheless, it is still quite costly. One of the concerns regarding the use of this method was about the possible overestimation of nematode DNA, due to dead organisms in the samples. However, in a study done using *P. thornei* it was concluded that by 7 d, 93% of the DNA of dead nematodes were undetectable and after 14 d dead nematodes were not detectable at all [61]. Therefore, the DNA of the dead nematodes has no significant contribution to the estimated nematode DNA in a sample.

Although DNA-based testing methods have been developed for cereal cyst nematode *H. avenae* [121], the test service offered by SARDI, Australia still employs counting of nematodes (cysts).The approach currently used to quantify *H. avenae* involves inoculation of seedlings grown in tubes or pots. In tube tests, seedlings are inoculated with a known

number of juveniles at the time of transplanting and then four times at 3 d intervals (aimed at observing at least 50 female nematodes in the susceptible lines). Nematode count is assessed by counting cysts under a dissection microscope [45]. The tube test is an accurate measurement, but it is time consuming and labour intensive. The pot test was developed to provide a less expensive approach for use in selection (John Lewis, personal communication). In the pot test, seeds are sown in a potting mix inoculated with 25 eggs/g and at the time of the assessment, only the number of cysts visible outside the root ball are counted, and only up to a maximum of 21 [88]. The pot test is less accurate than the tube test but is usually sufficient for distinguishing large differences in resistance. Although DNA-based methods have recently been reported to be sensitive enough to detect < 1 *H. avenae* egg/g of soil, they have not yet been implemented routinely at SARDI [121].

2.4 Molecular markers, linkage and QTL mapping

2.4.1 Molecular markers

The simplest way to define a DNA marker would be as an assay that detects a DNA sequence polymorphism. DNA markers are often used in the development of genetic linkage maps, MAS in plant and animal breeding programs, phylogenetic and evolutionary studies, disease/pest diagnostics, varietal identification and characterization [52]. There are different types of DNA markers, including RFLP, AFLP, randomly amplified polymorphic DNA, SSR, STS, Diversity Arrays Technology (DArT™), single nucleotide polymorphism (SNP), insertion site based polymorphism (ISBP) and Kompetitive allele-specific polymerase chain reaction (KASP™). In recent years, SSR, DArT™, KASP™, ISBP, SNP and STS markers have been widely used in wheat [3, 4, 6, 16, 129, 168]. Further,

genotyping-by-sequencing (GBS) seems to have a promising future [132]. In this section, marker types that were used in the research for this thesis will be discussed.

SSR markers (microsatellites) target small repetitive motifs that are abundant in eukaryotic genomes [52, 143]. The polymorphism is detected as a length polymorphism, which is a result of varied number of tandom repeats present in individuals as a result of replication errors. SSR markers are multi-allelic and co-dominant [133] and can be assayed as high-throughput marker assays using multiplexed genotyping methods [56]. Several wheat consensus maps were developed using SSR markers [143, 168, 169]. In hexaploid wheat SSR markers are evenly distributed except in some centromeric regions and clustering of markers is rare [143]. Due to the increasing popularity of new technologies, the use of SSR markers has declined, however, it is still advantageous to have SSR markers in linkage maps, as it facilitates comparison between maps.

Single nucleotide polymorphisms can be defined as single positions on the genome, at which alternative nucleotides are found among individuals, which is detected as a polymorphism [12]. In the wheat genome, SNP polymorphisms are abundant. With the wheat genome sequence information that is now available in the public domain [41, 85, 131, 176], new technologies have been developed that can be used to mine the genome to capture polymorphisms and develop assays. Current SNP resources include the wheat SNP databases [4, 30] and multiplexed SNP arrays such as a 9K iSelect Beadchip array [16], a 90K iSelect Beadchip array [189] and Axiom® Wheat Genotyping Arrays consisting of between 35,000 and 817,000 assays (to be released in 2014; Affymetrix, Inc., USA). Further, many SNPs can be detected through genotyping-by-sequencing [132]. Recent developments in SNP marker technologies have made it possible to generate high-resolution genetic maps for wheat [5, 6, 16].

The ISBP markers target the transposable-elements that are plentiful in wheat genome [129, 130]. The '*IsbpFinder.Pl*' software developed by Paux et al. [130] can be used to generate ISBP markers that are mostly genome specific. ISBP markers are designed by targeting sequences that flank transposable-elements and amplifying fragments that contain transposon junction sequences and/or sequences adjacent to them [130]. These markers can be assayed using a wide range of detection techniques including agarose gel electrophoresis, capillary electrophoresis, melt curve analysis, SNaPshot® Multiplex System and Illumina Bead Array technology [129, 130].

DArT™ technology involves hybridization-based assays on microarrays. The assays generate a genome-wide fingerprints based on the presence/absence of hybridisation to specific DNA fragments derived from samples representing genomic DNA libraries from one or more organisms [3, 74]. Prior knowledge of the genomic sequences is not required [74]. The DArT™ platform has been used to develop wheat linkage maps in many studies [3, 25, 157].

Another marker technology used in genotyping is the KASP™ technology. KASP™ markers are uniplex marker assays that interrogate SNPs or length polymorphisms. KASP™ assays involve polymerase chain reaction (PCR) amplification and the polymorphism is detected using fluorescence signals. KASP™ technology has been used in mapping to achieve high genome-wide marker coverage [5, 6, 180]. At the CerealsDB database [26, 194] there are details for approximately 100,000 KASP™ markers including map positions, primer sequences and contig sequences from which they were derived.

2.4.2 Linkage mapping

Genetic linkage maps and QTL maps are important resources for crop improvement. A genetic linkage map can be defined as a set of markers (phenotypic and/or molecular markers), ordered linearly according to their co-segregation pattern, along a chromosome or a part of a chromosome [18]. The distance between two adjacent markers is given in map units (centiMorgan (cM)) and it is defined as the number of genetic crossovers occurring between any two markers/factors among 100 such cases [174]. This basic concept was further improved later by the introduction of concepts such as logarithm of odds (LOD) scores and mapping functions. Mapping functions are used to estimate the genetic map distance between two markers. The Haldane mapping function [54], assumes that all crossovers happen independently, whereas Kosambi mapping function [81] takes into account the effect of one chiasma (the point where a crossover occur), over the occurrence of a second one in its close proximity.

The use of DNA markers led to the generation of large data sets and thus needed computer software to perform the computations in linkage mapping. As a result over the years linkage mapping software was developed to suite different requirements. Cheema and Dicks [18] discussed the use of several programs, including MapManager QTX, JoinMap, MapMaker and AntMap. In addition software like Multipoint [110], MSTMap [109] and statistical software such as R [136] can also be used for genetic linkage mapping.

There are three major steps in linkage mapping: grouping, ordering and spacing [18]. Grouping could be based on LOD scores (e.g. MapManager, MapMarker) or based on a graph partitioning approach (e.g. MSTMap) [18, 20]. Once markers are grouped into linkage groups, ordering of markers is done within each group. The biggest problem in ordering is dealing with the large number of possible marker orders and picking the best order. All linkage mapping software performs ordering, however, this is sometimes

supplemented with the use of specific software such as RECORD [181]. Once marker order has been established the map distances between adjacent markers are calculated and the cumulative length of all such intervals within a linkage group provides the total length of the linkage group [18].

The accuracy and precision of linkage mapping can be affected by many factors, including missing data points, genotyping errors, population size, chiasma interference and segregation distortion [18]. Curation of genetic linkage maps may involve exclusion of markers with many missing data points, use of a mapping function such as Kosambi to account for chiasma interference, checking for possibly erroneous data points and exclusion of markers with segregation distortion [18]. Another important aspect is the identification of lines that are genetically identical or nearly identical and that may not be independent in origin. If the data for such lines are not removed or combined, they will reduce the accuracy of the linkage map (e.g., over estimating map distances in chromosome regions in which the duplicated lines carry recombinations).

2.4.3 QTL mapping

Quantitative traits can be simply defined as traits that exhibit quantitative variation. The genomic regions that affect such traits are known as quantitative trait loci. A quantitative trait could be controlled by one or more QTL and/or affected by the environment. Given the fact that many agronomically important traits such as yield and its components, and tolerance and resistance to some abiotic and biotic stresses exhibit quantitative variation, the detection and mapping of QTL can be important for crop improvement [20]. QTL are detected based on associations between marker genotypes and trait data [20].

Over the years several methods of systematic mapping of QTL have been developed. The most commonly used approaches are: single marker analysis (SM), simple interval mapping (SIM), composite interval mapping (CIM), multiple interval mapping (MIM) and whole genome average interval mapping (WGAIM). In SM, the simplest approach, associations are identified by comparing mean trait values among genotypic classes at each marker locus [43]. One limitation of this method is that the further the QTL is from the closest markers, the more difficult it is to detect and accurately estimate QTL effects, due to recombination between the markers and the QTL [20]. Other limitations of SM are that without prior knowledge about the marker positions, the QTL position relative to a marker locus cannot be estimated and when two markers detect strong trait associations it is not possible to determine whether they are detecting the same QTL or two different QTL. In SIM, associations with trait variation are tested at positions within marker intervals along each chromosome [86]. In CIM, which was developed by Zeng [203], background interference is removed from the final model by fitting other markers/QTL in the statistical model as controls. In MIM [79] analysis is based on models that simultaneously consider multiple marker intervals and putative QTL into a single QTL analysis. WGAIM is an extension of interval mapping implemented in R package [136], where all intervals of the linkage map is considered simultaneously for QTL analysis [183].

The test statistics from interval mapping (usually LOD score or likelihood ratio statistics (LRS) are often presented as profiles plotted against marker positions on the linkage map [20]. As reviewed by Collard et al. [20], a LOD score of 1 corresponds to an LRS value of 4.6. For a QTL to be considered statistically significant, its test statistic needs to exceed a significance threshold [20]. One means of establishing a significance threshold is to perform an empirical permutation test using the actual experimental data [19]. Once significant test statistics values have been detected in a chromosome region, the position of

the QTL is usually estimated as the map position at which the maximum (peak) test statistic value was observed.

The detection of QTL can be affected by many factors such as: genetic factors, environmental effects, population size and experimental error [20]. Some of the software commonly used for QTL mapping include MapManager QTX, QTL Cartographer, QGene, MapMaker/QTL [20]. In addition, Multipoint, GenStat and R packages dedicated for QTL mapping are in use.

2.5 Research gaps

Based on the literature reviewed here the following research gaps were identified:

1. The QTL mapping of RLN *P. neglectus* resistance locus *Rlnn1* was done using a chromosome 7A linkage map with few markers, constructed using a consensus approach [200]. Edwards [42] had constructed a good linkage map for a population (Excalibur/Kukri) that segregates for *Rlnn1*, and that population had been evaluated for resistance against *P. neglectus* (Haydn Kuchel and James Edwards, personal communication). In our laboratory at the University of Adelaide, Elise Tucker had implemented a comparative mapping approach using wheat-rice synteny to develop several molecular markers that are closely linked to the *Rlnn1*, and one of these (designated *wri2* in this thesis) had been made available to wheat breeders in Australia through the Australian Wheat and Barley Molecular Marker Program [135]. With new marker technologies and genetic resources there was scope to further improve the chromosome 7A genetic map and fine map the *Rlnn1* resistance locus as an initiative towards cloning of *Rlnn1*.
2. The Trident/Molineux linkage map that was used to map the *H. avenae* resistance locus *Cre8* had few markers on chromosome 6B [197]. The QTL was estimated to

be in a marker interval of 14.7 cM. In our laboratory at the University of Adelaide, Julia Brueggemann had added additional SSR markers to the linkage map, and Elise Tucker had used a comparative mapping approach to exploit wheat-rice synteny and design new markers, one of which had been made available to wheat breeders [135]. There was still potential to improve the marker density around the QTL region and to develop genetic material to fine map the *Cre8* resistance locus to facilitate cloning.

3. Given the high phenotyping costs involved with both *P. neglectus* and *H. avenae*, the development of diagnostic markers were needed for MAS, so that the phenotyping could be limited to situations where it is essential.

2.6 Overall research goal

With the increasing world population and scarce land availability for cultivation, the need to reduce losses incurred due to biotic stresses such as plant parasitic nematodes is a pressing need. The use of moderately resistant varieties has reduced the yield losses, however, the absence of varieties that confer complete resistance have stressed on the need to release such varieties through wheat breeding programmes. While identification of resistance QTL and development of closely-linked molecular markers have contributed for the recent advancements, a much deeper understanding about the resistance loci would accelerate the progress. Thus, the overall research conducted for this thesis addressed the following scientific questions:

1. Can wheat QTL regions conferring nematode resistance, be characterised to identify and validate new diagnostic markers for MAS using new marker technologies?

2. Can recent advances in genomic resources be used for the identification of causal genes conferring resistance against two important nematode pests?

Chapter 3

Genetic mapping and marker development for resistance of wheat against the root lesion nematode *Pratylenchus neglectus*

BMC Plant Biology 13:230.doi:10.1186/1471-2229-13-230; published article

Authors: Dimanthi V. Jayatilake[1], Elise J. Tucker[1,2], Harbans Bariana[3], Haydn Kuchel[1,4], James Edwards[1,2,4], Alan C. McKay[5], Ken Chalmers[1,2] and Diane E. Mather[1,2]**

[1]School of Agriculture, Food and Wine, Waite Research Institute, The University of Adelaide, PMB 1, Glen Osmond, SA 5064, Australia

[2]Australian Centre for Plant Functional Genomics, Waite Research Institute, The University of Adelaide, PMB 1, Glen Osmond, SA 5064, Australia

[3]The University of Sydney Plant Breeding Institute – Cobbitty, PMB 4011, Narellan, NSW 2567, Australia

[4]Australian Grain Technologies, PMB 1, Glen Osmond, SA 5064, Australia

[5]South Australian Research and Development Institute, Plant Research Centre, 2b Hartley Grove, Urrbrae, SA 5064 Australia

**Corresponding author: diane.mather@adelaide.edu.au

Email addresses of other authors:

DJ: dimanthi.jayatilake@adelaide.edu.au

ET: elise.tucker@acpfg.com.au

HB: harbans.bariana@sydney.edu.au

HK: haydn.kuchel@ausgraintech.com

JE: james.edwards@ausgraintech.com

AM: alan.mckay@sa.gov.au

KC: ken.chalmers@adelaide.edu.au

The text, figures and tables presented in this thesis chapter are exactly the same as the published article, except for minor numbering changes in figures and tables, which were reformatted to be consistant with the rest of the thesis. The information from the author contribution statement of the manuscript is presented in a Statement of Authorship at the beginning of the chapter. The information from the statement of acknowledgement, list of abbreviations and the reference list of the manuscript is included in the corresponding sections of the thesis. Additional files are presented in Appendix 1.

3.1 Statement of Authorship

Title of the paper	Genetic mapping and marker development for resistance of wheat against the root lesion nematode *Pratylenchus neglectus*
Publication Status	■Published ☐ Accepted for publication ☐ Submitted for publication ☐ Publication style
Publication Details	Jayatilake DV, Tucker EJ, Bariana H, Kuchel H, Edwards J, McKay AC, Chalmers K, Mather DE: Genetic mapping and marker development for resistance of wheat against the root lesion nematode *Pratylenchus neglectus* BMC Plant Biol 2013, 13:230.

Author Contributions

By signing the Statement of Authorship, each author certifies that their stated contribution to the publication is accurate and that permission is granted for the publication to be included in the candidate's thesis.

Name of Principal Author (Candidate)	Dimanthi V. Jayatilake		
Contribution to the paper	Critically examined all genotypic and phenotypic data, assayed additional markers, reconstructed the linkage map, conducted QTL analysis, assayed selected markers on a panel of cultivars and interpreted the results and wrote the first draft of the manuscript and took primary responsibility for manuscript revision.		
Signature		Date	26/03/2014

Name of Co-author	Elise J. Tucker		
Contribution to the paper	Joint first author. Conducted wheat-rice comparative analysis, designed new markers and assayed them on the population (prior to the candidature of DVJ). Provided input for the manuscript.		
Signature		Date	14·4·2014

Name of Co-author	Haydn Kuchel
Contribution to the paper	Prior to the candidature of DVJ, designed the experiment to evaluate the Excalibur/Kukri population for resistance against *P. neglectus*.
Signature	Date 26/3/14

Name of Co-author	James Edwards
Contribution to the paper	Prior to the candidature of DVJ, analysed the phenotypic data from that experiment and constructed an initial genetic linkage map.
Signature	Date 26/3/14

Name of Co-author	Harbans Bariana
Contribution to the paper	Evaluated the population for resistance against leaf rust and stem rust.
Signature	Date 12/3/14

Name of Co-author	Alan C. McKay
Contribution to the paper	Prior to the candidature of DJV, designed the methods used to quantify *P. neglectus* DNA in plant root systems.
Signature	Date 26/3/14

Name of Co-author	Ken Chalmers
Contribution to the paper	Supervised the marker design, genotyping and linkage mapping.
Signature	Date 26/3/14

Name of Co-author	Diane E. Mather
Contribution to the paper	Provided overall supervision of the research and helped write the manuscript.
Signature	Date 26 MARCH 2014

All authors read and approved the final manuscript and declared that they have no competing interests.

3.2 Abstract

Background

The *Rlnn1* locus, which resides on chromosome 7A of bread wheat (*Triticum aestivum* L.) confers moderate resistance against the root lesion nematode *Pratylenchus neglectus*. Prior to this research, the exact linkage relationships of *Rlnn1* with other loci on chromosome 7A were not clear and there were no simple codominant markers available for selection of *Rlnn1* in wheat breeding. The objectives of the research reported here were to (1) develop an improved genetic map of the *Rlnn1* region of chromosome 7A and (2) develop molecular markers that could be used in marker-assisted selection to improve resistance of wheat against *P. neglectus.*

Results

A large-effect quantitative trait locus (QTL) for resistance against *P. neglectus* was genetically mapped using a population of Excalibur/Kukri doubled haploid lines. This QTL coincides in position with the rust resistance gene(s) *Lr20/Sr15*, the phytoene synthase gene *Psy-A1* and 10 molecular markers, including five new markers designed using wheat-rice comparative genomics and wheat expressed sequence tags. Two of the new markers are suitable for use as molecular diagnostic tools to distinguish plants that carry *Rlnn1* and *Lr20*/*Sr15* from those that do not carry these resistance genes.

Conclusions

The genomic location of *Rlnn1* was confirmed to be in the terminal region of the long arm of chromosome 7A. Molecular markers were developed that provide simple alternatives to costly phenotypic assessment of resistance against *P. neglectus* in wheat breeding. In Excalibur, genetic recombination seems to be completely suppressed in the *Rlnn1* region.

3.3 Keywords

Root lesion nematode, *Pratylenchus neglectus*, wheat, molecular markers, *Rlnn1*, *Lr20*, *Sr15*, *Psy-A1*

3.4 Background

The root lesion nematode *Pratylenchus neglectus* infects a wide range of host plants, including wheat (*Triticum aestivum* L.) and crops that are grown in rotation with wheat. As a migratory endoparasite, *P. neglectus* moves in and out of roots, feeding as it moves through the root cortex. It causes lesions on roots, stunts plant growth and can significantly reduce crop yield. Plants that reduce the nematode population in root systems and in the soil are considered to be resistant. Resistant crop species and cultivars are valuable in crop rotations because they reduce the threat to subsequent crops.

The Australian wheat cultivars Excalibur and Krichauff have long been known to be at least moderately resistant against *P. neglectus* [177, 182]. Williams et al. [200] attributed the *P. neglectus* resistance of these cultivars to a locus (*Rlnn1*) on the long arm of chromosome 7A (7AL). They estimated *Rlnn1* to be 9.1-cM distal to the gene *Lr20*, which confers resistance against leaf rust (*Puccinia triticina*). *Lr20* has in turn been reported to co-segregate with *Sr15* and *Pm1* [114, 178], which confer resistance against stem rust (*Puccinia graminis* f. sp. *tritici*) and powdery mildew (*Blumeria graminis* f. sp. *tritici*), respectively.

Evaluation of resistance against *P. neglectus* can be laborious and costly, requiring replicated inoculated trials involving counting of nematodes (e.g., [200]) or the extraction of DNA from soil and root systems, followed by real-time polymerase chain reaction (PCR) to estimate the quantity of *P. neglectus* DNA [121]. Molecular markers for *Rlnn1*

could therefore be very useful selection tools in wheat breeding, allowing phenotyping resources to be allocated only to progeny that had been pre-selected as likely to carry the resistance allele. Williams et al. [200] suggested conversion of the restriction fragment length polymorphism (RFLP) marker *cdo347* and the amplified fragment length polymorphism (AFLP) marker *AGC/CCT179*, both of which they had reported to be at the same position as *Lr20*, into PCR-based assays for use in marker-assisted selection of *Rlnn1*. To our knowledge, no such assays have been developed. This may have been because the reported distance of 9.1 cM seemed too large for such markers to be very useful in wheat breeding.

The phytoene synthase locus *Psy-A1* is also in the distal region of 7AL [59]. At this locus, there are multiple alleles, conferring different levels of yellow pigment in wheat grain and flour [24, 70, 139]. Krichauff and several other cultivars with moderate resistance against *P. neglectus* have been reported to carry either the *Psy-A1s* or *Psy-A1t* allele [24, 70], both of which are associated with high levels of yellow pigment in flour. Wheat breeders in Australia are interested in developing cultivars with both white flour and resistance against *P. neglectus*, but, to our knowledge, they have not identified any materials with this combination of traits.

In the research reported here, a large mapping population was used to map *Rlnn1* relative to molecular markers and to the genes *Lr20*, *Sr15* and *Psy-A1*, and new markers were developed and validated for use in selection for resistance against *P. neglectus.*

3.5 Results

Resistance against leaf rust, stem rust and *Pratylenchus neglectus*

Evaluation of disease responses against the *P. triticina* pathotype 104-2,3,6,7 and the *P. graminis* f. sp. *tritici* pathotype 98-1,2,(3),5,6 indicated that Excalibur and 98 Excalibur/Kukri doubled haploid (DH) lines carry *Lr20/Sr15* resistance, while Kukri and 74 other Excalibur/Kukri DH lines are susceptible to both rust pathogens. No lines were observed to be resistant against one pathogen and susceptible to the other, indicating that if *Lr20* and *Sr15* are two genes (not a single pleiotropic gene), they are in complete coupling linkage in the Excalibur/Kukri population.

The estimated quantity of *P. neglectus* DNA in the roots of inoculated plants, was 27,553 pg per plant for Kukri, but only 11,447 pg per plant for Excalibur. Quantitative variation for this measure of nematode resistance was observed within both the rust-resistant and rust-susceptible categories of Excalibur/Kukri DH lines (Figure 3.1), with the amount of *P. neglectus* DNA detected being significantly ($t = 16.4$, $p < 0.001$) lower for rust-resistant lines (9,959 pg) than for rust-susceptible lines (21,428 pg). Greater variability was observed for the more susceptible class than for the more resistant class (Figure 3.1), probably because of inoculation failures (‘escapes’) broadening the phenotypic range observed for susceptible lines. Failure of inoculation of individual plants (whether genetically resistant or susceptible) would be much more likely to occur than high multiplication of nematodes on genetically resistant plants.

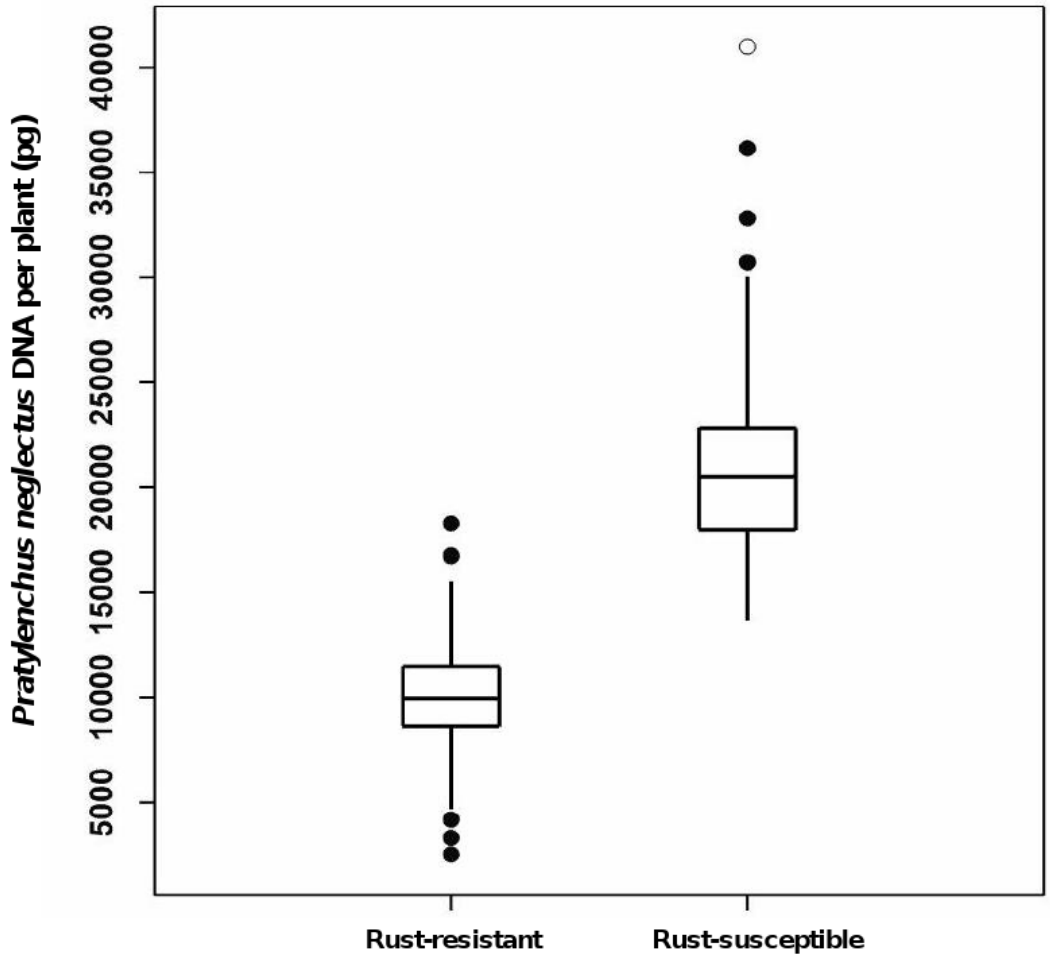

Figure 3.1: *Pratylenchus neglectus* resistance of rust-resistant and rust-susceptible Excalibur/Kukri doubled haploid lines.

Classification of lines as carrying or not carrying *Lr20/Sr15* rust resistance was based upon disease responses observed after inoculation of seedlings with appropriate pathotypes of *Puccinia triticina* and *Puccinia graminis* f. sp. *tritici.* Evaluation of resistance against the root lesion nematode *Pratylenchus neglectus* was based upon estimation of the quantity of *P. neglectus* DNA in the roots of inoculated wheat plants. The box spans the interquartile range of the estimated quantity of *P. neglectus* DNA per plant, the horizontal line within each box indicates the median. The whiskers extend to show the spread of data within the 'inner fence' (1.5 times the interquartile range beyond the quartiles). The solid black dots represent outliers within the 'outer fence' (3 times the interquartile range beyond the quartiles). The white dot represents an outlier outside of the 'outer fence'.

Genetic mapping

Analysis of data from the Excalibur/Kukri mapping population, resulted in a high-quality genetic linkage map of chromosome 7A (Figure 3.2; Appendix 1- Additional file S1.1: Figure S1.1), with *Lr20/Sr15* and *Psy-A1* collocating with each other and with the sequence tagged site (STS) markers *schfc3* and *sts638,* the simple sequence repeat (SSR) markers *gwm344* and *cfa2240* and the Diversity Arrays Technology (DArT^{TM}) marker *wPt-0790* at the distal end of 7AL. Sequencing of the products amplified with *PSY7A5_F/R* primers [24] indicated that Excalibur carries the *Psy-A1t* ('very yellow') allele (see Appendix 1- Additional file S1.2: Figure S1.2), while amplification with *csPSY* primers [70] confirmed that Kukri carries the *Psy-A1p* ('pale yellow') allele.

With QTL analysis using the estimated quantity of *P. neglectus* DNA per plant as the trait value, *Rlnn1* was detected as a highly significant QTL (peak LOD = 34; Figure 3.2) at the same position as *Lr20*, *Sr15*, *Psy-A1* and the collocating STS, SSR and DArT™ markers. This locus accounted for 60 % of the observed phenotypic variation.

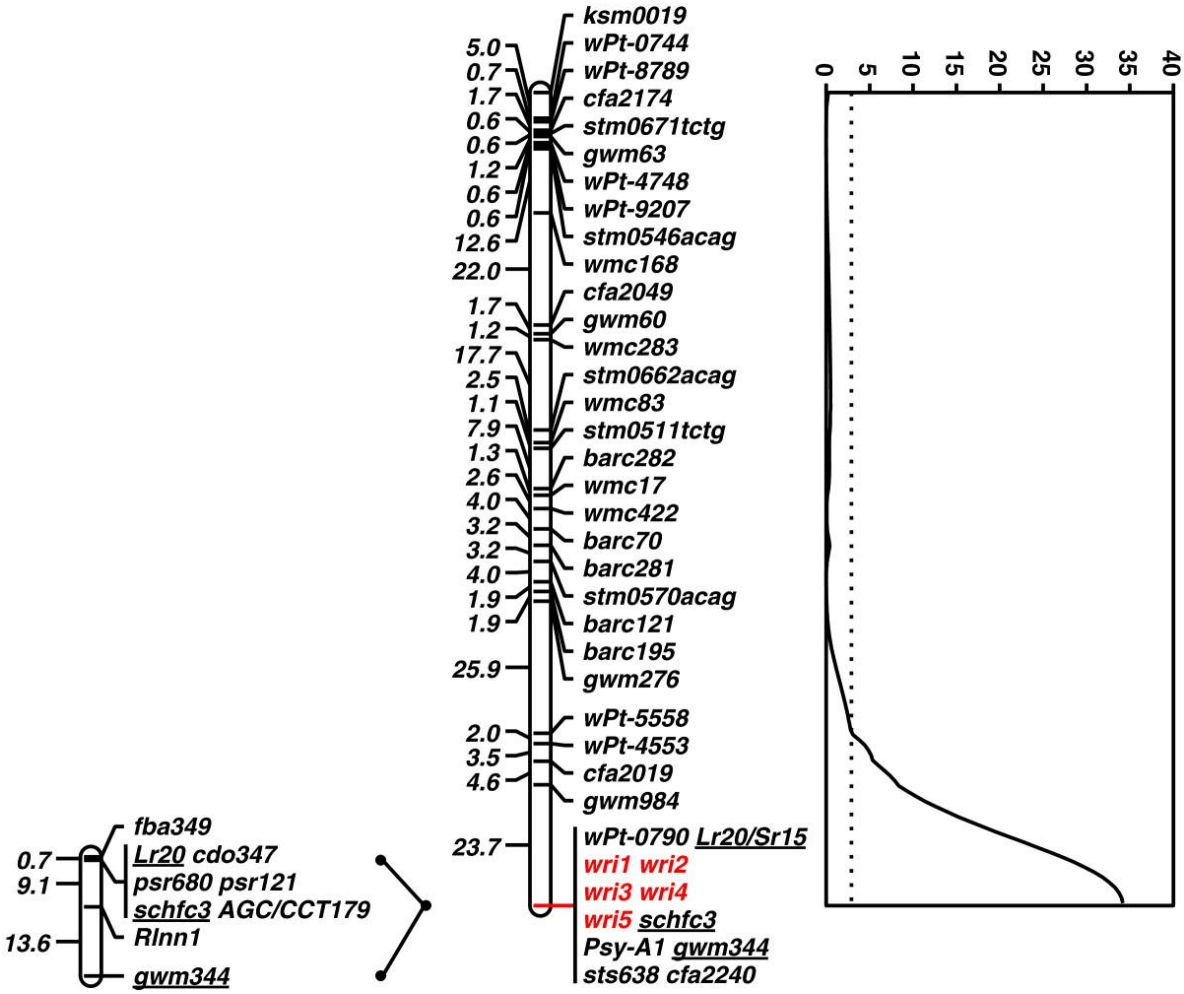

Figure 3.2: Genetic map of chromosome 7A showing *Rlnn1*, *Lr20/Sr15*, *Psy-A1* and molecular marker loci.

From left to right: a map showing the relative locations of the *Pratylenchus neglectus* resistance locus *Rlnn1*, the leaf rust resistance locus *Lr20* and seven molecular markers, as reported by Williams et al. [200]; a map showing the relative locations of the resistance locus *Lr20/Sr15*, the phytoene synthase gene *Psy-A1* and 39 molecular markers mapped on the chromosome 7A using a population of Excalibur/Kukri doubled haploid lines; and a graph showing a LOD test-statistic scan from simple interval mapping of resistance against the root lesion nematode *Pratylenchus neglectus* in the Excalibur/Kukri population, with resistance evaluated based upon estimation of the quantity of *P. neglectus* DNA in the roots of inoculated wheat plants. The names of three loci common to both maps are underlined. The names of five newly developed EST-based markers are shown in red.

Development of new markers based on comparative analysis between wheat and rice

Since the physical locations of the SSR markers *cfa2240* (in the above-mentioned terminal marker cluster) and *cfa2019* (28.3 cM proximal to the cluster) had both previously been assigned to the wheat deletion bin 7AL16-0.86-0.90 [171], 42 unique expressed sequence tags (ESTs) from that deletion bin and 45 unique ESTs from the deletion bin 7AL18-0.90-1.00 were selected for use in comparative genomic analysis with rice (see Appendix 1-Additional file S1.3: Table S1.1). Of these 87 ESTs, 60 had BLASTN E-values less than e-10. Consistent with previous evidence of synteny between the distal part of 7AL and chromosome 6 of rice [170], more than half of these ESTs were similar to sequences in the terminal region of rice chromosome 6 (19 of 30 ESTs from 7AL16-0.86-0.90, and 15 of 30 ESTs from 7AL18-0.90-1.00).

Similarly, the probe sequences of three RFLP markers that had previously been reported to be linked with *Rlnn1*, *Lr20* and/or *Pm1* [114, 200] showed high similarity with predicted genes in the terminal region of rice chromosome 6: PSR148 with LOC_Os06g51150 (1.2e-260), PSR680 with LOC_Os06g49380 (5.4e-103), and CDO347 with LOC_Os06g51270 (1.2e-98). The CDO347 sequence also had a significant BLASTN hit (5.7e-88) on rice chromosome 2 (LOC_Os02g58560). For PSR121, a probe that had been used to map another RFLP near *Rlnn1*, *Lr20* and *Pm1* [114, 200] the most significant hit (7.6e-161) was on rice chromosome 5 (LOC_Os05g31140).

Given the evidence that the terminal region of rice chromosome 6 is syntenic with the *Rlnn1* region of wheat chromosome 7A, sequences from the terminal region of rice chromosome 6 were used to retrieve orthologous wheat ESTs and primers were designed to flank predicted introns. Analysis of PCR products amplified with primers designed from five wheat ESTs [GenBank:BE445506, GenBank:BE445653, GenBank:BF484041,

GenBank:CN010180, GenBank:BF483039] detected readily assayable polymorphisms between the parents Excalibur and Kukri:

1. **BE445506:** The primer pair BE445506_F/R amplified products of approximately 150 bp from both parents and from an artificial heterozygote (a 1:1 mixture of Excalibur and Kukri DNA) (Figure 3.3A). Similar amplicons were obtained for all six Chinese Spring group-7 nullisomic-tetrasomic lines (CS N7A-T7B, CS N7A-T7D, CS N7B-T7A, CS N7B-T7D, CS N7D-T7A and CS N7D-T7B), indicating that this primer pair is not genome-specific. With high-resolution melting analysis, a polymorphism between Excalibur and Kukri was detected, providing a codominant marker assay (*wri1*) (Figure 3.4A).
2. **BE445653:** The primer pair BE445653_F/R (*wri2*) amplified 7A-specific products with differing sizes from Excalibur (586 bp) and Kukri (512 bp). This length polymorphism can be scored visually after electrophoretic separation on agarose gels (Figure 3.3B), providing a codominant marker assay. Sequencing of the amplicons revealed that the 74-bp length polymorphism between Excalibur and Kukri is due to the net effect of a number of insertion/deletion polymorphisms, which range in length from 1 to 30 nucleotides. Sequence polymorphisms between Excalibur and Kukri were also observed at 80 nucleotide sites (see Appendix 1- Additional file S1.4: Figure S1.3).
3. **BF484041:** The primer pair BF484041_F/R (*wri3*) amplified three distinct products from Kukri (approximately 250 bp, 450 bp and 350 bp which are apparently specific to chromosomes 7A, 7B and 7D respectively). In Excalibur, only the 7B- and 7D-specific products showed strong amplification (Figure 3.3C). With high-resolution melting analysis, Excalibur, Kukri and an artificial heterozygote (a 1:1 mixture of Excalibur and Kukri DNA) each had a distinct melting curve, providing a codominant marker assay (Figure 3.4B).

4. **CN010180**: The primer pairs CN010180_F1/R and CN010180_F2/R amplified 7A-specific products from Excalibur and Kukri, respectively. The two clearly visible amplicons were of similar size (approximately 175 bp). With sequential loading of the two PCR products onto gels, the two complementary allele-specific primer pairs (CN010180_F1/R and CN010180_F2/R) provided a codominant marker assay (*wri4*) (Figure 3.3D).
5. **BF483039**: The primer pair BF483039A_F2/ BF483039_cpR1, obtained from the Wheat SNP Database [4, 30] amplified a product of approximately 600 bp from Kukri, but no product from Excalibur, providing a 7A-specific dominant marker (*wri5*, Figure 3.3E).

When assayed on the Excalibur/Kukri DH lines, all five EST-based markers co-segregated with *gwm344*, *cfa2240*, *wPt-0790*, *schfc3*, *sts638*, *Psy-A1*, *Lr20* and *Sr15*.

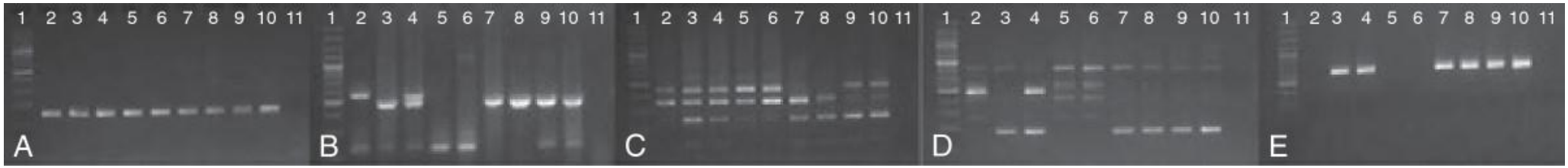

Figure 3.3: Amplicons of markers *wri1*, *wri2*, *wri3*, *wri4* and *wri5* separated by agarose gel electrophoresis.

(A) *wri1*, (B) *wri2*, (C) *wri3*, (D) *wri4*, (E) *wri5*, (1) GeneRuler® 100 bp DNA ladder (Thermo Fisher Scientific Inc.), (2) Excalibur, (3) Kukri, (4) 1:1 mixture of Excalibur and Kukri DNA (artificial heterozygote), the Chinese Spring nullisomic-tetrasomic lines (5) CS N7A-T7B, (6) CS N7A-T7D, (7) CS N7B-T7A, (8) CS N7B-T7D, (9) CS N7D-T7A, (10) CS N7D-T7B and (11) water**.**

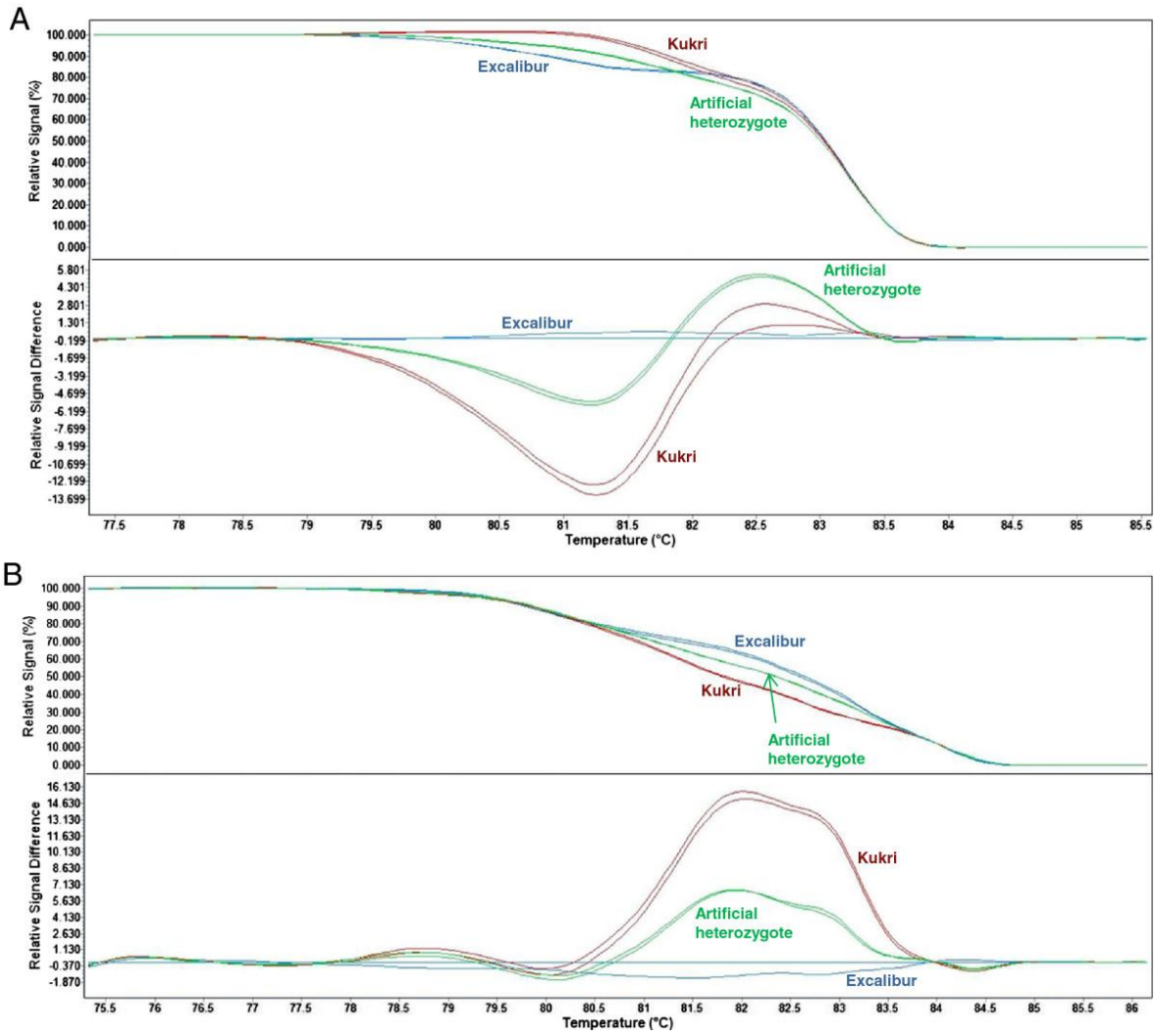

Figure 3.4: High-resolution melting curves for amplicons of markers *wri1* (A) and *wri3* (B).

Above: normalised and shifted melting curves; Below: normalised and temperature-shifted difference plot. Curves are shown for products amplified from genomic DNA of Excalibur, Kukri and a 1:1 mixture of Excalibur and Kukri DNA (artificial heterozygote).

Molecular marker genotypes of resistant and susceptible wheat cultivars

When assayed on a panel of 25 wheat cultivars, the markers *wri2*, *wri3*, *wri4*, and *wri5* all clearly distinguished Excalibur and 11 other resistant cultivars (i.e., known to have moderate resistance against *P. neglectus* and/or to carry *Lr20*/*Sr15*) from Kukri and 14 other susceptible cultivars (i.e., known to be susceptible to *P. neglectus* and to lack *Lr20/Sr15* resistance). Marker *wri1* was able to distinguish Excalibur from Kukri, and it additionally detected polymorphisms within the resistant and susceptible classes, for which there were three distinct melting curves among the resistant cultivars and at least two others among the susceptible cultivars (Figure 3.5). This variation within phenotypic classes may reflect sequence polymorphism in homoeologous regions on chromosomes 7B and 7D.

With the *csPSY* marker, all 11 resistant cultivars provided the same result as Excalibur, indicating the presence of the *Psy-A1s* or *Psy-A1t* ('very yellow') alleles. None of the susceptible cultivars gave this result. With sequencing of the region in which the *Psy-A1s* or *Psy-A1t* alleles have been reported to differ, it was confirmed that all 11 resistant cultivars carry the *Psy-A1t* allele [GenBank:HM006895] (see Appendix 1- Additional file S1.2: Figure S1.2). With *BstN1* restriction of the *csPSY* amplicon, each of the susceptible cultivars was classified as carrying either the *Psy-A1p* ('pale yellow') or *Psy-A1e* ('white') allele.

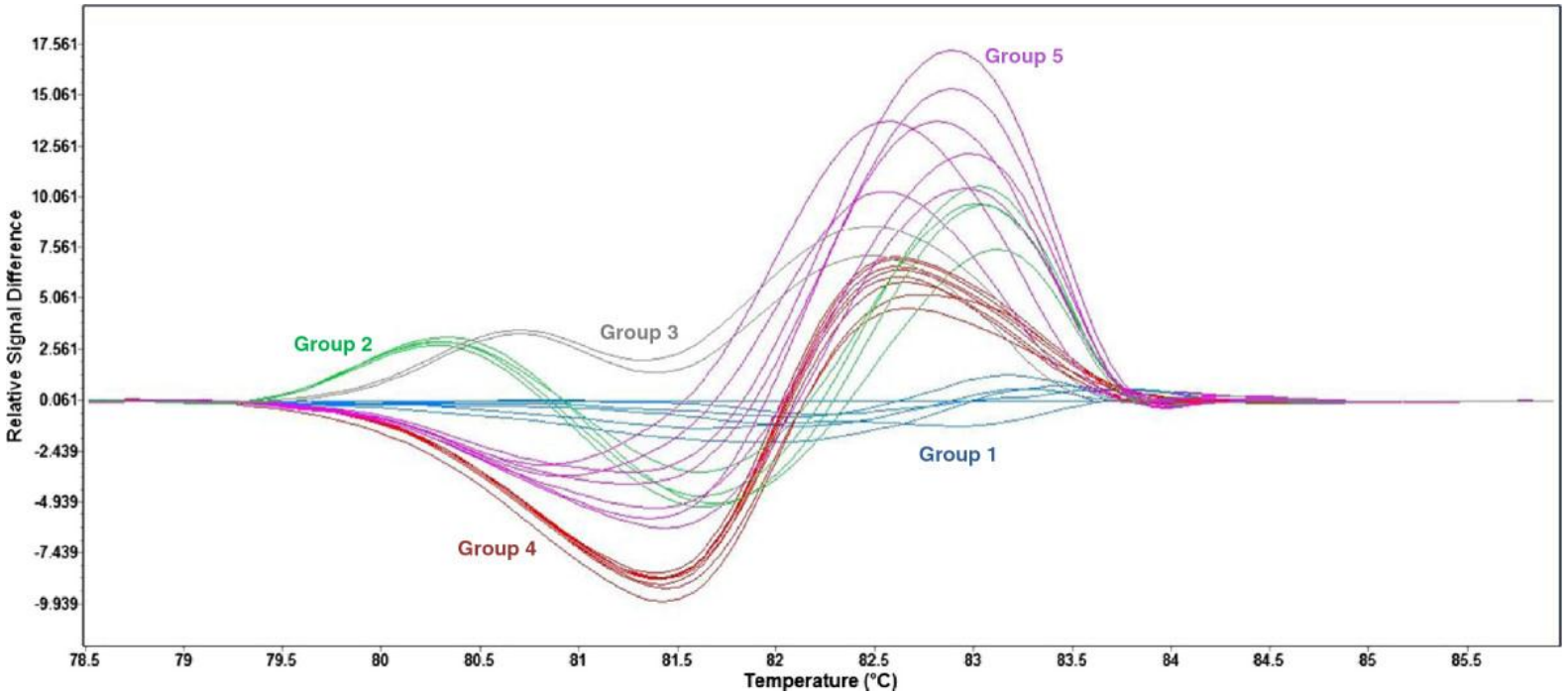

Figure 3.5: High-resolution melting curves for amplicons of the co-dominant marker *wri1*.

Normalized and temperature- shifted difference plot for products amplified from genomic DNA of, Excalibur and 11 other cultivars known to carry *Rlnn1* and/or known to carry *Lr20*/*Sr15* (Group 1: Excalibur, Bindawarra, Bowie, Vectis, Wyalkatchem, Orion; Group 2: Aroona, Tatiara, Thew, Cascades; Group 3: BT- Schomburgk, Krichauff) and Kukri and 14 other cultivars known to lack *Rlnn1* and/or known to lack *Lr20*/*Sr15* (Group 4: Kukri, Sunbri, Calingiri, Sunlin, Sunvale, AGT Scythe, Annuello, Machete; Group 5: Sunstate, Chara, Babbler, Hartog, Buckley, Gladius, Yitpi)

3.6 Discussion

Data on 182 progeny lines derived from a cross between Excalibur and Kukri wheat were used to map the root lesion nematode resistance locus *Rlnn1* as a QTL on 7AL, at a position that coincides with several molecular markers and with the rust resistance loci *Lr20* and *Sr15*. As expected, the allele from Excalibur conferred greater resistance. For *P. neglectus* and other parasitic nematodes, resistance refers to the ability of the plant to limit nematode multiplication and thereby reduce the nematode population in the soil. In field experiments, measures of resistance require data on initial and final nematode populations. In inoculated experiments such as the one conducted here, estimates of the final populations are sufficient, given that the initial population is the same for all plants. In this experiment, *P. neglectus* DNA was quantified in the root systems only (and not in the surrounding soil). Accordingly, there could be some unknown confounding from differences in the size of the root system. Although root mass was not recorded in this experiment, no obvious differences in root size or density were noticed. Given that the moderate resistance of Excalibur was originally detected in field experiments [177, 182] and that it has been repeatedly classified as moderately resistant using a range of methods, its resistance cannot be dismissed as simply an artefact of any variation in root size.

Our linkage map can be compared to a previously published map [200] based on the relative positions of the SSR marker *gwm344*, the rust resistance gene *Lr20* and the STS marker *schfc3* (Figure 3.2). In addition, the positions of the new markers *wri3* and *wri4* can be compared with the position of the RFLP locus *cdo347*. This is because *wri3* and *wri4* were designed based on EST sequences [GenBank:BF484041 and GenBank:CN010180] with high similarity (1.0e-56 and 4.0e-113, respectively) to the rice gene LOC_Os06g51270, which was the most significant hit for the CDO347 probe.

On the Excalibur/Kukri map, the *Rlnn1* QTL and four molecular markers (*gwm344, schfc3, wri3* and *wri4*) all collocate with *Lr20*. In the earlier map [200], *schfc3* and *cdo347* collocated with *Lr20,* but *gwm344* was 22.7 cM distal to *Lr20* and *Rlnn1*was about halfway between *Lr20* and g*wm344*. These discrepancies are probably due to differences in sample size and methodology. The original estimate of the position of *Rlnn1* [200] relied upon data from three small samples of progeny lines (25, 30 and 31 lines), each derived from a different cross. Each line was classified as either resistant or susceptible to *P. neglectus* and a consensus mapping approach was used to map *Rlnn1* as a discrete locus. With that approach and those sample sizes, any misclassification of lines or mis-scoring of markers could have considerably expanded the estimated distance between loci. In our work, trait data for *P. neglectus* resistance, which exhibited bimodal quantitative variation (Figure 3.1), were used to map *Rlnn1* as a QTL, without any attempt to classify the lines into distinct categories.

We detected a very strong association of resistance against *P. neglectus* with *Lr20/Sr15, Psy-A1* and 10 collocating molecular markers (*gwm344, cfa2240, schfc3, wPt-0790, sts638, wri1, wri2, wri3, wri4* and *wri5*). Of these, *sts638* had already been recommended [114] for selection of resistance conferred by *Lr20* and/or *Pm1,* but it has the disadvantage of being a dominant marker. The markers *schfc3, wPt-0790* and *wri5* are also dominant, as is *wri3* when assayed using gel electrophoresis with scoring of the presence or absence of a 250-bp chromosome 7A-specific amplicon. The markers *csPSY, gwm344, cfa2240, wri2* and *wri4* can all be assayed as codominant markers using electrophoresis, while *wri1* and *wri3* can be assayed as codominant markers using high-resolution melting analysis. We confirmed that *csPSY, wri2, wri3, wri4* and *wri5* all distinguish Excalibur and 11 wheat cultivars that are known to have moderate resistance against *P. neglectus* and/or to carry *Lr20*/*Sr15,* from Kukri and other 14 wheat cultivars that lack the resistance conferred by *Rlnn1* and *Lr20/Sr15*.

For marker-assisted selection of the root lesion nematode resistance locus *Rlnn1*, we recommend *wri2* for gel electrophoresis (Figure 3.3B) and *wri3* for high-resolution melting analysis (Figure 3.4B). The 7A-specific marker *wri2* is suitable for electrophoretic separation because it involves a substantial (74-bp) length polymorphism, whilst *wri3* can be scored as a high-throughput codominant marker using high-resolution melting analysis. Either of these markers would also be suitable for selection of the resistance genes *Lr20/Sr15* and *Pm1*. They both clearly distinguish between all of the resistant and susceptible materials that we have assayed, so they are likely to be useful across a wide range of wheat breeding germplasm.

Other loci within the wheat genome have also been reported to carry sets of co-segregating genes conferring resistance against rusts and powdery mildew. These include the *Lr34/Yr18/Pm38* locus on chromosome 7D, *Lr46/Yr29/Pm39* locus on chromosome 1B and *Lr67/Yr46* locus on chromosome 4D [62, 63, 90, 100, 161, 172, 195]. For the *Lr34/Yr18/Pm38* locus, a single gene encoding a protein resembling an adenosine triphosphate-binding cassette (ABC) transporter has been determined to confer resistance against leaf rust, stripe rust (caused by *Puccinia striiformis* f. sp. *tritici*) and powdery mildew [82]. For *Lr20/Sr15* and *Pm1,* McIntosh [99] found that changes to the *Lr20* disease reaction were always accompanied by changes to the *Sr15* reaction, while changes to *Pm1* were independent, indicating that the genetic determinant of *Pm1* resistance is not the same as for *Lr20/Sr15*. There is no particular reason to assume that the *Rlnn1* resistance effect is due to the same gene(s) as the *Lr20/Sr15* or *Pm1* resistance effects.

While coupling-phase linkage of alleles conferring resistance against multiple pathogens may be advantageous, the linkage of resistance alleles with a *Psy-A1* allele that confers high levels of yellow pigment in wheat flour is disadvantageous for markets that favour white flour. Recombinant progeny carrying the nematode resistance gene in combination

with a low-pigment allele of *Psy-A1* would be useful in wheat breeding. We have not found any such recombinants. Neu et al. [114] have suggested that *Lr20* and *Pm1* are in a region of suppressed recombination. They proposed that this could be due to an alien introgression or a genetic rearrangement. Based on the results presented here, it seems likely that *Rlnn1* and *Psy-A1* are also within the region of suppressed recombination. Based on previously reported sequence similarity of the *Psy-A1t* allele with B-genome alleles [24], it seems possible that chromosome 7A of Excalibur and the other resistant cultivars carries an ancestral translocation from the terminal region of the long arm of chromosome 7B.

Both the observed collocation of the *Rlnn1* QTL with *Psy-A1* (Figure 3.2) and the hypothesis that these loci are in a region of suppressed recombination are consistent with the experience of wheat breeders in Australia, who have not (to our knowledge) been able to combine *Rlnn1* resistance with white flour colour. In addition to limiting the opportunity to obtain favourable recombinants between *Rlnn1* and *Psy-A1* for wheat breeding purposes, suppression of recombination could impede positional cloning of *Rlnn1*, *Lr20/Sr15* and *Pm1*.

3.7 Conclusions

The research reported here has clarified the position of the *Rlnn1* locus for resistance against the root lesion nematode *P. neglectus*, by using a large wheat population to map *Rlnn1* as a QTL, rather than relying upon consensus mapping from small samples. The approach adopted here has clearly shown that *Rlnn1* is very closely linked with the rust resistance gene(s) *Lr20* and *Sr15*, the *t* allele of the phytoene synthase gene *Psy-A1* and several molecular markers. Some of the molecular markers developed here are useful for wheat breeding; they provide simple alternatives to costly phenotypic assessment of

resistance against *P. neglectus* and they have been confirmed to be diagnostic across a panel of wheat cultivars. The results reported here are consistent with the hypothesis that materials with *Rlnn1* resistance carry a chromosome rearrangement on 7AL and that this suppresses genetic recombination in this region.

3.8 Methods

Plant materials

The plant materials used here included the Australian wheat cultivars Excalibur (RAC177(*Sr26*)/Uniculm492//RAC311S; released by the University of Adelaide in 1991) and Kukri (76ECN44/76ECN36//RAC549; Madden/6*RAC177; released by the University of Adelaide in 1999), 182 DH lines produced from the F_1 generation of a cross between Excalibur and Kukri, a panel of 25 other wheat cultivars (sourced from the Australian Winter Cereals Collection) and six Chinese Spring nullisomic-tetrasomic lines (CS N7A-T7B, CS N7A-T7D, CS N7B-T7A, CS N7B-T7D, CS N7D-T7A and CS N7D-T7B, developed by Sears [155]).

The 182 Excalibur/Kukri DH lines were selected from 233 such lines for which molecular markers had previously been assayed [42]. The remaining 51 DH lines were excluded based on examination of the molecular marker data: 43 because they seemed to be genetically identical to other lines in the population, 6 because the DNA samples representing those lines exhibited more than one allele for numerous markers, indicating possible contamination of the lines or DNA samples, and 2 due to possible errors in DNA extraction.

Among the 25 wheat cultivars in the panel, 11 (Aroona, Bindawarra, Bowie, BT-Schomburgk, Wyalkatchem, Cascades, Krichauff, Thew, Tatiara, Orion and Vectis) are

known to have moderate resistance against *P. neglectus* and/or to carry *Lr20*/*Sr15*, while the other 14 (AGT Scythe, Annuello, Babbler, Buckley, Calingiri, Chara, Gladius, Hartog, Machete, Sunbri, Sunlin, Sunstate, Sunvale and Yitpi) are susceptible to *P. neglectus* and do not carry *Lr20/Sr15*.

Evaluation of resistance against leaf rust, stem rust and *Pratylenchus neglectus*

Resistance against rust pathogens was evaluated using the methods described by Bariana and McIntosh [8]. Two sets of seedlings were sown, one for inoculation with the *P. triticina* (Pt) pathotype 104-2,3,6,7 (PBI culture no. 231) and one for inoculation with the *P. graminis* f. sp. *tritici* (Pgt) pathotype 98-1,2,(3),5,6 (PBI culture no. 279). For each pathogen, 176 Excalibur/Kukri DH lines (six of the lines that had been genotyped were excluded due to insufficient seed availability or poor germination) were sown in 9-cm plastic pots (five seeds per line and four lines per pot) filled with a mixture of pine bark and river sand. Sown pots were fertilized with balanced fertilizer Aquasol® (10 g/10 L for 100 pots). Seedlings were raised in a controlled-environment microclimate room maintained at 20 ± 2 °C. At 7 d after sowing, urea was applied at the same rate as the Aquasol®. At the two-leaf stage (10 to 12 d after sowing), urediniospores suspended in light Shellsol T® mineral oil were atomised on the seedlings using a hydrocarbon pressure pack. The Pt-inoculated seedlings were incubated for 24 h in a misting room fitted with an ultrasonic humidifier. The Pgt-inoculated seedlings were incubated for 48 h under natural light conditions at 18 ± 2 °C on water-filled steel trays covered with plastic hoods. Seedlings were then transferred to a microclimate room maintained at 18 ± 2 °C. Infection type assessments of each line were made 14 d after inoculation using the 0 - 4 scales described by McIntosh et al. [101]. Each line was classified as resistant or susceptible to leaf and stem rust.

Evaluation of resistance against *P. neglectus* was carried out by the South Australian Research and Development Institute Root Disease Testing Service, Adelaide [121]. Plants were grown in a partially replicated experiment using four blocks sown at weekly intervals. Thirteen lines had to be excluded from this experiment due to insufficient availability of viable seed. Excalibur, Kukri and each of 170 Excalibur/Kukri DH lines, were each assigned to one block, while each of 50 Excalibur/Kukri DH lines was assigned to two blocks. Seeds of Excalibur, Kukri and the Excalibur/Kukri DH lines were pre-germinated over a period of 2 d in a misting chamber maintained between 22 and 24 ^{0}C. For each experimental unit, five pre-germinated seeds were sown in tubes (55 × 120 mm) containing 350 g of steam-pasteurised sand. These tubes were arranged in crates according to a pre-determined design, with each experimental unit consisting of a row of five adjacent tubes. Watering was carried out by flooding the tubes up to a 100-mm depth for 4 min, every 3 d. The *P. neglectus* inoculum used in the study was sourced from plants grown in Cambrai soil in South Australia. The culture was maintained in carrot calli using methods modified from Moody et al. [108] and was subcultured every 90 d. The nematodes were extracted from the carrot calli using a mist chamber as described by Hooper [68]. Nematodes were counted in three 250-µL samples of extract and the inoculum was adjusted to a final concentration of 1,500 nematodes /mL by diluting with sterile water. One week after sowing, each tube was inoculated by making two 50-mm-deep holes close to the seedling and dividing a 1-mL aliquot of the inoculum between the two holes. After inoculation, watering was suspended for 3 d. On the second day after inoculation, 1.4 g of a slow-release fertiliser (Osmocote, Scotts Miracle-Gro, USA) was added to each tube and the sand surface was covered with a layer of plastic beads to reduce evaporation and mould development.

Eight weeks after inoculation, the plants were removed from the tubes. The roots were cut, washed with running water to remove all soil and dried at 60 ^{0}C. For each plant, total DNA

was extracted from air dried roots as has been described for soil DNA extraction [55, 141]. Quantitative real-time PCR (qPCR) was performed on an ABI PRISM® 7900HT instrument using TaqMan® Minor Groove Binder probe (Applied Biosystems, Foster City, CA, USA). The TaqMan probe (6FAM- 5´- CATTGGGCTCAGAAAC -3´) was used at 200 nM final concentration with a forward primer (5´- CACGGACCAAGGAGTTTATCG - 3´) and a reverse primer (5'- CGAGGACATGTTTCACTTTCATTG - 3´), each at 400 nM final concentration. The qPCR reactions were prepared using the QuantiTect Probe PCR Master Mix (QIAGEN GmbH, Hilden, Germany). The PCR conditions were 50 °C for 2 min; 95 °C for 15 min followed by 40 cycles of 95 °C for 15 s and 60 °C for 1 min. The quantity of *P. neglectus* DNA per plant was calculated using a standard calibration curve obtained from 10-fold serial dilution series of purified *P. neglectus* genomic DNA.

The resulting phenotypic data were analysed using the REML directive in GenStat v15.3.0.9425 (VSN International Ltd., UK), employing a model that included random effects for the experimental block and the parental or DH line. Comparisons of the *P. neglectus* resistance between the rust-resistant and rust-susceptible groups were carried out by applying a two-sample *t* test to line best linear unbiased predictions (BLUPs) for *P. neglectus* DNA per plant, assuming unequal group variances.

Wheat-rice comparative analysis and development of new markers from wheat ESTs

Because the physical locations of the *Rlnn1*-linked SSR markers *cfa2019* and *cfa2240* had previously been assigned to wheat deletion bin 7AL16-0.86-0.90 [171], 87 unique ESTs from the two terminal deletion bins 7AL16-0.86-0.90 and 7AL18-0.90-1.00 of wheat physical EST maps in GrainGenes database [27] were used as BLASTN queries to search the rice genome sequence at Rice Genome Annotation Project database [28, 80]. In

addition, probe sequences of the *Rlnn1* and/or *Lr20*/*Sr15*/*Pm1*-linked RFLP markers *cdo347, psr121*, *psr148,* and *psr680* from the GrainGenes database [27] were used as BLASTN queries against the GenBank *Triticum* EST database at NCBI [112]. BLAST hits with E-values less than e-40, were retrieved and used to query rice coding sequences at the Rice Genome Annotation Project database [28, 80]. Once an orthologous region of the rice genome was identified, the sequences of predicted rice genes in that region were used as BLASTN queries to search the GenBank *Triticum* EST database at NCBI [112] for wheat orthologues. Sequence comparisons of the rice genes with their putative wheat EST orthologues were used to predict the positions of wheat introns, and PCR primers were designed to span predicted introns. In addition, primer sequences that had previously been designed for wheat ESTs assigned to 7AL16-0.86-0.90 and 7AL18-0.90-1.00 were obtained from the Wheat SNP Database [4, 30]. Newly designed PCR primer pairs and those obtained from the SNP database (Table 3.1) were used to amplify products from genomic DNA of Excalibur and Kukri using PCR conditions described in Appendix1 (Additional file S1.5). For each primer pair, the amplicons from Excalibur and Kukri were examined for polymorphism using electrophoresis on agarose gels, high-resolution melting analysis in a Roche LightCycler® 480 and/or sequencing.

Table 3.1: PCR markers designed based on five wheat expressed sequence tags (ESTs).

Marker	EST	Forward primer (5'-3')		Reverse primer (5'-3')	
wri1	BE445506	BE445506_F	TCAGACAATTTAGTGGATGCTCG	BE445506_R	CCGCAAAGTAGCACGCCTT
wri2	BE445653	BE445653_F	TGGACACTGGGTTCATCGAGGA	BE445653_R	AGCAAGCACACTAGCCACTCTGTTT
wri3	BF484041	BF484041_F	TTCTCGCTGCAAAACTATGGC	BF484041_R	TTCACAGATCCAGTGCTTATGTCG
wri4	CN010180	CN010180_F1	ATGGGGCCTCTTCGG	CN010180_R	GSAAACATCTGTCTGATTACARAATAAG AA
		CN010180_F2	ATGGGGCCTCTTCGC		
wri5	BF483039	BF483039A_F2	GCAGCTACTTTGAACCCTTCAG	BF483039_cpR1	CGACCGTCTTCCCGAACAGC

Partial sequencing of *Psy-A1* and BE445653

The primer pair *PSY7A5_F/R* [24] was used to amplify a region of the gene *Psy-A1* from the cultivars Excalibur, Aroona, Bindawarra, Bowie, BT-Schomburgk, Wyalkatchem, Cascades, Krichauff, Thew, Tatiara, Orion and Vectis using conditions given in Appendix 1 (Additional file S1.5). PCR products were cleaned up using NucleoSpin® Gel and PCR clean-up kit (MACHEREY-NAGEL GmbH & Co. KG). Sequencing was carried out at Australian Genome Research Facility Ltd., Adelaide by capillary separation on the Applied Biosystems 3730xl DNA analyzer (Applied Biosystems, CA, USA). The sequences of Excalibur and 11 other cultivars were aligned to *Psy-A1t* allele sequence of the breeding line WAWHT2074 [GenBank:HM006895] [24] and *Psy-A1s* allele sequence of the cultivar Schomburgk [GenBank:EU649795] [70] with the multiple align module implemented in Geneious® 6.0.4 (Biomatters Ltd., New Zealand) with default settings.

Primer pair *wri2_F/R* was used to amplify a region of BE445653 from the cultivars Excalibur, Bowie, Wyalkatchem, Cascades, Krichauff, Kukri, Machete, AGT Scythe, Chara, Gladius, Buckley and Yitpi using the conditions described in Appendix 1 (Additional file S1.5). PCR purification, sequencing and sequence analysis and alignment were performed as described above.

Genotyping of molecular markers

The STS markers *schfc3* (designed based on the STS marker *FC7* [126]) and *sts638* [114], the *Psy-A1* marker *csPSY* [70] (see Appendix 1 - Additional file S1.5: Table S1.2) and five new markers (*wri1*, *wri2*, *wri3*, *wri4* and *wri5*, Table 1.1) were assayed on Excalibur, Kukri and each of the 182 Excalibur/Kukri DH lines, using PCR conditions described in Appendix 1 (Additional file S1.5). For markers *wri2*, *wri4*, *wri5*, *schfc3* and *csPSY*, genotypes were assayed on 2.0 to 2.5 % agarose gels (see Appendix 1 - Additional file

S1.5). For markers *wri1*, *wri3* and *sts638*, genotypes were assayed using high-resolution melting technology [201] in a Roche LightCycler® 480 using conditions reported in Appendix 1 (Additional file S1.5). Melting curves were analysed using the gene scanning module of Roche LightCycler® software version 1.5.0. The five new markers (*wri1*, *wri2*, *wri3*, *wri4* and *wri5*) and *csPSY* were also assayed on the panel of 25 wheat cultivars, on the Chinese Spring nullisomic-tetrasomic lines (CS N7A-T7B, CS N7A-T7D, CS N7B-T7A, CS N7B-T7D, CS N7D-T7A and CS N7D-T7B) and on an artificial heterozygote (created by combining equal amounts of Excalibur and Kukri 50-ng/µl DNA).

Genetic mapping

For each rust pathogen, each Excalibur/Kukri DH line for which all plants were resistant (infection type of 0 - 2) was classified as carrying the Excalibur allele of the corresponding rust resistance gene and each line for which all plants were susceptible (infection type of 3 - 4) were classified as carrying the Kukri allele. Four lines that exhibited mixed responses (some resistant plants and some susceptible) were treated as having missing data for the rust resistance loci. Similarly, for each molecular marker, each DH line was classified as carrying the same allele as Excalibur or the same allele as Kukri. Six markers that had originally been mapped on chromosome 7A [42] were excluded due to ambiguous genotypic scores (*gdm125*, *gwm681*, *wPt-7299*, *wPt-2260* and *wPt-1259*) or a high frequency of missing data (*wPt-6668*). The newly assayed markers (*wri1*, *wri2*, *wri3*, *wri4*, *wri5*, *sts638* and *schfc3*), the phytoene synthase gene *Psy-A1* and the rust resistance locus *Lr20/ Sr15* were added to the existing chromosome 7A genetic linkage map [42] using the 'distribute' function of MapManager QTXb20 [96] (search linkage criterion set at a LOD threshold of p = 1e-6; map distance estimation done using Kosambi mapping function [81]). The marker order was refined using RECORD [181] and the goodness-of-fit of the

marker order was examined by plotting pairwise recombination fractions against LOD linkage statistics. Line BLUPs of the quantity of *P. neglectus* DNA per plant were used to map *Rlnn1* as a QTL on the resulting genetic map by interval mapping as implemented in Qgene 4.3.10 [77] with a step size of 1 cM and a significance threshold for detection of QTL set by performing 1000 permutations with a genome wide Type I error rate of 0.05. The final linkage map and QTL graph was plotted using MapChart v2.2 [184].

Chapter 4

Suppressed recombination in a region of wheat chromosome 7A that carries loci affecting resistance against a root lesion nematode and fungal pathogens

Dimanthi V. Jayatilake[1], Harbans Bariana[3], Melissa Garcia[1, 2], John Toubia[2], Peng Zhang[3], Matthew Hayden[4], Ken Chalmers[1,2] and Diane E. Mather[1,2]

[1]School of Agriculture, Food and Wine, Waite Research Institute, The University of Adelaide, PMB 1, Glen Osmond, SA 5064, Australia

[2]Australian Centre for Plant Functional Genomics, Waite Research Institute, The University of Adelaide, PMB 1, Glen Osmond, SA 5064, Australia

[3]The University of Sydney Plant Breeding Institute – Cobbitty, PMB 4011, Narellan, NSW 2567, Australia

[4] Department of Primary Industries Victoria, Victorian AgriBiosciences Center, Bundoora, VIC 3083, Australia

Email addresses of other authors:

DJ: dimanthi.jayatilake@adelaide.edu.au

HB: harbans.bariana@sydney.edu.au

MG: melissa.garcia@acpfg.com.au

JT: john.toubia@acpfg.com.au

PZ: peng.zhang@sydney.edu.au

MH: matthew.hayden@dpi.vic.gov.au

KC: ken.chalmers@adelaide.edu.au

4.1 Statement of Authorship

Title of the paper	Suppressed recombination in a region of wheat chromosome 7A that carries loci affecting resistance against a root lesion nematode and fungal pathogens
Publication Status	☐ Published ☐ Accepted for publication ☐ Submitted for publication ☐ Publication style
Publication Details	This chapter will be prepared as a manuscript for submission to BMC Genomics. We plan to augment it soon with results of additional work still being undertaken by collaborators.

Author Contributions

By signing the Statement of Authorship, each author certifies that their stated contribution to the publication is accurate and that permission is granted for the publication to be included in the candidate's thesis.

Name of Principal Author (Candidate)	Dimanthi V. Jayatilake
Contribution to the paper	Critically examined all genotypic and phenotypic data, designed and assayed markers, reconstructed the linkage map, conducted QTL analysis, screened for informative recombinants, conducted seed multiplication in the glasshouse, sequencing, conducted phylogenetic analysis, interpreted the results and wrote the first draft of the manuscript and took primary responsibility for manuscript revision.
Signature	Date 26/03/2014

Name of Co-author	Harbans Bariana
Contribution to the paper	Evaluated the population for resistance against leaf rust.
Signature	Date 12/3/14

Name of Co-author	Melissa Garcia		
Contribution to the paper	Designed new molecular markers		
Signature		Date	26.03.14

Name of Co-author	John Toubia		
Contribution to the paper	Assembled the sequences and wrote other custom scripts to identify polymorphisms		
Signature		Date	26.03.2014

Name of Co-author	Peng Zhang		
Contribution to the paper	Conducted the cytology experiments and assisted in interpreting findings		
Signature		Date	12-03-2014

Name of Co-author	Matthew Hayden		
Contribution to the paper	Carried out 9K- iSelect SNP genotyping on DNA pools		
Signature		Date	28-03-2014.

Name of Co-author	Ken Chalmers		
Contribution to the paper	Supervised the marker design, genotyping and linkage mapping.		
Signature		Date	26/3/14

Name of Co-author	Diane E. Mather		
Contribution to the paper	Provided overall supervision of the research and helped write the manuscript.		
Signature		Date	26 MARCH 2014

4.1 Introduction

The results reported in Chapter 3 provided strong evidence that the root lesion nematode *P. neglectus* resistance QTL on 7AL (*Rlnn1*) collocates with the rust resistance genes *Lr20* (conferring resistance against leaf rust caused by *Puccinia triticina* [13, 190]) and *Sr15* (conferring resistance against stem rust caused by *Puccinia graminis* f. sp. *tritici* [191]), a phytoene synthase gene (*Psy-A1*; [59]) and 10 molecular markers in Excalibur/Kukri genetic background. This clustering of markers/genes and a QTL at the distal end of 7AL, is consistent with the suggestion of Neu et al. [114] that suppressed recombination in the *Lr20*/*Pm1* (*Pm1*:conferring resistance against powdery mildew *Blumeria graminis* f. sp. *tritici* [156]) region. Neu et al. [114] speculated that the suppression of recombination could be due to an alien introgression or a genetic rearrangement.

The resistance alleles of *Rlnn1*, *Lr20*/*Sr15* and *Pm1* are in tight coupling linkage with the '*t*' allele of *Psy-A1* (Chapter 3; [99, 114, 178]). This coupling phase linkage of the resistance alleles with an allele associated with 'very yellow' flour colour (*Psy-A1t*) is not desirable for bread-making (Chapter 3). To my knowledge, no released wheat variety carries the desirable resistance alleles for *Rlnn1*and *Lr20*/*Sr15* and whiter flour colour (i.e., any *Psy-A1* allele other than '*t*'). This further indicates the difficulty of finding natural recombinants between these genes, despite much effort by the breeders.

Among the collocated loci mentioned above, only *Psy-A1* has been extensively characterised at the molecular level. The availability of *Psy1* allele sequences from wheat and close relatives presented opportunities to investigate the evolutionary history of the *Psy1* gene (and thus its genomic region). Results of phylogenetic analysis conducted by Crawford et al. [24] indicated that even though the *Psy-A1t* allele has been genetically mapped on 7AL [24, 125], it is more closely related to the *Psy1* alleles of the S genome of *Aegilops speltoides* (a likely progenitor of the wheat B genome [53]) and to some B

genome alleles from *T. aestivum* and *Triticum turgidum* ssp. *dicoccon* than to other A-genome *Psy1* alleles. Crawford et al. [24] proposed that this could be due to an ancient allele sorting or a genetic rearrangement such as a translocation.

In the research reported here, further investigations were conducted to 1) improve the Excalibur/Kukri chromosome 7A linkage map and refine the map position of the *Rlnn1* locus (presented in Part A of this chapter, which reports on addition of new molecular markers); 2) investigate if there is suppressed recombination at the distal end of 7AL in the cultivar Excalibur (presented in Part B of this chapter, which reports evidence from other mapping populations, a syntenic build of Chinese Spring chromosome 7A and a set of Excalibur/Kukri recombinant inbred lines); and 3) if there is suppressed recombination, to understand the biological basis for this phenomenon (presented in Part C of this chapter, which reports on evidence based on *Psy1* allele sequences and analysis of selected amplicons of markers mapped to the region).

4.2 Part A – Improving the Excalibur/Kukri chromosome 7A linkage map and refining the map position of the *Rlnn1* locus

4.2.1 Objectives

1. Improve the Excalibur/Kukri chromosome 7A linkage map by taking a targeted approach to fill the large intervals and to map molecular markers distal to the 'terminal cluster'.
2. Refine the marker order and the mapped position of the *Rlnn1* locus.

3. Identify additional diagnostic markers for MAS.

4.2.2 Methods

Plant materials

The materials used in this part were the Australian cultivars Excalibur and Kukri, 182 DH lines developed from the F_1 generation of a cross between Excalibur and Kukri, a panel of 25 wheat cultivars sourced from the Australian Winter Cereals Collection (Aroona, Bindawarra, Bowie, BT-Schomburgk, Wyalkatchem, Cascades, Krichauff, Orion, Thew, Tatiara, Vectis, AGT Scythe, Annuello, Babbler, Buckley, Calingiri, Chara, Gladius, Hartog, Machete, Sunbri, Sunlin, Sunstate, Sunvale and Yitpi) and six Chinese Spring nullisomic-tetrasomic lines CS N7A-T7B, CS N7A-T7D, CS N7B-T7A, CS N7B-T7D, CS N7D-T7A and CS N7D-T7B developed by Sears [155].

Marker assays

Pre-existing markers

KASP™ marker assays

Fifty-three published KASP™ markers mapped to chromosome 7A were selected from the CerealsDB database [26] and from those reported by Allen et al. [6]. These markers were assayed on Excalibur, Kukri and 20 Excalibur/Kukri DH lines at LGC Genomics Ltd., UK and/or on a Roche LightCycler® 480 (Roche Products Pty. Ltd., Switzerland), according to methods described in Appendix 2 (Additional file S2.1). Genotypic calls were made using the end-point genotyping module implemented in Roche LightCycler® 480 software release 1.5.0 (Roche Products Pty. Ltd., Switzerland).

Gel-based marker assays

The markers *AWW5L7* [153], a marker for a polymorphism in *Cat3-A1* [23] and *AWW622* (*AWW622_F* 5`- CCTCTTCAGGTGGCTGACCAAGTAG - 3`; *AWW622_R* 5`- CCTTGTCAGATTAGGAGAATTTTGC - 3`; Margaret Pallotta, unpublished) were assayed on Excalibur, Kukri and the Excalibur/Kukri DH lines using the conditions described in Appendix 2 (Additional file S2.1), with polymorphisms visualised using agarose gel electrophoresis.

Development of new HRM-based marker assays

One sample of Excalibur DNA, one sample of Kukri DNA, two samples of an artificial heterozygote (prepared by combining equal amounts of 50-ng/µl parental DNA), and three samples of each of two DNA pools (an 'Excalibur-like pool' and a 'Kukri-like pool' prepared by combining 50 ng/µl DNA from 20 Excalibur/Kukri DH lines each, with fixed Excalibur haplotype or Kukri haplotypes in the *Rlnn1* QTL region) were genotyped using the Illumina Infinium 9K iSelect genotyping array [16]. Based on the results of this assay, sequence polymorphisms that were strongly associated with polymorphism in the *Rlnn1* region were selected and were used as the basis for primer design with BatchPrimer 3 [202] for the development of high-resolution melting (HRM)-based marker assays.

Using a BLASTN search approach, molecular markers mapped to the end of 7AL in the Excalibur/Kukri linkage map were anchored to the Chinese Spring chromosome 7A syntenic build 7AL_v0.1 and 7A_SynBuild_v2.0 at the Wheat Genome Database [29, 85]. Contig sequences of the syntenic builds were extracted from selected regions and ISBP markers suitable for assaying with HRM technology were designed using the *IsbpFinder* program [129].

Whole-genome shotgun survey sequences (Illumina 100-bp paired-end, 10× coverage) of cultivars Excalibur and Kukri that had been generated by Bioplatforms Australia [7, 41] were quality checked and filtered using custom scripts that were designed to trim and remove adapter sequences and low quality reads. The Chinese Spring contig sequences from positions 16,900,000 through 17,969,999 of 7A_SynBuild_v2.0 were extracted from the Wheat Genome Database [29] and used as reference sequences for mapping of the Excalibur and Kukri shotgun sequence reads with Bowtie2 [87] (parameters: --very-sensitive --mp 30,25 --rfg 15,13 --rdg 15,13 --np 15 --no-unal --no-mixed, and all remaining parameters kept as default). Polymorphisms were detected using custom scripts in a semi-automated approach. Candidate SNPs were selected based on two criteria: 1) coverage was required to be greater than 5 for each sample and 2) the base call had to be constant within the samples (no ambiguous calls), but different between samples. The output was visualized using Tablet 1.13.07.31 [105]. Sequences from targeted regions with SNP polymorphisms between cultivars Excalibur and Kukri were extracted and were used to design HRM-based assays using BatchPrimer 3 [202].

All HRM-based primer pairs were assayed on a Roche LightCycler® 480 based on methods described in Appendix 2 (Additional file S2.1). The normalized shifted melting curves and/or normalized temperature-shifted difference plots were examined for polymorphism between Excalibur and Kukri using the gene scanning feature of Roche LightCycler® software 1.5.0. All polymorphic HRM-based primers were assayed on 182 Excalibur/Kukri DH lines.

Selected polymorphic primer pairs were also assayed on Chinese Spring nullisomic-tetrasomic lines CS N7A-T7B, CS N7A-T7D, CS N7B-T7A, CS N7B-T7D, CS N7D-T7A and CS N7D-T7B to assess genome specificity. In addition the marker *AWW5L7* was assayed on the cultivars Halberd, Cranbrook and on the artificial heterozygote.

Linkage and QTL mapping of the DH mapping population

New markers were added to the existing Excalibur/Kukri chromosome 7A linkage map (Chapter 3) using MapManager QTXb20 [96] with the function 'distribute' (search linkage criteria set at p = 1e-6) and the marker order was refined using RECORD [181]. Using the same BLUPs of the *P. neglectus* nematode DNA (pg) per plant that were used in Chapter 3, SIM was implemented in Qgene 4.3.10 [77] with a step size of 1 cM to map *Rlnn1* QTL on the new chromosome 7A genetic map. The LOD threshold to identify significant QTL was estimated by performing 1000 permutations with a genome-wide Type 1 error of 0.05. The linkage map and QTL graph were plotted in MapChart v2.2 [184].

Marker validation

All markers mapped to the 'terminal cluster' were assayed on a wheat panel of 25 cultivars (Aroona, Bindawarra, Bowie, BT-Schomburgk, Wyalkatchem, Cascades, Krichauff, Orion, Thew, Tatiara, Vectis, AGT Scythe, Annuello, Babbler, Buckley, Calingiri, Chara, Gladius, Hartog, Machete, Sunbri, Sunlin, Sunstate, Sunvale and Yitpi).

4.2.3 Results

Marker assays

The Excalibur/Kukri genetic linkage map reported in Chapter 3 had a large 23.7-cM interval proximal to the 'terminal cluster' and no molecular markers mapped distal to the 'terminal cluster'. Additional markers, both pre-existing and newly designed for the purpose, were assayed on the Excalibur/Kukri DH lines.

Pre-existing marker assays

Out of 53 KASP™ assays (Appendix 2 – Additional file S2.1: Table S2.1) that had previously been mapped to chromosome 7A in other materials [6, 26], 22 detected clear polymorphisms between Excalibur and Kukri.

With the *AWW5L7* primer pair, which had previously been reported to detect a length polymorphism between Halberd (956 bp) and Cranbrook (877 bp) that mapped on chromosome 7B [153], an 877-bp product was amplified from Kukri and two products were amplified from Excalibur. One of the Excalibur products was similar in length to the products from Cranbrook and Kukri, while the other was slightly longer than the product from Halberd (Figure 4.1). The presence/absence polymorphism was readily detected through gel electrophoresis.

The *Cat3-A1* marker [23], also resulted a presence/absence polymorphism, with a 761-bp product amplified from Kukri but no product amplified from Excalibur (Figure 4.2A). The polymorphism was readily detected through gel electrophoresis. The primer pair *AWW622_F/R* amplified products of approximately 300 bp and 600 bp from Kukri, but only a 600-bp product from Excalibur (Figure 4.2B). That polymorphism was readily assayed with gel electrophoresis and scored as a dominant marker based on the presence or absence of the smaller amplicon. Application of this marker to nullisomic-tetrasomic aneuploid stocks indicated that the larger amplicon is specific to chromosome 7B, while the smaller one is specific to chromosome 7A.

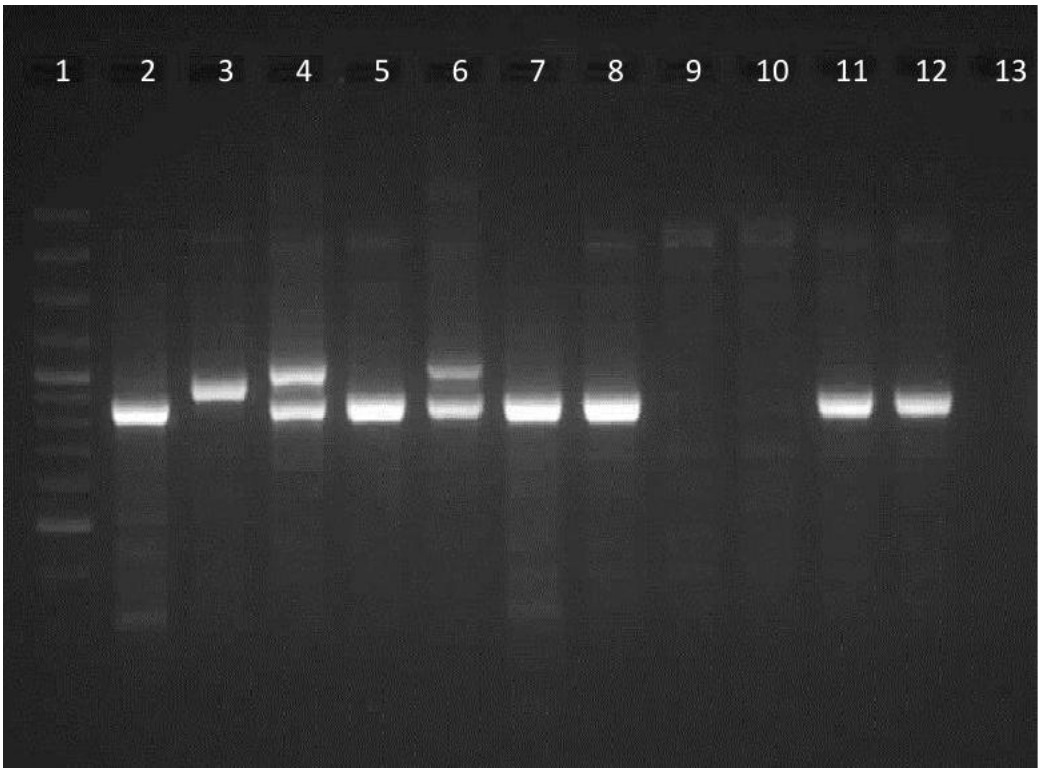

Figure 4.1: Amplicons of marker *AWW5L7* separated by agarose gel-electrophoresis.

From left to right: (1) GeneRuler® 100 bp DNA ladder (Thermo Fisher Scientific Inc.), (2) Cranbrook, (3) Halberd, (4) Excalibur, (5) Kukri, (6) an 1:1 mixture of Excalibur and Kukri DNA (artificial heterozygote), (7) CS N7A-T7B, (8) CS N7A-T7D, (9) CS N7B-T7A, (10) CS N7B-T7D, (11) CS N7D-T7A, (12) CS N7D-T7B and (13) Water.

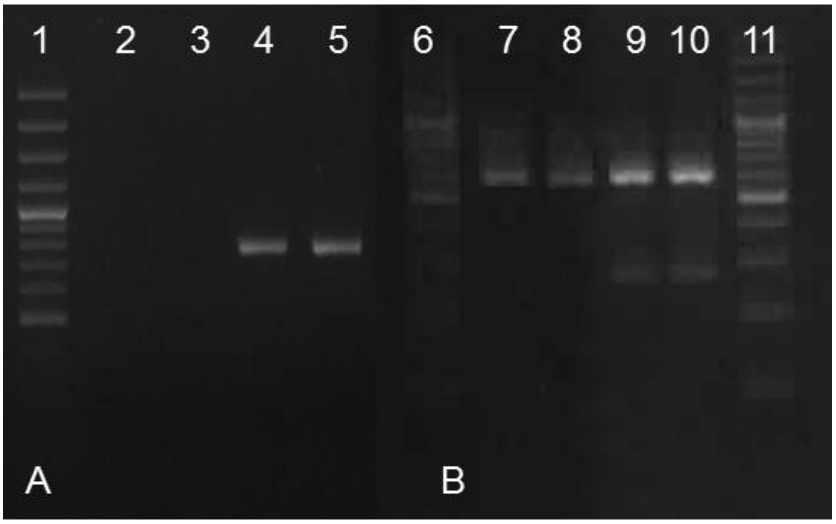

Figure 4.2: Amplicons of markers *Cat3-A1* (A) and *AWW622* (B) separated by agarose gel-electrophoresis.

From left to right: (1) GeneRuler® 100 bp DNA ladder (Thermo Fisher Scientific Inc.), (2) Excalibur, (3) Excalibur, 4) Kukri, 5) Kukri, 6) GeneRuler® 100 bp DNA ladder (Thermo Fisher Scientific Inc.), (7) Excalibur, (8) Excalibur, 9) Kukri, 10) Kukri and 11) GeneRuler® 100 bp DNA ladder (Thermo Fisher Scientific Inc.).

Development of new HRM-based marker assays

Thirty-four HRM assays (Table 4.1 to 4.3) were developed for sequence polymorphisms between Excalibur and Kukri. These comprised: (1) 15 polymorphisms identified by genotyping pooled DNA from each of two contrasting sets of Excalibur/Kukri DH lines on an iSelect genotyping array [16]; (2) 16 putative ISBP sites identified from genomic sequence of chromosome 7A; and (3) 3 SNPs between Excalibur and Kukri sequences.

Table 4.1: Primer sequences of newly designed molecular markers based on the 9K-iSelect genotyping array

Marker name	SNP index	Primer sequence (5` to 3`)	Marker type
wri17	*iwa4601*	Forward: GCGTTGCCAATACTGAAGAAGC	Codominant
		Reverse: TTACCGAAACAGTTCAATCCACA	
wri18	*iwa2012*	Forward: GGGTATGACTGTCAAACTGATACGG	Codominant
		Reverse: ATGCCGATGTTGTTCCAGTGA	
wri19	*iwa7074*	Forward: CTCAGGTTCTCTGTTAGAAGGCAA	Codominant
		Reverse: GAGGGTTTGTCAAGGAAACCAA	
wri20	*iwa4993*	Forward: TTAGAGGCGCGCTGAATAAG	Codominant
		Reverse: TGACCTGACCTGACCTGACC	
wri21	*iwa4994*	Forward: TGTGGTGATGAACTGGTTGTGTAAT	Codominant
		Reverse: TAAAACAAAACAACTGGACCCTT	
wri22	*iwa7184*	Forward: CATGTCTTGTGCCTTGGATTTG	Codominant
		Reverse: GAGAGCAGGATTGGACTCGG	
wri23	*iwa3371*	Forward: AGTCAATAAGTTACTCCTCCTGGG	Codominant
		Reverse: CGAGGAAGAATAGGTAGGTGTCG	

wri24	*iwa4364*	Forward: TCGTGGTTATAAGGTTACGATGTG	Codominant
		Reverse: TCCGTACGAGAAACTCACTCTG	
wri25	*iwa4433*	Forward: CATTCTATCGCATGCACCAA	Codominant
		Reverse: TCACTGCAAGACCGTGATTC	
wri26	*iwa4176*	Forward: AGCATGAAGCTGTGGAACCT	Codominant
		Reverse: TATGATGCAGAGCCAGCAAA	
wri27	*iwa6424*	Forward: GCCTGCCAATGTGAAGTTG	Codominant
		Reverse: CAAAGTTGCTACTGAGTTGACTGCTA	
wri28	*iwa6772*	Forward: GAGGTCGTTGCCGGTAAAAT	Codominant
		Reverse: GGTTCTATCCCGGCTACCTT	
wri29	*iwa7005*	Forward: CCTTGCCTTCCTTGATCTTG	Codominant
		Reverse: GGCTTGTGAAATCACAGTGG	
wri30	*iwa5904*	Forward: CGCTTCAGAGGAGATCCAAG	Dominant
		Reverse: AGGACCATCTGCCACTCATC	
wri31	*iwa0795*	Forward: GGTAGACCACCACACCATGC	Dominant
		Reverse: GCGTACGAGTATGGCAACAG	

Table 4.2: Primer sequences of newly designed insertion site-based polymorphism markers

Marker name	Primer sequence (5` to 3`)	Marker type
wri32	Forward: GAGAGCACTCCAAAACTGGC	Codominant
	Reverse: TTCAGAATCGGGACAAAAGG	
wri33	Forward: TGGCCCATCTTACATTCTCA	Codominant
	Reverse: CTGCGCAGAGACAATGATTC	
wri34	Forward: GCTTGGTTCTGCATTGGATT	Codominant
	Reverse: TGGTCAAACTTTACGAGGCTT	
wri35	Forward: CACACATGCTTCATCCGAAC	Codominant
	Reverse: GTGGCCTTGGGCTTACTGT	
wri36	Forward: GGCTCAGTCTTTCGAAGGTG	Dominant
	Reverse: CTACGGGAGAGCTATTCGCC	
wri37	Forward: GGCTCAGTCTTTCGAAGGTG	Dominant
	Reverse: CTACGGGAGAGCTATTCGCC	
wri38	Forward: TGCCCGAGGAATAGCATATC	Dominant
	Reverse: TTCGATGATGATTCCAGTTG	
wri39	Forward: TTCTCCTCGTTTCGACTCGT	Dominant
	Reverse: TGCAAAAACATCTCATATTGTGG	
wri40	Forward: ATGGGGAAGGGACGACTAAG	Dominant
	Reverse: TAAAGGTCCCATTTGAACCG	
wri41	Forward: TGTTGGTCTCTTCCTCCTCG	Dominant
	Reverse: TGTGATCATGCACAACATGG	
wri42	Forward: AAAGGGCACAGGAGCTATGA	Dominant
	Reverse: CATTTCTACGACAAGTAATTCCGA	
wri43	Forward: TGTCAAAGTAGCATCGAAAACG	Dominant
	Reverse: ATCTATATGCGGTGAAGGCG	
wri44	Forward: CTCTATGCATGGGTGCAATG	Dominant

	Reverse: GCCGACTAAGAAGTTGGCTG	
wri45	Forward: TTGCACCGTTCCATTGAATA	Dominant
	Reverse: ACGGAGGGAGTATCACACAA	
wri46	Forward: CACCCAACCCTAGTTAGCGA	Dominant
	Reverse: TGAGGCAAATCTTTTGCATTT	
wri47	Forward: GGTAAAAGTTGTGACCTAAAACGTC	Dominant
	Reverse: CGTGCACCTTATCACCTCCT	

Table 4.3: Primer sequences of molecular markers designed based on single nucleotide polymorphisms between Excalibur and Kukri sequences

Marker name	**Primer sequence (5` to 3`)**	**Marker type**
wri48	Forward: CTCGGGTAGGTCCATGAAAA	Codominant
	Reverse: AATCCTGCATCGAGATTTGG	
wri49	Forward: CAAAACCGTACCCAATCTCG	Codominant
	Reverse: GTACGTGCCAGGTTTTGGTT	
wri50	Forward: GCTACCAGTCGGTGTCCTG	Codominant
	Reverse: ATCCGACACGTCAACACAAA	

Among the 34 newly designed HRM-based markers, 20 could be scored as codominant markers based on normalised-shifted melting curves and/or normalized temperature-shifted difference plots (e.g., Figure 4.3A and B) and the other 14 could be scored as dominant (presence/absence) markers (e.g., Figure 4.3C).

A

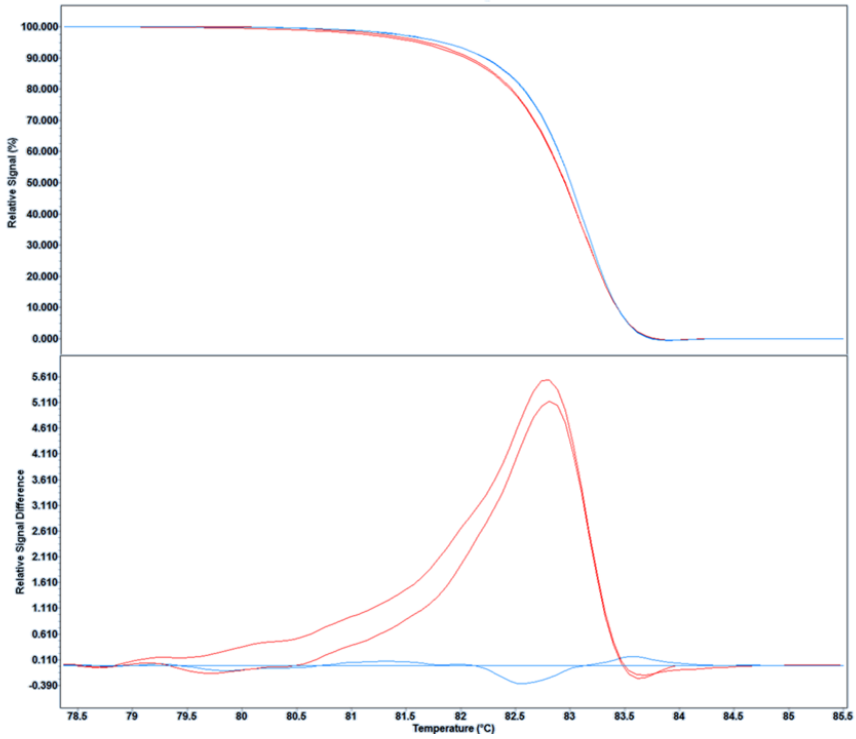
Relative Signal (%)
100.000
90.000
80.000
70.000
60.000
50.000
40.000
30.000
20.000
10.000
0.000
Relative Signal Difference
5.610
5.110
4.610
4.110
3.610
3.110
2.610
2.110
1.610
1.110
0.610
0.110
-0.390
78.5
79
79.5
80
80.5
81
81.5
82
82.5
83
83.5
84
84.5
85
85.5
Temperature (°C)

B

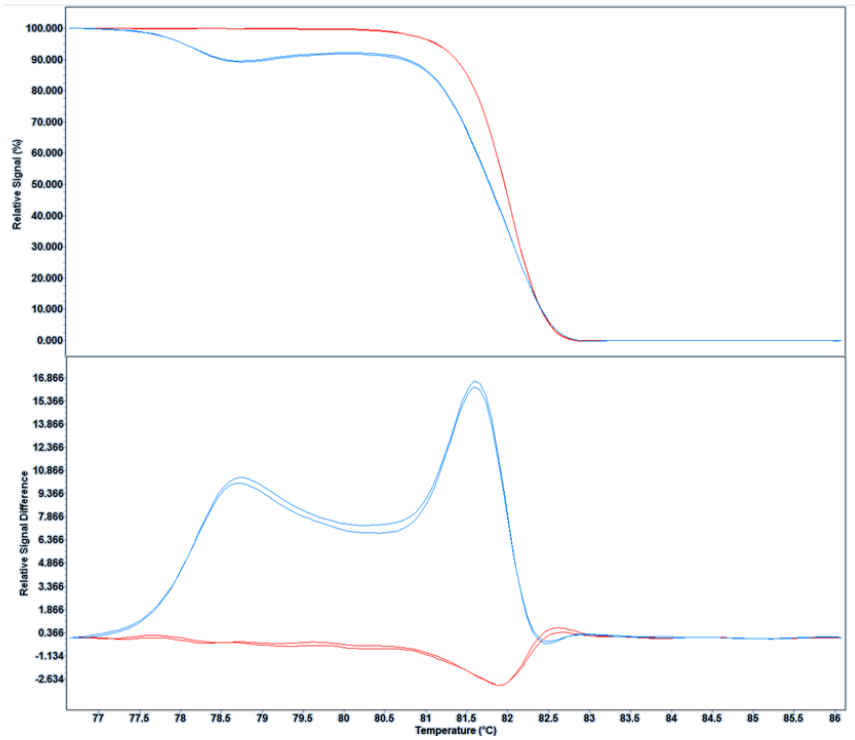
Relative Signal (%)
100.000
90.000
80.000
70.000
60.000
50.000
40.000
30.000
20.000
10.000
0.000
Relative Signal Difference
16.866
15.366
13.866
12.366
10.866
9.366
7.866
6.366
4.866
3.366
1.866
0.366
-1.134
-2.634
77
77.5
78
78.5
79
79.5
80
80.5
81
81.5
82
82.5
83
83.5
84
84.5
85
85.5
86
Temperature (°C)

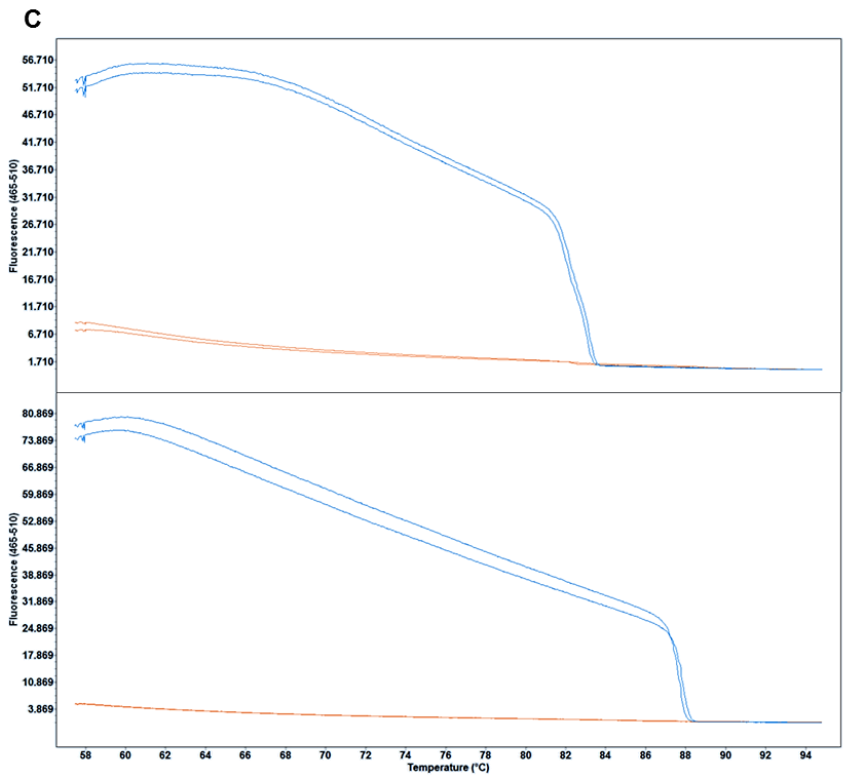

Figure 4.3: High-resolution melting curves of insertion site based polymorphism marker *wri41* and *wri34* and 9K-iSelect array derived markers *wri30* and *wri28*.

Codominant markers ISBP marker *wri34* (A) and 9K-iSelect marker *wri28* (B) above: normalised and shifted melting curves; below: normalised and temperature-shifted difference plot. Dominant markers (C) above: melting curves of ISBP marker *wri41* and below: melting curves of 9K-iSelect marker *wri30*.

Linkage and quantitative trait locus mapping

A total of 59 markers (34 newly developed markers, 22 published KASP™ markers, *AWW622*, *AWW5L7* and a marker that assays a polymorphism in a catalase gene *Cat3-A1* [23]), were added to the existing Excalibur/Kukri linkage map of chromosome 7A (Figure 4.4). The *Cat3-A1* marker and 24 other markers cosegregated with *Lr20*/*Sr15*, *Psy-A1* and 10 previously mapped markers that collocate with the estimated position of the *Rlnn1* QTL as reported in Chapter 3. There were also clusters of three or more cosegregating markers

at 1.1 cM (7 markers), 4.4 cM (11 markers) and 8.2 cM (3 markers) proximal to the large 'terminal cluster'. The position and effect of the *Rlnn1* QTL (LOD - 32; R^2 - 59%; additive effect - 5452) remained consistent with that reported in Chapter 3.

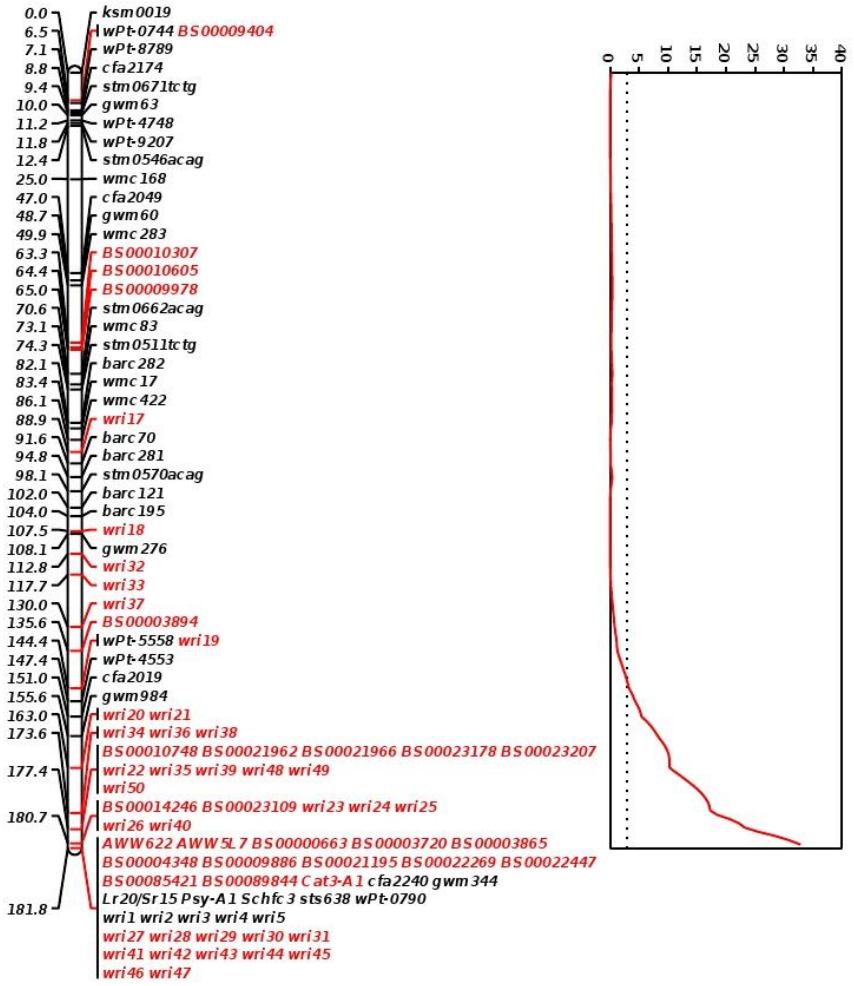

Figure 4.4: Genetic map of chromosome 7A showing *Rlnn1, Lr20, Sr15, Psy-A1, Cat3-A1* and molecular marker loci.

From left to right: a map showing the relative locations of the resistance loci *Lr20* and *Sr15*, the phytoene synthase gene *Psy-A1*, catalase gene *Cat3-A1* and 97 molecular markers mapped on chromosome 7A using a population of Excalibur/Kukri doubled haploid lines; and a graph showing a LOD test-statistic scan from simple interval mapping of resistance against the root lesion nematode *Pratylenchus neglectus* in the Excalibur/Kukri population, with resistance evaluated based upon estimation of the quantity of *P. neglectus* DNA in the roots of inoculated wheat plants as reported in Chapter 3. The newly added 59 molecular markers are coloured in red.

Marker assisted selection and genome specificity

When assayed on a panel of 11 wheat lines known to be moderately resistant to *Rlnn1* and/or carry the resistance loci at *Lr20*/*Sr15* (Aroona, Bindawarra, Bowie, BT-Schomburgk, Wyalkatchem, Cascades, Krichauff, Orion, Thew, Tatiara and Vectis) and 14 wheat lines known to be at least moderately susceptible and not carry the *Rlnn1* resistance allele (AGT Scythe, Annuello, Babbler, Buckley, Calingiri, Chara, Gladius, Hartog, Machete, Sunbri, Sunlin, Sunstate, Sunvale and Yitpi), products from 8 markers (ISBP markers *wri43* and *wri45*; 9K-iSelect array derived markers *wri31*, *wri27*, *wri28* and *wri29*; *AWW5L7* and the *Cat3-A1* marker) were diagnostic. Out of these the HRM-based markers *wri27*, *wri28* and *wri29* can be recommended for the use in MAS of *Rlnn1* (as others were dominant markers), along with the *wri2* and *wri3* markers recommended in Chapter 3.

Results obtained by assaying the new markers from the 'terminal cluster' on a series of nullisomic-tetrasomic stocks indicated that all ISBP markers (*wri41*, *wri42*, *wri43*, *wri44*, *wri45*, *wri46* and *wri47*) and one 9K-iSelect marker (*wri31*) were specific to chromosome 7A. The product amplified from the *Cat3-A1* gene and the smaller-size product from marker *AWW622* were also specific to chromosome 7A.

4.3 Part - B: Is recombination suppressed in the distal end of chromosome 7AL?

4.3.1 Objective

Investigate if the clustering of markers/genes and the *Rlnn1* QTL at the distal end of 7AL is a result of suppressed recombination.

4.3.2 Method

Plant material

The plant material used in this part includes 1988 $F_{4:5}$ recombinant inbred (RI) lines developed from the F_1 generation of a cross between Excalibur and Kukri.

Other mapping populations

Map positions of the markers mapped to chromosome 7A of Avalon/Cadenza linkage map were downloaded from the CerealsDB SNP database [26] and of CPI133872/Janz from the supplementary material of Cavanagh et al. [16]. The map positions of the common markers between the Excalibur/Kukri linkage map and Avalon/Cadenza and/or CPI133872/Janz were compared.

Anchoring molecular markers to the Chinese Spring chromosome 7 syntenic builds

As described in Part A, the molecular markers from the ‘terminal cluster’ were anchored to the Chinese Spring chromosome 7 syntenic builds at the Wheat Genome Database [29] by

a BLASTN query (comparison matrix - BLOSUM62; E-value - 1e-32) using relevant amplicon/contig/EST sequences. The best hit position with a sequence identity of ≥ 97% was considered as the putative anchor position on the Chinese Spring syntenic builds 7A, 7B and 7D.

Screening of Excalibur/Kukri recombinant inbred lines

DNA was extracted from 1988 Excalibur/Kukri RI lines using a method described by Fox et al. [46]. For 863 of these lines, the DNA had already been extracted from bulks of leaf tissue collected from five $F_{4:5}$ plants per line. For, the other 1127 lines, the DNA were extracted from leaf tissue sampled from one F_5 plant. Markers *wri34* and *wri2* were assayed (according to methods described in Appendix 2 (Additional file S2.1) and Appendix 1 (Additional file S1.5) respectively) to identify recombinants between markers *wri34* and *wri2* ('recombinant sub-set') and lines with residual heterozygosity at marker *wri2* for further investigation.

For each line from the 'recombinant sub-set' a new DNA extraction was done using a phenol-chloroform method modified by Pallotta et al. [123] from Rogowsky et al. [144] and the DNA was used to assay 59 molecular markers/gene markers according to the methods described in Appendix 1 (Additional file S1.5) and Appendix 2 (Additional file S2.1). The markers were re-ordered according to the recombination break-points based on a graphical representation of the genotypes. Further a marker *csPSY* that distinguishes between the *Psy-A1* (phytoene synthase) alleles of Excalibur and Kukri [70] was assayed on 1167 of the Excalibur/Kukri RI lines using conditions described in Appendix 1 (Additional file S1.5).

From each line in which residual heterozygosity was detected, four $F_{5:6}$ plants per line were grown to maturity in a glasshouse. Leaf tissue was sampled from each plant at the seedling stage and DNA was extracted using the method described by Fox et al. [46]. Seven codominant markers (*wri34*, *wri22*, *wri23*, *wri24*, *BS0014249*, *BS0004348* and *wri2*) and two dominant markers (*wri40* and *wri41*) were assayed on the progeny lines to identify recombinants, pairs of sibling plants with different alleles at the distal end of 7AL ('sister-lines') and plants with residual heterozygosity at *wri2* (according to methods described in Appendix 1 (Additional file S1.5) and Appendix 2 (Additional file S2.1).

Evaluation of resistance against the root lesion nematode *Pratylenchus neglectus* and the leaf rust pathogen *Puccinia triticina*

Resistance against *P. neglectus* was evaluated according to methods described in Chapter 3 with a slight modification in *P. neglectus* DNA quantified per pot than per plant. That is, the DNA was extracted from both the root and soil as opposed to just the roots in the method described in Chapter 3.

Evaluation of resistance against *P. neglectus* was carried out by the SARDI Root Disease Testing Service, Adelaide [121] in four experimental blocks sown at weekly intervals. Three separate sets of entries were included in this experiment:

a. Set A: 25 F_5-derived pairs of Excalibur/Kukri RI 'sister-lines'.
   In each of the four experimental blocks, each of these pairs was represented by one F_7 plant homozygous for the Excalibur *wri2* allele and (in an adjacent position) one F_7 plant homozygous for the Kukri allele. These pairs of lines were included in order to verify the effect of the *Rlnn1* region.
b. Set B: Excalibur, Kukri, 14 Excalibur/Kukri RI lines (with recombinations between marker cluster 4 and the 'terminal cluster') and 6 Excalibur/Kukri

RI progeny lines (descending from heterozygous plants with recombinations between marker cluster 5 and the 'terminal cluster'). The recombinant RI and RI progeny lines were included to check whether *Rlnn1* was proximal or distal to the recombination breakpoints.

Three plants of each of these lines were allocated to each of the four experiment blocks, providing a total of 12 replicates for these entries. These lines were included to check whether *Rlnn1* was proximal or distal to the recombination breakpoints. Another eight lines (seven DH and one RI) were also included at the same level of replication.

c. Set C: 749 other Excalibur/Kukri RI lines and 39 other Excalibur/Kukri RI progeny lines carrying the Excalibur allele at *wri2*.

   Each line was represented by a single plant in the entire experiment. These plants were included in order to screen a large number of progeny for possible recombination between *Rlnn1* and its linked markers. Only one replicate was included for each line in order to maximise the number of lines that could be screened in the available experimental units. Lines with the Excalibur allele at *wri2* were deliberately chosen as it was anticipated that in a single-plant evaluation, apparently susceptible plants from those lines would be more reliable indicators of recombination than apparently resistant plants from lines with the Kukri allele at *wri2*, because the latter could be plants that had escaped infection.

Subsequently, Excalibur, Kukri, one Excalibur/Kukri DH line, the *Triticale* cultivar Abacus as a resistant check, two pairs of Excalibur/Kukri RI 'sister-lines' and six other Excalibur/Kukri RI lines were re-evaluated with eight plants of each line arranged according to a pre-determined design in a single experimental block (Set D).

Statistical analysis of the data was performed using the AS-Reml package in the R statistical environment [136]. For the replicated set (Set B) a linear mixed model was fitted with *P. neglectus* DNA as the response variable, genotype as a fixed effect, and the various design factors as random effects. These included block, crate, row and column with a separate residual variance for each block. Best linear unbiased estimates (BLUEs) were calculated for each genotype along with the *p*-value from the test of whether each genotype was significantly different to both Excalibur and Kukri. The genotypes in the un-replicated set (Set C) and the replicated set (Sets A and D) were fitted as random effects and hence BLUPs were calculated for each genotype along with the *p*-value from the test of whether each genotype was significantly different to Excalibur.

Evaluation of resistance against *P. triticina* was done on 1283 Excalibur/Kukri lines (including 1207 Excalibur/Kukri RI lines, 17 pairs of Excalibur/Kukri RI 'sister-lines' (8 pairs had to be excluded due to insufficient seed availability) and 42 Excalibur/Kukri RI progeny lines) using methods described by Bariana and McIntosh [8] and under the same conditions that are described in Chapter 3. The infection assessment was done based on the scale described by McIntosh et al. [101].

4.3.3 Results

Other mapping populations

Some of the markers that collocate in the Excalibur/Kukri linkage map have also been assayed on other wheat populations, and were widely separated in the resulting maps. In an Avalon/Cadenza map (CerealDB SNP database [26]), markers span a genetic distance of 6.5 cM, while in CPI133872/Janz (supplementary material of Cavanagh et al. [16]) markers span a genetic distance of 28.5 cM (Figure 4.5)

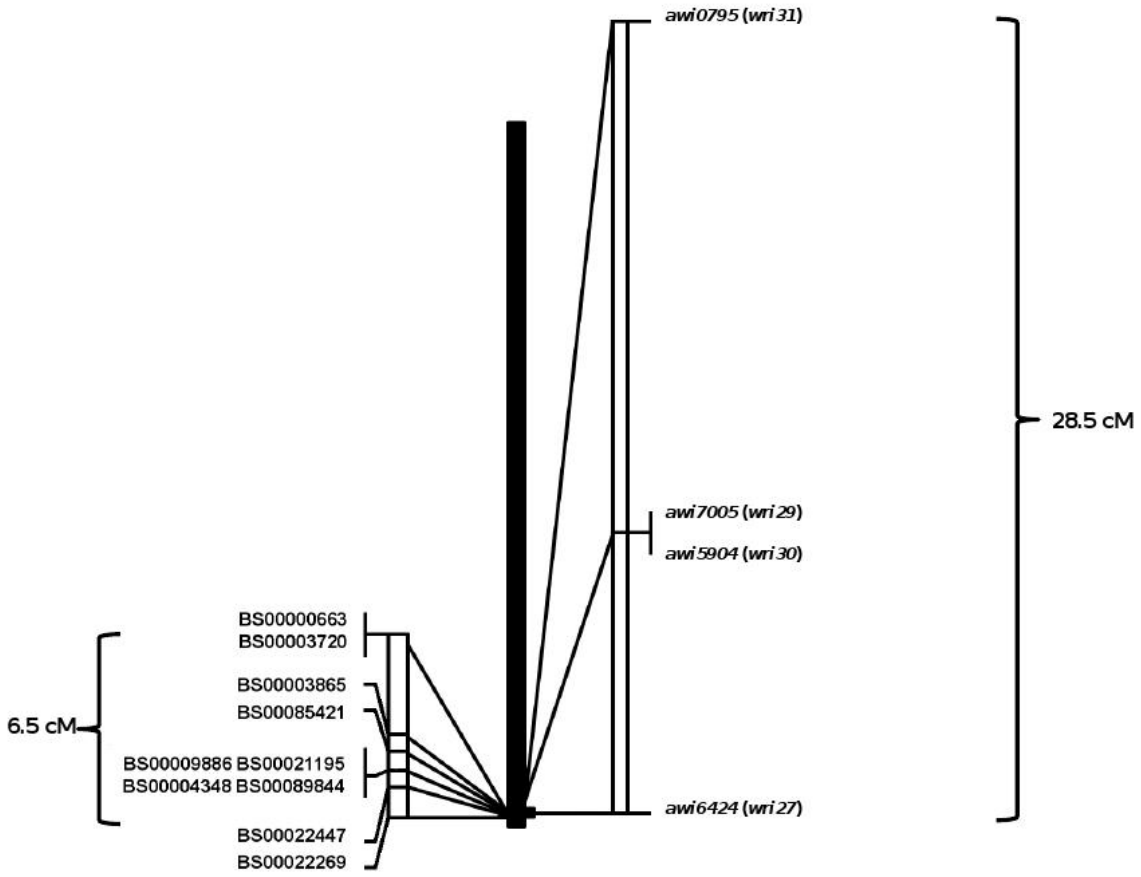

Figure 4.5: Schematic representation of the map positions of common markers between Excalibur/Kukri and other published linkage maps.

Comparison between Excalibur/Kukri and Avalon/Cadenza [6] linkage maps (Left) and Excalibur/Kukri and CPI133872/Janz [16] linkage maps (right).

Anchoring markers to the Chinese Spring chromosome 7 syntenic builds

Some of the markers could be anchored onto short-read genomic sequence syntenic builds of one, two or all three Chinese Spring group-7 chromosomes at the Wheat Genome Database [29, 85]. Markers that could be anchored to a syntenic build with at least 97% sequence identity and E-value ≤ 1e-33 spanned estimated physical distances of 0.9 Mb on 7A_SynBuild_v2.0, 0.3 Mb on 7B_SynBuild_v2.0 and 0.3 Mb on 7D_SynBuild_v2.0 (Figure 4.6; Appendix 2 - Additional file S2.2: Table S2.2 to S2.4).

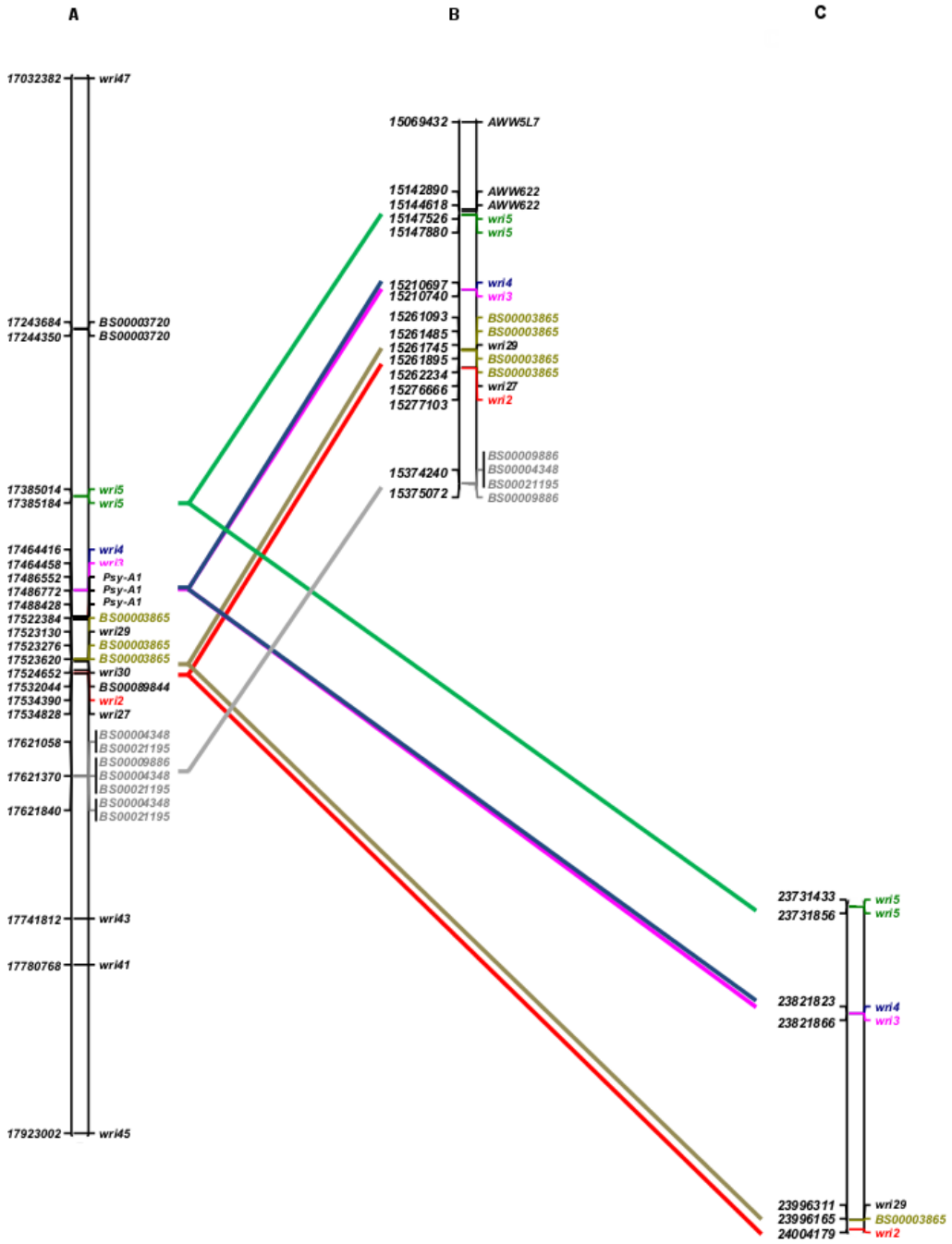

Figure 4.6: A graphical illustration of the anchored positions of markers from the 'terminal cluster' on the Chinese Spring syntenic builds 7A (A), 7B (B) and 7D (C).

The homoeologous marker positions between the builds are connected with lines coloured to correspond to the marker or marker cluster. Numbers on the left-hand side of the vertical bars represent the BLAST hit start position on the syntenic builds.

Identification of recombinant progeny and reordering markers

A large set of Excalibur/Kukri RI lines that had already been developed by the Australian Centre for Plant Functional Genomics provided a genetic resource to screen for additional informative recombinants.

Among 1934 Excalibur/Kukri RI lines with unambiguous genotypic calls for both *wri2* (from the 'terminal cluster') and *wri34* (which mapped 8.2 cM proximal to that cluster), 194 were identified as carrying recombinations between *wri2* and *wri34*. When 56 molecular markers that mapped at the distal end of 7AL were assayed on this 'recombinant subset', some of the markers that were collocated in the Excalibur/Kukri DH linkage map (Figure 4.4) could be separated and ordered based on recombination break-points (Figure 4.7; Appendix 2 – Additional file S2.3: Table S2.5). However, even in the 'recombinant subset', *Lr20*/*Sr15*, *Cat3-A1*, *Psy-A1* and 34 markers co-segregated.

When 94 lines from the 'recombinant sub-set' with the Excalibur allele at *wri2* were evaluated for resistance against *P. neglectus* using single plants, only two had estimates of *P. neglectus* DNA/pot that differed significantly from the corresponding estimate for Excalibur ($p < 0.05$; Figure 4.8). The lines were selected from 194 lines found to be recombinant between markers *wri2* and *wri34* known as the 'recombinant sub-set'.

Similarly, when individual plants from another 626 Excalibur/Kukri RI lines with the Excalibur allele at *wri2* were assessed for resistance against *P. neglectus,* only 13 lines differed significantly from Excalibur (Figure 4.9). Among the 39 Excalibur/Kukri recombinant inbred line progeny none differed significantly from Excalibur ($p < 0.05$; data not shown).

These numbers are less than would be expected by chance (5 % of 94 = 4.7; 5 % of 626 = 31.3). For six of these apparently susceptible lines, there was sufficient seed available to

permit re-evaluation in a replicated experiment. In that experiment, all six lines had estimated amounts of *P. neglectus* DNA/pot that were significantly lower than that of Kukri and very similar to that of Excalibur (Figure 4.10), making it unlikely that these lines actually carry recombinations between *wri2* and *Rlnn1*.

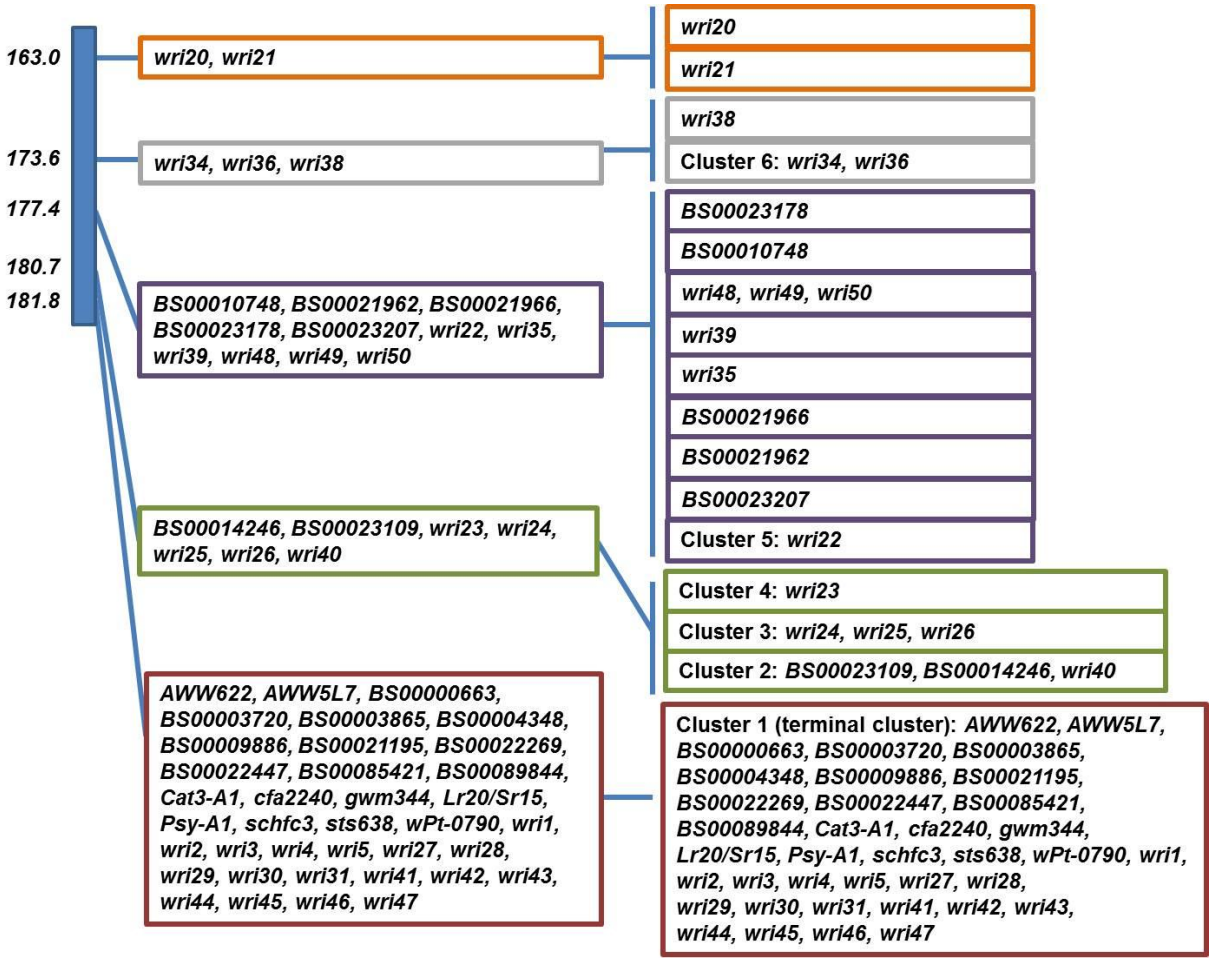

Figure 4.7: A graphical representation of the separation and re-ordering of molecular markers from the distal-end of chromosome 7AL.

Schematic representation of the marker positions in the distal end of chromosome 7AL in cM (left), marker clusters with 182 Excalibur/Kukri DH mapping population (middle), and separation and ordering of markers/marker clusters using the 194 Excalibur/Kukri RI lines in the 'recombination sub-set' and the recombinants identified among the progeny of heterozygous lines at *wri2* (right).

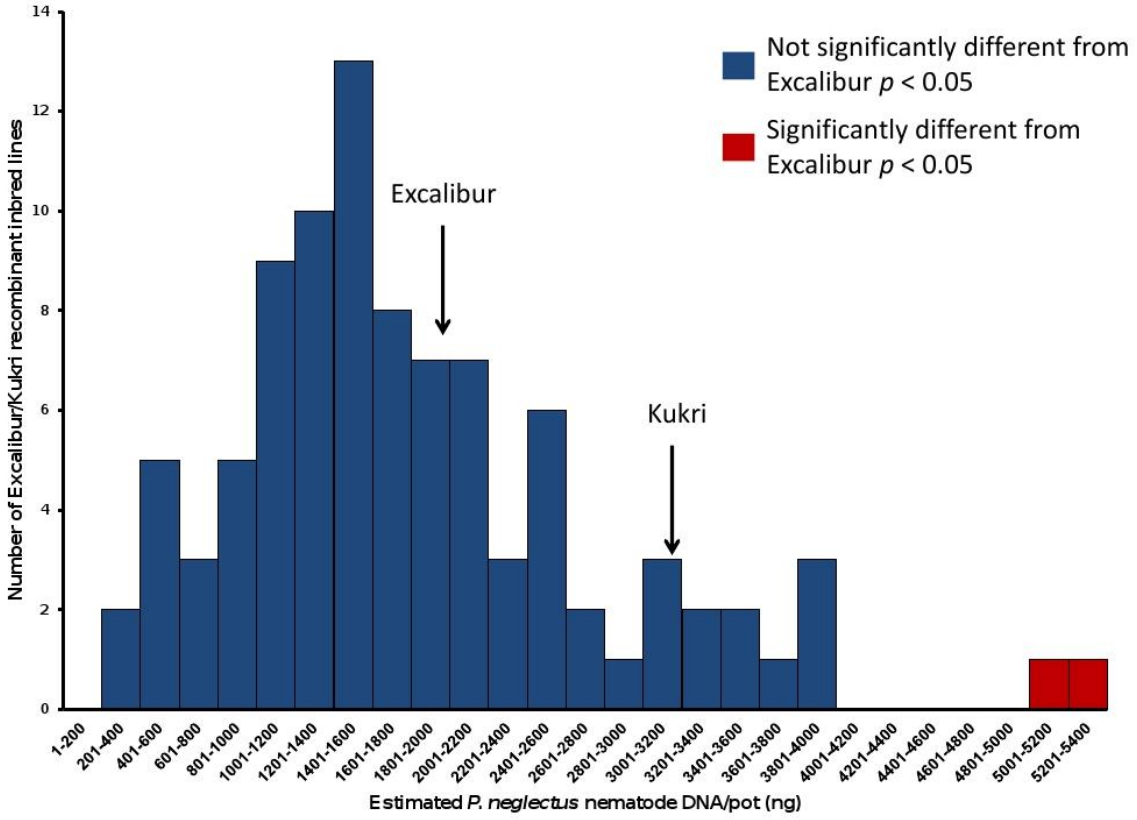

Figure 4.8: Frequency histogram showing the distribution of 94 Excalibur/Kukri recombinant lines carrying the Excalibur allele at the marker *wri2*.

The lines, which were selected from a 'recombinant sub-set' of 194 lines with recombination between markers *wri2* and *wri34*, were assayed using single plants. The parents Excalibur and Kukri were assayed with 12 replicates each.

Among 1934 Excalibur/Kukri RI lines assayed with marker *wri2*, residual heterozygosity was detected in only 104 lines (5%). From 72 of these, it was possible to isolate individual F_5 plants that were heterozygous at *wri2*. When nine molecular markers that flank recombination break-points (Figure 4.7; Appendix 2 (Additional file S2.3: Table S2.5); cluster 6: *wri34*, cluster 5: *wri22*, cluster 4: *wri23*, cluster 3: *wri24*, cluster 2: *BS0014246* and *wri40*, terminal cluster: *BS0004348*, *wri41* and *wri2*) were assayed on selfed progeny (four plants each) of the 72 heterozygous F_5 plants, 25 pairs (referred to as the 'sister-lines'), 32 additional recombinants (including 12 of the lines identified as 'sister-lines')

and 77 RI lines with residual heterozygosity at *wri2* were identified. The resulting order of the 9 markers evaluated on the 32 additional recombinants was consistent (with no changes or improvement) with the order shown in Figure 4.7 and Appendix 2 (Additional file S2.3: Table S2.5).

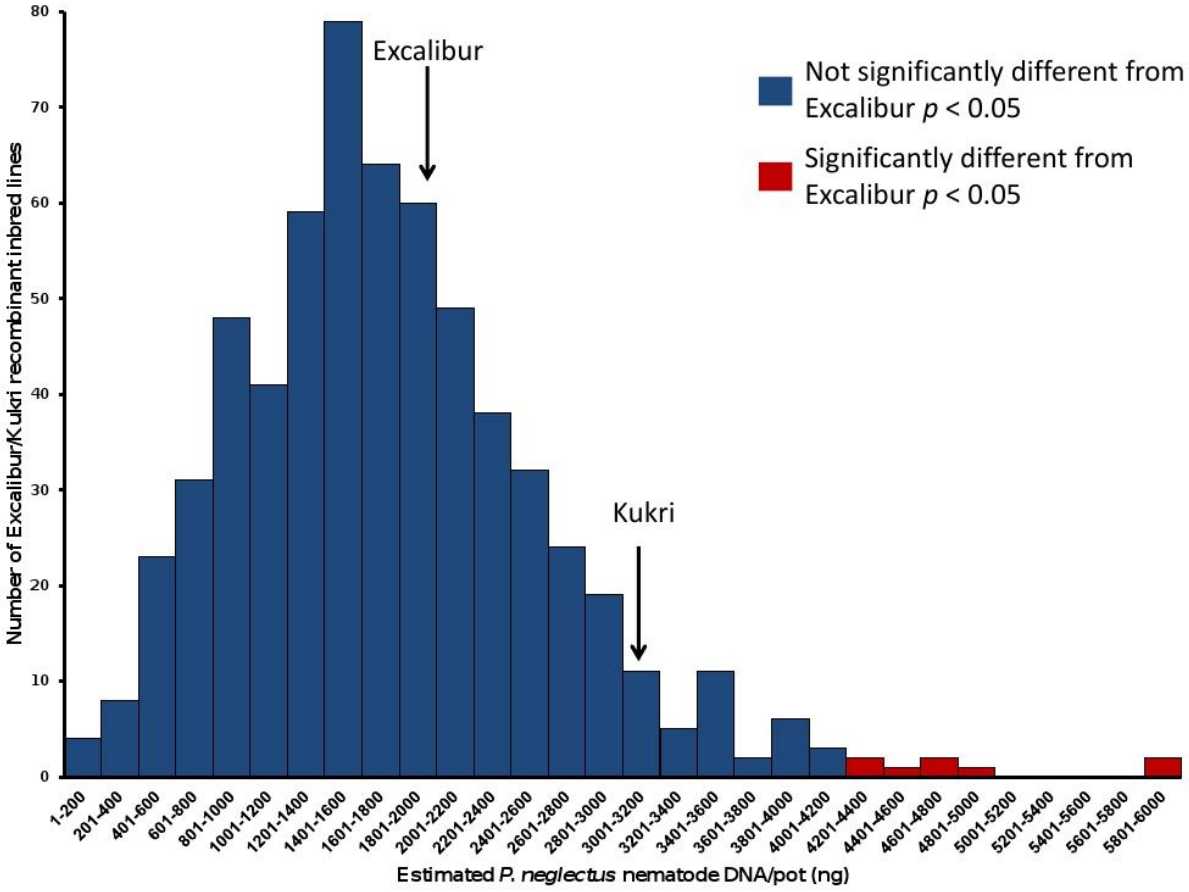

Figure 4.9: Frequency histogram showing the distribution of 626 Excalibur/Kukri recombinant inbred lines carrying Excalibur allele at the marker *wri2.*

The Excalibur/Kukri RI lines were assayed as single plants. The parents Excalibur and Kukri were assayed with 12 replicates each.

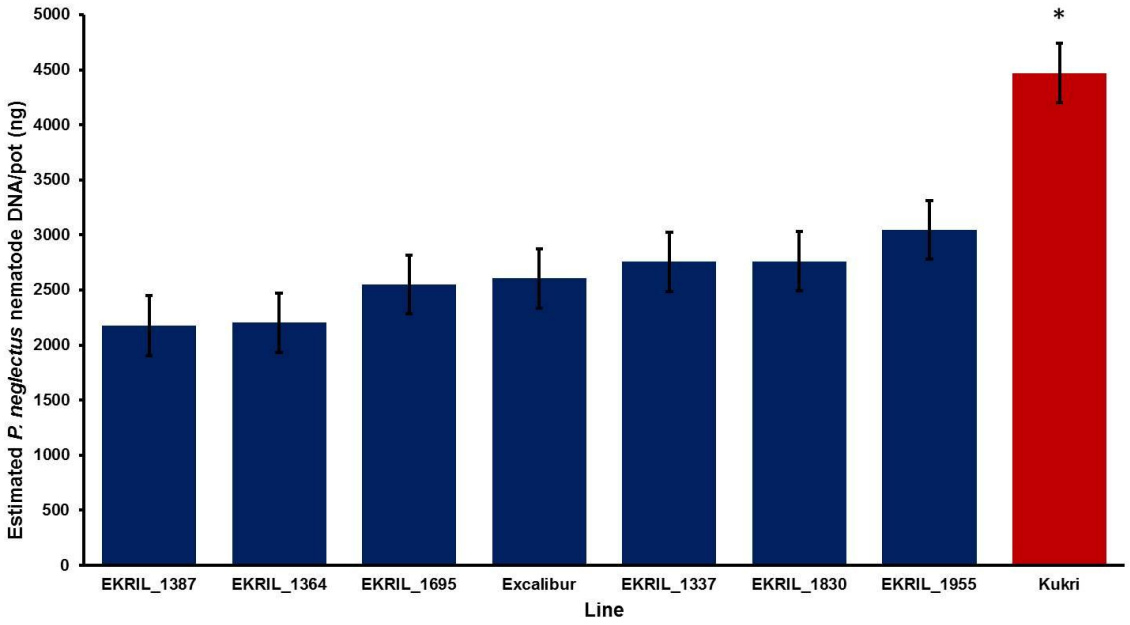

Figure 4.10: Re-evaluation of *P. neglectus* DNA/pot in Excalibur, Kukri and six Excalibur/Kukri recombinant inbred lines carrying Excalibur allele at the marker *wri2.*

The lines were assayed using eight replicates. The standard deviation of each line is shown by whiskers. * The best linear unbiased prediction for Kukri was significantly different from Excalibur ($p < 0.05$).

Six of these RI progeny lines (from additional recombinants) and 14 RI lines ('recombinant sub-set'), all with recombinant haplotypes across the most distal marker clusters (the terminal cluster and clusters 2, 3, 4 and 5 in Figure 4.7 and Appendix 2 (Additional file S2.3: Table S2.5), were evaluated for resistance against *P. neglectus*. None of the lines carrying the Excalibur allele at *wri2* had a significantly higher estimated *P. neglectus* nematode DNA amount than Excalibur (Figure 4.11), while all the lines carrying a Kukri allele at *wri2* were significantly different from Excalibur. Thus this replicated

assay confirmed the close association of the terminal cluster marker *wri2* with resistance against *P. neglectus* and did not identify any lines recombinant between *wri2* and *Rlnn1*.

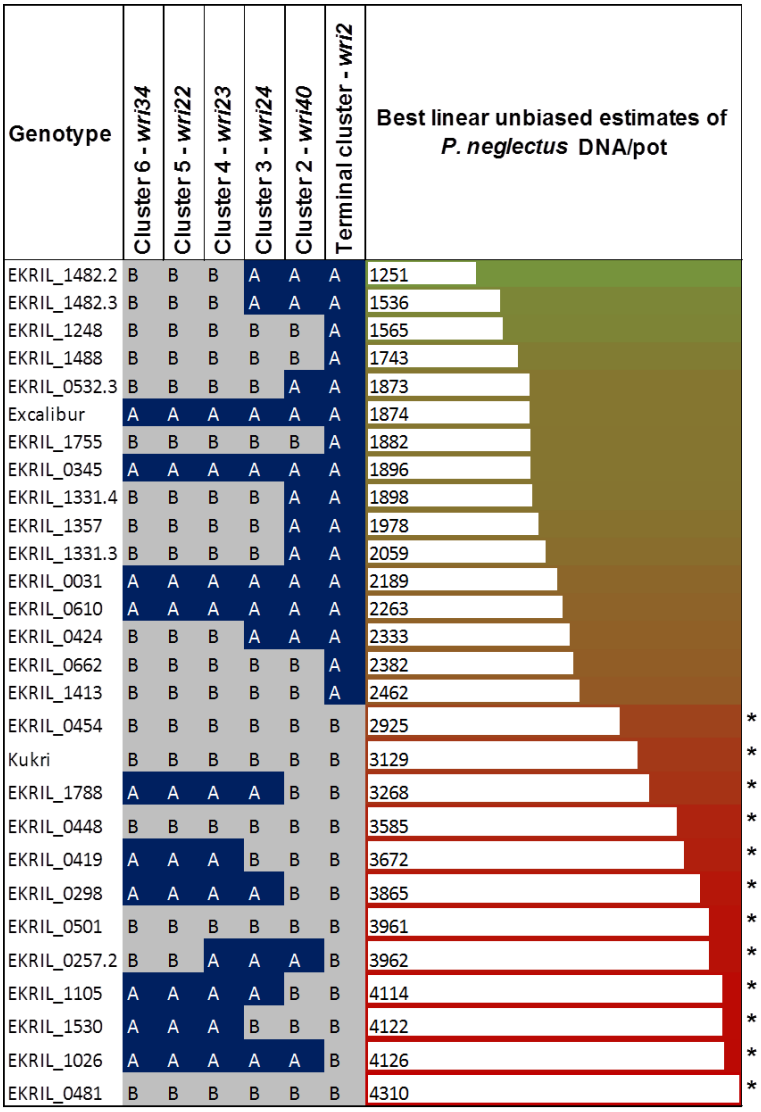

Figure 4.11: Best linear unbiased estimates of *P. neglectus* DNA/pot of Excalibur, Kukri and 14 Excalibur/Kukri recombinant lines and 6 Excalibur/Kukri recombinant inbred line progeny carrying informative recombinations at the distal end of 7AL.

The lines were selected from 194 lines found to be recombinant between markers *wri2* and *wri34* known as the 'recombinant sub-set' and the 32 recombinant progeny of heterozygous lines. The genotypic data is given for each line for markers assayed from 'terminal cluster' through to the cluster 5. The lines that are significantly different from Excalibur at $p < 0.05$ are indicated with an asterisk.

The 25 pairs of 'sister-lines' presented an additional opportunity to evaluate the effects of the *Rlnn1* region on resistance against *P. neglectus*. In 23 pairs, the line carrying the Excalibur allele at *wri2* had lower *P. neglectus* DNA/pot than its sister-line carrying the Kukri allele (Figure 4.12). Two pairs (pair 12 and pair 16) exhibited the opposite result, but when they were re-tested, the new test results were in agreement with the rest of the 'sister-pairs' (data not shown). When 17 pairs of 'sister-lines' were evaluated for rust resistance (*P. triticina*), no recombination was observed between *Lr20* and the marker *wri2*.

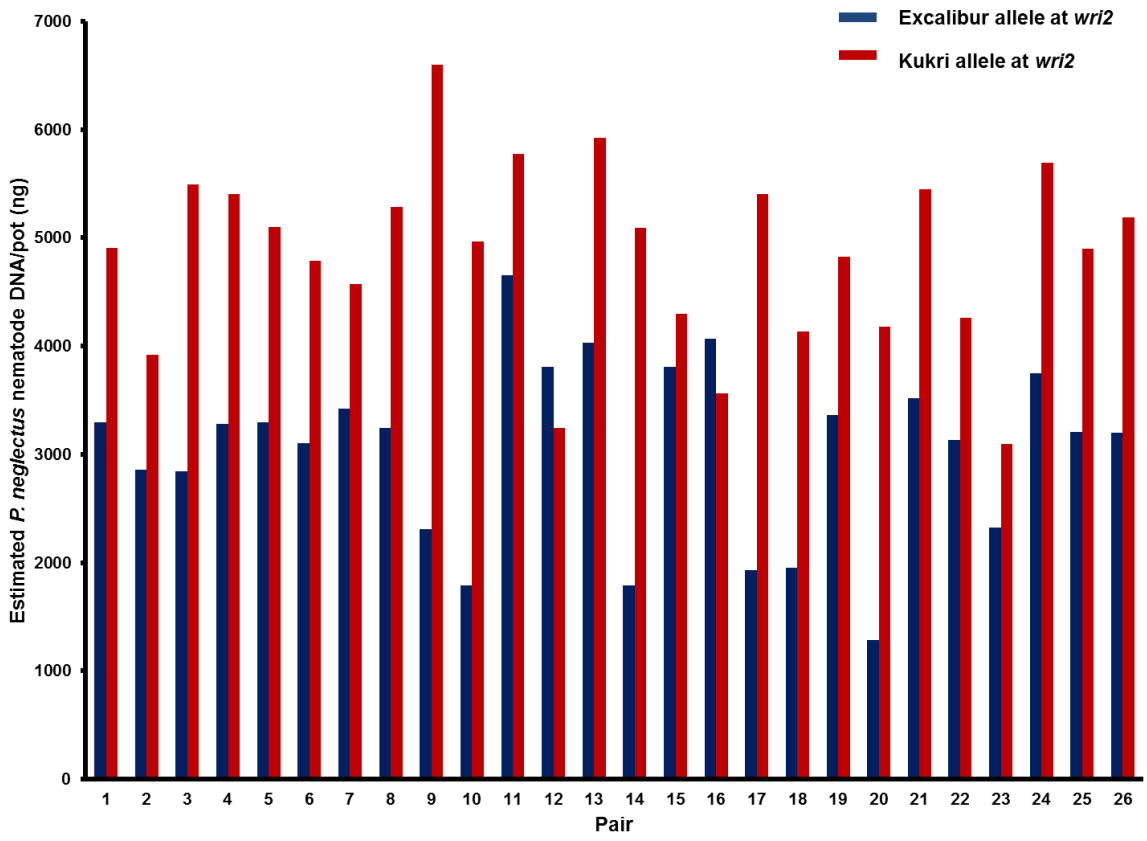

Figure 4.12: Estimated *P. neglectus* nematode DNA/pot in Excalibur, Kukri and 25 pairs of Excalibur/Kukri recombinant inbred 'sister-lines'.

The 'sister-lines' (pairs 1-25) are pairs of sibling plants with different alleles at marker *wri2* and a similar/opposite haplotype at the rest of the *Rlnn1* region. Excalibur (blue) and Kukri (red) are presented as pair 26.

4.4 Part - C: What causes the suppressed recombination?

4.4.1 Objective

Investigate the cause of suppressed recombination at the distal end of chromosome 7AL.

4.4.2 Method

Plant materials

The materials used in this part includes the wheat cultivars Schomburgk and Raven sourced from the Australian Winter Cereals Collection, accession AEG357-4 of *Ae. speltoides* provided by The Harold and Adele Lieberman Germplasm Bank, Tel Aviv, Israel courtesy of Dr Jacob Manisterski.

Partial sequencing of the *Psy-A1* allele of Schomburgk

In order to verify the *Psy-A1* allele carried by the cultivar Schomburgk, the region was re-sequenced using the primer pair *PSY7A5_F/R* [24], where a region of the gene *Psy-A1* was amplified from genomic DNA of the cultivar Schomburgk according to the methods described in Appendix 1 (Additional file S1.5). The resulting sequence was aligned to the *Psy-A1t* allele sequence of the breeding line WAWHT2074 [GenBank:HM006895] [24] and the previously reported *Psy-A1s* allele sequence of the cultivar Schomburgk [GenBank:EU649795] [70] using the multiple align module implemented in Geneious® v6.0.4 (Biomatters Ltd., New Zealand) with default settings (global alignment with free

end gaps, the 65% similarity (5.0/-4.0) cost matrix, a gap open penalty of 12, a gap extension penalty of 3 and two refinement iterations).

Phylogenetic analysis of *Psy1* gene alleles

A BLASTN search using the *Psy-A1t* allele sequence [GenBank:HM006895] as the query was used to retrieve genomic sequences of *Triticum* and *Aegilops Psy1* alleles from NCBI [112]. The retrieved genomic sequences (except the one for *Psy-A1s*) were aligned in Geneious® v6.0.4 (Biomatters Ltd., New Zealand) using the multiple alignment feature (with the default settings mentioned above). An ungapped sequence alignment was generated using the conserved block module of SeqFire [2], with a 1% accepted gap and default settings for the amino acid conservation threshold (75%), the amino acid substitution group (none), the minimum size of conserved block (3) and the maximum size of non-conserved block (3). A maximum likelihood inference of the phylogeny was done using RAxML v7.2.6 [173] with *Thinopyrum ponticum* [GenBank:EU096095] as the out-group (following Crawford et al. [24]), a general-time-reversible (GTR) substitution model and 200 maximum likelihood searches with node support estimated using 1000 bootstrap searches.

Fluorescent *in-situ* hybridisation

Fluorescent *in-situ* hybridisation (FISH) was carried out on root samples obtained from Excalibur and Kukri cultivars according to the method described by Zhang et al. [205], using the BAC clone 676D4 with repetitive sequences specific to A genome (red, labeled with rhodamine-dUTP) and BAC clone 9M13 with repetitive sequences specific to D

genome (green, labeled with biotin-dUTP and detected with FITC avidin). The cells were counterstained with DAPI (blue).

Partial sequencing of an *AWW5L7* amplicon from Excalibur and Raven

In order to investigate the origin of the fragment amplified from the primer pair *AWW5L7-Left3/Right* [152], products were amplified from the cultivars Excalibur and Raven using conditions given in Appendix 2 (Additional file S2.1). The PCR product was gel-extracted and cleaned up using NucleoSpin® Gel and polymerase chain reaction clean-up kit (MACHEREY-NAGEL GmbH & Co. KG, Germany). Sequencing was carried out at Australian Genome Research Facility Ltd., Australia by capillary separation on an Applied Biosystems 3730xl DNA analyzer (Applied Biosystems, CA, USA). The sequences obtained were aligned with an *AWW5L7* Halberd sequence [GenBank:BV693737] with the multiple align module implemented in Geneious® v6.0.4 (Biomatters Ltd, New Zealand) with default settings (global alignment with free end gaps, the 65% similarity (5.0/-4.0) cost matrix, a gap open penalty of 12, a gap extension penalty of 3 and two refinement iterations). The sequence of the Excalibur product was used as a query in a BLAST search against all nucleotide collections using a program optimised for 'somewhat similar sequences' (BLASTN) and other parameters set to default at the NCBI BLAST portal [112], and against the International Wheat Genome Sequencing Consortium (IWGSC [22]) and other *Triticeae* shot-gun assemblies (IWGC), using an in-house BLAST portal at the Australian Centre for Plant Functional Genomics, Australia with an E-value threshold set to 1e-5. Further, BLAST searches were performed against the BAC libraries of chromosome 7A and 7B (kindly conducted by Gabriel Keeble-Gagnère, Murdoch University, Australia and Simen Rød Sandve, Norwegian University of Life Sciences, Norway).

4.4.3 Results

Phylogenetic analysis of *Psy1* alleles

Phylogenetic analyses of *Psy1* alleles by Wang et al. [187] and Crawford et al. [24] provided opportunities to understand the evolution of *Psy1* alleles, but neither of these analyses include all of the *Psy1* alleles for which sequences are now available.

Out of the best 100 returned hits from a BLASTN search using the *Psy-A1t* allele sequence [GenBank:HM006895] against NCBI databases [112] 59 *Psy1* alleles from *Triticum* and *Aegilops* and one *Psy-E1* sequence from *Thinopyrum ponticum* was retrieved.

Given conflicting reports [24, 70] about the *Psy-A1* allele carried by the cultivar Schomburgk, a 793-bp portion of *Psy-A1* was sequenced from Schomburgk. Comparison of the sequence obtained with the sequences reported for *Psy-A1s* [GenBank:EU649795] [70] and *Psy-A1t* [GenBank:HM006895] [24] alleles revealed that Schomburgk carries the *Psy-A1t* allele (Figure 4.13). It was concluded that the original sequence reported for the *Psy-A1s* allele had a single-base sequencing error (at 409 bp; Figure 4.13), so *Psy-A1s* was excluded from further analysis.

In a maximum likelihood phylogeny using an ungapped 1864-nucleotide sequence, the 59 *Psy1* alleles formed four strongly supported (bootstrap support (BS) >70) monophyletic clades: (1) an 'A-genome clade': containing alleles *g* and *f* from A^u (*Triticum urartu*), *a, b, c, e, k, n, p, q,* and *r* from *T. aestivum* and *a, d, e, k, l* and *m* from *T. turgidum*; (2) a 'B-genome clade': containing alleles *a, b, c, d, e* and *m* from *T. aestivum* and *a, e, f, g, h, i, j, k, l* and *m* from *T. turgidum*; (3) a 'D-genome clade': containing *a, e, f, g, k, l* and *m* from *T. aestivum* and *b, c, d, h, i* and *j* from *Aegilops tauschii*; and (4) a 'mixed clade': containing *Psy1* alleles from the A genome (*t* from *T. aestivum* and *o* from *T. turgidum*), B genome (*c, m* and *d* from *T. aestivum* and *m* and *k* from *T. turgidum*), A^m genome (*h, i* and *j*

from *T. monococcum*) and S genome (*a*, *b* and *c* from *Ae. speltoides*) (Figure 4.14; Appendix 2 – Additional file S2.4: Figure S2.1 and Table S2.6). The 'mixed clade' consists of two distinct subclades (BS >70; Figure 4.14; Appendix 2 – Additional file S2.4: Figure S2.1 and Table S2.6). One consists of the three A^m-genome alleles and one A genome allele from *T. turgidum*. The other consists of three S-genome alleles from *Ae. speltoides*, five B-genome alleles (3 from *T. aestivum* and 2 from *T. turgidum*) and the *Psy-A1t* allele. Within the latter subclade, the *Psy-A1t* allele showed a basal relationship to all of the S-genome and B-genome alleles (Figure 4.14; Appendix 2 – Additional file S2.4: Figure S2.1 and Table S2.6). Within an ungapped sequence alignment of the sequences from the 'mixed clade' (Appendix 2 – Additional file S2.4: Figure S2.2), there are 191 SNPs, of which 16 distinguish the *Psy-A1t* allele from the other members of the clade. The sequence identity between *Psy-A1t* allele and the other alleles in the 'mixed clade' ranges between 95 and 97%, compared to only 92, 93 and 93% between *Psy-A1t* and the 'A-genome', 'B-genome' and 'D-genome' clades, respectively.

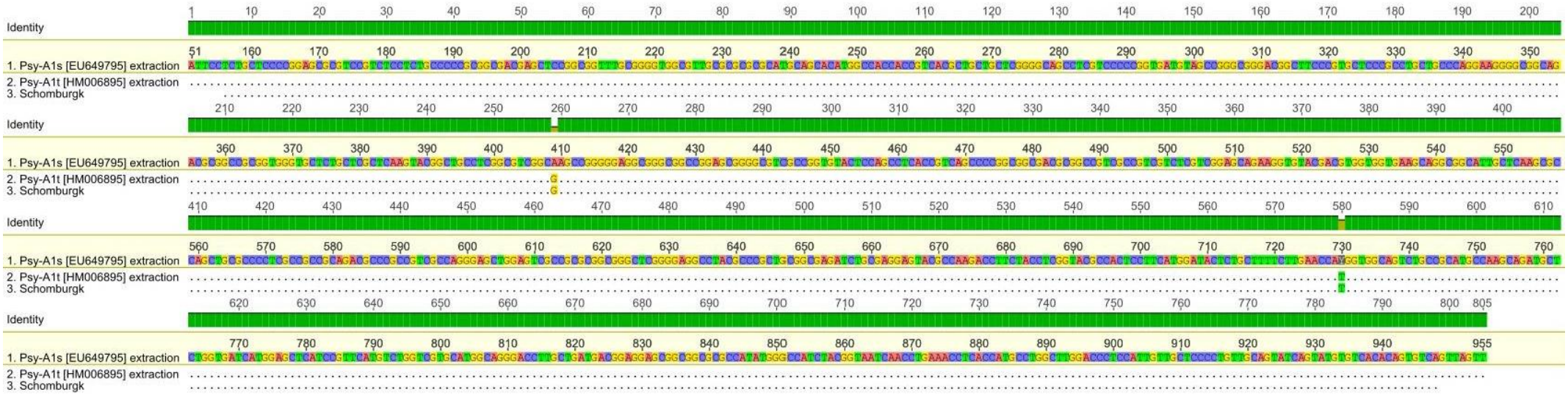

Figure 4.13: Alignment of sequences of *PSY7A5_F/R* amplicons from cultivar Schomburgk to an extraction of the *Psy-A1t* allele sequence of the breeding line WAWHT2074 [GenBank:HM006895] and the *Psy-A1s* allele sequence of the cultivar Schomburgk [GenBank:EU649795].

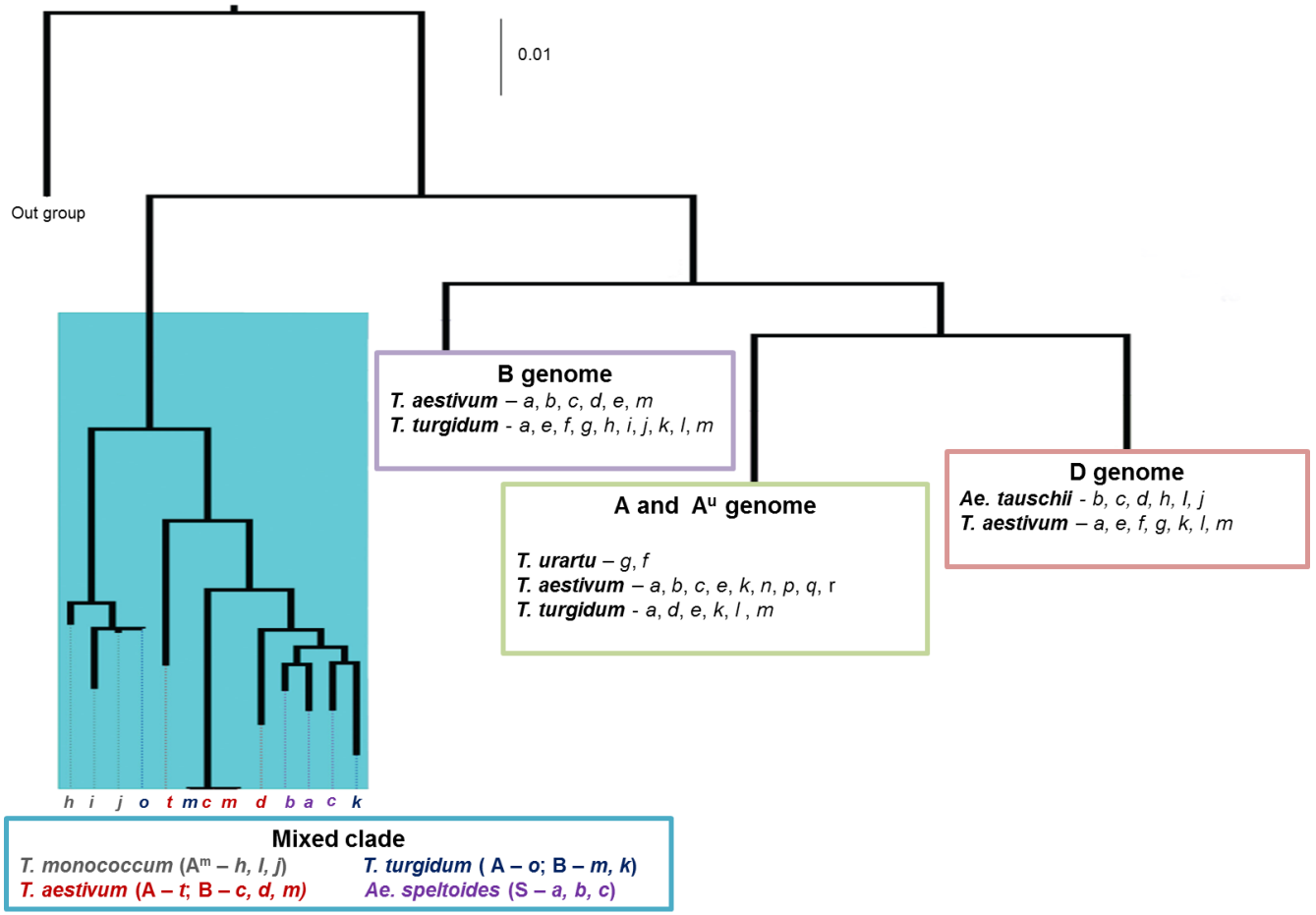

Figure 4.14: An illustration of the gene tree of *Psy1* alleles of wheat and related species

Unique amplification patterns in markers

Among the dominant markers mapped in the 'terminal cluster', all ISBP markers, two 9K-iSelect markers (*wri30* and *wri31*), the DArT marker *wPt-790*, one EST-based marker (*wri3*) and the *Cat3-A1* gene amplified products from Kukri but not from Excalibur. Most of these markers were derived from Chinese Spring sequences. Conversely, the markers *sts638*, *schfc3* and *AWW5L7* amplified products from Excalibur that were not amplified from Kukri. The markers *sts638* and *schfc3* were derived from sequences from cultivars known to carrying the *Lr20* and/or *Pm1* resistance alleles and carrying the '*t*' allele at *Psy-A1* gene. Other markers seemed to amplify products from both Excalibur and Kukri, and the two gel-based markers *wri2* and *Psy-A1* amplified longer products from Excalibur than from Kukri. In contrast to what was observed for markers in the 'terminal cluster', markers that were derived from Chinese Spring sequences and that mapped elsewhere on chromosome 7A did amplify products from Excalibur.

The longer product of marker *AWW5L7*

For the marker *AWW5L7*, a product similar to the 877-bp amplicon from Cranbrook was amplified from both Excalibur and Kukri. In addition, a longer product was amplified from Excalibur. This product provided a presence/absence polymorphism that was mapped to the 'terminal cluster' of 7AL in the Excalibur/Kukri linkage map (Figure 4.4). When the *AWW5L7* marker was assayed on 11 other cultivars (Aroona, Bindawara, Bowie, Wyalkatchem, Cascades, Orion, Thew, Tatiara, Vectis, Krichauff and BT-Schomburgk) that are thought to carry the resistance allele at the *Rlnn1* QTL, they all exhibited the longer product that had been observed in Excalibur. Two of the cultivars (Krichauff and BT-Schomburgk, both of which have Halberd in their ancestry) also exhibited the 956-bp 'Halberd' product.

Sequencing of the longer amplicon from Excalibur (Appendix 2 - Additional file S2.5) and from Raven (an ancestor common to some of the lines that are moderately resistant to RLN) provided identical partial sequences (Figure 4.15). Alignment of these sequences with the Halberd *AWW5L7* amplicon sequence [GenBank:BV693737] revealed SNPs at 41 sites and a series of insertion/deletion polymorphisms that range in length from 1 to 34 nucleotides and result in a net 78-bp length polymorphism between Halberd and Excalibur (Figure 4.15).

Figure 4.15: Alignment of trimmed partial sequence of *AWW5L7-Left3/Right* from cultivar Excalibur and Raven to the *AWW5L7-Left3/Right* sequence of cultivar Halberd [Genbank:BV693737]

When the sequence from Excalibur (Appendix 2 - Additional file S2.5) was used in a BLASTN query against the NCBI [112] nucleotide collection, the best hits were to a barley (*Hordeum vulgare*) catalase 1 (*Cat1*) gene [GenBank:AF021938] with a sequence identity of just 88% (E-value 0.0; query coverage 100%). The sequence did not retrieve any significant hits from the IWGSC survey sequences (identity ≥ 99%; [22]), *Triticeae* shot-gun sequence assemblies of *T. turgidum* ssp. *durum, Ae. speltoides, Ae. tauschii, Aegilops sharonensis, T. monococcum and T. urartu* (identity ≥ 95%), chromosome-7A BAC library assemblies (Gabriel Keeble, personal communication) or chromosome-7B BAC library assemblies (Simen Rød Sandve, personal communication; 93% identity).

FISH imaging

In the FISH image the A genome is stained in red fluorescence, the D genome is stained in green fluorescence (Figure 4.16A and C). With counterstaining, the A genome is visible in pink, the D genome in turquoise blue and unstained double stranded DNA that includes the B genome in blue (Figure 4.16B and D). Chromosomes with an A-B translocation would therefore be red with an unstained telomere (Figures 4.16A and C) and, with counterstaining, a purple chromosome with a blue telomere (Figure 4.16B and D).

Two chromosomes with putative A-B translocations at both ends (T5 and T6 in Figure 4.16A and B, T3 and T4 in Figure 4.16C and D) were observed in each cultivar. In addition, chromosomes with possible terminal A-B translocations were observed: two in Kukri (Figure 4.16C and D; T1 and T2) and four in Excalibur (Figure 4.16A and B; T1 to T4).

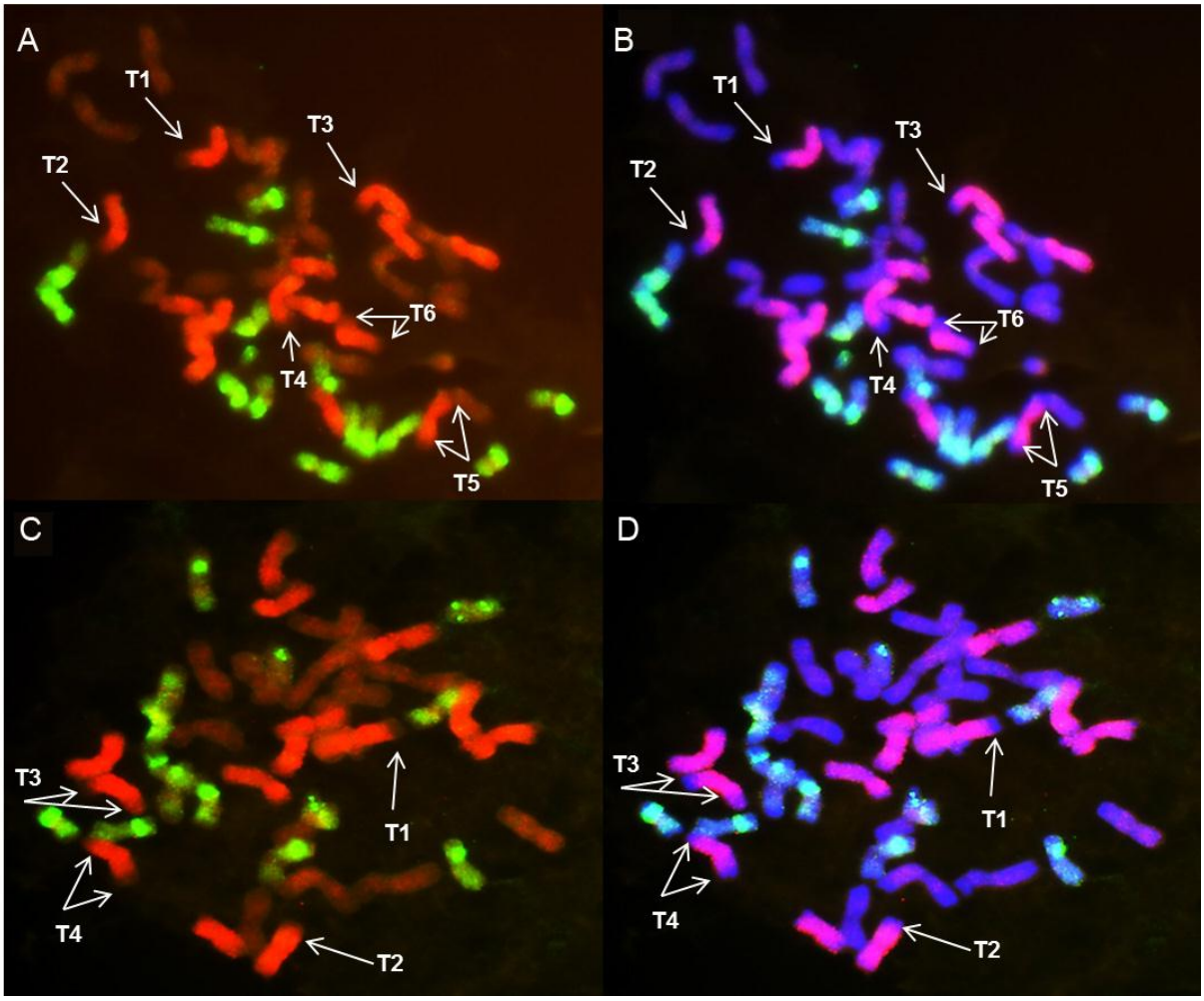

Figure 4.16: Fluorescence *in-situ* hybridization in Excalibur and Kukri.

(A) Excalibur initial stain of A genome (red), D genome (green) and the unstained B genome is in brown; (B) Excalibur counterstain of A genome (purple) and D genome (turquoise) and the counterstain of B genome and other doubled stranded DNA is in blue; (C) Kukri initial stain of A genome (red), D genome (green) and the unstained B genome is in brown; (D) Kukri counterstain of A genome (purple) and D genome (turquoise) and the counterstain of B genome and other doubled stranded DNA is in blue; The putative translocations are indicated by the letter 'T'.

4.5 Discussion

In cultivars that carry the phytoene synthase *Psy-A1t* allele, *Rlnn1* resistance against *P. neglectus* and *Lr20*/*Sr15* resistance against rust pathogens, recombination seems to be

suppressed in the distal region of 7AL. This chapter presents new evidence that supports the hypothesis of suppressed recombination at the distal end of 7AL and examines possible genetic phenomena that led to it.

This work improved the Excalibur/Kukri chromosome 7A linkage map relative to the one presented in Chapter 3, by adding a total of 59 molecular markers (Figure 4.4). Of these, 49 markers were mapped distal to the SSR marker *gwm984*: 2 at 163.0 cM, 3 at 173.6 cM, 11 at 177.4 cM, 7 at 180.7 cM, and 26 at 181.8 cM (collocating with the 'terminal cluster' in Chapter 3). Thus, the earlier interval of 23.7 cM between the marker *gwm984* and the 'terminal cluster' was split in to several smaller intervals with each interval not more than 10 cM. No new markers mapped distal to the 'terminal cluster' (181.8 cM), which now consists of 36 molecular markers and the rust resistance gene(s) *Lr20/Sr15* and coincides with the estimated position of *Rlnn1* (Figure 4.4).

The high cost of phenotyping for resistance against *P. neglectus* makes it a suitable trait for MAS. For a marker to be useful in MAS, the allele associated with resistance should be detected in all materials but not in any susceptible materials. Such a marker is considered as a diagnostic marker. For a marker to be used effectively in MAS, it should ideally be codominant, so that it can identify heterozygous individuals. The current research identified several apparently diagnostic HRM-based markers, including three codominant markers (*wri27*, *wri28* and *wri29*) that seem suitable for MAS.

The targeted approach taken here involved actively selecting markers that had previously been mapped to the distal end of 7AL in other populations [6, 16] and also developing new markers based on genomic sequences that were thought to be near the distal end of 7AL [29, 41, 85]. Given this approach, the clustering of markers at the distal end of 7AL, could be an artifact of ascertainment bias. However, several findings reported in this chapter indicate otherwise:

a. Some of the markers/genes mapped to the ‘terminal cluster’ in the Excalibur/Kukri 7A genetic linkage map were not clustered in other published maps

   In two other mapping populations considered here (CPI133872/Janz [16] and Avalon/Cadenza [6]), some markers collocated in the terminal cluster of the Excalibur/Kukri chromosome 7A linkage map were separated by up to 28.5 cM (Figure 4.5).

b. Some of the markers in the ‘terminal cluster’ were anchored to widely separated positions on the Chinese Spring 7A, 7B and 7D syntenic builds

   When markers from the Excalibur/Kukri ‘terminal cluster’ were anchored onto Chinese Spring group-7 syntenic builds [29, 85], they spread over regions of approximately 0.9 Mb (7A) and 0.3 Mb (7B and 7D) (Figure 4.6; Appendix 2 (Additional file S2.2: Table S2.2 to S2.4).

c. No natural recombinants were detected in a large set of Excalibur/Kukri DH and RI lines

   When these markers were assayed across a large number of Excalibur/Kukri RI lines, some of the markers that were initially in clusters (in the Excalibur/Kukri DH linkage map; Figure 4.4) could be separated (Figure 4.7), but the ‘terminal cluster’ remained intact. Similarly, among the *Psy-A1*, *Lr20*, *Rlnn1* and *wri2* loci, there was no convincing evidence of recombination, even in a large RI population with more recombination history than the DH mapping population used in Chapters 3 and 4 (Figures 4.8 to 12).

Consistent with this, no cultivar has been released which has very white flour colour in combination with moderate resistance to *P. neglectus* (*Rlnn1*) and *Lr20/Sr15* resistance against rust pathogens.

Thus, it seems that the genetic clustering of many markers on 7AL is due to restricted recombination in the Excalibur/Kukri population and not simply due to a focus on developing markers that would map in the terminal region of 7AL. Such suppressed recombination has been reported in wheat chromosome 3DL (at leaf rust resistance gene *Lr24*) due to an introgressed fragment from *Agropyron elongatum* chromatin [150], wheat 2B (at leaf rust resistance gene *Lr35*) due to an introgression of *Triticum speltoides* chromatin [158], wheat chromosome 6BL (at leaf rust resistance gene *Lr9*) due to an introgressed alien chromatin from *Aegilops umbellulata* [149], at the proximal region of wheat chromosome 7AL (at strip rust resistance gene *Sr22*), due to an introgression of *Triticum boeoticum* chromatin [128].

The findings of clustering of molecular markers in 7AL linkage map of Excalibur/Kukri are consistent with the speculations made by Neu et al. [114], who mapped a cluster of molecular markers (8 and 12) that collocated with *Lr20* and *Pm1* and suggested suppressed recombination at the distal end of 7AL. Previous research using a cytology-based physical map [65, 66] did not detect any suppression of recombination at the distal ends of group-7 chromosomes, but that research used Chinese Spring wheat, whereas the suppressed recombination discussed here is postulated to be limited to materials that carry resistance alleles at *Lr20*/*Sr15* and *Rlnn1*.

Given the strong evidence for suppression of recombination, further investigations were done to find out the reason behind this genetic phenomenon. Possible reasons for suppressed recombination could include genetic rearrangements (translocations, inversions) or deletions or duplications of chromosomal segments [49]. With no recombination of genetic markers at the distal end of 7AL, it was not possible to critically evaluate the possibility of an inversion. No explicit evidence was found for either a duplication at the distal end of 7AL and the fact that some markers in the ‘terminal cluster’ amplified products from Excalibur indicate that the entire region is not deleted. The

findings reported in this chapter are very consistent with there being a translocation at the distal end of 7AL in Excalibur:

a. Close relationship of the *Psy-A1t* allele with *Ae. speltoides* alleles and some of the B-genome alleles of *T. aestivum* cultivars and *T. turgidum* ssp. *dicoccon* isolates

   The results of the phylogenetic analysis indicate a possibility that due to a significant mutation(s) the ancestral *Psy1* allele initially diverged into two groups, and since that divergence the *Psy-A1t* allele evolved separately from most wheat *Psy-A1*, *Psy-B1* and *Psy-D1* alleles (Figure 4.14; Appendix 2 – Additional file S2.4: Figure S2.1 and Table S2.6; [24]). Subsequently the clade with the *Psy-A1t* allele divided into two sub-clades, with the *Psy-A1t* allele recovered in the sub-clade that included the S genome alleles from *Ae. speltoides* and several B-genome alleles from *T. aestivum* and *T. turgidum* (Figure 4.14; Appendix 2 - Additional file S2.4: Figure S2.1 and Table S2.6; [24]). This close relationship of the *t* allele (genetically mapped to chromosome 7AL) with the S and B genome alleles, could be because of a translocation that was transferred through certain lineages. The current phylogeny information it is not sufficient to determine where this segment came from, but it is suggestive of an involvement of a 7B-like chromosome.

b. Unique amplification pattern in markers mapped to the 'terminal cluster'

   The markers *Psy-A1* and *wri2* from the 'terminal cluster' both amplified products from both Excalibur and Kukri. This indicates that the sequence at the distal end of the Excalibur 7A chromosome is not entirely alien but is similar to group -7 chromosomes.

   Most of the markers that amplified a product from Kukri but not from Excalibur were derived based on Chinese Spring sequences. The two markers (*sts638* and

schfc3) that amplified a product from Excalibur but not from Kukri were developed based on sequences derived from cultivars carrying the resistance allele at *Pm1*/*Lr20* [71, 114] and the *Psy-A1t* allele at *Psy-A1* [126]. Thus, it is Excalibur sequence in the region of interest differs from that of Chinese Spring more than the Kukri sequence does.

c. Genetic mapping of the longer product from the 7B-specific marker *AWW5L7* in Excalibur to the terminal marker cluster of 7AL

The chromosome 7B specific marker *AWW5L7* had previously [152] been genetically mapped to 7BL in a Halberd/Cranbrook population. Here, based on a presence/absence polymorphism of a second, longer, product that was amplified from Excalibur but not from Kukri, the marker *AWW5L7* was mapped to the chromosome 7A 'terminal cluster' in the Excalibur/Kukri linkage map. Excalibur also exhibited the 877-bp 'Cranbrook' product. Although this product could not be mapped due to lack of polymorphism in the Excalibur/Kukri population, it seems safe to assume that it is on 7B and would segregate independently from the longer product and the other loci in the terminal cluster. Consistent with this, the combination of the 956-bp 'Halberd' product and the longer product was observed in two other cultivars.

The observation of close sequence similarity between parts of the longer product from Excalibur and the product from Halberd is consistent with the idea that Excalibur carries a translocation from a 7B-like chromosome.

The longer product was also amplified by the 11 wheat cultivars in the panel that are known to be moderately resistant to RLN *P. neglectus* and to carry the *Rlnn1* resistance locus and the and 'very yellow' *Psy-A1t* allele. Despite the close relationship indicated by the *Psy1* phylogeny, *Ae. speltoides* (accession AEG357-4)

amplified neither the 956 bp nor the longer product, this indicate that this particular accession is not directly related to the putative translocation. The partial sequences derived from the longer product (Appendix 2 - Additional file S2.5) had no significant hits to any of the Chinese Spring wheat sequences from IWGSC or to the *Triticeae* shot-gun sequence assemblies. The absence of a significant BLAST hit could be due to the fact that the query sequence comes from a source that is not represented in the databases searched or due to incomplete sequence coverage in the current sequence databases. Of the databases searched, the ones with the greatest coverage are those for which the sequences came from Chinese Spring, in which the variant was not expected to be present.

d. <u>Presence of a putative A-B translocation in Excalibur FISH images that was absent in Kukri</u>

The FISH images (Figure 4.16) revealed four chromosomes (two possible pairs) with putative A-B translocations in Excalibur and only two (one possible pair) Kukri. In wheat, there is a common cyclic translocation (7BS-5AL-4AL) on chromosome 4A [93]. This previously documented translocation could be the A-B translocation observed in Kukri and one of the two observed in Excalibur. The other putative A-B translocation in Excalibur might be on chromosome 7A. However, none of the chromosomes on which possible A-B translocations were observed have the metacentric morphology that is expected for wheat chromosome 7A. It is possible that at the time of translocation there was a truncation and the chromosome became submetacentric. Further work needs to be done to come to a definitive conclusion. To pursue the possibility of an A-S translocation, some work has been conducted on *in-situ* hybridisation with probes from *Ae. speltoides*, but with no A-S translocation detected on chromosome 7A of Excalibur (Peng Zhang,

personal communication).

All of the findings reported here are consistent with Excalibur carrying a translocation at the distal end of 7AL, yet none of them give a clear indication of the source of the translocated segment, except that it seems to have come from the homoeologous region of another group-7 chromosome. Such a translocation could have happened naturally due to intergeneric, interspecific or intraspecific crossing or could have been a result of deliberate wide crossing. Some other modern wheat cultivars carry translocations derived from deliberate interspecific or intergeneric crossing. Some of these translocations are on group-7 chromosomes, including those that carry the leaf rust resistance genes *Lr19, Lr47* and the greenbug resistance gene *Gb5* [37, 148]. However, in the absence of any reports of *Lr20, Sr15, Pm1* or *Rlnn1* tracing back to a deliberate attempt at introgression, it seems more likely that the translocation happened naturally. The fact that *Lr20* is known to be present in many wheat cultivars from different parts of the world could indicate that the translocation may pre-date hexaploidisation. If so, it could have either happened in a tetraploid or diploid ancestor. There are no reports of suppressed recombination in the chromosome 7A of modern tetraploid wheat but it is possible that the translocation in question occurred only in some of the ancestors that participated in ancient hybridisation, and was passed on to only some lineages of wheat through ancestral allele sorting.
If recombination is completely suppressed in the distal end of 7AL in all materials with *Psy-A1t*, no natural recombinants will be found that carry *Rlnn1, Lr20/Sr15* and/or *Pm1* resistance in combination with any alternative (lower yellow pigment) *Psy-A1* allele. However, the desired combination (with resistance alleles to the rust and *P. neglectus*, coupled with whiter flour colour) might be achieved by screening for *Psy1* mutants within a TILLING (Targeting Induced Local Lesions IN Genomes; [98]) population that carries the resistance alleles. Lack of recombination precludes the isolation of the resistance genes

Rlnn1, *Lr20/Sr15* and/or *Pm1* with a standard positional cloning approach, but gene isolation might be achieved with a radiation hybrid approach [69].

Chapter 5

Genetic mapping of the *Cre8* locus for resistance against cereal cyst nematode (*Heterodera avenae* Woll.) in wheat

Dimanthi V. Jayatilake[1*], Elise J. Tucker[1,2*], Julia Brueggemann[1], John Lewis[3], Melissa Garcia[1,2], Susanne Dreisigacker[4], Matthew J. Hayden[5], Ken Chalmers[1,2] and Diane E. Mather[1,2, **]

[1]School of Agriculture, Food and Wine, Waite Research Institute, The University of Adelaide, PMB 1, Glen Osmond, SA 5064, Australia

[2]Australian Centre for Plant Functional Genomics, Waite Research Institute, The University of Adelaide, PMB 1, Glen Osmond, SA 5064, Australia

[3] South Australian Research and Development Institute, Waite Campus, Plant Research Centre, 2b Hartley Grove, Urrbrae, SA 5064, Australia

[4] CIMMYT, Apdo. Postal 6-641, 06600 Mexico, D.F., Mexico

[5] Department of Environment and Primary Industries Victoria, AgriBio Centre, Bundoora, VIC 3083, Australia

* Joint first authors

**Corresponding author: diane.mather@adelaide.edu.au; telephone +61 8 8313 7156; fax +61 8 8313 7102

Email addresses of other authors:

DJ: dimanthi.jayatilake@adelaide.edu.au

ET: elise.tucker@acpfg.com.au

JB: julia.brueggemann@adelaide.edu.au

JL: john.lewis@sa.gov.au

MG: melissa.garcia@acpfg.com.au

SD: s.dreisigacker@cgiar.org

MH: matthew.hayden@depi.vic.gov.au

KC: ken.chalmers@adelaide.edu.au

The text, figures and tables presented in this thesis chapter are exactly the same as the submitted manuscript, except for minor numbering changes in figures and tables, which were reformatted to be consistant with the rest of the thesis. The the author contributions are presented in a Statement of Authorship at the beginning of the chapter. The information from the statement of acknowledgement and the reference list of the manuscript is included in the corresponding sections of the thesis. Online Resources are presented in Appendix 3.

5.1 Statement of Authorship

Title of the paper	Genetic mapping of the *Cre8* locus for resistance against cereal cyst nematode (*Heterodera avenae* Woll.) resistance in wheat
Publication Status	☐ Published ☐ Accepted for publication ■ Submitted for publication ☐ Publication style
Publication Details	This chapter has been prepared as a manuscript and was submitted to Molecular Breeding for publication on the 06/03/2014.

Author Contributions

By signing the Statement of Authorship, each author certifies that their stated contribution to the publication is accurate and that permission is granted for the publication to be included in the candidate's thesis.

Name of Principal Author (Candidate)	Dimanthi V. Jayatilake		
Contribution to the paper	Critically examined all genotypic and phenotypic data, designed and assayed additional markers, reconstructed the linkage map, conducted QTL analysis, assayed selected markers on a panel of cultivars, analysed the data on the selected lines and interpreted the results, and wrote the first draft of the manuscript and took primary responsibility for manuscript revision.		
Signature		Date	26 · 03 · 2014

Name of Co-author	Elise J. Tucker		
Contribution to the paper	Joint first author. Conducted wheat-rice comparative analysis, designed new markers and assayed them on the population (prior to the candidature of DVJ). Selected lines for the re-evaluation of *H. avenae* resistance. Provided input for the manuscript.		
Signature		Date	14 · 4 · 2014

Name of Co-author	Julia Brueggemann
Contribution to the paper	Prior to the candidature of DVJ assayed markers on the population
Signature	Date 26/3/14

Name of Co-author	John Lewis
Contribution to the paper	Conducted the re-evaluation of *H. avenae* resistance in selected lines
Signature	Date 14/4/14

Name of Co-author	Melissa Garcia
Contribution to the paper	Designed new molecular markers
Signature	Date 26.03.14

Name of Co-author	Susanne Dreisigacker
Contribution to the paper	Designed a new marker
Signature	Date 01 - 04 - 2014

Name of Co-author	Matthew J. Hayden
Contribution to the paper	Carried out 9K- iSelect SNP genotyping on DNA pools
Signature	Date 29 - 03 - 2014

Name of Co-author	Ken Chalmers
Contribution to the paper	Supervised the marker design, genotyping and linkage mapping.
Signature	Date 23/3/14

Name of Co-author	Diane E. Mather
Contribution to the paper	Provided overall supervision of the research and helped write the manuscript.
Signature	Date 26 MARCH 2014

All authors read and approved the final manuscript and declared that they have no competing interests.

5.2 Abstract

The cereal cyst nematode (CCN, *Heterodera avenae* Woll.) resistance locus *Cre8* on the long arm of chromosome 6B (6BL) of wheat (*Triticum aestivum* L.) is effective in lowering the nematode population in soil. Identification of reliable and high-throughput molecular markers linked to the *Cre8* locus is important for the successful deployment of *Cre8*-derived resistance in wheat breeding programs. Here we report the addition of over 600 markers to improve an existing linkage map for the Trident/Molineux wheat population. With the improved map, *Cre8* was mapped as a large-effect quantitative trait locus (QTL) near the distal end of 6BL. This QTL explained up to 35 % of the phenotypic variation in CCN resistance. New marker assays were developed for DNA polymorphism in the *Cre8* region. Seven molecular markers closely linked with *Cre8* (at 0.9, 2.2 or 5.9 cM from the estimated QTL position) were found to be diagnostic across a panel of wheat cultivars and are recommended for use in marker-assisted selection of the *Cre8* resistance locus in wheat breeding. Prospects for the isolation of the causal gene are discussed.

5.3 Keywords

Cereal cyst nematode, *Heterodera avenae*, wheat, molecular markers, *Cre8*

5.4 Introduction

Cereal cyst nematode (CCN, *Heterodera avenae* Woll.) is a sedentary endoparasitic nematode that causes significant yield loss in wheat (*Triticum aestivum* L.) and other important cereal crops such as barley (*Hordeum vulgare* L.) and oat (*Avena sativa* L.). Murray and Brennan [111] estimated that without control measures, wheat yield losses due to CCN would be as high as A$ 572 million annually. Cereal cyst nematode, which has one

life cycle per cropping season, produces the characteristic root damage symptoms in wheat of a knotted and stunted root system with white lemon-shaped females (white cysts) filling with eggs and becoming visible during the spring as the crop matures, with susceptible cultivars hosting large numbers, but with only few present on resistant cultivars. Upon their death, the CCN females turn into brown cysts with the cuticle transformed into a protective shell. These remain in the soil, enabling the over-summer survival of the eggs in a dormant state until late autumn when the eggs are stimulated to hatch with the presence of cool and moist soil conditions [175]. Virtually all eggs produced by a female CCN hatch over the subsequent two years. Due to the limited host range and hatching characteristics of CCN, incorporation of resistant cultivars into crop rotations is critical to maintain CCN populations at non-damaging levels.

Accordingly, the development of CCN-resistant cereal cultivars is an important ongoing objective of breeding programs for the southern and western cereal growing belt of Australia. Screening of breeding material to select for CCN resistance relies partly on phenotypic bioassays and partly on molecular marker assays for specific CCN resistance loci. Several bread wheat loci that confer resistance against *H. avenae* have been genetically mapped: *Cre1* [164, 198]; *Cre8* [197, 199] and *QCre.srd-1B* [197]. In addition, several genes have been introgressed into bread wheat from other species to improve its CCN resistance: *Cre2* [33], *Cre5* [75, 76] and *Cre6* [118] from *Aegilops ventricosa* Tausch; *Cre3* and *Cre4* [39, 40] from *Ae. tauschii* Cosson; and *Cre7* [145] from *Ae. triuncialis* (L.) Á. Löve.

Genetic research on *Cre8* began with the observation [127] that the moderately CCN-resistant cultivar Festiguay and its moderately resistant derivatives Molineux, Barunga and Frame all carry the same allele of the restriction fragment length polymorphism (RFLP) marker *cdo347*. Using a Trident/Molineux doubled haploid (DH) population, Williams et

al. [199] confirmed the strong association of differences in CCN resistance with a polymorphism revealed by *cdo347*. Using nullisomic-tetrasomic lines, Williams et al. [199] assigned the resistance locus to chromosome 6B and designated it *Cre8*. Williams et al. [197] then used RFLP markers and simple sequence repeat (SSR) markers to construct a linkage map for Trident/Molineux. They mapped three QTL for CCN resistance. At two of these loci (*QCre.srd-1B* on chromosome 1B and *Cre8* on chromosome 6B), the resistance alleles were from Molineux. At the third locus (*Cre5* on chromosome 2A) the resistance allele was from Trident. The linkage group onto which Williams et al. [197] mapped *Cre8* consisted of only six markers (three RFLP and three SSR), with *Cre8* estimated to be within a 14.7-cM interval between the SSR marker *gdm147* and the collocating RFLP markers *cdo347* and *awbma20*. Of these markers, *gdm147* had the strongest association with CCN resistance.

The research reported here was undertaken to improve the Trident/Molineux linkage map by adding new markers, to re-evaluate the position of the *Cre8* resistance QTL on chromosome 6B, and to develop and evaluate molecular markers that could be suitable for use in marker-assisted selection of *Cre8* resistance.

5.5 Materials and methods

Plant materials

The plant materials used include the Australian wheat cultivars Trident (VPM1/5*Cook//4* Spear) and Molineux (Pitic62/Festiguay//2*Warigal), a set of 182 DH lines developed from F_1 progeny of a cross between Trident and Molineux [137], Chinese Spring, the Chinese Spring deletion lines CS 6BS-2, CS 6BS-3, CS 6BS-5, CS 6BL-3 and CS 6BL-5 (http://www.k-state.edu/wgrc/Germplasm/Deletions/group6.html), Chinese

Spring nullisomic-tetrasomic lines CS N6A-T6B, CS N6A-T6D, CS N6B-T6A, CS N6B-T6D, CS N6D-T6A and CS N6D-T6B [155] and a panel of 13 wheat cultivars. The panel consisted of six cultivars (Barunga, Correll, Festiguay, Frame, Stylet and Yitpi) known to be moderately resistant to CCN and thought to carry *Cre8* resistance and seven cultivars (Mace, Aroona, Axe, Drysdale, Egret, Gladius and Krichauff) known to be at least moderately susceptible to CCN and assumed to lack *Cre8* resistance. Seeds of these cultivars were obtained from the Australian Winter Cereals Collection.

Polymorphism discovery, marker assay development and marker genotyping

DNA was extracted from leaf tissue sampled from individual seedlings of each of the cultivars and lines mentioned above using the method described by Rogowsky et al. [144], with modifications described by Pallotta et al. [123].

Diversity Arrays Technology (DArT™) assays were performed at Triticarte Pty. Ltd., Australia, according to the methods described by Akbari et al. [3] on Trident, Molineux and each of the 182 Trident/Molineux DH lines using DNA normalized to 50 ng/µl.

A total of 73 SSR markers selected from the GrainGenes database [27] were assayed on Trident and Molineux using the multiplex-ready PCR assay protocol described by Hayden et al. [56]. Amplicons were separated using capillary electrophoresis on an AB3730xl DNA fragment analyser (Applied Biosystems®, USA) and genotypes were called using GeneMapper® software v4.0 (Applied Biosystems®, USA). Polymorphic markers were assayed on the 182 Trident/Molineux DH lines.

Thirty one Kompetitive Allele Specific PCR (KASP™) markers that had been reported by Allen et al. [6] and/or in the CerealDB database [26] as mapping on 6BL were assayed on 22 Trident/Molineux DH lines at LGC Genomics Ltd., UK and/or on a Roche

LightCycler® 480 (Roche Products Pty. Ltd., Switzerland). For the latter, genotypes were called using the end-point genotyping module implemented in Roche LightCycler® 480 software release 1.5.0 (Roche Products Pty. Ltd., Switzerland). Polymorphic markers were assayed on the remaining 160 Trident/Molineux DH lines (conditions described in Appendix 3 - Online Resource S3.1).

To select informative single nucleotide polymorphisms (SNP) from the 9K Wheat Illumina Infinium iSelect genotyping array [16], a pooled-DNA approach was undertaken. This involved the preparation of two DNA pools, one by combining equal amounts of 50 ng/µl DNA from 20 DH lines fixed for the Trident haplotype (non-*Cre8* pool) in the *Cre8* QTL region on chromosome 6B and one by combining equal amounts of 50 ng/µl DNA from 20 DH lines fixed for the Molineux haplotype (*Cre8* pool) in that region. Three replicates of each of the two DNA pools were assayed on the 9K iSelect genotyping array, along with one DNA sample from each of two individual DH lines (the *Cre8* line TMDH150 and the non-*Cre8* line TMDH109) and two 'artificial heterozygote' samples developed by combining equal amounts of DNA from TMDH150 and TMDH109. Polymorphisms between the pools were selected based on differences in normalized theta values of the two DNA pools based on a t-test and were filtered to favour those that had previously been mapped on chromosome 6B [16]. For polymorphisms captured in this manner, assays were developed using high-resolution melting (HRM) technology [201] or KASP™ technology. Primers for HRM assays were designed using BatchPrimer3 v1.0 [202] and were tested on TMDH109 and TMDH150 on a Roche LightCycler® 480 (Roche Products Pty. Ltd., Switzerland), using the assay conditions described in Appendix 3 (Online Resource S3.1). Genotypes were assigned using the gene scanning module implemented in Roche LightCycler® 480 software release v1.5.0 (Roche Products Pty. Ltd., Switzerland). Primers for KASP™ assays were designed with Primer3 software [146] as implemented in Geneious® v6.0.4. (Biomatters Ltd., New Zealand). Each assay involved two forward

primers and a common reverse primer. Each forward primer complemented one of the SNP alleles at its 3' end and had a standard tail complementary to the universal FRET cassettes present in the KASP™ Mastermix (LGC Genomics Ltd., UK) at its 5' end (FAM tail: 5'-GAAGGTGACCAAGTTCATGCT - 3'; VIC tail: 5' - GAAGGTCGGAGTCAACGGATT - 3'; Trick et al. [180]). The KASP™ assays were initially tested on 22 Trident/Molineux DH lines as described above (Appendix 3 - Online Resource S3.1).

To identify additional polymorphisms in the *Cre8* region, sequences of the *Cre8*-linked RFLP probes AWBMA20 (sequenced specifically for this work and submitted to the GrainGenes database [27] and CDO347 (already in the GrainGenes database [27]) were used as BLAST queries against the rice genome sequence at Rice Genome Annotation Project database [28] to identify the syntenous region in the rice genome. The sequence of the predicted rice gene in the orthologous region was used as a BLASTN query to search the GenBank *Triticum* EST database at NCBI [112] for wheat orthologues. Primers were designed to amplify products from Trident and Molineux genomic DNA and the amplified products were sequenced (Appendix 3 - Online Resource S3.1). Primers were designed to capture polymorphisms between Trident and Molineux. Polymorphic sites were assigned to wheat deletion bins using the chromosome-6B Chinese Spring deletion lines. Expressed sequence tags (ESTs) from that deletion bin were subsequently targeted for polymorphism discovery and assay design using an approach similar to the one described above.

All new markers were assayed on all 182 Trident/Molineux DH lines and all markers that mapped to the distal region of 6BL were assayed on the panel of 13 wheat cultivars.

Linkage and quantitative trait locus analyses

The genotypic data used by Williams et al. [197], supplemented by genotypic data for the newly assayed markers, were used to construct a linkage map. Based on examination of the

genotypic data, 21 of 182 Trident/Molineux DH lines were excluded from analysis: 6 due to possible DNA contamination, 12 that seem genetically identical to other lines in the population and 3 due to high proportions of missing data. Markers with a high proportion of missing data and/or ambiguous allele calls and markers with segregation distortion were also excluded from the analysis. The linkage map was constructed using MapManager QTXb20 [96] using a search linkage criterion of $p = 0.001$, with newly developed markers assigned to linkage groups using the 'distribute' function with a search linkage criterion of $p = 1e\text{-}6$. The marker order was refined using RECORD [181] and the map distances were estimated using the Kosambi mapping function [81]. Linkage groups were assigned to chromosomes and oriented by comparing marker positions to those on published maps [3, 6, 16, 25, 168, 197]. Linkage maps were plotted using MapChart v2.2 [184]. QTL mapping was implemented with the composite interval mapping feature of Windows QTL Cartographer v2.5_011 [188] using a step size of 0.5 cM, a co-factor dropping window of 10 cM, 5 co-factors selected based on forward regression and the same trait values that had been used by Williams et al. [197]: line means for *H. avenae* nematode counts from experiments conducted in 2004 and in 2005 and the means across both years. The threshold to test for statistical significance of QTL was set for a genome-wide Type I error rate of 0.05 by performing 1000 permutations.

Phenotyping of selected lines

Trident, Molineux and 43 Trident/Molineux DH lines, most of which had recombination events on 6BL, were re-evaluated for resistance against *H. avenae* using the "pots test" method described by Lewis et al. [88], with 12 replicates of each line. Each experimental unit consisted of a single plant grown in a tapering 10-cm-long black tube filled with soil infested with *H. avenae* cysts to provide a CCN population density of approximately 25

eggs/g. The tubes were arranged in wire mesh crates and placed in outdoor plant beds with supplementary sprinkler irrigation. After approximately four months, the root balls were removed from the tubes and the number of white female nematodes visible on the surface of each root ball was counted (up to 21, above which it is considered unambiguous that the plant is susceptible).

The lines were then classified into four main genotypic classes based on marker genotypes in the *Cre5* and/or *QCre.srd-1B* QTL regions: (a) resistance alleles at both *Cre5* (Trident) and *QCre.srd-1B* (Molineux*)*; (b) *Cre5* only; (c) *QCre.srd-1B* only; and (d) neither *Cre5* nor *QCre.srd-1B*. Within each of these four main classes, lines were further classified into two *Cre8* subclasses based on their genotypes (Trident or Molineux allele) at a marker representing the *Cre8* QTL region. The effect of the *Cre8*-linked marker allele on the number of nematodes was modeled using mixed-effects Poisson regression with genotypic subclass as a fixed effect and line as a random effect, using a custom script written in R [136]. Subsequently, pairwise comparisons were performed between the *Cre8* subclasses within each main class.

5.6 Results

New molecular marker assays

Based on the analysis of pooled DNA samples using the wheat 9K iSelect genotyping array [16], eight polymorphic SNPs were selected for assay design. For four of these (*iwa2098, iwa1495, iwa0824* and *iwa4245*), primer pairs were designed for analysis with HRM technology (*wri6_F/R, wri7_F/R, wri8_F/R* and *wri9_F/R*, respectively; Appendix 3 - Online Resource S3.1: Table S3.2). For each of these markers, polymorphism can be scored using melting curves and/or difference plots (Appendix 3 - Online Resource S3.2;

Figure S3.1). For the other four SNPs (*iwa3224, iwa3880, iwa4246* and *iwa8441*), assays were developed for analysis with KASP™ technology (*wri10, wri11, wri12* and *wri13*, respectively; Appendix 3 - Online Resource S3.1: Table S3.1) with polymorphisms scored based on differences in SNP allele assignment by end-point genotyping (Appendix 3 - Online Resource S3.1 and Online Resource S3.2; Figure S3.2).

The *Cre8*-linked RFLP probe sequences for AWBMA20 (http://wheat.pw.usda.gov/cgi-bin/graingenes/report.cgi?class=sequence;name=AWBMA20) and CDO347 had significant BLAST hits (E-value 5.6e-10 and 3.2e-127 respectively) to the predicted rice gene Os02g58560. The wheat EST GH723564 (Unigene 93111; E-value 0.0) was identified as a wheat orthologue of Os02g58560. Chromosome-6B-specific primers (*oET0041_F 5*'- CGAGCCCCTCAAATACTCCG - 3' and *oET0041_R* 5'-ACAGCCCCACGCTCATGATC - 3') were designed to wheat EST GH723564 (Unigene93111). This primer pair amplified 768-bp amplicons from both Trident and Molineux. Sequencing of these amplicons revealed two SNP sites. The primer pair *wri14_LSPF/R_ASP* (Appendix 3 - Online Resource S3.1: Table S3.2) was designed to assay these polymorphisms. It amplified two products from Molineux (approximately 750 bp and 675 bp) but only one (750 bp) from Trident. This polymorphism can be readily detected with agarose gel electrophoresis, providing a chromosome-6B-specific dominant marker assay that can be scored based on the presence/absence of the 675 bp product (Appendix 3 - Online Resource S3.2; Figure S3.3A).

Two chromosome-6B-specific primers (BE403950A_F1_UCD 5'-TTTACTTTAAATGAACATTTCAGCAGC - 3' and BE403950_cpR1_UCD 5'-CGCGACCCTACTCTTCTGAC - 3'; Wheat SNP Database [30]; Akhunov et al. [4]) which had been designed to EST BE403950 (Unigene53224) and assigned to the terminal deletion bin 6BL5-0.40-1.00, were used to amplify products from Trident and Molineux

genomic DNA (see Appendix 3 - Online Resource S3.1). Sequencing of these products revealed one SNP between Trident and Molineux. To detect this SNP, a pair of complementary dominant assays (*wri15*; Appendix 3 - Online Resource S3.1: Table S3.2) was designed. The primer pair *wri15_F/R1* amplifies a 350-bp product from Trident and the primer pair *wri15_F/R2* amplifies 350-bp product from Molineux. Results for this pair of assays can be conveniently scored (as if it were a co-dominant assay) by loading the products from one primer pair onto an agarose gel, running electrophoresis for 15 minutes, then loading the products from the other primer pair and continuing electrophoresis (Appendix 3 - Online Resource S3.2; Figure S3.3B). A codominant KASP™ marker assay (*wri16*) was also developed to assay the same SNP (Appendix 3 - Online Resource S3.1: Table S3.1; Appendix 3 - Online Resource S3.2; Figure S3.3C).

Linkage map and QTL results

A total of 771 molecular markers were mapped: 164 SSR markers that were previously assayed and reported by Williams et al. [197] and 607 newly assayed markers (569 DArT™ markers, 19 additional SSR markers, 8 published KASP™ markers and 11 new molecular markers). The resulting map consists of 25 linkage groups, two for each of chromosomes 1B, 3A, 3B and 7D and one for each of the other 17 chromosomes of wheat (Appendix 3 - Online Resource S3.3: Figure S3.4). As expected, all three of the QTL that Williams et al. [197] had reported to be associated with CCN resistance were detected (Table 5.1). The *Cre8* region on chromosome 6B had higher test statistics and larger additive effect estimates than the other two loci (*QCre.srd-1B* and *Cre5*).

Table 5.1: Composite interval mapping (CIM) statistics of major quantitative trait loci (QTL) for resistance against cereal cyst nematode in the Trident/Molineux doubled haploid population as assessed in experiments conducted in 2004 and 2005.

QTL	Chromosome	Donor of resistance allele	Closest markers to the QTL peak	CIM statistics[1] at the QTL peak								
				2004			2005			Mean of 2004 and 2005		
				LRS	R^2	Additive effect	LRS	R^2	Additive effect	LRS	R^2	Additive effect
Cre8	6B	Molineux	*BS00011603* and *BS00022529*	86.1	0.33	25	76.1	0.31	9	100.5	0.35	16
QCre.srd-1B	1B2	Molineux	*wmc719*[2], *gwm140*[3] and *wmc367*[4]	55.1	0.19	20	43.6	0.16	7	62.5	0.19	12
Cre5	2A	Trident	*wmc177*	30.9	0.10	-14	30.8	0.11	-6	41.5	0.12	-10

[1]Calculated using the composite interval mapping feature of Windows QTL Cartographer v2.5_011 (Wang et al. [188]) using a step size of 0.5 cM, a co-factor dropping window of 10 cM, 5 co-factors selected based on forward regression, with the significance threshold set for a genome-wide Type I error rate of 0.05 by performing 1000 permutations. [2] 2004 [3]2005 [4] Mean of 2004 and 2005

The new linkage map of chromosome 6B (Figure 5.1A) is 156.4 cM long and includes 80 markers: 58 DArT markers, 3 SSR markers, 8 published KASP™ markers, 8 markers developed based on sequences that were included on the 9K iSelect genotyping array and 3 newly developed EST-based markers. The peak test statistic (LRS = 100.5) for the *Cre8* QTL, as mapped based on two-year means, is at the 154.2 cM position, 0.9 cM proximal to the position of markers *BS00011603* and *BS00022529* (Table 5.1; Figure 5.1A). This 0.9 cM interval is closely flanked by two clusters of markers (at 148.3 and 156.4 cM), each consisting of eight cosegregating markers, all of which are strongly associated with CCN resistance (Figure 5.1A).

Of the 43 Trident/Molineux DH lines that were re-evaluated for resistance against *H. avenae*, 38 could be unambiguously classified based on their genotypes (Trident or Molineux) at other CCN-resistance loci (i.e., in the *Cre5* and *QCre.srd-1B* regions). The remaining five lines could not be classified due to recombination events in the *Cre5* region of chromosome 2A and due to missing genotypic data. Consistent with the QTL analysis results, nematode counts were lowest for the lines with Trident alleles at *Cre5* and Molineux alleles at *QCre.srd-1B* (Appendix 3 - Online Resource S3.4: Figure S3.5A and B), highest for the opposite combination (Appendix 3 - Online Resource S3.4: Figure S3.5G and H) and intermediate for the other two combinations (Appendix 3 - Online Resource S3.4: Figure S3.5C and D; Figure S3.5E and F). When the lines within the four main genotypic classes were further classified based on their genotypes at the *Cre8*-linked marker *BS0011603*, the overall effect of *Cre8* subcategories on the nematode count was significant in the global test (log-likelihood ratio test $p < 0.0001$). When pairwise comparisons between *Cre8* subcategories were made, the lines with the Molineux allele at *BS0011603* had lower mean nematode counts than the corresponding *Cre8* subcategory with the Trident allele at that marker (Figure 5.2).

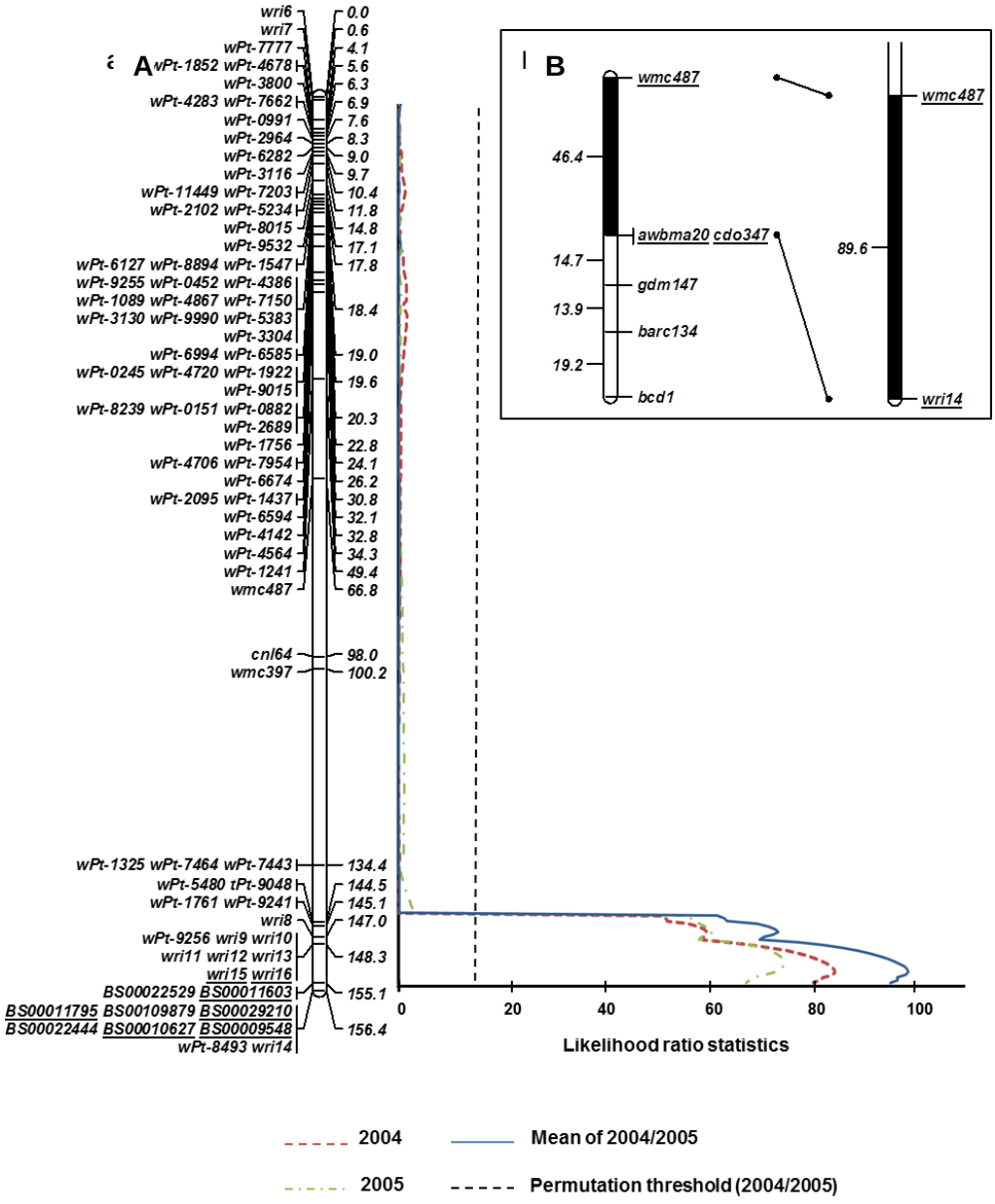

Figure 5.1: A) Genetic linkage map and LRS test-statistic scans for cereal cyst nematode resistance on chromosome 6B based on composite interval mapping using data from 161 Trident/Molineux doubled haploid lines. B) A comparison of the Trident/Molineux chromosome 6B linkage map of Williams et al. [197] (left) with the corresponding region of the current map (right).

Line means of nematode counts of tube test experiments carried out by Williams et al. [197] in 2004 and 2005 and the mean counts across these two years were used as trait data. The diagnostic markers recommended for marker-assisted selection are underlined.

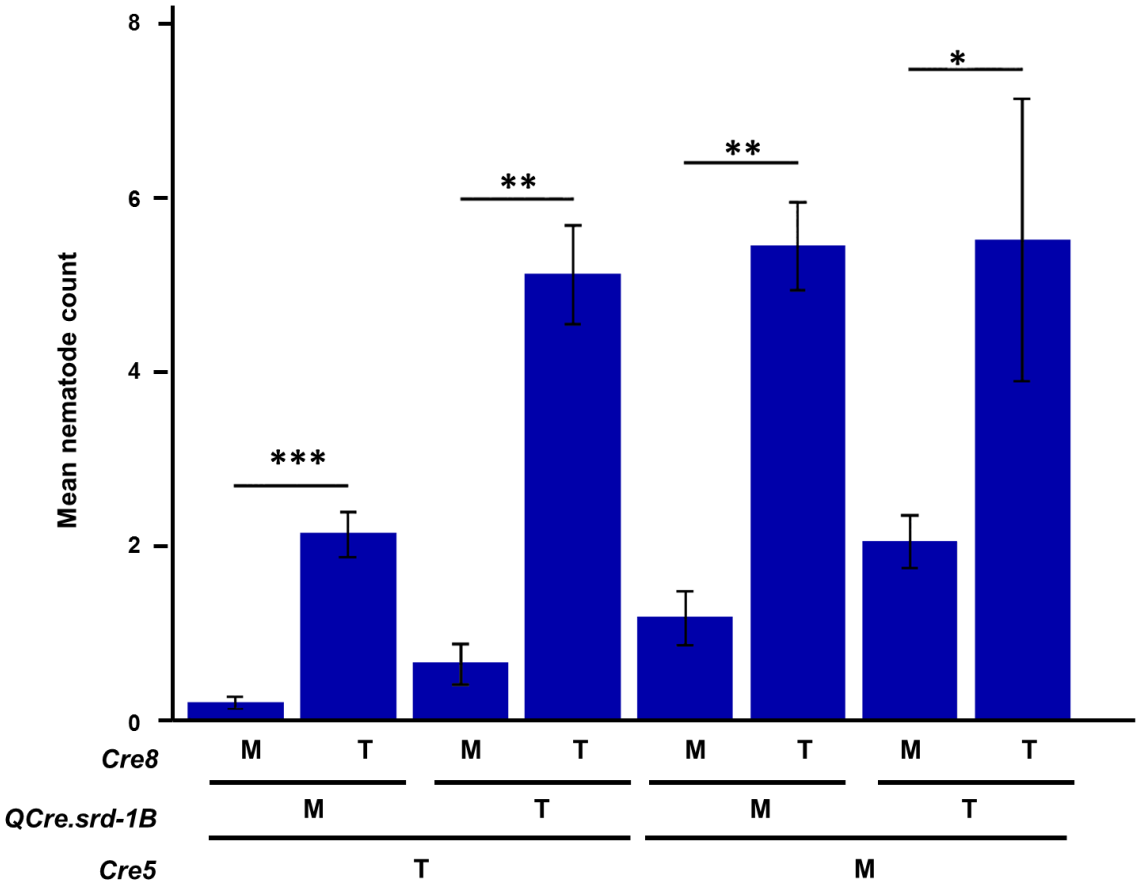

Figure 5.2: Mean nematode counts for eight genotypic classes of Trident/Molineux lines with different combinations of alleles at markers linked with the *H. avenae* resistance loci *Cre5* (*gwm359-wmc177*), *QCre.srd-1B* (*wmc367-gwm140*) and *Cre8* (*BS00011603*).

T: Trident M: Molineux allele; *, ** and ***: pairwise comparison significant at the 0.05, 0.001 and 0.0001 probability levels, respectively.

Marker validation

Marker assays applied to a panel of 13 cultivars verified that cultivars that are moderately resistant to CCN and are thought to carry the resistance allele at the *Cre8* locus (Barunga, Cornell, Festiguay, Frame, Stylet and Yitpi) have the same allele as Molineux for 17 markers (Figure 5.3). For seven of these markers (*wri15* and *wri16* from the 148.3 cM position; *BS00011603* from the 155.1 cM position*; BS00010627, BS00011795, BS0009548* and *BS00029210* from the 156.4 cM position), all of the moderately susceptible cultivars

that were assayed (Mace, Aroona, Axe, Drysdale, Egret, Gladius and Krichauff) exhibited the same allele as Trident (Figure 5.3). These seven markers could therefore be useful as diagnostic markers. For each of the other 10 markers tested (one that mapped at 147.0 cM, five that mapped at 148.3 cM, one that mapped at 155.1 cM and three that mapped at 156.4 cM), at least some of the moderately susceptible cultivars exhibited the same allele as Molineux (Figure 5.3), limiting the usefulness of these markers for selection.

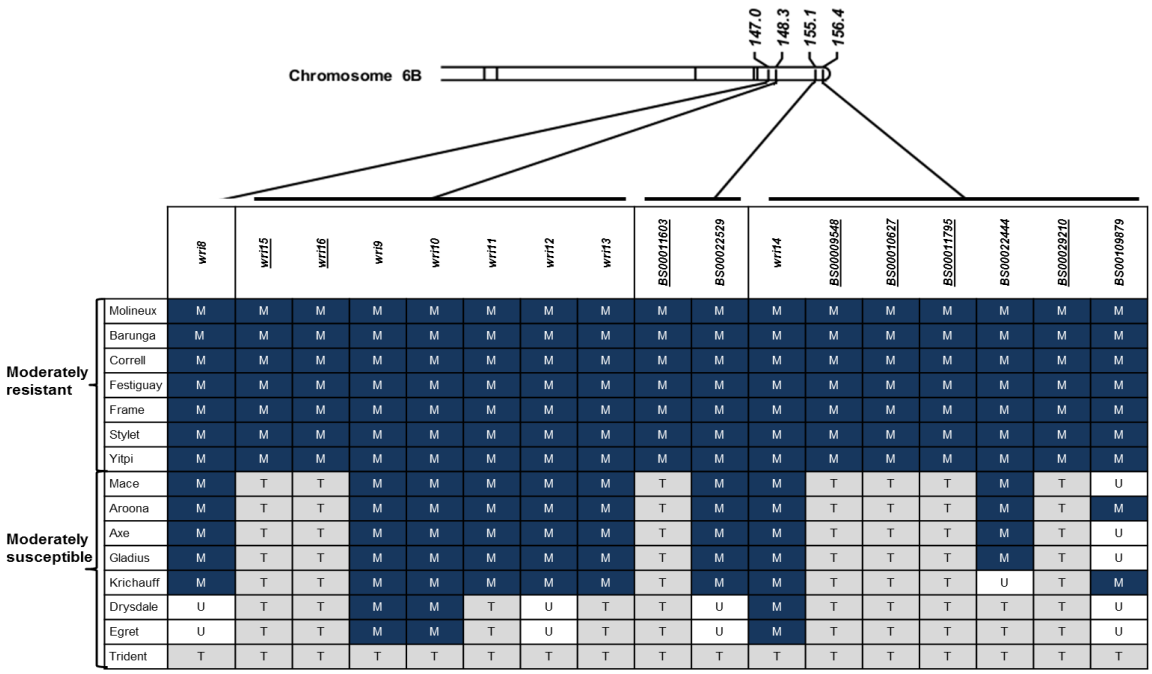

		wri8	wri15	wri16	wri9	wri10	wri11	wri12	wri13	BS00011603	BS00022529	wri14	BS00009548	BS00010627	BS00011795	BS00022444	BS00029210	BS00109879
Moderately resistant	Molineux	M	M	M	M	M	M	M	M	M	M	M	M	M	M	M	M	M
	Barunga	M	M	M	M	M	M	M	M	M	M	M	M	M	M	M	M	M
	Correll	M	M	M	M	M	M	M	M	M	M	M	M	M	M	M	M	M
	Festiguay	M	M	M	M	M	M	M	M	M	M	M	M	M	M	M	M	M
	Frame	M	M	M	M	M	M	M	M	M	M	M	M	M	M	M	M	M
	Stylet	M	M	M	M	M	M	M	M	M	M	M	M	M	M	M	M	M
	Yitpi	M	M	M	M	M	M	M	M	M	M	M	M	M	M	M	M	M
Moderately susceptible	Mace	M	T	T	M	M	M	M	M	T	M	M	T	T	T	M	T	U
	Aroona	M	T	T	M	M	M	M	M	T	M	M	T	T	T	M	T	M
	Axe	M	T	T	M	M	M	M	M	T	M	M	T	T	T	M	T	U
	Gladius	M	T	T	M	M	M	M	M	T	M	M	T	T	T	M	T	U
	Krichauff	M	T	T	M	M	M	M	M	T	M	M	T	T	T	U	T	M
	Drysdale	U	T	T	M	M	T	U	T	T	U	M	T	T	T	T	T	U
	Egret	U	T	T	M	M	T	U	T	T	U	M	T	T	T	T	T	U
	Trident	T	T	T	T	T	T	T	T	T	T	T	T	T	T	T	T	T

Figure 5.3: Marker haplotypes for Molineux, Trident and 13 other wheat cultivars.

M and T indicate that the result was the same as that obtained for Molineux or Trident, respectively, while U (unknown) indicates that it was not possible to unambiguously classify the result as being the same as that of either Molineux or Trident. Diagnostic markers recommended for marker-assisted selection are underlined.

5.7 Discussion

Here, we report the improvement of the Trident/Molineux linkage map by the addition of DArT™, SSR, EST-based and SNP markers to the linkage map reported by Williams et al. [197]. Although the focus of this report is on the *Cre8* region of chromosome 6B, some of the additional markers mapped could also be of interest relative to other traits that have been mapped in Trident/Molineux [83].

As expected, considering that we used the same population and phenotypic data as Williams et al. [197], the same three QTL for CCN resistance were detected, with *Cre8* being the most significant (Table 5.1). Williams et al. [197] had assigned the *Cre8* QTL to a 14.7 cM interval between markers *awbma20*/*cdo347* and *gdm147* at the end of 6BL. Here, the *Cre8* QTL was mapped to the same chromosome region, but the molecular marker map is much more saturated. The linkage map reported by Williams et al. [197] for chromosome 6B consisted of just three SSR and three RFLP markers. Here, the 6B linkage map (Figure 5.1A) was improved by adding 79 new markers and by retaining only the SSR marker *wmc487* from the previous map. The other two SSR markers were excluded because of some ambiguous genotypic data and all three RFLP markers were excluded because many data points were missing. Accordingly, direct comparison of the current Trident/Molineux chromosome-6B linkage map with that of Williams et al. [197] relies only on the SSR marker *wmc487* and on the relationship of the EST-based marker *wri14* with the RFLP marker *awbma20* (Figure 5.1B). On the earlier map, marker *wmc487* was 46.4 cM distal to *awbma20/cdo347.* In contrast, on the current map, *wmc487* is 89.6 cM proximal to *wri14.* Based on comparisons with other published maps [6, 16, 168], the genetic distance on the current map of chromosome 6B seems correct. In the construction of the earlier map, the lack of markers between *wmc487* and *awbma20* would have made it difficult to establish the correct orientation and marker order for the linkage group. Based

on our examination of all of the genotypic data, it seems that the correct orientation of the *awbma20/cdo347 – bcd1* region is opposite to that reported by Williams et al. [197]. This would explain much of the apparent discrepancy between the distance estimates of 46.4 and 89.6 cM and it indicates that *Cre8* is in fact genetically very close to the distal end of 6BL.

When the existing CCN resistance data were evaluated using the improved maker map, the *Cre8* QTL was mapped just proximal to markers *BS00011603* and *BS00022529* (Figure 5.1A, Table 5.1). Further, in a new phenotypic evaluation of a subset of the Trident/Molineux lines, the Molineux alleles of these markers were confirmed to be strongly associated with lower nematode counts, as evidenced by the differences between the paired genotypic subclasses with different alleles at *BS00011603* (Figure 5.2; Appendix 3 - Online Resource S3.4: Figure S3.5).

The large number of markers mapped within a few cM of the estimated position of *Cre8* provides a range of potential markers for use in selection. Here, some of these markers were tested across a panel of cultivars. For all of these markers, the alleles exhibited by Molineux were completely conserved across all of the cultivars that are thought to carry the *Cre8* resistance allele, providing further supporting evidence for the close linkage of these markers with *Cre8* (Figure 5.3).

Due to the high cost involved in phenotypic evaluation of CCN resistance, this trait is a very good example for which molecular markers are useful for selection. For a marker to be widely useful in plant breeding, a particular marker allele must be present in all sources of the gene of interest and absent from other germplasm into which the gene of interest is to be introgressed. Seven of the 17 markers tested here seem to satisfy both criteria, with the allele exhibited by Trident conserved across all of the cultivars that are thought not to carry the *Cre8* resistance allele. For the other 10 markers, the allele exhibited by Molineux

was observed in at least some of the non-*Cre8* cultivars. This validation failure of most of the markers evaluated here (10 of 17) is not surprising, given that the initial marker discovery was based on polymorphism between Trident and Molineux, without consideration of allele frequencies across other germplasm. This indicates that many of the polymorphisms identified are varietal differences that are not universally associated with differences in CCN resistance, and it demonstrates the importance of validating linked markers across characterised germplasm. Of the seven markers that validated well here, six (*BS00009548, BS00029210, BS00010627, BS00011603, BS00011795* and *wri16*) can be screened with KASP™ technology and one (*wri15*, assaying the same SNP as *wri16*) can be screened using electrophoresis on agarose gel.

Genes for resistance against cyst nematodes have been cloned in sugar beet [15], tomato [44, 104] and potato [122] but not in any monocots. Positional cloning approaches have been used to attempt to isolate the genes responsible for CCN resistance at the *Cre1* and *Cre3* loci of wheat [32, 84]. This led to identification of two sequences with nucleotide-binding-site leucine-rich domains (NBS-LRR): one a functional gene expressed in roots and the other a pseudogene (due to a frame shift directed by a deletion). Although nematode resistance genes from other plant species (e.g. $Hs1^{pro-1}$ [15], *Hero* [44], *Mi* [104] and *Gro1-4* [122] are known to have NBS-LRR domains, there has been no definitive proof-of-function evidence published for any CCN resistance genes in wheat.

To implement a positional cloning approach for *Cre8* resistance, one would need to screen large numbers of progeny with flanking markers to identify potential recombinants. Based on the current map, this might be done with a marker from the *wri16* position and one from either the *BS00011603* or *BS00009548* position. To safeguard against the possibility that the causal gene is not actually within the selected interval, this screening might be carried out in an iterative manner. Initially, more widely spaced markers might be used. On the

proximal side, the marker *wri8* could be useful for this. On the distal side, there is no corresponding option, given that *BS00009548* is at the terminal position of the genetic map of 6BL.

If screening was done and recombinants identified, those plants and/or their progeny would need to be phenotyped for CCN resistance. This presents another challenge. With the pot-based phenotyping method that was applied here, we were not able to unambiguously classify all lines as resistant or susceptible even when 12 replications were used. Some plants that lack the resistance allele had quite low nematode counts (Appendix 3 - Online Resource S3.4: Figure S3.5). These may be 'escapes'. In any single-plant evaluation, such plants could be misclassified as carrying the resistance allele. More accurate and precise data might be obtained using other methods such as tube tests [45] or DNA-based quantification [121], but these methods would also require assessment of multiple-plant families.

Considering the rapidly expanding sequence information that is becoming available for chromosome 6B of wheat [176] and the bioinformatic resources exploiting synteny with closely related species such as barley, an alternate (or complementary) strategy for the identification of the *Cre8* resistance gene could involve the use of marker sequence information from this mapping study as the starting point for a candidate-gene approach.

The research reported here has improved the Trident/Molineux genetic linkage map by adding many molecular markers, some of which were designed specifically for this purpose. The orientation of the region of chromosome 6B that carries *Cre8* was corrected. A large number of markers in that region were found to be closely associated with resistance against CCN. Some of these markers were confirmed as diagnostic across a panel of wheat cultivars and can be used in wheat breeding as an alternative to costly and time-consuming phenotypic assays used in the resistance screening for CCN *H. avenae.*

Chapter 6

Development of materials for fine mapping *Cre8*

6.1 Introduction

In Chapter 5, the prospects for isolation of the CCN resistance locus *Cre8* through a positional cloning approach were discussed. For positional cloning, generally a large population that has gone through several meiosis events is preferred (e.g., RI lines, F_2, progeny of F_2, backcross F_1 or near-isogenic lines developed through backcrossing). Further, it is ideal to use material in which no other loci that affect the trait are segregating.

In the Trident/Molineux DH population used in the Chapter 5, *Cre8* is one of three CCN resistance loci that are segregating. The others are *QCre.srd-1B*, at which the resistance allele is from Molineux and *Cre5*, at which the resistance allele is from Trident [197]. This chapter reports the development of a large F_2 population from a cross between two Trident/Molineux DH lines: one that carries the *Cre8* resistance allele but neither of the other two resistance alleles and one that does not carry resistance alleles at any of the three loci, for use as a genetic resource for fine mapping of *Cre8*.

6.2 Methods

Based on marker genotypes in the *QCre.srd-1B* region (*wmc719* - *wPt-3950*) of chromosome 1B and the *Cre5* region (*gwm359* - *wmc177*) of chromosome 2A, Trident/Molineux DH lines that have the Trident allele at *QCre.srd-1B* and the Molineux allele at *Cre5* were selected. Out of these lines, two were selected to be crossed with each

other: one with Trident alleles in the *Cre8* region and one with Molineux alleles in the *Cre8* region.

The F_1 cross was carried out in a glasshouse in Urrbrae, South Australia, Australia. Six seeds of each line (maternal and paternal lines) were planted in plastic pots (20 cm in diameter) filled with coco peat and watered every 2 d until maturity. At spike emergence, the apical spikelet and the immature basal spikelets were removed from the maternal plants (Figure 6.1A). In each of the remaining spikelets, the central floret was removed (Figure 6.1B) and the top 1/3 of each of the remaining florets was cut off at a slight angle and emasculation was carried out by removing all the immature anthers with forceps (Figure 6.1C and D). The spikes were labeled and were individually covered with glassine envelopes to prevent cross pollination. The emasculated spikelets were kept for 2 to 3 d until the stigma became receptive (indicated by the fluffy appearance in Figure 6.1E). Fresh pollen from the donor paternal parent was applied on to the receptive stigma of the emasculated florets (Figure 6.1F and G). The spikes were again labeled and individually covered with glassine envelopes (Figure 6.1H). After several weeks, plump seeds were visible indicating successful crosses (Figure 6.1I). Plants were maintained until they were ready for harvesting and were harvested as separate heads.

Each of the F_1 seeds was planted in a plastic pot (15 cm in diameter) filled with coco peat and watered every 2 d until maturity. At 14 d after sowing, leaf tissues were collected and freeze-dried at -50 °C, under a 0.110-mbar vacuum pressure for 17 h in a Christ® ALPHA 1-2 LD freeze dryer (Martin Christ Freeze Dryers GmbH, Germany). DNA was extracted using the method described by Fox et al. [46]. To confirm heterozygosity of the F_1 plants, marker *wri15* was assayed across all the F_1 plants according to the conditions described in Chapter 5. The confirmed F_1 progeny were grown to maturity. Prior to flowering, the spikes were bagged with glassine envelopes and allowed to self-pollinate. Watering was

continued until maturity and seeds from each F_1 plant were harvested separately and were kept in a cold room (10 °C) in an airtight container.

Figure 6.1: An illustration of the crossing procedure in wheat.

Spike after removing apical and basal spikelets (A), removal of the central floret (B), spikelets after removal of the top 1/3 (C), removal of immature anthers (D), receptive stigma (E), pollen from a mature anther (F), shedding pollen on to an emasculated floret (G), a spike bagged with a glassine envelope (H) and developing seeds from successful crosses (I).

6.3 Results and Discussion

Out of 161 Trident/Molineux DH lines used in Chapter 5, two lines that carry the Trident alleles at markers near the *QCre.srd-1B* locus and Molineux alleles at markers near the *Cre5* locus were selected. One (TMDH006) has a Molineux-like haplotype throughout the

entire 6B chromosome and thus carries the resistance allele at *Cre8* (*Cre8*-carrying), while the other (TMDH082) has a Trident-like haplotype throughout the entire 6B chromosome and therefore lacks the resistance allele at *Cre8* (non-*Cre8*-carrying) (Figure 6.2).

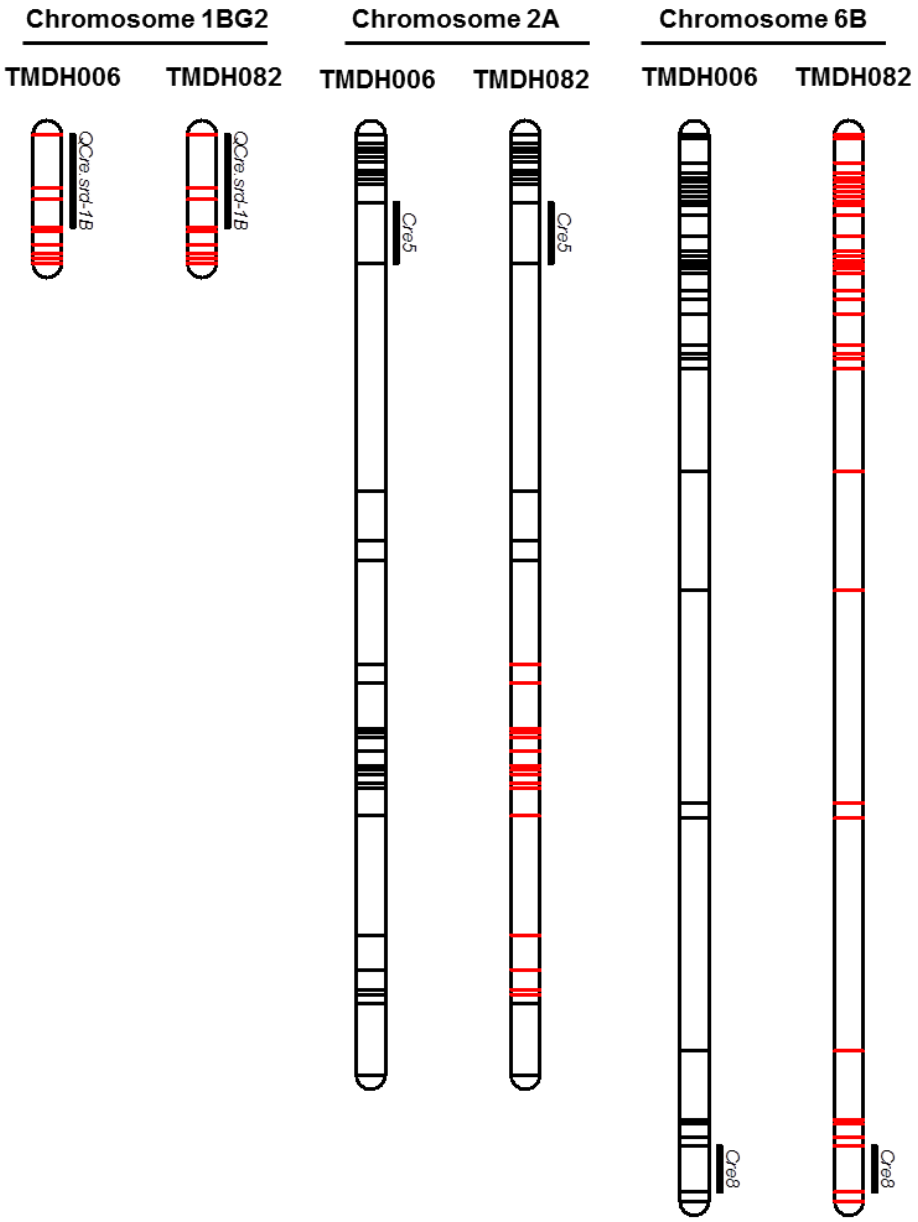

Figure 6.2: A graphical representation of the chromosome 1BG2, 2A and 6B of TMDH006 and TMDH082.

Marker positions are coloured according to the corresponding parental genotypes: Molineux-like (black) and Trident-like (red). The approximate QTL positions shown with solid bars.

Consistent with the QTL effects reported by Williams et al. [197] and in Chapter 5 of this thesis, the nematode counts observed by Williams et al. [197] were low for the *Cre8*-carrying line TMDH006 and high for the non-*Cre8*-carrying line TMDH082 (Figure 6.3A). This confirmed that these two lines are suitable as parental lines for population development. For the cross, TMDH082 was used as the maternal parent and the TMDH006 was used as the paternal parent. As these DH lines were developed from a Trident/Molineux cross, both should carry the same cytoplasm from their maternal parent Trident. Therefore a reciprocal cross was not performed to test for maternal effects.

Out of the 101 F_1 seeds from the TMDH082/TMDH006 cross, 98 provided plants that were confirmed to be heterozygous at marker *wri15* (seeds 11 and 33 did not germinate, while the genotypic data indicated that plant 28 had resulted from accidental self-pollination of the maternal parent; Figure 6.4). From the 98 F_1 plants, approximately 3300 F_2 seeds were harvested.

Thus, the confirmed F_1 plants used here permitted the establishment of an F_2 population that is large enough to be useful for fine mapping. For some traits, both phenotyping and genotyping can be done in the F_2 generation. This is not feasible for CCN resistance, because phenotyping of individual plants would not be sufficient to unambiguously assign each plant to a resistant or susceptible category. To address this issue, progeny tests will be required. Given that phenotyping for CCN resistance is costly, it would be most efficient to limit the phenotyping to the progeny of the genetically informative F_2 plants: those that carry chromosomes with recombinant haplotypes in the *Cre8* region. To identify the informative plants, one approach would be to grow all F_2 plants, extract DNA from leaf tissues and assay markers to select for the plants with recombinant haplotypes. However, this approach may require a large space to maintain the plants until the selections are

completed, and preferably until maturity (so as not to waste the genetic resource) as it is possible that the causal gene might be outside the expected region.

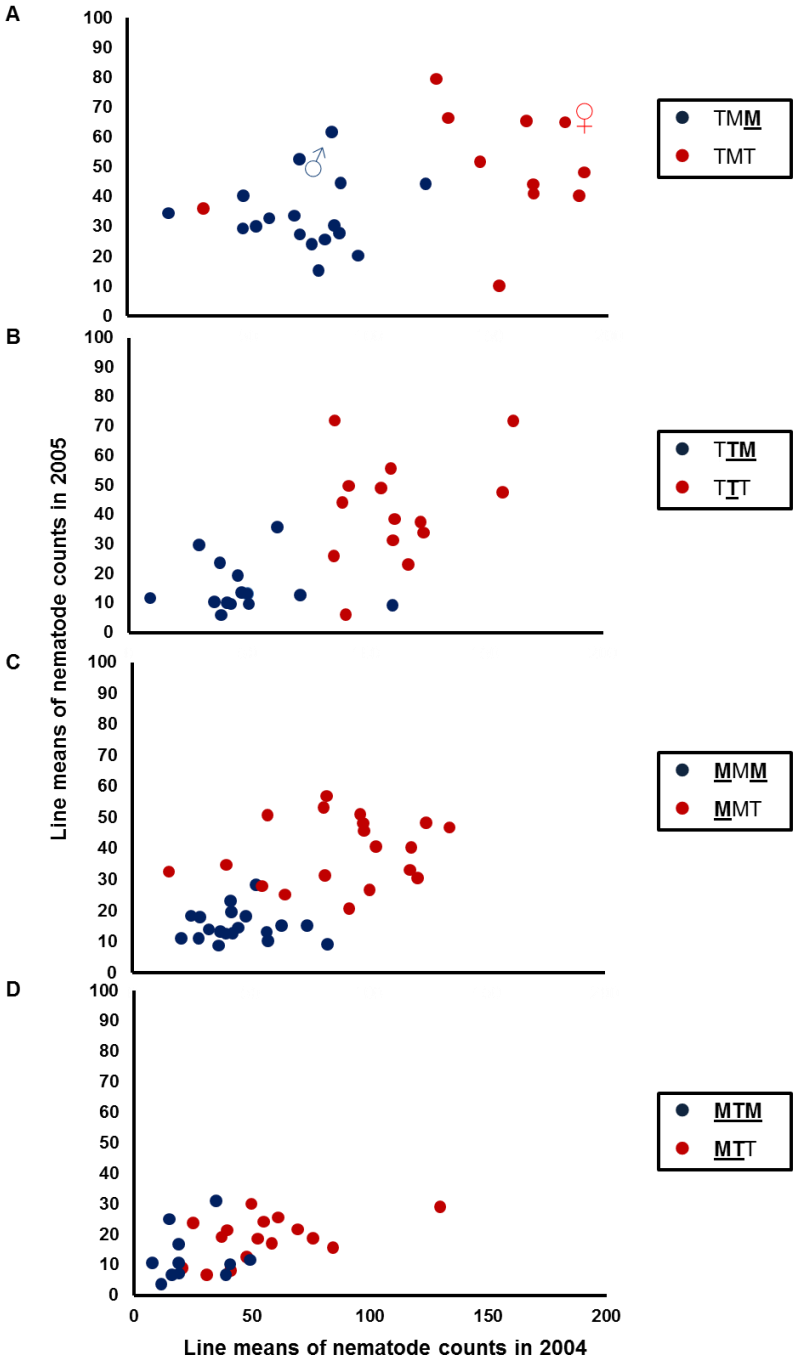

Figure 6.3: Line means of nematode counts in 2004 *versus* 2005 of 121 Trident/Molineux doubled haploid lines.

The first, second and third characters in each legend entry represent the alleles (M from Molineux or T from Trident) at *QCre.srd-1B*, *Cre5* and *Cre8* respectively. Alleles that confer resistance are underlined. ♂ - TMDH006 and ♀ - TMDH082.

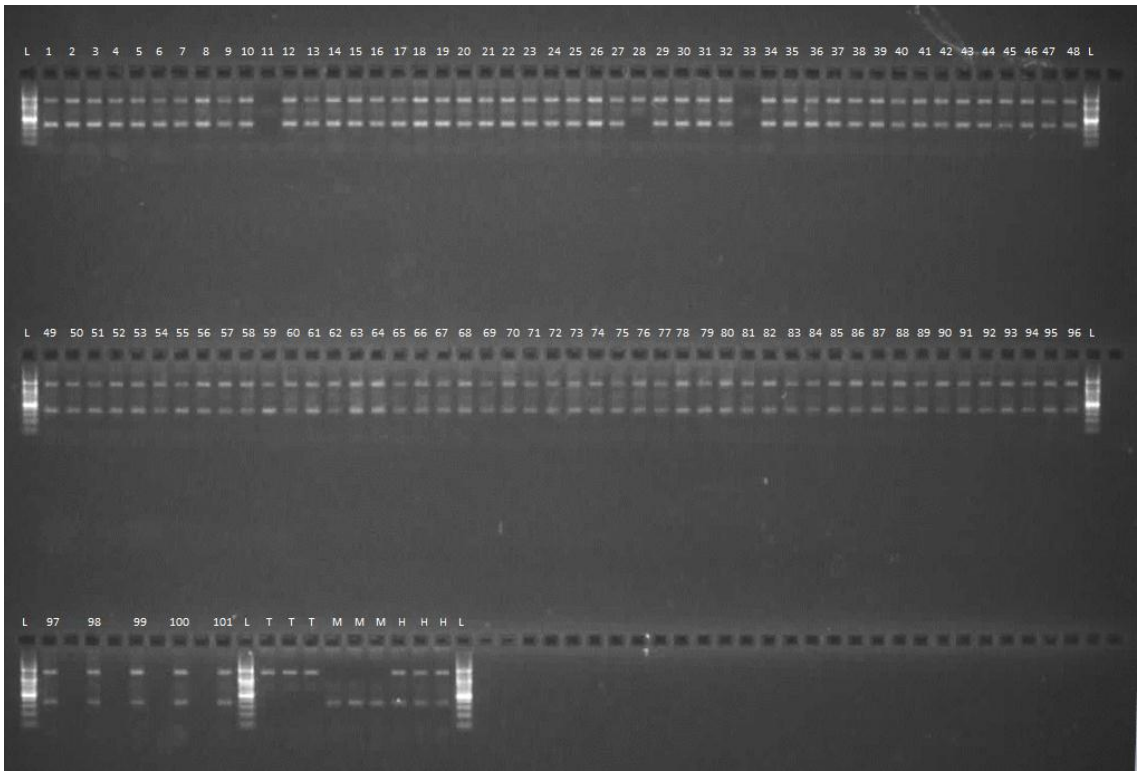

Figure 6.4: *wri15* assay on 101 F_1 progeny of a cross between TMDH082 and TMDH006.

L - GeneRuler® 100 bp DNA Ladder (Thermo Fisher Scientific Inc.); 1- 101: F_1 progeny of TMDH082/TMDH006 cross; T - TMDH082, M - TMDH006; H - artificial heterozygote (combining equal amounts of TMDH082 and TMDH006 DNA)

An alternative approach is to cut each of the F_2 seeds in half and use the non-embryo-carrying half for the DNA extraction and marker assays and retain the embryo-carrying half for future use (Figure 6.5). With an automated DNA extraction system, DNA extraction for 3300 half-seeds can be completed quite quickly. The molecular markers *wri8*, *wri16*, *BS00011603* and *BS0009548* (from map positions 147.0, 148.3, 155.1 and 156.4 cM respectively, representing the *Cre8* QTL region in the chromosome 6B linkage map of Chapter 5) could be then assayed and the marker order be further refined. Only the retained embryo-carrying half-seed of the informative recombinants (heterozygous at one flanking marker and homozygous for the Molineux allele at the other) can then be grown

to maturity to obtain $F_{2:3}$ families. If not all of the informative recombinants can be carried forward for phenotyping, preference should be given to the Molineux parental haplotype over the Trident parental haplotype.

The plants with the Molineux haplotype (*Cre8*-carrying plants) are likely to exhibit less phenotypic variation than plants with the Trident haplotype (Figure 6.3A to D). This will provide a more uniform 'control' phenotype to which the phenotypes of recombinant progeny can be compared.

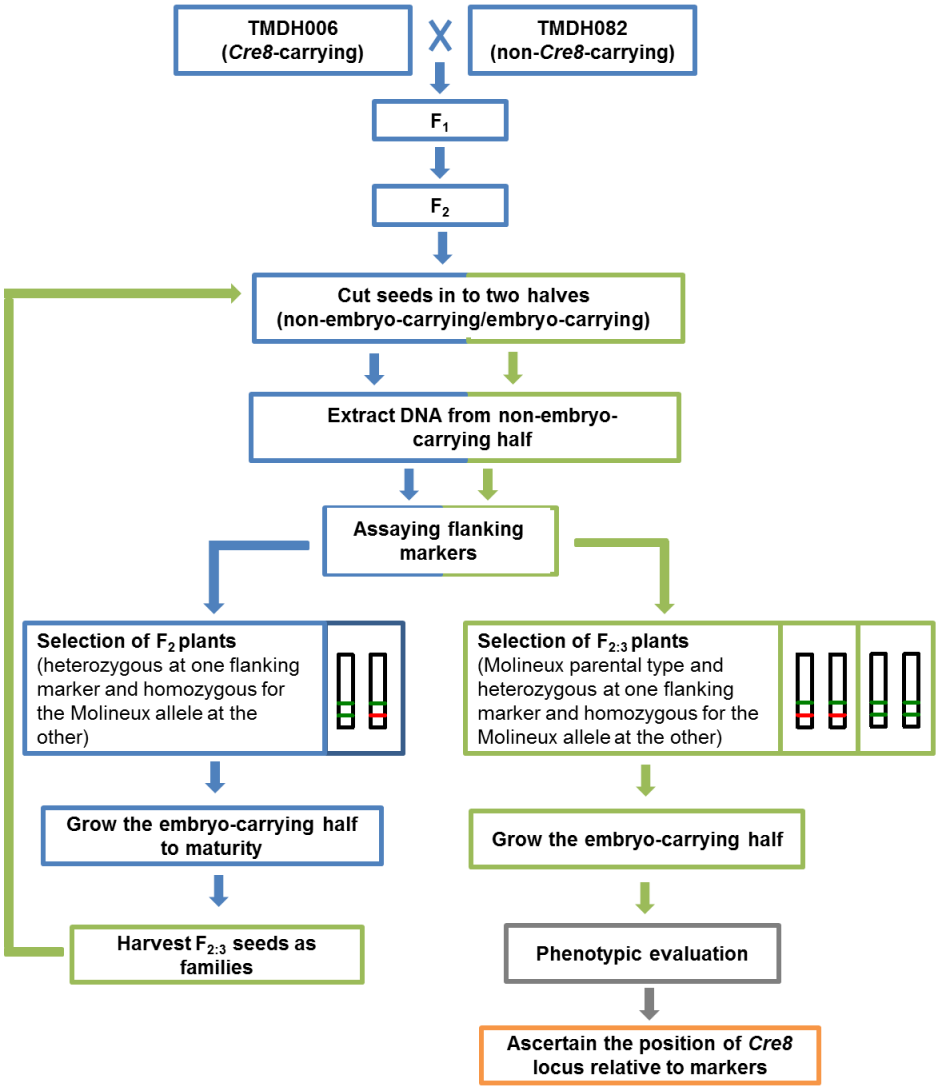

Figure 6.5: A flow diagram illustrating the population development and screening for informative recombinants.

The haplotypes of the plants in $F_{2:3}$ families could be determined by a similar genotyping approach involving half-seed DNA extraction method described above (Figure 6.5). Within each family, individuals with Molineux parental haplotype (about 8 plants) and recombinant haplotype (heterozygous for one flanking marker and homozygous for the Molineux allele at the other; about 8 plants) could be selected and the embryo-carrying halves of the seeds could be sown to grow F_3 plants in an inoculated tube test [88] to evaluate CCN resistance. Within the same $F_{3:4}$ family, higher nematode counts among the recombinants compared to the Molineux parental type plants would indicate that the causal gene may be absent in the recombinants and thus a putative location of *Cre8* could be defined in relation to recombination break-points.

The cluster of markers mapped to the most distal position of the 6BL linkage map show a very close association with the CCN resistance. As no other molecular markers are mapped beyond this point in the current map (Chapter 5), it will be important to investigate the possibility of the causal gene for resistance residing further distal in the 6BL linkage map. Other published linkage maps [6, 16] do have some markers mapped distal to the most distal markers in the current Trident/Molineux map. Some of these were tested here, but they did not exhibit polymorphism between Trident and Molineux. With the availability of whole-genome shotgun contigs for chromosome 6B [176] and the wider use of markers developed by GBS [132], it may be possible to identify polymorphic sequences that are distal to the current markers. If not, it may be necessary to develop new crosses between a *Cre8* carrying line and another parent.

One of the main advantages of using the population developed here for fine mapping (over using a line that also has other resistance genes that affect the trait) would be the fact that the phenotypic data will be reflective of the *Cre8*-derived resistance, as *Cre8* is the only major resistance QTL that segregates in this population. The approach described here

should quickly improve map resolution of *Cre8* region. The map resolution could be further improved by phenotyping and genotyping of additional progeny and/or the development of additional recombinants through further self-pollination and/or backcrossing. Further, by comparing the phenotypic data and the recombinant breakpoints of informative recombinants, a tentative position for the *Cre8* resistance locus could be estimated, relative to the molecular markers. However, the success will largely depend on whether *Cre8* itself is proximal or distal to the most distal mapped marker.
Through the IWGSC [22], a 6BL survey sequence with a 90× coverage (36 Gb) is already available [176] and the wheat chromosome 6B genome sequence assembly should be available in the near future [22, 176]. Access to genomic sequences enables identification of orthologous candidate genes through synteny to other well annotated genomes such as rice and *Brachypodium*. Before proceeding with functional analysis, the most likely candidate needs to be identified. For that, knowledge about biological pathways involved in triggering and delivering resistance responses could be very useful.

The underlying resistance mechanisms and the biological pathways involved in delivering resistance responses are poorly understood in most CCN resistance loci. Some work has been done on *Cre1* and *Cre3* resistance loci of wheat, in terms of understanding the penetration, establishment and initial development of nematodes, and/or on the initiation and development of syncytia, designated nematode feeding sites [51, 117, 154, 196]. However, no research has been reported investigating the resistance mechanisms involved with *Cre8* CCN resistance locus and the biological pathways involved in its defence responses. To begin to fill this knowledge gap, I conducted some observational work (described in Appendix 4) on nematode penetration and syncytium development in inoculated plants of the Trident/Molineux DH lines TMDH006 (*Cre8*-carrying) and TMDH082 (non-*Cre8*-carrying). It was observed that initial penetration of the nematodes and their early development and/or the initiation and early development of the syncytia (up

to 18 d after inoculation) happened successfully in both lines. However, as sampling was not carried beyond 18 days after inoculation, no definitive conclusion could be drawn as to whether the effect of the *Cre8* resistance locus is to trigger defence responses such as extensive vacuolation, lowered protoplasm activity and degradation of syncytia, all leading to nutrient deprivation in developing nematodes, as seen in root tissues carrying *Cre1* or *Cre3* CCN resistance loci. The knowledge gained through root response studies could be important in understanding the key changes associated with these resistance loci and will provide insight to identify potential candidates for isolation of the *Cre8* resistance gene(s) *via* a candidate gene approach.

Due to time restrictions defined by the PhD candidature, neither fine mapping of the *Cre8* region using the developed F_2 mapping population nor further examination of root responses of *Cre8* and non-*Cre8* lines was undertaken. The population will be an important resource in future attempts of fine mapping the *Cre8* resistance locus and the initial results that are presented in Appendix 4 provide a basis for the design of future experiments to investigate the *Cre8* resistance mechanism.

Chapter 7

General discussion

The RLN genus *Pratylenchus* and the CCN genus *Heterodera* are capable of causing significant yield loss when proper control strategies are not in place. The research reported in this thesis was on the *P. neglectus* resistance locus *Rlnn1* and *H. avenae* resistance locus *Cre8* in wheat.

7.1 Genetic mapping of the nematode resistance loci *Rlnn1* and *Cre8*

Use of genetic resistance is very important to keep nematode densities below the economic threshold levels. The research reported in this thesis was aimed at fine mapping of the *Rlnn1* and *Cre8* resistance loci, to identify diagnostic markers for MAS and as an initiative towards positional cloning.

Prior to this thesis research, *Rlnn1* had been mapped to the distal end of chromosome 7AL using Excalibur/Kukri DH lines [200] and *Cre8* had been mapped to the distal end of 6BL using Trident/Molineux DH lines [197, 199]. At the beginning, the prospects for fine mapping the *Rlnn1* resistant locus seemed much better than those for *Cre8*, due to the fact that 1) new markers targeting the distal end of 7AL could be developed using the chromosome 7AL sequences that were already available at the time (e.g., Chinese Spring syntenic build for chromosome 7A though the IWGSC Wheat Genome Database [29] and whole-genome shot-gun sequences of Excalibur and Kukri though Bioplatforms Australia [7, 41]) and 2) there was a large fine mapping population (Excalibur/Kukri $F_{4:5}$ RI lines) readily available for use. Chromosome 6BL sequencing was not as advanced at the time

and no large mapping population was available for fine mapping of *Cre8*. Therefore at the beginning of the candidature progress in fine mapping of *Cre8* was expected to proceed at a slower pace compared to *Rlnn1*.

For Excalibur/Kukri, improvements to the linkage map were targeted only at the chromosome 7A, because a map with good genome-wide coverage was already available [42]. The targeted approaches reported in Chapters 3 and 4 included selecting and assaying markers that had been mapped to 7AL in other population maps [6, 16, 26], marker databases [4, 30], ESTs [27, 171] or were designed based on sequences selected from the distal end of the Chinese Spring chromosome 7A syntenic build [29, 85] or were designed based on the Excalibur and Kukri polymorphisms detected based on the chromosome 7AL shot-gun sequences [7, 41]. This targeted approach substantially improved the Excalibur/Kukri chromosome 7AL linkage map (Chapters 3 and 4).

In contrast, at the outset of the project the Trident/Molineux linkage maps had a low coverage with just RFLP and SSR markers. Even though the Trident/Molineux DH lines had been genotyped for DArT® markers, two EST-based markers and several SSR markers, a well curated linkage map was not available. In the research reported in Chapter 5, the Trident/Molineux genetic linkage map was improved by adding new markers throughout the genome. As the emphasis of the thesis research was on the distal end of chromosome 6BL, the 6B linkage map was further improved by implementing a targeted approach of selecting markers that had previously been mapped to chromosome 6BL [6, 16, 26] and by designing new markers using an EST-based approach [27, 171]. A sequence-based approach was not feasible for chromosome 6B as the IWGSC [22] chromosome 6B sequences were only made available to public recently and are still not available as an assembly to target the region of interest [176].

Through new marker technologies such as the 90K-iSelect array for wheat [189], the 820K-Axiom® Wheat Genotyping array (Affymetrix, Inc., USA) and genotyping-by-sequencing (GBS; [132]) very large numbers of markers can be mapped to improve regions of interest. During the course of this research, GBS data were obtained for the 182 Excalibur/Kukri lines used in the Chapters 3 and 4 (Diane Mather and Ken Chalmers, unpublished data), but by the time these data were obtained, the lack of recombination in the *Rlnn1* region of 7AL in Excalibur/Kukri materials, was already evident. Accordingly, development of additional molecular markers for this region seemed unlikely to be informative. In contrast, for the *Cre8* resistance locus, there is no indication of suppressed recombination and thus, high-density mapping technologies could be used to fill the 'gap' region proximal to the *Cre8* QTL peak (Chapter 5) and to look for markers that may map distal to the current terminal marker cluster (Chapter 5). If successful, any new markers that map to the distal end of the 6BL linkage map could assist in refining the marker order and the position of the *Cre8* QTL.

A high-quality genetic linkage map is a necessity for accurately defining a QTL position and its effects. Quality control can improve the accuracy of the linkage maps. Incorrect genotypic calls can lead to apparent double recombinants and affect the marker order and overestimate the map distance by increasing the distance around the particular marker region. If the marker with incorrect genotypic calls is near the QTL such artefacts further affect the accuracy of the QTL position and effect estimates. Another issue that can affect the accuracy of a linkage map is the presence of genetically identical or highly similar line(s), as a result of accidental duplication of lines. Inclusion of more than one copy of a particular line will lead to overestimation of genetic distances in regions in which that line is recombinant and to underestimation of genetic distances in regions where the lines is not recombinant. Taking these issues into account, some quality control measures were adopted here. Markers with very high missing genotypic calls, suspected DNA

contamination, ambiguous genotypic calls and markers with segregation distortion were removed. The lines with identical or very similar genotypes were replaced by a single 'consensus line'.

These stringent quality control measures improved the current linkage maps of Excalibur/Kukri and Trident/Molineux. Even though the Excalibur/Kukri genetic linkage map of Edwards [42] was well curated, there were a few markers with ambiguous data calls near the *Rlnn1* QTL region. In the research conducted for this thesis, these were identified through examination of pairwise recombination fractions and LOD linkage plots. These markers were re-assayed and the genotypic errors were corrected. To improve the quality of the curated map, several other markers that could not be readily re-assayed were removed due to ambiguous data calls and others due to high missing values (e.g, RFLP and DArT™ markers). Several DH lines had to be removed as a result of DNA contamination and mix-ups. Further several sets of genetically similar lines (26 sets including 43 lines) were identified and were replaced with consensus lines for each set, which improved the accuracy of the genetic distances, QTL effect estimates and refined the QTL position.

Similarly, in the Trident/Molineux DH population dataset there were markers with large number of missing data points (e.g, RFLP and SSR) and ambiguous allele calls (due to genotypic errors or as a result of contaminated DNA). In the Trident/Molineux linkage map, the stringent curation criteria led to removal of five of the six markers mapped to chromosome 6B in the original map [197]. That, along with the addition of new markers to chromosome 6B, made it possible to correct the orientation of the distal region of the chromosome and to map the *Cre8* QTL to the distal end of 6BL.

In genome-wide linkage and QTL mapping with large populations and large genotypic and phenotypic datasets, minor errors such as duplication of a few lines or mis-scoring of a few genotypes are unlikely to substantially affect the results. However, when fine mapping a

particular QTL, stringent quality control as adopted above is critical. If not, it will largely affect the accuracy of fine mapping and the subsequent cloning attempts.

The mapping of the *Rlnn1* resistance locus to the distal end of 7AL, using Excalibur/Kukri DH lines (in Chapter 3), is the first report of mapping of the *Rlnn1* locus as a QTL in a single large bi-parental mapping population, without classification of lines into resistant and susceptible categories. The use of a large single biparental population as opposed to combining information from few smaller populations avoided artefacts that can be created as a result of a consensus mapping approach. Further with a trait such as resistance against *P. neglectus* it is difficult to accurately categorise lines as resistant or susceptible, mainly due to the variability of trait data (even with many replicates as seen in Chapter 4). As a result misclassification of some lines is very likely and this can affect the overall accuracy of the analysis.

In Chapter 5, all three expected QTL (*Cre8, Cre5* and *QCre.srd-1B*) initially mapped by Williams et al. [197], were detected and their QTL effects were estimated accurately using a CIM approach. Even though the main interest was in the locus on chromosome 6B, the Trident/Molineux genetic linkage maps of the rest of the chromosomes were also improved as a result of adding new molecular markers. Although this would be outside of the scope of this thesis, this could present opportunities to refine the positions of other trait QTL such as milling yield and baking quality traits previously reported by Kuchel et al. [83].

In Australian wheat breeding programs and national variety trials, regular screening for resistance against RLN *P. neglectus* and CCN *H. avenae* is done to assess resistance levels of currently grown cultivars, in newly developed cultivars and in advanced breeding lines. The phenotypic assays for nematode screening are costly, labour intensive and time consuming. Markers had been implemented to some extent, but the available markers had limitations. Therefore the development of new diagnostic markers was important. The

research reported in this thesis resulted in several molecular markers that were recommended for MAS of resistance loci *Rlnn1* and *Cre8*. These markers were confirmed to be diagnostic across a panel of wheat cultivars that are at least moderately resistant to the nematode of interest (*P. neglectus* or *H. avenae*) and/or were known to carry the resistance allele at the particular nematode resistance loci (*Rlnn1* or *Cre8*). In the current thesis five markers were recommended for the use in MAS of *Rlnn1* (*wri2, wri3, wri27, wri28* and *wri29*) and seven markers were recommended for the MAS of *Cre8* (*wri15, wri16, BS00011603, BS00010627, BS00011795, BS00009548* and *BS00029210*).

These markers allow faster screening of the progeny of parents that carry the *Rlnn1* or *Cre8* resistance, at a much lower cost than phenotypic assays. This enables researchers and breeders to do phenotypic evaluations only when they are absolutely necessary, such as for discovery of new sources of resistance, verification of the resistance of advanced lines, descriptions of new cultivars and assessment of the informative recombinants during fine mapping.

7.2 Towards cloning of *Cre8*

Most of the markers mapped in the *Cre8* QTL region cosegregated with one or more other markers in the Trident/Molineux DH mapping population. With a large fine mapping population, it might be possible to find more informative recombinants to separate some of these clustered markers, to achieve a better map resolution and a marker order for the *Cre8* region. This would also be an initial step towards map-based cloning of the *Cre8* resistance locus. In Chapter 6 of the thesis, I reported the development of genetic material for fine mapping *Cre8*. There are many different types of mapping populations that can be used for fine mapping. The material that I developed is based on a cross between two DH lines: one carrying the *Cre8* resistance allele and the other carrying the susceptible allele. Apart from

carrying opposite alleles on chromosome 6B, the two DH lines lack the resistance alleles at the *Cre5* and *QCre.srd-1B* loci, and thus the progeny of the cross will segregate for *Cre8* but not for either of the other resistance loci. The F_2 seeds produced are now being used to fine map the *Cre8* QTL region and revise the marker order according to the method described in Chapter 6. Progeny of these informative recombinants will be phenotyped to more precisely map *Cre8*. One disadvantage of this early-generation approach is that there are fewer opportunities for recombination than in materials with more recombination history such as RI lines. However, the screening of a large F_2 population (~ 3300 plants) and the following generations, will give greater opportunity to capture potential recombinants early than waiting for the development of advanced-generation RI lines.

Once the *Cre8* region is fine mapped and is anchored to assembled genomic sequence, there may be multiple candidate genes that seem worthy of investigation. An understanding of the biological pathways involved in conveying resistance could be important for narrowing down the choice of candidate genes for functional analysis. Three resistance genes against cyst nematodes have been cloned in dicots ($Hs1^{pro-1}$ for resistance to sugar beet cyst nematode (*Heterodera schachtii*) [15], *Hero* for resistance to potato cyst nematode (*Globodera rostochiensis*) in tomato [44] and *Gro1-4* in potato [122]). The *Hero* gene is not similar to any known gene, but it includes a coiled-coil NBS-LRR domain (CC/NBS/LRR resistance gene class) similar to many other reported disease resistance genes [44]. In a transgenic tomato plant expressing the *Hero* gene, cells adjacent to the tracheal elements were necrotised, preventing the syncytium from encroaching into xylem tissues [35]. This isolation of the syncytia leads to the degradation of syncytial nuclei, followed by the degradation of the syncytium itself due to lack of sufficient nutrients. This leads to a nutrient deficit environment that is unfavourable for the growing juveniles [35]. The condition induces an imbalanced sex ratio, as under poor nutrient availability the juveniles morph into males rather than females. The *Hero* gene is expressed in all tissues,

but its expression is upregulated in the roots upon nematode infection, and the timing coincides with the degradation of syncytia [35]. The *Hs1*$^{pro-1}$ gene has an imperfect leucine-rich region and a putative transmembrane domain, but it does not belong to the NBS-LRR class or any other known plant resistance gene categories [15]. Similar to *Hero*, *Hs1*$^{pro-1}$ is thought to exert resistance through degradation of syncytia, however, the mechanism is different from that of *Hero*. In *Hs1*$^{pro-1}$ carrying lines, the syncytia degradation involves processes within the structure of the syncytium [67]. The mechanism is suspected to have a relationship to membrane aggregations observed exclusively in lines carrying the *Hs1*$^{pro-1}$ gene. These membrane aggregations are thought to be formed by degradation of the endoplasmic reticulum [67]. The *Gro1-4* gene contains Toll-Interleukin 1 receptor, NBS and LRR domains (TIR/NBS/LRR resistance gene class) [122]. To my knowledge no response studies have been done on the *Gro1-4* gene.

In wheat, candidate genes have been proposed for the homeologous loci *Cre1* and *Cre3* [84], but functional analysis of these genes was not discussed and it is not clear whether these are the only potential causal genes in the region. One of the two candidate sequences is from a pseudogene and the other encodes a polypeptide that is expressed in roots. Both contain cytoplasmic NBS-LRR domains [32, 84]. The resistance responses of *Cre1* and *Cre3* are thought to be involved in early degradation of syncytia in resistant lines (discussed later in this Chapter) [51, 154, 196].

The chromosome 6B survey-sequence assembly should be available soon through the IWGSC [22, 176]. As described in the Chapter 4 of this thesis, markers that are closely associated with the *Cre8* nematode resistance QTL could be anchored on to the chromosome 6B survey-sequence assembly. This will give the opportunity to retrieve genomic sequences from the targeted region for the development of new molecular markers to further improve the marker density at the *Cre8* region for fine mapping and

refine the marker order and QTL position further. In addition often genome assembly is likely to be annotated based on similarities to orthologous genes [29, 85] and/or the orthologous genes for specific sequences can be found using a comparative genomics approach. This should make it possible to narrow down the choice of candidate genes based on their functional relatedness to nematode resistance. Given that most genes reported for cyst nematode resistance carry the NBS-LRR domains, such features may be important to narrow down the choice of candidates genes for functional analysis..

Since Chinese Spring is the cultivar used for the development of the IWGSC assemblies, it will be important to know the resistance state of Chinese Spring against CCN *H. avenae*. Given that Chinese Spring amplifies a chromosome 6B-specific product similar to that of Molineux, for the diagnostic marker *wri16* (Chapter 5), it is possible that Chinese Spring carries the resistance allele at the *Cre8* resistance locus. In order to confirm the resistance status, I recommend phenotyping Chinese Spring for resistance against CCN *H. avenae.*

7.3 Suppressed recombination at the distal end of chromosome 7AL in Excalibur/Kukri genetic material

Although Neu et al. [114] had suggested a suppressed recombination at the distal end of 7AL in materials with *Lr20/Pm1* resistance, Williams et al. [200] estimated that the *Rlnn1* resistance locus and the SSR marker *gwm344* are distal to *Lr20* by 9.1 and 13.6 cM, respectively. It therefore seemed unlikely that *Rlnn1* would be within the region of suppressed recombination. Once the Excalibur/Kukri population was phenotyped for resistance against *P. neglectus* and the rust pathogens *P. triticina* and *P. graminis* f. sp. *tritici* and *Lr20*/*Sr15* loci were mapped, it became clear that the region of interest for resistance against *P. neglectus* is exactly the same as the one studied by Neu et al. [114].

The results presented in Chapter 4 of this thesis provide considerable additional evidence for suppression at the distal end of 7AL in materials for which one parent (Excalibur) carries the resistance alleles at *Lr20, Sr15* and *Rlnn1*: 1) assaying markers/genes from the 'terminal cluster' on a larger Excalibur/Kukri RI population revealed no natural recombinants; 2) evaluating a large number of Excalibur/Kukri RI lines for resistance against *P. neglectus* revealed no recombinants between the *Rlnn1* locus and *wri2* marker; 3) comparing the map position of markers mapped to the 'terminal cluster' (in Excalibur/Kukri linkage map) with other published maps revealed that some common markers are mapped as separate loci; and 4) anchoring of the 'terminal cluster' markers to the Chinese Spring syntenic builds revealed that most markers were physically mapped to different positions. These findings strongly indicate suppressed recombination in the *Rlnn1* region. Based on the findings reported in Chapters 3 and 4, the suppressed recombination is limited to Excalibur and to other cultivars that carry the resistance alleles at *Rlnn1*, *Lr20*/*Sr15* and the *Psy-A1t* allele for 'very yellow' flour colour. In the linkage block in which recombination is suppressed, there are several genes that are of interest to breeders. Thus investigating the genetic phenomenon that lead to this suppressed recombination may have broader implications than just breeding for RLN resistance.

Suppressed recombination in chromosomes can happen due to various genetic phenomenon including chromosomal rearrangements such as translocations or inversions or due to deletions or duplications of chromosomal segments [49]. Out of these possibilities, the results presented in Chapters 3 and 4 mostly support a translocation at the distal end of chromosome 7AL.

7.4 A translocation at the distal end of 7AL?

Wheat has a long evolutionary history that involved two separate hybridisation events that occurred over a long time period. The progenitors of A, B, D and S genomes (*Triticum* and *Aegilops*) of cultivated wheat radiated from each other between 2.5 and 6 million years ago [17, 72]. Less than 0.5 to 3 million years ago, as a result of a hybridisation between *T. urartu* (A^uA^u) and B-genome progenitor(s), tetraploid wild Emmer wheat *T. turgidum* (A^uA^uBB) emerged. Emmer wheat was domesticated around 10,000 to 12,000 years ago. Around 8,000 years ago, the hybridisation of domesticated Emmer wheat with *Ae. tauschii* (DD) resulted in the hexaploid wheat *T. aestivum* (AABBDD) [72]. A translocation in wheat can be an ancient one that is present in some or all wheat cultivars or it can be more recent as a result of an intergeneric (between genera)/interspecific (between species)/intraspecific (within species) crossing. Therefore an observed translocation could have occurred within the history of modern wheat breeding or at any time in the last 8,000 years of wheat evolution or it could have pre-dated hexaploid wheat and could have occurred in one of its diploid or tetraploid progenitors.

Although translocations are rare events, several have been identified in modern wheat. Most identified translocations are telomeric [47]. The cyclic translocation of chromosome 7BS-5AL-4AL in all wheat is an ancient translocation involving wheat chromosome group 7 [93, 113]. More recent translocations involving group-7 chromosomes include translocations of the leaf rust resistance gene *Lr19* from *Agropyron elongatum* to wheat chromosome 7DL [148] and the leaf rust resistance gene *Lr47* and the greenbug resistance gene *Gb5* both from *Ae. speltoides* [37] to chromosome 7A. These resulted from deliberate intergeneric crosses performed on selected lines and they are present only in materials derived from those crosses. In contrast, *Lr20* is known to be present in a large number of wheat cultivars that are not known to be derived from any deliberate interspecific or

intergeneric crossing, and that have not been traced back to any common ancestor in modern wheat breeding. Accordingly, it seems unlikely that the suppressed recombination observed in Excalibur and other cultivars discussed in Chapter 4 is due to a translocation introduced by deliberate intergeneric/interspecific/intraspecific crossing.

If a translocation occurred naturally then it could have been (1) an intergenomic translocation within hexaploid wheat or a tetraploid ancestor or (2) an intergeneric/interspecific/intraspecific translocation following a natural outcrossing event. To my knowledge, the segment is present only in some hexaploid wheat and is not known to be present in any tetraploid wheat. Although this favours the possibility of a translocation taking place after hexaploidation, it is also possible that the translocation occurred prior to hexaploidisation or even prior to tetraploidisation, and was present in some but not all of the ancestors that participated in ancient hybridisation, and was passed on to only some lineages of wheat through ancestral allele sorting.

Based on the results reported in this thesis it seems likely that a translocation at the distal end of 7AL in Excalibur is the underlying cause for the suppressed recombination. The evidence can be summarized as follows:

a. Although Excalibur's *Psy-A1t* allele genetically maps to chromosome 7AL, its sequence is very different from other *Psy-A1* alleles

   In the phylogenetic analysis reported in Chapter 4 and by Crawford et al. [24] on the *Psy1* alleles of wheat and close relatives, the *Psy-A1t* allele was found to be more closely related to the *Ae. speltoides* S genome alleles and to some wheat B genome alleles, than to the A genome alleles from chromosome 7A to which it was genetically mapped. A translocation from a 7B-like chromosome carrying the *Psy-A1t* allele could have led to this phenomenon. The origin and the time at which the translocation occurred remain unknown.

To trace back the origin of the translocation it can be recommended to genotype all known cultivars that carry the *Lr20* gene, with *Psy-A1* and other markers mapped to the region, to see if they carry the Excalibur-like haplotype. It is also recommended to evaluate those cultivars for resistance against *P. neglectus* to estimate their level of resistance.

b. The amplification of an additional 7B-like product from Excalibur for the marker *AWW5L7*

As reported in Chapter 4 of this thesis, the *AWW5L7* amplifies two products from Excalibur, one of which was not polymorphic between Excalibur and Kukri but was confirmed to be specific to 7BL using nullisomic-tetrasomic stocks. The other (somewhat longer) product was amplified from Excalibur but not from Kukri. Mapping of this polymorphism assigned this product to the 'terminal cluster' of 7AL (not to the expected position of marker *AWW5L7* on chromosome 7BL [152]). The 7B-specific smaller fragment in Excalibur is amplified by both Kukri and Cranbrook and is probably from the chromosome 7B itself. The longer product from Excalibur, has similarities to the product from the Halberd, but shows length and SNP polymorphisms. Thus, it is likely to be 1) an intraspecific translocation from a 7B chromosome of an ancestor related to Halberd or 2) an interspecific/intergeneric translocation from a 7B-like donor. The *Psy-A1* phylogeny of Chapter 4 and of Crawford et al. [24] indicated that the B-genome progenitor *Ae. speltoides* may be a possible donor. Accessions of *Ae. speltoides* could be screened to determine if *AWW5L7* marker amplifies the longer Excalibur product and a cytogentics approach could be used to screen for putative translocations between the A genome and *Ae. speltoides*. The marker *AWW5L7* did not amplify the longer Excalibur product for the *Ae. speltoides* the accession AEG357-4 and genomic *in-situ* hybridisation images with *Ae. speltoides* (PBI

cytogenetic stock C64.69) used as a probe detected no putative A-B translocation with *Ae. speltoides* (Peng Zhang, personal communication).

The sequence from Excalibur had no significant BLAST hits to any of the sequence databases that are currently available including the survey sequences of Chinese Spring chromosomes at IWGSC and sequences of wheat close relatives at IWGC [22]. It is not surprising to see that no hit was found in IWGSC sequences as the variant is not expected to be present in the cultivar Chinese Spring that was used to generate the sequences. The variant may not have had significant hits to other databases, either because it did not originate from those genera or because the region is still not adequately represented among currently available reads. Through IWGSC and IWGC [22], more complete sequence assemblies will be available for wheat and other related species in the near future and thus it will be important to update the BLAST search as new sequence resources/assemblies get available.

c. Unique amplification patterns observed in the markers mapped to the 'terminal cluster'

Among the markers that were mapped to the 'terminal cluster', there were codominant markers that amplify products from both Excalibur and Kukri and dominant markers that amplify a product from Kukri only and those that only amplified a product from Excalibur. Most markers in the group that amplified products from Kukri only were derived based on Chinese Spring sequence information. In contrast, the few markers that amplified a product from Excalibur only were derived based on sequences from cultivars that are known to carry resistance allele at *Lr20* and the 'very yellow' flour colour allele at *Psy-A1*. This implies that Excalibur has a unique sequence, which is different to that of both Kukri and Chinese Spring that carry the susceptibility allele at *Lr20* and the paler

flour colour alleles at *Psy-A1*. Among the 'terminal cluster' markers are the chromosome 7A-specific codominant markers *Psy-A1* and *wri2*. The amplification of products from both Excalibur and Kukri indicates that the sequence at chromosome 7AL in Excalibur is not completely alien, but should be coming from a genome that is chromosome 7-like.

In regions proximal to the 'terminal cluster' all three types of markers (with fragments amplified by either or from both Excalibur and Kukri) were found. Interestingly, there were dominant markers derived from Chinese Spring sequences that amplified a product from Excalibur. Thus, the unique amplification patterns of the 'terminal cluster' markers suggest a translocation at the distal end with a chromosome 7- like genome.

d. FISH images that show a putative unknown translocation at the distal end of Excalibur which is absent in Kukri.

   In Chapter 4 a FISH-based cytogenetic approach was taken to explore if a putative translocation can be visualized in Excalibur that is not present in Kukri. One such chromosome pair with a putative translocation at one of the distal ends was present in the Excalibur FISH images (that was absent in Kukri). However, with a FISH approach it is not possible to narrow down the putative chromosome.

As supported by the above evidence it is most likely that the suppressed recombination is a result of a translocation. However, further research needs to be done to test the current theory. In the meantime it is important not to discard other possibilities prior to a proper investigation.

7.5 Other possibilities

Inversions are not common in the wheat genome. One example of an inversion is on the short arm of chromosome 4A, which carries a pericentric inversion [113]. However, due to the lack of recombination among the markers in the terminal marker cluster, it is not possible to compare the marker order to other maps, and this makes it impossible to know whether the part of the region is inverted. Other possibilities include deletion or duplication of a chromosomal segment at the distal end of 7AL. As mentioned above the terminal cluster did carry markers that amplify products from Excalibur, thus the distal region does carry chromatin in Excalibur and therefore a deletion of the entire region can be ruled out. Further, no explicit evidence was present to suggest a duplication of a chromosome segment at the distal end. As summarised above, the findings of the current thesis support a translocation theory. It seems likely that the suppressed recombination is due to a translocation at the distal end of 7AL.

7.6 Future prospects for *Rlnn1*

Further investigations need to be carried out to determine whether the suppressed recombination at the chromosome 7AL is a result of a translocation and to figure out its origin and extent. Some of the suggestions are as follows:

a. Other cultivars carrying the resistance alleles for *Lr20/Sr15* and their common ancestors could be assayed with the cs*PSY* marker [70] and with the proposed diagnostic markers for *Rlnn1* to find out which alleles they carry.
b. Further upgrading the *Psy1* phylogeny by looking at a wider range of *Triticeae* species (ones that are compatible to cross with wheat or *T. urartu*) could be important to deepen the understanding about the origins of the alleles in the 'mixed-clade'.

c. The FISH approach taken in the current analysis, is only capable of detecting putative A-B translocations, but is unable to pin-point on which chromosome the translocation has occurred. FISHIS (Fluorescent *In-Situ* Hybridization in Suspension) is a more recently introduced method that enables successful hybridisation of the fluorescent probes with the denatured target DNA in a suspension [50, 95]. This coupled with chromosome flow-sorting can separate chromosomes in high purity [50, 95]. The FISHIS approach combined with chromosome flow-sorting could be used to separate the 7A chromosomes of Excalibur and Kukri in high purity and then FISH labeling can be done to investigate possible translocations.

d. Over the course of this research, 25 *Rlnn1* 'sister-lines' were identified (Chapter 4). These were useful in confirming the effect of *Rlnn1*. It was hoped that heterozygotes identified from the same families would be useful for fine mapping, but this was not pursued due to the suppressed recombination. However, given that the members of each pair of 'sister-lines' are known to differ in the region of interest, they could provide a useful resource through next generation sequencing to identify additional sequence variants and potentially a candidate gene.

   The first step would be to choose the most appropriate pairs of 'sister-lines'. This could be done by assaying markers from the distal end of 7AL representing other clusters that were not included in initial genotyping in Chapter 4. A pair that has the smallest possible region of polymorphism on the distal end of 7AL will be identified. To direct the focus on to chromosome 7A, FISHIS could be applied to each of the two lines followed by flow-sorting to recover purified chromosome 7A DNA. Genomic DNA of each 7A chromosome of each of the two lines could be sequenced using a next generation sequencing method and through bioinformatics analysis polymorphic sequences could be identified, including presence/absence

polymorphisms given the possibility that the gene itself may be present in only one member of the pair. Bioinformatic approaches could then be applied to the sequences that may be associated with resistance to narrow down the candidate sequences for functional analysis. To my knowledge no RLN resistance genes have been cloned, but several cyst nematode resistance genes have been successfully isolated (isolation of *Mi* from tomato and *Hero* and *Gro1-4* from potato and an attempt on isolating the CCN resistance genes *Cre1* and *Cre3* genes of wheat [32, 44, 84, 104, 122]). However, no causal genes have been confirmed. As discussed before the cloned regions contained NBS-LRR domains (e.g. $Hs1^{pro-1}$ [15], *Hero* [44], *Mi* [104], *Gro1-4* [122], *Cre1* and *Cre3* [32, 84]).Many plant disease resistance genes contain NBS-LRR domains. The Chinese Spring chromosome 7A syntenic build has revealed many syntenic *Brachypodium* genes containing NBS-LRR domains at the regions corresponding to the *Rlnn1* QTL [29, 85]. Once the region of interest is narrowed down, these genes may be a good starting point to look for candidate genes.

For *P. thornei* it has been reported that in resistant wheat 1) the nematode egg deposition was significantly lower, 2) hatching inhibitors lowered the nematode multiplication rate, 3) the nematode maturation was suppressed and 4) the migration and motility of the nematodes were significantly affected [92]. Thus, for *P. thornei*, resistance was not triggered at root penetration stage, but occurred after penetration *via* genes that affect suppression of reproduction, secretion of hatching inhibitors, suppression of nematode migration and motility and suppression of juvenile maturation [92]. In CCN, it has been shown that resistance was associated with early degradation of syncytia leading to nutrient deprivation, which affects the maturation of nematodes [154, 196]. To my knowledge no research has been done to understand the factors affecting *P. neglectus* resistance in wheat.

While it may be a good starting point, there is no reason to think that the resistance mechanisms exerted by *P. thornei* and the cyst nematodes will be applicable for *P. neglectus*. Thus, as a result of poor understanding about the defence responses of wheat against *P. neglectus*, specific target genes and mechanisms cannot be recommended at the time.

e. The *Ph1* gene on chromosome 5B prevents the pairing of non-homoeologous chromosomes from pairing during meiosis [185]. If a chromosome carries alien chromatin, the *Ph1* gene action will prevent the chromosome pairing and thus results a suppressed recombination. If this was the reason for the suppressed recombination in Excalibur, a mutated *Ph1* gene should reverse the situation and allow recombination to happen between Excalibur and Kukri. Thus, I recommend a cross between a *Ph1* mutant line, which is carrying the susceptibility allele at *Rlnn1* ($Ph^-/Rlnn1^-$) to be crossed to Excalibur ($Ph^+/Rlnn1^+$). The F_1 progeny of the above cross can be selfed to get the F_2 population. The homozygous F_2 lines carrying the Ph^- ($Ph^-/Rlnn1^+$ and $Ph^-/Rlnn1^-$) can be selfed to get the enhanced F_3 generation. F_3 generation will be used to map molecular markers and to identify informative recombinants.

f. Isolation and functional analysis of causal genes are important for understanding the biological processes that trigger resistance responses. To my knowledge no RLN resistance genes have been isolated. However, positional cloning approaches have been used to, isolate causal genes for cyst nematode resistance in tomato and potato (*Mi* [104] and *Hero* [44] genes) and attempts have been made to isolate CCN resistance genes in wheat (*Cre1* and *Cre3* genes [32, 84]), At the beginning of this thesis research, the *Rlnn1* resistance gene seemed amenable for fine mapping and positional cloning, however, the progress towards these goals was hampered by the suppressed recombination at the distal end of 7AL. Given that the *Rlnn1* resistance

gene is mapped to a region with suppressed recombination, use of a conventional map-based/candidate gene-based cloning approach to isolate the causal genes would not be feasible, but a modified method with an initial mutagenesis approach might still work.

Radiation could be used to isolate the DNA fragment carrying the resistance gene, using an approach that would involve the use of γ-ray radiation to fragment chromosomes and analysis the presence/absence of DNA markers [69]. The theory behind this technique is that when two loci are further apart they are more likely to end up in two different fragments, when subjected to γ -ray irradiation. Radiation hybridisation has been used in wheat to isolate the *scs*^{ae} gene from a region of supressed recombination [69]. Such a method could be used to isolate the causal gene(s) of *Rlnn1* resistance locus.

g. The suppressed recombination in the distal end of chromosome 7A has led to the collocation of the resistance loci *Rlnn1* and *Lr20*/*Sr15* with the phytoene synthase *Psy-A1t* allele responsible for the 'very yellow' flour colour in wheat. The 'very yellow' flour colour in wheat is undesirable for bread-making and its tight linkage with the resistance loci *Rlnn1* and *Lr20*/*Sr15* makes it difficult for breeders to develop a cultivar that carries resistance alleles against *P. neglectus* and the rust pathogens and has very white flour. To my knowledge, no such cultivar has been developed. Based on the evidence presented in Chapters 3 and 4, it is unlikely to find natural recombinants.

   An approach to identify mutants with the desired phenotype would be through TILLING: a non-transgenic approach of creating and detecting new variants, which combines chemical mutagenesis to create mutations and detection of point mutations using a high-throughput system [21, 98, 163]. TILLING has been used successfully in wheat [162, 163]. For the purpose we could either develop or use an

already available TILLING population derived from a cultivar that carries the resistance alleles for *Rlnn1*, *Lr20*/*Sr15* loci and the *Psy-A1t* allele. Such a TILLING population derived from Wyalkatchem (~ 1400 lines) has already been developed (Peter Sharp, personal communication). The sequence of the *Psy-A1t* gene is known [24] and primers specifically designed to detect TILLING mutants could be used to amplify products from the M_2 lines. Using a multiplexed high-throughput screening method, mutants can be identified rapidly. These mutants can be phenotyped to see if there are any lines with the desired phenotypic combination (resistance alleles for *Rlnn1*, *Lr20*/*Sr15* and whiter flour colour).

7.7 Resistance responses of *Cre8* and *Rlnn1* resistance locus

In addition to the research covering these main aims, I also conducted an experiment as a first look at the *Cre8* resistance responses in resistant and susceptible wheat lines (reported in Appendix 4).

Based on the responses that had previously been reported for the *Cre1* locus in wheat, the *Cre3* locus from *Ae. tauschii* and CCN resistance loci in barley, it was already evident that resistance responses against CCN are not triggered at the nematode penetration, establishment or development stages. Effects were seen later, leading to degradation of syncytia in the resistant lines, which was observed by 13 to 15 DAI. This degradation would create nutrient-deprived conditions, in which the CCN females fail to mature and bear eggs [51, 117, 154, 196]. The experiment that is reported in Appendix 4 of this thesis was the first attempt to compare the responses to infection between lines with and without *Cre8* resistance. The exercise revealed that similar to what has been seen for lines with *Cre1* and *Cre3*, the nematodes do manage to enter the root tissue, establish themselves and feed on the nutrients from the host plant without triggering defence responses. No

significant differences in syncytial development were observed up to 18 DAI, which I had chosen to be the final sampling time based on an expectation from the literature [154, 196] that differences would be observable by 15 DAI. Further research needs to be carried out to understand what happens beyond 18 DAI.

To my knowledge, no resistance response investigations have been done on lines carrying the *Rlnn1* resistant locus. With *P. thornei* it has been seen that the resistance mechanisms are triggered after the initial nematode penetration stage, through interference to nematode migration, development of juveniles and the reproduction [92]. Further, it was also observed that the deposition of eggs and the hatching of the eggs were also affected by possible inhibitors in root exudates [92]. However, no investigations have been done to understand the responses of plants carrying resistance against *P. neglectus*. These findings cannot be extrapolated to *Rlnn1*, which does not confer resistance against *P. thornei*, but similar investigations could be carried out for *P. neglectus* possibly using the 'sister-lines' developed in Chapter 4.

Overall, the research conducted for this thesis has contributed towards the advancement in knowledge and understanding of two important nematode resistance loci in wheat, has generated molecular markers that can be used as effective selection tools in wheat breeding, has provided a basis for designing strategies and materials for future isolation of *Cre8* and possibly *Rlnn1*. The suppression of recombination at the distal end of 7AL limits the prospects of cloning the *Rlnn1* gene(s). However, several other strategies were proposed to develop a line with resistance alleles for *Rlnn1*, *Lr20*/*Sr15* and a much whiter flour colour suitable for bread-making and also to find possible candidate sequences/genes associated with *Rlnn1*.

Chapter 8

Contributions to knowledge

The research reported in this thesis was targeted at fine mapping of two of the important nematode resistance genes: 1) *Rlnn1* that conveys resistance against the RLN *P. neglectus* and 2) *Cre8* that conveys resistance against the CCN *H. avenae*. The significant contributions made by the current thesis research to the advancement of scientific knowledge include:

1. **Substantial improvement of two genetic linkage maps in wheat.**

   The improved chromosome 7A of Excalibur/Kukri and all chromosomes of Trident/Molineux presents a reference linkage map that include DArT™, SSR, SNP, ISBP, KASP™ and EST-based markers. The improved linkage maps could be used to identify and/or refine the positions of important trait loci.

2. **Clarification of the positions of one important nematode-resistance locus on each of these maps.**

   The map position of the nematode resistance loci, *Rlnn1* and *Cre8* was confirmed to be at the distal end of 7AL and 6BL, respectively. Their position and QTL effects were further refined.

3. **Development of diagnostic marker assays that can be used in marker-assisted selection of *Rlnn1* and *Cre8*.**

   Several markers that are diagnostic across a panel of wheat cultivars (including cultivars known to be at least moderately resistant and cultivars that are known to be susceptible to the nematodes) were identified. Most of the markers can be used as a high-throughput, cost-effective alternative to the costly phenotypic screening assay during MAS.

4. **Development of new genetic materials for further research on *Cre8*.**

   To pursue positional cloning of *Cre8* resistance locus, a large mapping population was developed. The newly developed genetic material does not have any other resistance loci that affect CCN resistance and thus, presents an opportunity to focus entirely on the *Cre8* resistance locus and its effects.

5. **Confirmation of a suppressed recombination in the cultivar Excalibur.**

   Recombination suppression at the distal end of 7AL in Excalibur resulted the collocation of numerous molecular markers, the rust resistance genes *Lr20*/*Sr15*, a phytoene synthase gene *Psy-A1*, a catalase gene *Cat3-A1* and the *Rlnn1* resistance QTL. The supressed recombination impeded the fine mapping and positional cloning of *Rlnn1* resistance gene(s). It was suggested that the supressed recombination may be a consequence of a translocation involving an unknown ancestor with a genome closely related to the wheat chromosome 7B.

References

1. Agrios GN: *Plant Diseases Caused by Nematodes.* 5th edn. London, UK: Elsevier Acedamic Press; 2005.
2. Ajawatanawong P, Atkinson GC, Watson-Haigh NS, MacKenzie B, Baldauf SL: **SeqFIRE: a web application for automated extraction of indel regions and conserved blocks from protein multiple sequence alignments.** *Nucleic Acids Res* 2012, **40:**W340-W347.
3. Akbari M, Wenzl P, Caig V, Carling J, Xia L, Yang S, Uszynski G, Mohler V, Lehmensiek A, Kuchel H, et al: **Diversity arrays technology (DArT) for high-throughput profiling of the hexaploid wheat genome.** *Theor Appl Genet* 2006, **113:**1409-1420.
4. Akhunov ED, Akhunova AR, Anderson OD, Anderson JA, Blake N, Clegg MT, Coleman-Derr D, Conley EJ, Crossman CC, Deal KR, et al: **Nucleotide diversity maps reveal variation in diversity among wheat genomes and chromosomes.** *BMC Genomics* 2010, **11:**702.
5. Allen AM, Barker GLA, Berry ST, Coghill JA, Gwilliam R, Kirby S, Robinson P, Brenchley RC, D'Amore R, McKenzie N, et al: **Transcript-specific, single-nucleotide polymorphism discovery and linkage analysis in hexaploid bread wheat (*Triticum aestivum* L.).** *Plant Biotechnol J* 2011, **9:**1086-1099.
6. Allen AM, Barker GLA, Wilkinson P, Burridge A, Winfield M, Coghill J, Uauy C, Griffiths S, Jack P, Berry S, et al: **Discovery and development of exome-based, co-dominant single nucleotide polymorphism markers in hexaploid wheat (*Triticum aestivum* L.).** *Plant Biotechnol J* 2012, **11:**279-295.
7. **Bioplatforms Australia** [http://www.bioplatforms.com.au/]

8. Bariana HS, McIntosh RA: **Cytogenetic studies in wheat. XV. Location of rust resistance genes in VPM1 and their genetic linkage with other disease resistance genes in chromosome 2A.** *Genome* 1993, **36:**476-482.

9. Birch ANE, Robertson WM, Fellows LE: **Plant products to control plant parasitic nematodes.** *Pestic Sci* 1993, **39:**141-145.

10. Blanco A, Colasuonno P, Gadaleta A, Mangini G, Schiavulli A, Simeone R, Digesù AM, De Vita P, Mastrangelo AM, Cattivelli L: **Quantitative trait loci for yellow pigment concentration and individual carotenoid compounds in durum wheat.** *J Cereal Sci* 2011, **54:**255-264.

11. Boerma HR, Hussey RS: **Breeding plants for resistance to nematodes.** *J Nematol* 1992, **24:**242-252.

12. Brookes AJ: **The essence of SNPs.** *Gene* 1999, **234:**177-186.

13. Browder LE: **Designation of two genes for resistance to *Puccinia recondit*a in *Triticum aestivum*.** *Crop Sci* 1972, **12:**705-706.

14. Brown RH: **Ecology and control of cereal cyst nematode (*Heterodera avenae*) in Southern Australia.** *J Nematol* 1984, **16:**216-222.

15. Cai D, Kleine M, Kifle S, Harloff H-J, Sandal NN, Marcker KA, Klein-Lankhorst RM, Salentijn EMJ, Lange W, Stiekema WJ, et al: **Positional cloning of a gene for nematode resistance in sugar beet.** *Science* 1997, **275:**832-834.

16. Cavanagh CR, Chao S, Wang S, Huang BE, Stephen S, Kiani S, Forrest K, Saintenac C, Brown-Guedira GL, Akhunova A, et al: **Genome-wide comparative diversity uncovers multiple targets of selection for improvement in hexaploid wheat landraces and cultivars.** *Proc Natl Acad Sci USA* 2013, **110:**8057-8062.

17. Chantret N, Salse J, Sabot F, Rahman S, Bellec A, Laubin B, Dubois I, Dossat C, Sourdille P, Joudrier P, et al: **Molecular basis of evolutionary events that shaped**

the hardness locus in diploid and polyploid wheat species (*Triticum* and *Aegilops*). *Plant Cell* 2005, **17:**1033-1045.

18. Cheema J, Dicks J: **Computational approaches and software tools for genetic linkage map estimation in plants.** *Briefings in Bioinformatics* 2009, **10:**595-608.

19. Churchill GA, Doerge RW: **Empirical threshold values for quantitative trait mapping.** *Genetics* 1994, **138:**963-971.

20. Collard BCY, Jahufer MZZ, Brouwer JB, Pang ECK: **An introduction to markers, quantitative trait loci (QTL) mapping and marker-assisted selection for crop improvement: The basic concepts.** *Euphytica* 2005, **142:**169-196.

21. Comai L, Greene EA, Henikoff S, McCallum CM: **Targeted screening for induced mutations.** *Nat Biotechnol* 2000, **18:**455+.

22. **International Wheat Genome Sequencing Consortium** [http://www.wheatgenome.org/]

23. Crawford A, Francki M: **Chromosomal location of wheat genes of the carotenoid biosynthetic pathway and evidence for a catalase gene on chromosome 7A functionally associated with flour b* colour variation.** *Mol Genet Genomics* 2013, **288:**483-493.

24. Crawford AC, Stefanova K, Lambe W, McLean R, Wilson R, Barclay I, Francki MG: **Functional relationships of *phytoene synthase 1* alleles on chromosome 7A controlling flour colour variation in selected Australian wheat genotypes.** *Theor Appl Genet* 2011, **123:**95-108.

25. Crossa J, Burgueño J, Dreisigacker S, Vargas M, Herrera-Foessel SA, Lillemo M, Singh RP, Trethowan R, Warburton M, Franco J, et al: **Association analysis of historical bread wheat germplasm using additive genetic covariance of relatives and population structure.** *Genetics* 2007, **177:**1889-1913.

26. **CerealDB SNP database** [http://www.cerealsdb.uk.net]

27. **GrainGenes Database** [http://wheat.pw.usda.gov/GG2/index.shtml]

28. **Rice Genome Annotation Project Database** [http://rice.plantbiology.msu.edu/analyses_search_blast.shtml]

29. **Wheat Genome Database** [http://wheatgenome.info/]

30. **Wheat SNP Database** [http://probes.pw.usda.gov:8080/snpworld/Map]

31. de la Peña RC, Murray TD, Jones SS: **Identification of an RFLP interval containing *Pch2* on chromosome 7AL in wheat.** *Genome* 1997, **40:**249-252.

32. de Majnik J, Ogbonnaya FC, Moullet O, Lagudah ES: **The *Cre1* and *Cre3* nematode resistance genes are located at homeologous loci in the wheat genome.** *Mol Plant Microbe Interact* 2003, **16:**1129-1134.

33. Delibes A, Romero D, Aguaded S, Duce A, Mena M, Lopez-Braña I, Andrés MF, Martin-Sanchez JA, García-Olmedo F: **Resistance to the cereal cyst nematode (*Heterodera avenae* Woll.) transferred from the wild grass *Aegilops ventricosa* to hexaploid wheat by a "stepping-stone" procedure.** *Theor Appl Genet* 1993, **87:**402-408.

34. Dibari B, Murat F, Chosson A, Gautier V, Poncet C, Lecomte P, Mercier I, Berges H, Pont C, Blanco A, Salse J: **Deciphering the genomic structure, function and evolution of carotenogenesis related phytoene synthases in grasses.** *BMC Genomics* 2012, **13:**221.

35. DSobczak M, Avrova A, Jupowicz J, Phillips MS, Ernst K, Kumar A: **Characterization of susceptibility and resistance responses to potato cyst nematode (*Globodera* spp.) infection of tomato lines in the absence and presence of the broad-spectrum nematode resistance *Hero* gene.** *Mol Plant Microbe Interact* 2005, **18:**158-168.

36. Doyle A, McLeod R, Wong P, Hetherington S, Southwell R: **Evidence for the involvement of the root lesion nematode *Pratylenchus thornei* in wheat yield decline in northern New South Wales.** *Aust J Exp Agric* 1987, **27:**563-570.

37. Dubcovsky J, Lukaszewski AJ, Echaide M, Antonelli EF, Porter DR: **Molecular characterization of two *Triticum speltoides* interstitial translocations carrying leaf rust and greenbug resistance genes.** *Crop Sci* 1998, **38:**1655-1660.

38. Duncan LW, Moens M: **Migratory endoparasitic nematodes.** In *Plant Nematology*. Edited by Perry RN, Moens M. Wallingford: CABI; 2006: 125 - 133

39. Eastwood R, Lagudah E, Appels R, Hannah M, Kollmorgen J: ***Triticum tauschii*: A novel source of resistance to cereal cyst nematode (*Heterodera avenae*).** *Aust J Agric Res* 1991, **42:**69-77.

40. Eastwood RF, Lagudah ES, Appels R: **A directed search for DNA sequences tightly linked to cereal cyst nematode resistance genes in *Triticum tauschii.*** *Genome* 1994, **37:**311-319.

41. Edwards D, Wilcox S, Barrero RA, Fleury D, Cavanagh CR, Forrest KL, Hayden MJ, Moolhuijzen P, Keeble-Gagnère G, Bellgard MI: **Bread matters: a national initiative to profile the genetic diversity of Australian wheat.** *Plant Biotechnol J* 2012, **10:**703-708.

42. Edwards J: **A genetic analysis of drought related traits in hexaploid wheat.** *PhD thesis.* The University of Adelaide, School of Agriculture, Food and Wine, 2012.

43. Edwards MD, Stuber CW, Wendel JF: **Molecular-marker-facilitated investigations of quantitative-trait loci in maize. I. Numbers, genomic distribution and types of gene action.** *Genetics* 1987, **116:**113-125.

44. Ernst K, Kumar A, Kriseleit D, Kloos D-U, Phillips MS, Ganal MW: **The broad-spectrum potato cyst nematode resistance gene (*Hero*) from tomato is the only**

member of a large gene family of NBS-LRR genes with an unusual amino acid repeat in the LRR region. *Plant J* 2002, **31:**127-136.

45. Fisher JM: **Towards a consistent laboratory assay for resistance to *Heterodera avenae*.** *Bull OEPP* 1982, **12:**445-449.

46. Fox RL, Warner P, Eglinton JK: **The application of rapid DNA extraction methods for MAS in barley and wheat improvement programs.** In *The 53rd Australian Cereal Chemistry Conference; Glenelg, South Australia*. 2003: 55-59.

47. Friebe B, Jiang J, Raupp WJ, McIntosh RA, Gill BS: **Characterization of wheat-alien translocations conferring resistance to diseases and pests: current status.** *Euphytica* 1996, **91:**59-87.

48. Gallagher CE, Matthews PD, Li F, Wurtzel ET: **Gene duplication in the carotenoid biosynthetic pathway preceded evolution of the grasses.** *Plant Physiol* 2004, **135:**1776-1783.

49. Gaut BS, Wright SI, Rizzon C, Dvorak J, Anderson LK: **Recombination: an underappreciated factor in the evolution of plant genomes.** *Nat Rev Genet* 2007, **8:**77-84.

50. Giorgi D, Farina A, Grosso V, Gennaro A, Ceoloni C, Lucretti S: **FISHIS: Fluorescence *in situ* hybridization in suspension and chromosome flow sorting made easy.** *PLoS ONE* 2013, **8:**e57994.

51. Grymaszewska G, Golinowski W: **Structure of syncytia induced by *Heterodera avenae* Woll. in roots of susceptible and resistant wheat (*Triticum aestivum* L.).** *J Phytopathol* 1991, **133:**307-319.

52. Gupta P, Varshney RK, Sharma P, Ramesh B: **Molecular markers and their applications in wheat breeding.** *Plant Breeding* 1999, **118:**369-390.

53. Haider N: **The origin of the B-genome of bread wheat (*Triticum aestivum* L.).** *Russ J Genet* 2013, **49:**263-274.

54. Haldane J: **The combination of linkage values and the calculation of distances between the loci of linked factors.** *J Genet* 1919, **8:**299-309.

55. Haling RE, Simpson RJ, McKay AC, Hartley D, Lambers H, Ophel-Keller K, Wiebkin S, Herdina, Riley IT, Richardson AE: **Direct measurement of roots in soil for single and mixed species using a quantitative DNA-based method.** *Plant Soil* 2011, **348:**123-137.

56. Hayden M, Nguyen T, Waterman A, McMichael G, Chalmers K: **Application of multiplex-ready PCR for fluorescence-based SSR genotyping in barley and wheat.** *Mol Breeding* 2008, **21:**271 - 281.

57. He X, Wang J, Ammar K, Peña RJ, Xia X, He Z: **Allelic variants at the *Psy-A1* and *Psy-B1* loci in durum wheat and their associations with grain yellowness** *Crop Sci* 2009, **49:**2058-2064.

58. He XY, He ZH, Ma W, Appels R, Xia XC: **Allelic variants of phytoene synthase 1 (*Psy1*) genes in Chinese and CIMMYT wheat cultivars and development of functional markers for flour colour.** *Mol Breed* 2009, **23:**553-563.

59. He XY, Zhang YL, He ZH, Wu YP, Xiao YG, Ma CX, Xia XC: **Characterization of phytoene synthase 1 gene (*Psy1*) located on common wheat chromosome 7A and development of a functional marker.** *Theor Appl Genet* 2008, **116:**213-221.

60. Heinrich T, Bartlem D, Jones MGK: **Molecular aspects of plant-nematode interactions and their exploitation for resistance strategies.** *Australas Plant Pathol* 1998, **27:**59-72.

61. Herdina, Ophel-Keller K, Wiebkin S, Dumitrescu I, Burns R, McKay A: **The detection of dead soil-borne pathogens measured by a DNA based assay.** In *Proceedings of the 3rd Australasian soilborne diseases symposium; Adelaide*. Edited by Ophel-Keller K, Hall B. Department of Primary Industry and Resources South Australia; 2004: 103--104.

62. Herrera-Foessel SA, Lagudah ES, Huerta-Espino J, Hayden MJ, Bariana HS, Singh D, Singh RP: **New slow-rusting leaf rust and stripe rust resistance genes *Lr67* and *Yr46* in wheat are pleiotropic or closely linked.** *Theor Appl Genet* 2011, **122:**239-249.

63. Hiebert CW, Thomas JB, McCallum BD, Humphreys DG, DePauw RM, Hayden MJ, Mago R, Schnippenkoetter W, Spielmeyer W: **An introgression on wheat chromosome 4DL in RL6077 (Thatcher*6/PI 250413) confers adult plant resistance to stripe rust and leaf rust (*Lr67*).** *Theor Appl Genet* 2010, **121:**1083-1091.

64. Hirschberg J: **Carotenoid biosynthesis in flowering plants.** *Curr Opin Plant Biol* 2001, **4:**210-218.

65. Hohmann U, Endo T, Gill K, Gill B: **Comparison of genetic and physical maps of group 7 chromosomes from *Triticum aestivum* L.** *Molec Gen Genet* 1994, **245:**644-653.

66. Hohmann U, Graner A, Endo TR, Gill BS, Herrmann RG: **Comparison of wheat physical maps with barley linkage maps for group 7 chromosomes.** *Theor Appl Genet* 1995, **91:**618-626.

67. Holtmann B, Kleine M, Grundler FMW: **Ultrastructure and anatomy of nematode-induced syncytia in roots of susceptible and resistant sugar beet.** *Protoplasma* 2000, **211:**39-50.

68. Hooper DJ: **Extraction of nematodes from plant material.** In *Laboratory methods for work with plant and soil nematodes.* 6th edition. Edited by Southey JF. London: HMSO Books; 1986: 51-58

69. Hossain KG, Riera-Lizarazu O, Kalavacharla V, Vales MI, Maan SS, Kianian SF: **Radiation hybrid mapping of the species cytoplasm-specific (*scs*^{ae}) gene in wheat.** *Genetics* 2004, **168:**415-423.

70. Howitt CA, Cavanagh CR, Bowerman AF, Cazzonelli C, Rampling L, Mimica JL, Pogson BJ: **Alternative splicing, activation of cryptic exons and amino acid substitutions in carotenoid biosynthetic genes are associated with lutein accumulation in wheat endosperm.** *Funct Integr Genomics* 2009, **9:**363-376.

71. Hu X, Ohm H, Dweikat I: **Identification of RAPD markers linked to the gene *Pm1* for resistance to powdery mildew in wheat.** *Theor Appl Genet* 1997, **94:**832-840.

72. Huang S, Sirikhachornkit A, Su X, Faris J, Gill B, Haselkorn R, Gornicki P: **Genes encoding plastid acetyl-CoA carboxylase and 3-phosphoglycerate kinase of the *Triticum*/*Aegilops* complex and the evolutionary history of polyploid wheat.** *Proc Natl Acad Sci USA* 2002, **99:**8133-8138.

73. **Department of Primary Industries** [www.dpi.vic.gov.au/graindiseases]

74. Jaccoud D, Peng K, Feinstein D, Kilian A: **Diversity arrays: a solid state technology for sequence information independent genotyping.** *Nucleic Acids Res* 2001, **29:**e25.

75. Jahier J, Abelard P, Tanguy M, Dedryver F, Rivoal R, Khatkar S, Bariana HS, Koebner R: **The *Aegilops ventricosa* segment on chromosome 2AS of the wheat cultivar 'VPM1' carries the cereal cyst nematode resistance gene *Cre5*.** *Plant Breeding* 2001, **120:**125-128.

76. Jahier J, Tanguy AM, Abelard P, Rivoal R: **Utilization of deletions to localize a gene for resistance to the cereal cyst nematode, *Heterodera avenae*, on an *Aegilops ventricosa* chromosome.** *Plant Breeding* 1996, **115:**282-284.

77. Joehanes R, Nelson JC: **QGene 4.0, an extensible Java QTL-analysis platform.** *Bioinformatics* 2008, **24:**2788-2789.

78. Jones MGK, Fosu-Nyarko J: **Molecular biology of root lesion nematodes (*Pratylenchus* spp.) and their interaction with host plants.** *Ann Appl Biol* 2014, **164:**163-181.

79. Kao C-H, Zeng Z-B, Teasdale RD: **Multiple interval mapping for quantitative trait loci.** *Genetics* 1999, **152:**1203-1216.

80. Kawahara Y, de la Bastide M, Hamilton JP, Kanamori H, McCombie WR, Ouyang S, Schwartz DC, Tanaka T, Wu J, Zhou S, et al: **Improvement of the *Oryza sativa* Nipponbare reference genome using next generation sequence and optical map data.** *Rice* 2013, **6:**4.

81. Kosambi DD: **The estimation of map distances from recombination values.** *Ann Eugen* 1944, **12:**172-175.

82. Krattinger SG, Lagudah ES, Spielmeyer W, Singh RP, Huerta-Espino J, McFadden H, Bossolini E, Selter LL, Keller B: **A putative ABC transporter confers durable resistance to multiple fungal pathogens in wheat.** *Science* 2009, **323:**1360-1363.

83. Kuchel H, Langridge P, Mosionek L, Williams K, Jefferies SP: **The genetic control of milling yield, dough rheology and baking quality of wheat.** *Theor Appl Genet* 2006, **112:**1487-1495.

84. Lagudah ES, Moullet O, Appels R: **Map-based cloning of a gene sequence encoding a nucleotide binding domain and a leucine-rich region at the *Cre3* nematode resistance locus of wheat.** *Genome* 1997, **40:**659-665.

85. Lai K, Berkman PJ, Lorenc MT, Duran C, Smits L, Manoli S, Stiller J, Edwards D: **WheatGenome.info: An integrated database and portal for wheat genome information.** *Plant Cell Physiol* 2011.

86. Lander ES, Botstein D: **Mapping mendelian factors underlying quantitative traits using RFLP linkage maps.** *Genetics* 1989, **121:**185-199.

87. Langmead B, Salzberg SL: **Fast gapped-read alignment with Bowtie 2.** *Nat Methods* 2012, **9:**357-359.

88. Lewis JG, Matic M, McKay AC: **Success of cereal cyst nematode resistance in Australia: History and status of resistance screening systems.** In *Cereal cyst nematodes: Status, research and outlook Proceedings of the first workshop of the international cereal cyst nematode initiative* Edited by Riley IT, Nicol JM, Dababat AA. Ankara, Turkey CIMMYT; 2009: 137-142

89. Li F, Vallabhaneni R, Wurtzel ET: ***PSY3,* a new member of the phytoene synthase gene family conserved in the Poaceae and regulator of abiotic stress-induced root carotenogenesis.** *Plant Physiol* 2008, **146:**1333-1345.

90. Lillemo M, Asalf B, Singh RP, Huerta-Espino J, Chen XM, He ZH, Bjørnstad Å: **The adult plant rust resistance loci *Lr34/Yr18* and *Lr46/Yr29* are important determinants of partial resistance to powdery mildew in bread wheat line Saar.** *Theor Appl Genet* 2008, **116:**1155-1166.

91. Lilley CJ, Atkinson HJ, Urwin PE: **Molecular aspects of cyst nematodes.** *Mol Plant Pathol* 2005, **6:**577-588.

92. Linsell KJ, Riley IT, Davies KA, Oldach KH: **Characterization of resistance to *Pratylenchus thornei* (*Nematoda*) in wheat (*Triticum aestivum*): Attraction, penetration, motility, and reproduction.** *Phytopathology* 2013, **104:**174-187.

93. Liu CJ, Atkinson MD, Chinoy CN, Devos KM, Gale MD: **Nonhomoeologous translocations between group 4, 5 and 7 chromosomes within wheat and rye.** *Theor Appl Genet* 1992, **83:**305-312.

94. Lu S, Li L: **Carotenoid metabolism: Biosynthesis, regulation, and beyond.** *J Integr Plant Biol* 2008, **50:**778-785.

95. Lucretti S, Giorgi D, Farina A, Grosso V: **FISHIS: A new way in chromosome flow sorting makes complex genomes more accessible.** In *Genomics of Plant Genetic Resources.* Springer; 2014: 319-348

96. Manly KF, Cudmore Jr. RH, Meer JM: **Map Manager QTX, cross-platform software for genetic mapping.** *Mamm Genome* 2001, **12:**930-932.

97. Mares DJ, Campbell AW: **Mapping components of flour and noodle colour in Australian wheat.** *Aust J Agric Res* 2001, **52:**1297-1309.

98. McCallum CM, Comai L, Greene EA, Henikoff S: **Targeting Induced Local Lesions IN Genomes (TILLING) for plant functional genomics.** *Plant Physiol* 2000, **123:**439-442.

99. McIntosh RA: **Nature of induced mutations affecting disease reaction in wheat.** In *Induced mutations against plant diseases: Proceedings of a symposium on the use of induced mutations for improving disease resistance in crop plants*; *31 January - 4 February 1977; Vienna*. International Atomic Energy Agency 1977: 551-564.

100. McIntosh RA: **Close genetic linkage of genes conferring adult-plant resistance to leaf rust and stripe rust in wheat.** *Plant Pathol* 1992, **41:**523-527.

101. McIntosh RA, Wellings CR, Park RF: *Wheat rusts: An atlas of resistance genes.* Melbourne: CSIRO; 1995.

102. McIntosh RA, Yamazaki Y, Dubcovsky J, Rogers J, Morris C, Somers DJ, Appels R, Devos KM: **Catalogue of gene symbols for wheat.** In *11 International Wheat Genetics Symposium; Queensland, Australia* 2008

103. Meagher JW: **World dissemination of the cereal-cyst nematode (*Heterodera avenae*) and its potential as a pathogen of wheat.** *J Nematol* 1977, **9:**9-15.

104. Milligan SB, Bodeau J, Yaghoobi J, Kaloshian I, Zabel P, Williamson VM: **The root knot nematode resistance gene *Mi* from tomato is a member of the leucine**

zipper, nucleotide binding, leucine-rich repeat family of plant genes. *Plant Cell* 1998, **10:**1307.

105. Milne I, Stephen G, Bayer M, Cock PJA, Pritchard L, Cardle L, Shaw PD, Marshall D: **Using Tablet for visual exploration of second-generation sequencing data.** *Briefings in Bioinformatics* 2013, **14:**193-202.

106. Miskelly DM: **Flour components affecting paste and noodle colour.** *J Sci Food Agric* 1984, **35:**463-471.

107. Montes MJ, Andres MF, Sin E, Lopez-Brana I, Martin-Sanchez JA, Romero MD, Delibes A: **Cereal cyst nematode resistance conferred by the *Cre7* gene from *Aegilops triuncialis* and its relationship with *Cre* genes from Australian wheat cultivars.** *Genome* 2008, **51:**315-319.

108. Moody EH, Lownsbery BF, Ahmed JM: **Culture of the root-lesion nematode *Pratylenchus vulnus* on carrot disks.** *J Nematol* 1973, **5:**225-226.

109. **MSTMap** [http://alumni.cs.ucr.edu/~yonghui/mstmap.html]

110. **MultiQTL** [http://www.multiqtl.com/]

111. Murray GM, Brennan JP: **The current and potential costs from diseases of wheat in Australia.** Grains Research and Development Corporation, Australia, 2009.

112. **NCBI** [http://blast.ncbi.nlm.nih.gov/]

113. Nelson JC, Sorrells ME, Van Deynze AE, Lu YH, Atkinson M, Bernard M, Leroy P, Faris JD, Anderson JA: **Molecular mapping of wheat: major genes and rearrangements in homoeologous groups 4, 5, and 7.** *Genetics* 1995, **141:**721-731.

114. Neu C, Stein N, Keller B: **Genetic mapping of the *Lr20-Pm1* resistance locus reveals suppressed recombination on chromosome arm 7AL in hexaploid wheat.** *Genome* 2002, **45:**737-744.

115. Nicol JM, Rivoal R: **Global knowledge and its application for the integrated control and management of nematodes on wheat.** In *Integrated management and biocontrol of vegetable and grain crops nematodes. Volume* 2. Edited by Ciancio A, Mukerji KG: Springer Netherlands; 2007: 251-294.[Ciancio A, Mukerji KG (Series Editor): *Integrated Management of Plant Pests and Diseases*].

116. Nicol JM, Turner SJ, Coyne DL, den Nijs L, Hockland S, Maafi ZT: **Current nematode threats to world agriculture.** In *Genomics and molecular genetics of plant-nematode interactions.* Edited by Jones J, Gheysen G, Fenoll C. Hobart: Springer Netherlands; 2011: 21-43

117. O'Brien P, Fisher J: **Development of *Heterodera avenae* on resistant wheat and barley cultivars.** *Nematologica* 1977, **23:**390-397.

118. Ogbonnaya FC, Seah S, Delibes A, Jahier J, López-Braña I, Eastwood RF, Lagudah ES: **Molecular-genetic characterisation of a new nematode resistance gene in wheat.** *Theor Appl Genet* 2001, **102:**623-629.

119. Ogbonnaya FC, Subrahmanyam NC, Moullet O, Majnik Jd, Eagles HA, Brown JS, Eastwood RF, Kollmorgen J, Appels R, Lagudah ES: **Diagnostic DNA markers for cereal cyst nematode resistance in bread wheat.** *Aust J Agric Res* 2001, **52:**1367-1374.

120. **NVT Online** [http://www.acasnvt.com.au]

121. Ophel-Keller K, McKay A, Hartley D, Herdina, Curran J: **Development of a routine DNA-based testing service for soilborne diseases in Australia.** *Australas Plant Pathol* 2008, **37:**243-253.

122. Paal J, Henselewski H, Muth J, Meksem K, Menéndez CM, Salamini F, Ballvora A, Gebhardt C: **Molecular cloning of the potato *Gro1-4* gene conferring resistance to pathotype *Ro1* of the root cyst nematode *Globodera rostochiensis,* based on a candidate gene approach.** *Plant J* 2004, **38:**285-297.

123. Pallotta MA, Graham RD, Langridge P, Sparrow DHB, Barker SJ: **RFLP mapping of manganese efficiency in barley.** *Theor Appl Genet* 2000, **101:**1100-1108.

124. Park RF, Williams M: *2010 -2011 Cereal rust survey - Annual report.* Australian cereal rust programme, Plant Breeding Institute, University of Sydney, Cobbitty.

125. Parker GD, Chalmers KJ, Rathjen AJ, Langridge P: **Mapping loci associated with flour colour in wheat (*Triticum aestivum* L.).** *Theor Appl Genet* 1998, **97:**238-245.

126. Parker GD, Langridge P: **Development of a STS marker linked to a major locus controlling flour colour in wheat (*Triticum aestivum* L.).** *Mol Breed* 2000, **6:**169-174.

127. Paull JG, Chalmers KJ, Karakousis A, Kretschmer JM, Manning S, Langridge P: **Genetic diversity in Australian wheat varieties and breeding material based on RFLP data.** *Theor Appl Genet* 1998, **96:**435-446.

128. Paull JG, Pallotta MA, Langridge P, The TT: **RFLP markers associated with *Sr22* and recombination between chromosome 7A of bread wheat and the diploid species *Triticum boeoticum*.** *Theor Appl Genet* 1994, **89:**1039-1045.

129. Paux E, Faure S, Choulet F, Roger D, Gauthier V, Martinant JP, Sourdille P, Balfourier F, Le Paslier MC, Chauveau A, et al: **Insertion site-based polymorphism markers open new perspectives for genome saturation and marker-assisted selection in wheat.** *Plant Biotechnol J* 2010, **8:**196-210.

130. Paux E, Gao L, Faure S, Choulet F, Roger D, Chevalier K, Saintenac C, Balfourier F, Paux K, Cakir M, et al: **Insertion site-based polymorphism: A swiss army knife for wheat genomics.** In *11th International Wheat Genetics Symposium*. Edited by Appels R, Eastwood R, Lagudah E, Langridge P, Lynne MM. Sydney University Press; 2008

131. Paux E, Sourdille P, Salse J, Saintenac C, Choulet F, Leroy P, Korol A, Michalak M, Kianian S, Spielmeyer W, et al: **A physical map of the 1-gigabase bread wheat chromosome 3B.** *Science* 2008, **322:**101-104.

132. Poland J, Brown P, Sorrells M, Jannink J-L: **Development of high-density genetic maps for barley and wheat using a novel two-enzyme genotyping-by-sequencing approach.** *PLoS ONE* 2012, **7:**e32253.

133. Powell W, Morgante M, Andre C, Hanafey M, Vogel J, Tingey S, Rafalski A: **The comparison of RFLP, RAPD, AFLP and SSR (microsatellite) markers for germplasm analysis.** *Mol Breed* 1996, **2:**225-238.

134. Pozniak CJ, Knox RE, Clarke FR, Clarke JM: **Identification of QTL and association of a phytoene synthase gene with endosperm colour in durum wheat.** *Theor Appl Genet* 2007, **114:**525-537.

135. **Australian Wheat and Barley Molecular Marker Program** [http://www.markers.net.au]

136. **R: A language and environment for statistical computing** [http://www.R-project.org/]

137. Ranjbar GA: **Production and utilization of doubled haploid lines in wheat breeding programs.** *PhD Thesis.* The University of Adelaide, Department of Plant Science; 1997.

138. Rathjen AJ, Eastwood RF, Lewis JG, Dube AJ: **Breeding wheat for resistance to *Heterodera avenae* in Southeastern Australia.** *Euphytica* 1998, **100:**55-62.

139. Ravel C, Dardevet M, Leenhardt F, Bordes J, Joseph JL, Perretant MR, Exbrayat F, Poncet C, Balfourier F, Chanliaud E, Charmet G: **Improving the yellow pigment content of bread wheat flour by selecting the three homoeologous copies of *Psy1*.** *Mol Breed* 2013, **31:**87-99.

140. Riley IT, Kelly SJ: **Endoparasitic nematodes in cropping soils of western Australia.** *Aust J Exp Agric* 2002, **42:**49-56.

141. Riley IT, Wiebkin S, Hartley D, McKay AC: **Quantification of roots and seeds in soil with real-time PCR.** *Plant Soil* 2010, **331:**151-163.

142. Rivoal R, Cook R: **Plant parasitic nematodes in temperate agriculture.** In *Plant parasitic nematodes in temperate agriculture.* Edited by Evans K, Trudgill DL, Webster JM. Wallingford, UK: CABI; 1993

143. Röder MS, Korzun V, Wendehake K, Plaschke J, Tixier M-H, Leroy P, Ganal MW: **A microsatellite map of wheat.** *Genetics* 1998, **149:**2007-2023.

144. Rogowsky P, Guidet F, Langridge P, Shepherd K, Koebner R: **Isolation and characterization of wheat-rye recombinants involving chromosome arm 1DS of wheat.** *Theor Appl Genet* 1991, **82:**537-544.

145. Romero MD, Montes MJ, Sin E, Lopez-Braña I, Duce A, Martín-Sanchez JA, Andrés MF, Delibes A: **A cereal cyst nematode (*Heterodera avenae* Woll.) resistance gene transferred from *Aegilops triuncialis* to hexaploid wheat.** *Theor Appl Genet* 1998, **96:**1135-1140.

146. Rozen S, Skaletsky H: **Primer3 on the WWW for general users and for biologist programmers.** In *Bioinformatics methods and protocols. Volume* 132. Edited by Misener S, Krawetz S: Humana Press; 1999: 365-386: *Methods in molecular biology*].

147. Safari E, Gororo NN, Eastwood RF, Lewis J, Eagles HA, Ogbonnaya FC: **Impact of *Cre1, Cre8* and *Cre3* genes on cereal cyst nematode resistance in wheat.** *Theor Appl Genet* 2005, **110:**567-572.

148. Sarma D, Knott DR: **The transfer of leaf-rust resistance from *Agropyron* to *Triticum* by irradiation.** *Can J Genet Cytol* 1966, **8:**137-143.

149. Schachermayr G, Siedler H, Gale MD, Winzeler H, Winzeler M, Keller B: **Identification and localization of molecular markers linked to the *Lr9* leaf rust resistance gene of wheat.** *Theor Appl Genet* 1994, **88:**110-115.

150. Schachermayr GM, Messmer MM, Feuillet C, Winzeler H, Winzeler M, Keller B: **Identification of molecular markers linked to the *Agropyron elongatum*-derived leaf rust resistance gene *Lr24* in wheat.** *Theor Appl Genet* 1995, **90:**982-990.

151. Schmidt AL, McIntyre CL, Thompson J, Seymour NP, Liu CJ: **Quantitative trait loci for root lesion nematode (*Pratylenchus thornei*) resistance in Middle-Eastern landraces and their potential for introgression into Australian bread wheat.** *Aust J Agric Res* 2005, **56:**1059-1068.

152. Schnurbusch T, Collins NC, Eastwood RF, Sutton T, Jefferies SP, Langridge P: **Fine mapping and targeted SNP survey using rice-wheat gene colinearity in the region of the *Bo1* boron toxicity tolerance locus of bread wheat.** *Theor Appl Genet* 2007, **115:**451-461.

153. Schnurbusch T, Langridge P, Sutton T: **The *Bo1*-specific PCR marker *AWW5L7* is predictive of boron tolerance status in a range of exotic durum and bread wheats.** *Genome* 2008, **51:**963-971.

154. Seah S, Miller C, Sivasithamparam K, Lagudah ES: **Root responses to cereal cyst nematode (*Heterodera avenae*) in hosts with different resistance genes.** *New Phytol* 2000, **146:**527-533.

155. Sears ER: **The aneuploids of common wheat.** *Res Bull Mo Agric Exp Sta* 1954, **572:**1-58.

156. Sears ER, Briggle LW: **Mapping the gene *Pm1* for resistance to *Erysiphe graminis* f. sp. *tritici* on chromosome 7A of wheat.** *Crop Sci* 1969, **9:**96-97.

157. Semagn K, Bjørnstad Å, Skinnes H, Marøy AG, Tarkegne Y, William M: **Distribution of DArT, AFLP, and SSR markers in a genetic linkage map of a doubled-haploid hexaploid wheat population.** *Genome* 2006, **49:**545-555.

158. Seyfarth R, Feuillet C, Schachermayr G, Winzeler M, Keller B: **Development of a molecular marker for the adult plant leaf rust resistance gene *Lr35* in wheat.** *Theor Appl Genet* 1999, **99:**554-560.

159. Sharma S, Sharma S, Kopisch-Obuch F, Keil T, Laubach E, Stein N, Graner A, Jung C: **QTL analysis of root-lesion nematode resistance in barley: 1. *Pratylenchus neglectus*.** *Theor Appl Genet* 2011, **122:**1321-1330.

160. Singh A, Reimer S, Pozniak CJ, Clarke FR, Clarke JM, Knox RE, Singh AK: **Allelic variation at *Psy1-A1* and association with yellow pigment in durum wheat grain.** *Theor Appl Genet* 2009, **118:**1539-1548.

161. Singh RP: **Genetic association of leaf rust resistance gene *Lr34* with adult plant resistance to stripe rust in bread wheat.** *Phytopathology* 1992, **82:**835-838.

162. Slade AJ, Fuerstenberg SI, Loeffler D, Steine MN, Facciotti D: **A reverse genetic, nontransgenic approach to wheat crop improvement by TILLING.** *Nat Biotechnol* 2005, **23:**75-81.

163. Slade AJ, Knauf VC: **TILLING moves beyond functional genomics into crop improvement.** *Transgenic Res* 2005, **14:**109-115.

164. Slootmaker LAJ, Lange W, Jochemsen G, Schepers J: **Monosomic analysis in bread wheat of resistance to cereal root eelworm.** *Euphytica* 1974, **23:**497-503.

165. Smiley RW, Nicol JM: **Nematodes which challenge global wheat production.** In *Wheat science and trade.* Edited by Carver BF: Wiley-Blackwell; 2009: 171-187

166. Smiley RW, Whittaker RG, Gourlie JA, Easley SA: **Suppression of wheat growth and yield by *Pratylenchus neglectus* in the pacific northwest.** *Plant Dis* 2005, **89:**958-968.

167. Smiley RW, Yan G, Smiley RW, Yan G: **Cereal cyst nematodes: biology and management in pacific northwest wheat, barley, and oat crops.** Oregon State University, Washington State University, University of Idaho, US Dept. of Agriculture, 2010.

168. Somers D, Isaac P, Edwards K: **A high-density microsatellite consensus map for bread wheat (*Triticum aestivum* L.).** *Theor Appl Genet* 2004, **109:**1105-1114.

169. Song QJ, Shi JR, Singh S, Fickus EW, Costa JM, Lewis J, Gill BS, Ward R, Cregan PB: **Development and mapping of microsatellite (SSR) markers in wheat.** *Theor Appl Genet* 2005, **110:**550-560.

170. Sorrells ME, La Rota M, Bermudez-Kandianis CE, Greene RA, Kantety R, Munkvold JD, Miftahudin, Mahmoud A, Ma X, Gustafson PJ, et al: **Comparative DNA sequence analysis of wheat and rice genomes.** *Genome Res* 2003, **13:**1818-1827.

171. Sourdille P, Singh S, Cadalen T, Brown-Guedira GL, Gay G, Qi L, Gill BS, Dufour P, Murigneux A, Bernard M: **Microsatellite-based deletion bin system for the establishment of genetic-physical map relationships in wheat (*Triticum aestivum* L.).** *Funct Integr Genomics* 2004, **4:**12-25.

172. Spielmeyer W, McIntosh RA, Kolmer J, Lagudah ES: **Powdery mildew resistance and *Lr34/Yr18* genes for durable resistance to leaf and stripe rust cosegregate at a locus on the short arm of chromosome 7D of wheat.** *Theor Appl Genet* 2005, **111:**731-735.

173. Stamatakis A: **RAxML-VI-HPC: maximum likelihood-based phylogenetic analyses with thousands of taxa and mixed models.** *Bioinformatics* 2006, **22:**2688-2690.

174. Sturtevant AH: **The linear arrangement of six sex-linked factors in *Drosophila*, as shown by their mode of association.** *J Exp Zool* 1913, **14:**43-59.

175. Talavera M, Stone VA: **Monitoring *Pratylenchus thornei* densities in SOCL and roots under resistant *(Triticum turgidum durum*) and susceptible (*Triticum aestivum*) wheat cultivars.** *Phytoparasitica* 2001, **29:**29-35.

176. Tanaka T, Kobayashi F, Joshi GP, Onuki R, Sakai H, Kanamori H, Wu J, Šimková H, Nasuda S, Endo TR, et al: **Next-generation survey sequencing and the molecular organization of wheat chromosome 6B.** *DNA Res* 2013.

177. Taylor SP, Hollaway GJ, Hunt CH: **Effect of field crops on population densities of *Pratylenchus neglectus* and *P. thornei* in southeastern Australia; Part 1: *P. neglectus*.** *J Nematol* 2000, **32:**591-599.

178. The TT, McIntosh RA: **Cytogenetical studies in wheat VIII.* Telocentric mapping and linkage studies involving *Sr22* and other genes in chromosome 7AL.** *Aust J Biol Sci* 1975, **28:**531-538.

179. Thompson J, Clewett T, Sheedy J, Reen R, O'Reilly M, Bell K: **Occurrence of root-lesion nematodes (*Pratylenchus thornei* and *P. neglectus*) and stunt nematode (*Merlinius brevidens*) in the northern grain region of Australia.** *Australas Plant Pathol* 2010, **39:**254-264.

180. Trick M, Adamski NM, Mugford SG, Jiang CC, Febrer M, Uauy C: **Combining SNP discovery from next-generation sequencing data with bulked segregant analysis (BSA) to fine-map genes in polyploid wheat.** *BMC Plant Biol* 2012, **12:**14.

181. Van Os H, Stam P, Visser RGF, Van Eck HJ: **RECORD: a novel method for ordering loci on a genetic linkage map.** *Theor Appl Genet* 2005, **112:**30-40.

182. Vanstone VA, Rathjen AJ, Ware AH, Wheeler RD: **Relationship between root lesion nematodes (*Pratylenchus neglectus* and *P. thornei*) and performance of wheat varieties.** *Aust J Exp Agric* 1998, **38:**181-188.

183. Verbyla A, Cullis B, Thompson R: **The analysis of QTL by simultaneous use of the full linkage map.** *Theor Appl Genet* 2007, **116:**95-111.

184. Voorrips RE: **MapChart: Software for the graphical presentation of linkage maps and QTLs.** *J Hered* 2002, **93:**77-78.

185. Wall AM, Riley R, Gale MD: **The position of a locus on chromosome 5B of *Triticum aestivum* affecting homoeologous meiotic pairing.** *Genet Res (Camb)* 1971, **18:**329-339.

186. Wallwork H, Zwer P: **Cereal variety disease guide 2014.** South Australian Research and Development Institute, 2014.

187. Wang J, He X, He Z, Wang H, Xia X: **Cloning and phylogenetic analysis of phytoene synthase 1 (*Psy1*) genes in common wheat and related species.** *Hereditas* 2009, **146:**208-256.

188. **Windows QTL Cartographer 2.5** [http://statgen.ncsu.edu/qtlcart/WQTLCart.htm]

189. Wang S, Wong D, Forrest K, Allen A, Chao S, Huang BE, Maccaferri M, Salvi S, Milner SG, Cattivelli L, et al: **Characterization of polyploid wheat genomic diversity using a high-density 90 000 single nucleotide polymorphism array.** *Plant Biotechnol J* 2014**:**10.1111/pbi.12183.

190. Watson IA, Baker EP: **Linkage of resistance to *Erysiphe graminis tritici* and *Puccinia triticina* in certain varieties of *Triticum vulgare* VIll.** In *Proceedings of The Linnean Society of New South Wales; Sydney, Australia*. Linnean Society of New South Wales; 1943

191. Watson IA, Luig NH: ***SR 15* - A new gene for use in the classification of *Puccinia graminis* var. *tritici*.** *Euphytica* 1966, **15:**239-247.

192. Welsch R, Wüst F, Bär C, Al-Babili S, Beyer P: **A third phytoene synthase is devoted to abiotic stress-induced abscisic acid formation in rice and defines**

functional diversification of phytoene synthase genes. *Plant Physiol* 2008, **147:**367-380.

193. Whitehead AG: *Plant Nematode Control.* Wallingford, UK: CAB international; 1997.

194. Wilkinson P, Winfield M, Barker G, Allen A, Burridge A, Coghill J, Edwards K: **CerealsDB 2.0: an integrated resource for plant breeders and scientists.** *BMC Bioinformatics* 2012, **13:**219.

195. William M, Singh RP, Huerta-Espino J, Islas SO, Hoisington D: **Molecular marker mapping of leaf rust resistance gene *Lr46* and its association with stripe rust resistance gene *Yr29* in wheat.** *Phytopathology* 2003, **93:**153-159.

196. Williams K, Fisher J: **Development of *Heterodera avenae* Woll. and host cellular responses in susceptible and resistant wheat.** *Fundam Appl Nematol* 1993, **16:**417-423.

197. Williams K, Willsmore K, Olson S, Matic M, Kuchel H: **Mapping of a novel QTL for resistance to cereal cyst nematode in wheat.** *Theor Appl Genet* 2006, **112:**1480-1486.

198. Williams KJ, Fisher JM, Langridge P: **Identification of RFLP markers linked to the cereal cyst nematode resistance gene (*Cre*) in wheat.** *Theor Appl Genet* 1994, **89:**927-930.

199. Williams KJ, Lewis JG, Bogacki P, Pallotta MA, Willsmore KL, Kuchel H, Wallwork H: **Mapping of a QTL contributing to cereal cyst nematode tolerance and resistance in wheat.** *Aust J Agric Res* 2003, **54:**731-737.

200. Williams KJ, Taylor SP, Bogacki P, Pallotta M, Bariana HS, Wallwork H: **Mapping of the root lesion nematode (*Pratylenchus neglectus*) resistance gene *Rlnn1* in wheat.** *Theor Appl Genet* 2002, **104:**874-879.

201. Wittwer CT, Reed GH, Gundry CN, Vandersteen JG, Pryor RJ: **High-resolution genotyping by amplicon melting analysis using LCGreen.** *Clin Chem* 2003, **49:**853-860.

202. You F, Huo N, Gu Y, Luo M-c, Ma Y, Hane D, Lazo G, Dvorak J, Anderson O: **BatchPrimer3: A high throughput web application for PCR and sequencing primer design.** *BMC Bioinformatics* 2008, **9:**253.

203. Zeng ZB: **Precision mapping of quantitative trait loci.** *Genetics* 1994, **136:**1457-1468.

204. Zhang L, Yan J, Xia X: **QTL mapping for kernel yellow pigment content in common wheat.** *Acta Agronomica Sinica* 2006, **32**.

205. Zhang P, Friebe B, Lukaszewski A, Gill B: **The centromere structure in robertsonian wheat-rye translocation chromosomes indicates that centric breakage-fusion can occur at different positions within the primary constriction.** *Chromosoma* 2001, **110:**335-344.

206. Zhang Y, Wu Y, Xiao Y, He Z, Zhang Y, Yan J, Zhang Y, Xia X, Ma C: **QTL mapping for flour and noodle colour components and yellow pigment content in common wheat.** *Euphytica* 2009, **165:**435-444.

207. Zwart R, Thompson J, Milgate A, Bansal U, Williamson P, Raman H, Bariana H: **QTL mapping of multiple foliar disease and root-lesion nematode resistances in wheat.** *Mol Breed* 2010, **26:**107-124.

208. Zwart RS, Thompson JP, Godwin ID: **Identification of quantitative trait loci for resistance to two species of root-lesion nematode (*Pratylenchus thornei* and *P. neglectus*) in wheat.** *Aust J Agric Res* 2005, **56:**345-352.

209. Zwart RS, Thompson JP, Sheedy JG, Nelson JC: **Mapping quantitative trait loci for resistance to *Pratylenchus thornei* from synthetic hexaploid wheat in the**

International *Triticeae* Mapping Initiative (ITMI) population. *Aust J Agric Res* 2006, **57:**525-530.

Appendix 1: Supplementary material of Chapter 3

This appendix presents the contents of five additional files that were published as supplements to the publication by Jayatilake et al. (2013) in BMC Plant Biology (Chapter 3).

Additional file S1.1

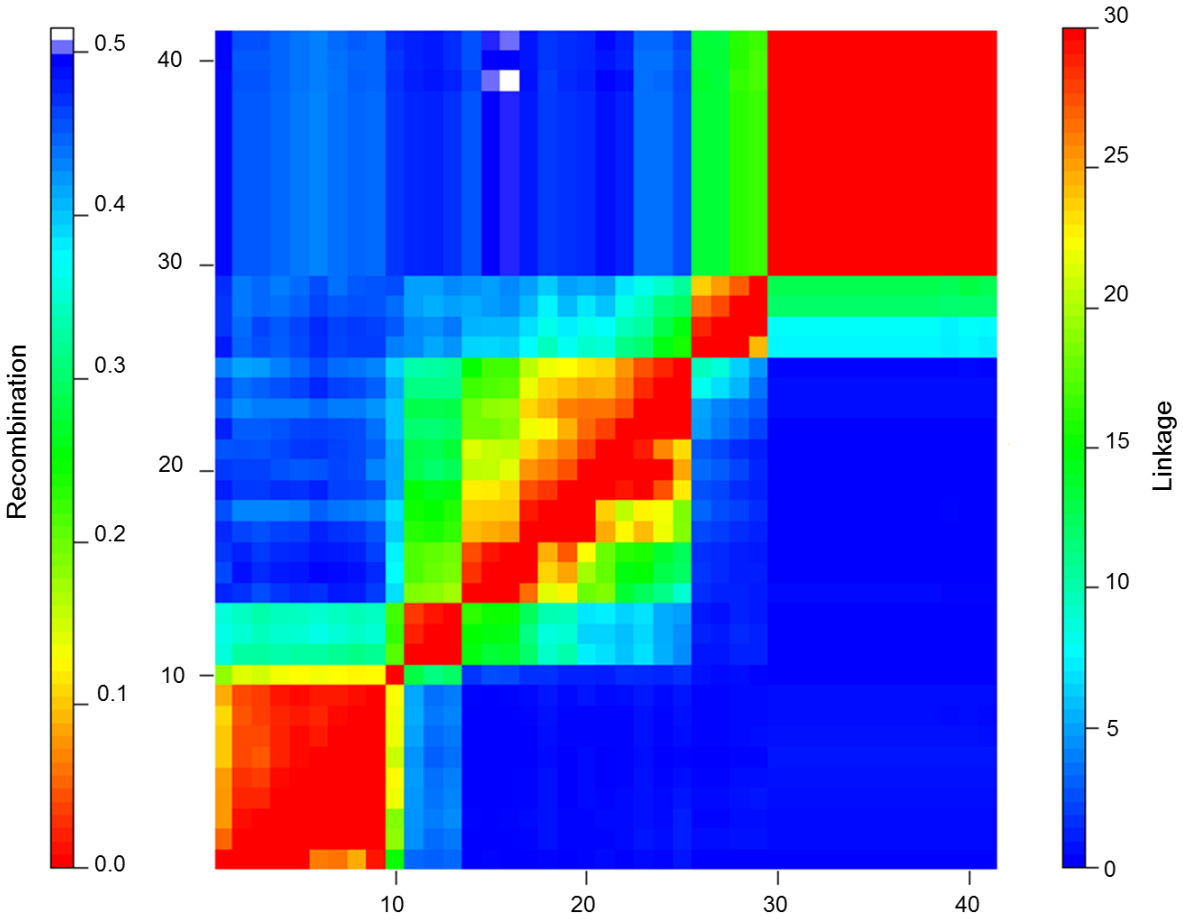

Figure S1.1: Pairwise recombination fraction and LOD linkage plot of chromosome 7A.

Additional file S1.2

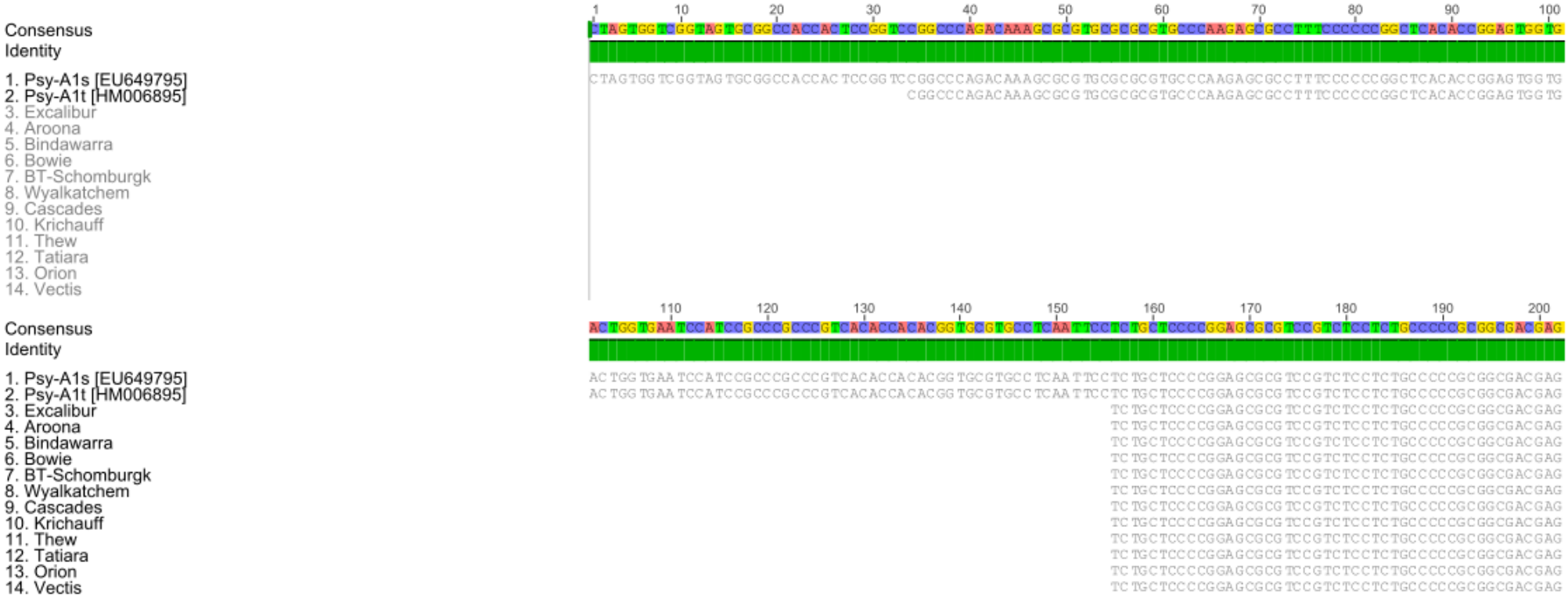

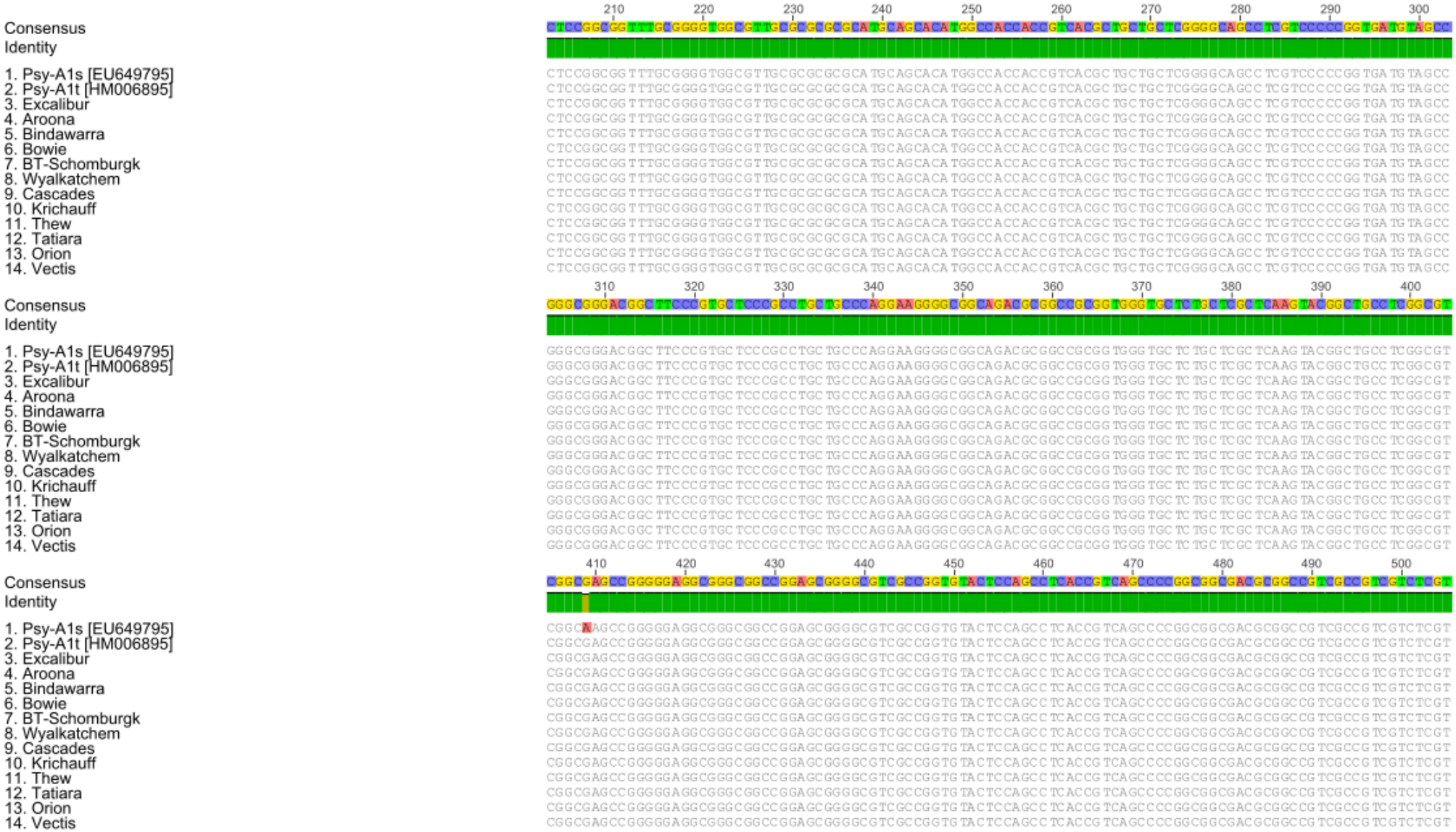
Consensus
Identity
1. Psy-A1s [EU649795]
2. Psy-A1t [HM006895]
3. Excalibur
4. Aroona
5. Bindawarra
6. Bowie
7. BT-Schomburgk
8. Wyalkatchem
9. Cascades
10. Krichauff
11. Thew
12. Tatiara
13. Orion
14. Vectis

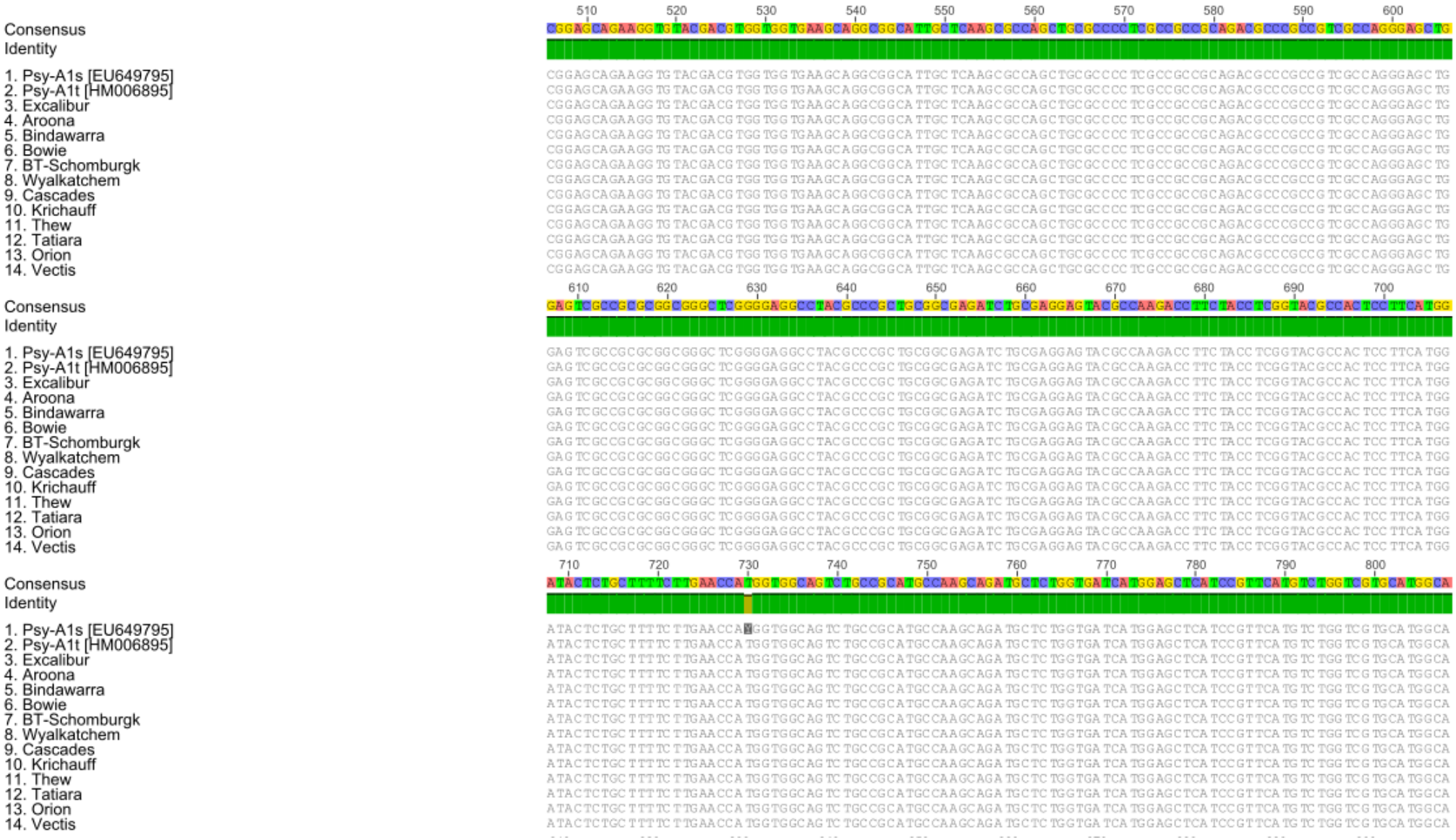
Consensus
Identity
1. Psy-A1s [EU649795]
2. Psy-A1t [HM006895]
3. Excalibur
4. Aroona
5. Bindawarra
6. Bowie
7. BT-Schomburgk
8. Wyalkatchem
9. Cascades
10. Krichauff
11. Thew
12. Tatiara
13. Orion
14. Vectis
510 520 530 540 550 560 570 580 590 600
610 620 630 640 650 660 670 680 690 700
710 720 730 740 750 760 770 780 790 800


Consensus
Identity
1. Psy-A1s [EU649795]
2. Psy-A1t [HM006895]
3. Excalibur
4. Aroona
5. Bindawarra
6. Bowie
7. BT-Schomburgk
8. Wyalkatchem
9. Cascades
10. Krichauff
11. Thew
12. Tatiara
13. Orion
14. Vectis
Consensus
Identity
1. Psy-A1s [EU649795]
2. Psy-A1t [HM006895]
3. Excalibur
4. Aroona
5. Bindawarra
6. Bowie
7. BT-Schomburgk
8. Wyalkatchem
9. Cascades
10. Krichauff
11. Thew
12. Tatiara
13. Orion
14. Vectis
Consensus
Identity
1. Psy-A1s [EU649795]
2. Psy-A1t [HM006895]
3. Excalibur
4. Aroona
5. Bindawarra
6. Bowie
7. BT-Schomburgk
8. Wyalkatchem
9. Cascades
10. Krichauff
11. Thew
12. Tatiara
13. Orion
14. Vectis

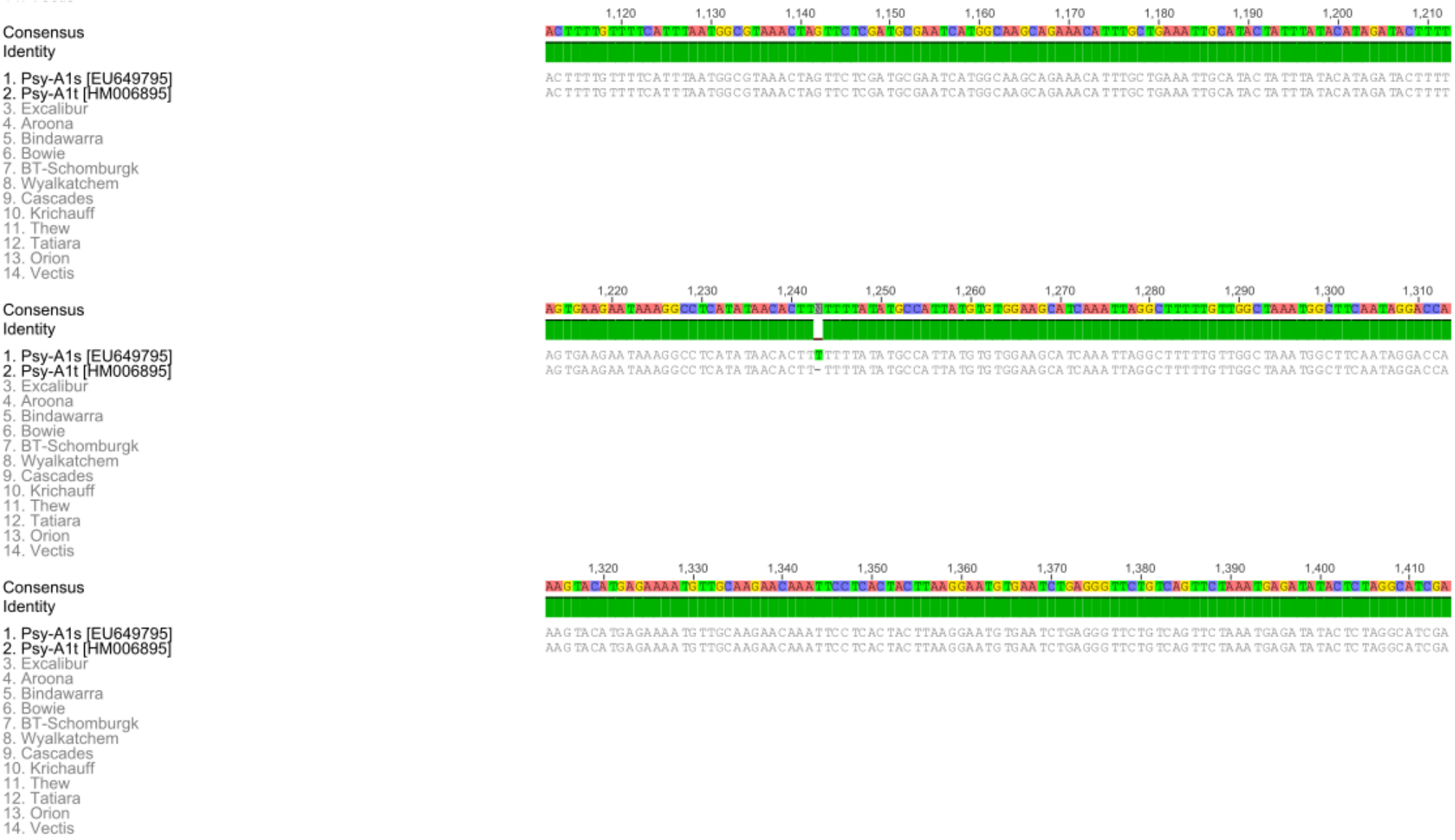
Consensus
Identity
1. Psy-A1s [EU649795]
2. Psy-A1t [HM006895]
3. Excalibur
4. Aroona
5. Bindawarra
6. Bowie
7. BT-Schomburgk
8. Wyalkatchem
9. Cascades
10. Krichauff
11. Thew
12. Tatiara
13. Orion
14. Vectis
1,120
1,130
1,140
1,150
1,160
1,170
1,180
1,190
1,200
1,210
1,220
1,230
1,240
1,250
1,260
1,270
1,280
1,290
1,300
1,310
1,320
1,330
1,340
1,350
1,360
1,370
1,380
1,390
1,400
1,410

Consensus
Identity

1. Psy-A1s [EU649795]
2. Psy-A1t [HM006895]
3. Excalibur
4. Aroona
5. Bindawarra
6. Bowie
7. BT-Schomburgk
8. Wyalkatchem
9. Cascades
10. Krichauff
11. Thew
12. Tatiara
13. Orion
14. Vectis

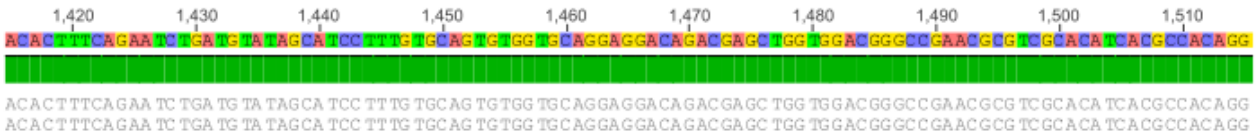

Consensus
Identity

1. Psy-A1s [EU649795]
2. Psy-A1t [HM006895]
3. Excalibur
4. Aroona
5. Bindawarra
6. Bowie
7. BT-Schomburgk
8. Wyalkatchem
9. Cascades
10. Krichauff
11. Thew
12. Tatiara
13. Orion
14. Vectis

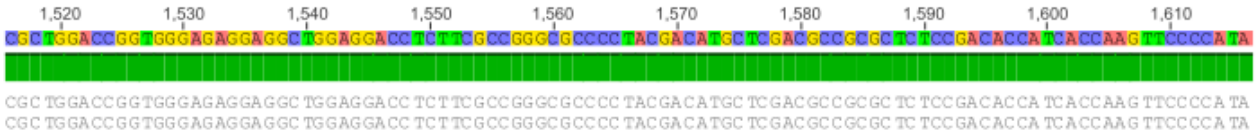

Consensus
Identity

1. Psy-A1s [EU649795]
2. Psy-A1t [HM006895]
3. Excalibur
4. Aroona
5. Bindawarra
6. Bowie
7. BT-Schomburgk
8. Wyalkatchem
9. Cascades
10. Krichauff
11. Thew
12. Tatiara
13. Orion
14. Vectis

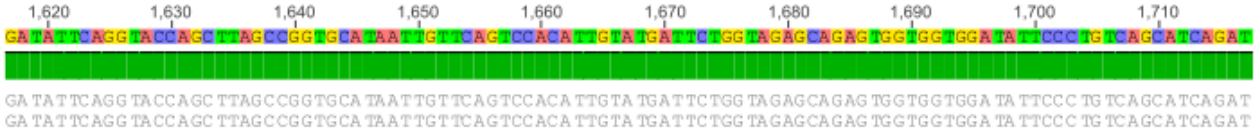


Consensus
Identity
1. Psy-A1s [EU649795]
2. Psy-A1t [HM006895]
3. Excalibur
4. Aroona
5. Bindawarra
6. Bowie
7. BT-Schomburgk
8. Wyalkatchem
9. Cascades
10. Krichauff
11. Thew
12. Tatiara
13. Orion
14. Vectis
1,720 1,730 1,740 1,750 1,760 1,770 1,780 1,790 1,800 1,810
1,820 1,830 1,840 1,850 1,860 1,870 1,880 1,890 1,900 1,910
1,920 1,930 1,940 1,950 1,960 1,970 1,980 1,990 2,000 2,010 2,020

Consensus
Identity

1. Psy-A1s [EU649795]
2. Psy-A1t [HM006895]
3. Excalibur
4. Aroona
5. Bindawarra
6. Bowie
7. BT-Schomburgk
8. Wyalkatchem
9. Cascades
10. Krichauff
11. Thew
12. Tatiara
13. Orion
14. Vectis

Consensus
Identity

1. Psy-A1s [EU649795]
2. Psy-A1t [HM006895]
3. Excalibur
4. Aroona
5. Bindawarra
6. Bowie
7. BT-Schomburgk
8. Wyalkatchem
9. Cascades
10. Krichauff
11. Thew
12. Tatiara
13. Orion
14. Vectis

Consensus
Identity

1. Psy-A1s [EU649795]
2. Psy-A1t [HM006895]
3. Excalibur
4. Aroona
5. Bindawarra
6. Bowie
7. BT-Schomburgk
8. Wyalkatchem
9. Cascades
10. Krichauff
11. Thew
12. Tatiara
13. Orion
14. Vectis

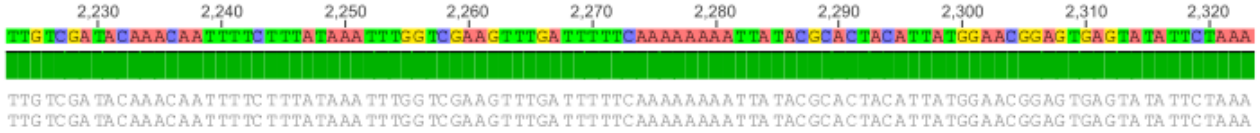


Consensus
Identity
1. Psy-A1s [EU649795]
2. Psy-A1t [HM006895]
3. Excalibur
4. Aroona
5. Bindawarra
6. Bowie
7. BT-Schomburgk
8. Wyalkatchem
9. Cascades
10. Krichauff
11. Thew
12. Tatiara
13. Orion
14. Vectis
2,330
2,340
2,350
2,360
2,370
2,380
2,390
2,400
2,410
2,420
ATGACAGACTCTTCATACATATGCCAGCCCTTCAAGGACATGATCGACGGGATGCGGACAGACCTCAAGAAGGCAAGATACAAGAACTTCGACGAGCTCTA
ATGACAGACTCTTCATACATATGCCAGCCCTTCAAGGACATGATCGACGGGATGCGGACAGACCTCAAGAAGGCAAGATACAAGAACTTCGACGAGCTCTA
2,430
2,440
2,450
2,460
2,470
2,480
2,490
2,500
2,510
2,520
CATGTACTGCTACTATGTCGCGGGTACGGTGGGGCTGATGAGCGTCCCGGTGATGGGCATTGCGCCCGAGTCCAAGGCGACGGCCGAGAGCGTCTACGGCG
CATGTACTGCTACTATGTCGCGGGTACGGTGGGGCTGATGAGCGTCCCGGTGATGGGCATTGCGCCCGAGTCCAAGGCGACGGCCGAGAGCGTCTACGGCG
2,530
2,540
2,550
2,560
2,570
2,580
2,590
2,600
2,610
2,620
CCGCTCTGGCTCTCGGGCTGGCGAACCAGCTCACCAACATACTCAGGGATGTTGGAGAAGAGTAAGCCACCCACTGATTACCACTAAAATGCAACGGTTTT
CCGCTCTGGCTCTCGGGCTGGCGAACCAGCTCACCAACATACTCAGGGATGTTGGAGAAGAGTAAGCCACCCACTGATTACCACTAAAATGCAACGGTTTT

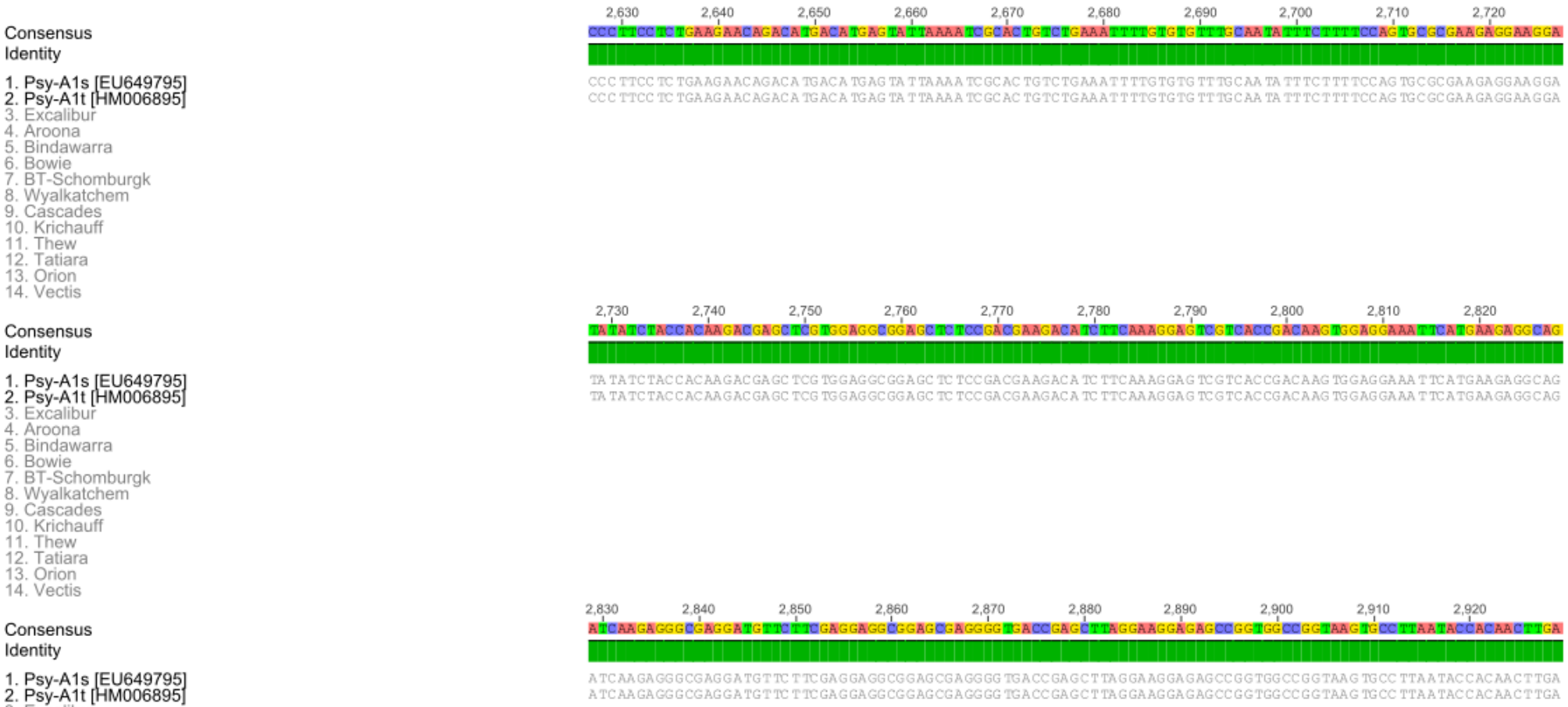
Consensus
Identity
1. Psy-A1s [EU649795]
2. Psy-A1t [HM006895]
3. Excalibur
4. Aroona
5. Bindawarra
6. Bowie
7. BT-Schomburgk
8. Wyalkatchem
9. Cascades
10. Krichauff
11. Thew
12. Tatiara
13. Orion
14. Vectis
2,630
2,640
2,650
2,660
2,670
2,680
2,690
2,700
2,710
2,720
CCCTTCCTCTGAAGAACAGACATGACATGAGTATTAAAATCGCACTGTCTGAAATTTTGTGTGTTTGCAATATTTCTTTTCCAGTGCGCGAAGAGGAAGGA
CCC TTCC TC TGAAGAACAGACA TGACA TGAG TA T TAAAA TCGCAC TGTCTGAAAT T TTGTGTG TT TGCAA TA TT TCT TT TCCAG TGCGCGAAGAGGAAGGA
Consensus
Identity
1. Psy-A1s [EU649795]
2. Psy-A1t [HM006895]
3. Excalibur
4. Aroona
5. Bindawarra
6. Bowie
7. BT-Schomburgk
8. Wyalkatchem
9. Cascades
10. Krichauff
11. Thew
12. Tatiara
13. Orion
14. Vectis
2,730
2,740
2,750
2,760
2,770
2,780
2,790
2,800
2,810
2,820
TATATCTACCACAAGACGAGCTCGTGGAGGCGGAGCTCTCCGACGAAGACATCTTCAAAGGAGTCGTCACCGACAAGTGGAGGAAATTCATGAAGAGGCAG
TA TATC TACCACAAGACGAGC TCG TGGAGGCGGAGC TC TCCGACGAAGACA TC TTCAAAGGAG TCGTCACCGACAAG TGGAGGAAA T TCATGAAGAGGCAG
Consensus
Identity
1. Psy-A1s [EU649795]
2. Psy-A1t [HM006895]
3. Excalibur
4. Aroona
5. Bindawarra
6. Bowie
7. BT-Schomburgk
8. Wyalkatchem
9. Cascades
10. Krichauff
11. Thew
12. Tatiara
13. Orion
14. Vectis
2,830
2,840
2,850
2,860
2,870
2,880
2,890
2,900
2,910
2,920
ATCAAGAGGGCGAGGATGTTCTTCGAGGAGGCGGAGCGAGGGGTGACCGAGCTTAGGAAGGAGAGCCGGTGGCCGGTAAGTGCCTTAATACCACAACTTGA
ATCAAGAGGGCGAGGATGTTC TTCGAGGAGGCGGAGCGAGGGG TGACCGAGCTTAGGAAGGAGAGCCGGTGGCCGGTAAG TGCC TTAATACCACAACTTGA

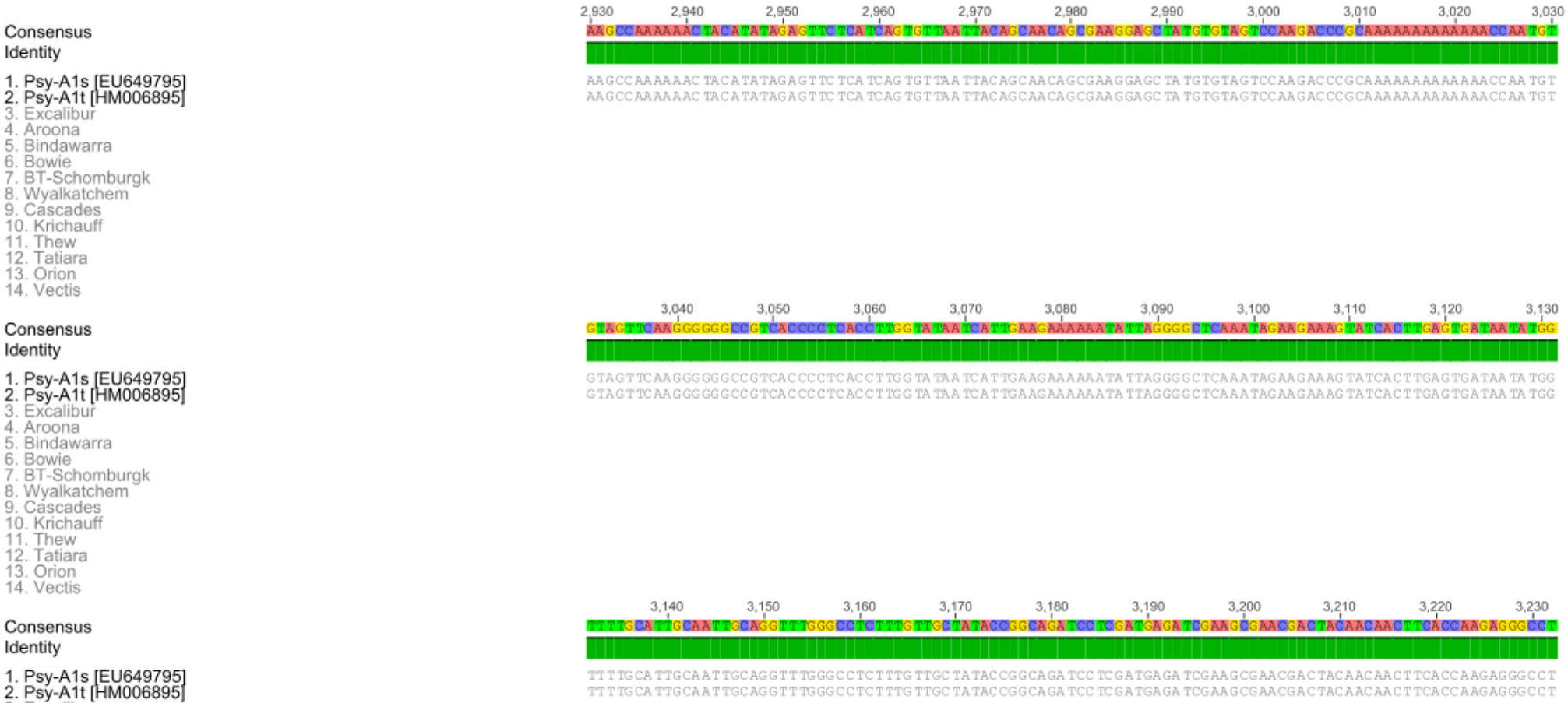
Consensus
Identity
1. Psy-A1s [EU649795]
2. Psy-A1t [HM006895]
3. Excalibur
4. Aroona
5. Bindawarra
6. Bowie
7. BT-Schomburgk
8. Wyalkatchem
9. Cascades
10. Krichauff
11. Thew
12. Tatiara
13. Orion
14. Vectis
2,930 2,940 2,950 2,960 2,970 2,980 2,990 3,000 3,010 3,020 3,030
AAGCCAAAAAACTACATATAGAGTTCTCATCAGTGTTAATTACAGCAACAGCGAAGGAGCTATGTGTAGTCCAAGACCCGCAAAAAAAAAAAAAACCAATGT
AAGCCAAAAAACTACATATAGAGTTCTCATCAGTGTTAATTACAGCAACAGCGAAGGAGCTATGTGTAGTCCAAGACCCGCAAAAAAAAAAAAAACCAATGT
3,040 3,050 3,060 3,070 3,080 3,090 3,100 3,110 3,120 3,130
GTAGTTCAAGGGGGGCCGTCACCCCTCACCTTGGTATAATCATTGAAGAAAAAATATTAGGGGCTCAAATAGAAGAAAGTATCACTTGAGTGATAATATGG
GTAGTTCAAGGGGGGCCGTCACCCCTCACCTTGGTATAATCATTGAAGAAAAAATATTAGGGGCTCAAATAGAAGAAAGTATCACTTGAGTGATAATATGG
3,140 3,150 3,160 3,170 3,180 3,190 3,200 3,210 3,220 3,230
TTTTGCATTGCAATTGCAGGTTTGGGCCTCTTTGTTGCTATACCGGCAGATCCTCGATGAGATCGAAGCGAACGACTACAACAACTTCACCAAGAGGGCCT
TTTTGCATTGCAATTGCAGGTTTGGGCCTCTTTGTTGCTATACCGGCAGATCCTCGATGAGATCGAAGCGAACGACTACAACAACTTCACCAAGAGGGCCT

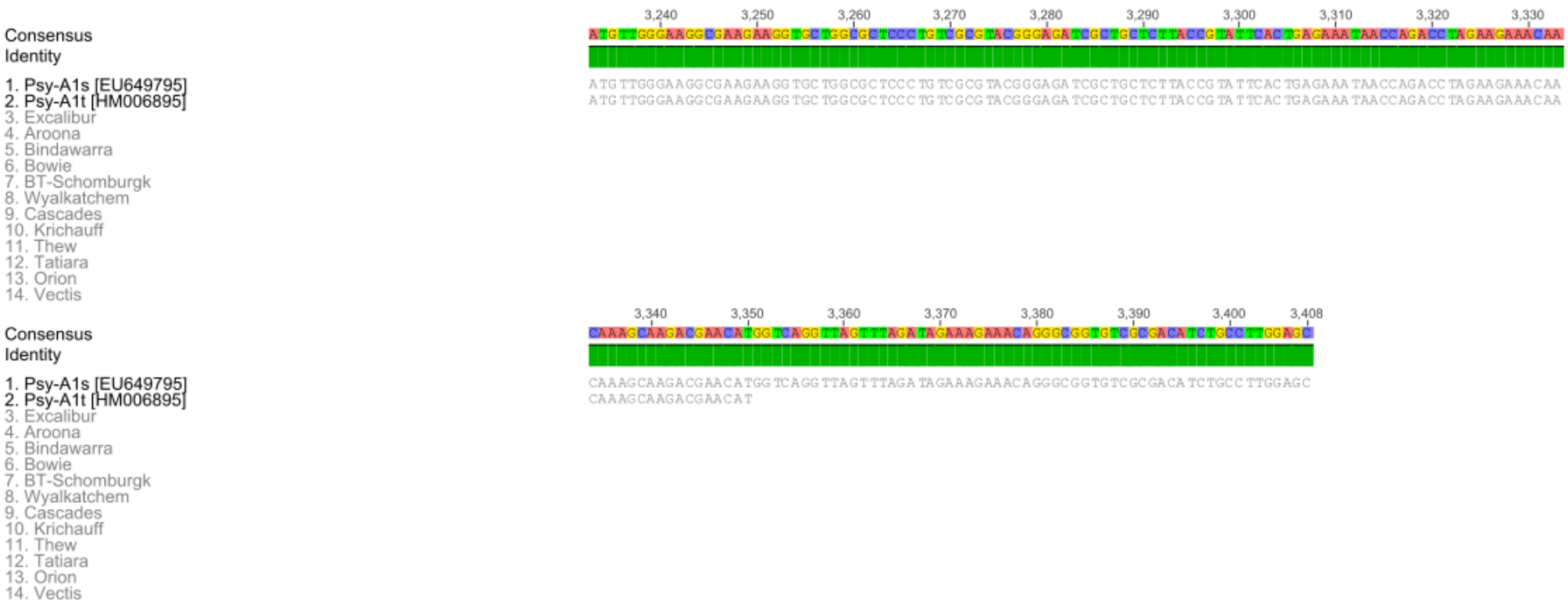

Figure S1.2: Alignment of sequences of *PSY7A5_F/R* amplicons from Excalibur and 11 other cultivars to the *Psy-A1t* allele sequence of the breeding line WAWHT2074 [GenBank:HM006895] and the *Psy-A1s* allele sequence of the cultivar Schomburgk [GenBank:EU649795].

Additional file S1.3

Table S1.1: Rice BLASTN results using query sequences for ESTs from wheat deletion bins 7AL16-0.86-0.90 and 7AL18-0.90-1.00.

BLAST query		BLAST hit						
EST accession	Wheat deletion bin	Rice chromosome	Rice chromosome start position (bp)	Rice chromosome end position (bp)	BLAST hit to rice CDS database	E value	Top Query Coverage	Top Identity
BE404790	7AL16-0.86-0.90	-	-	-	no significant hits	-	-	-
BE426715	7AL16-0.86-0.90	-	-	-	no significant hits	-	-	-
BE590621	7AL16-0.86-0.90	-	-	-	no significant hits	-	-	-
BE591497	7AL16-0.86-0.90	-	-	-	no significant hits	-	-	-
BF294048	7AL16-0.86-0.90	-	-	-	no significant hits	-	-	-
BF482648	7AL16-0.86-0.90	-	-	-	no significant hits	-	-	-
BG263870	7AL16-0.86-0.90	-	-	-	no significant hits	-	-	-
BG314165	7AL16-0.86-0.90	-	-	-	no significant hits	-	-	-
BM140333	7AL16-0.86-0.90	-	-	-	no significant hits	-	-	-
BM140366	7AL16-0.86-0.90	-	-	-	no significant hits	-	-	-
BE405531	7AL16-0.86-0.90	1	-	-	LOC_Os01g05960.1	2.00E-29	98.73%	61.41%

BE426680	7AL18-0.90-1.00	1	-	-	LOC_Os01g23620.1	2.20E-97	100.00%	90.35%
BF482714	7AL16-0.86-0.90	1	-	-	LOC_Os01g42090.1	1.60E-73	100.00%	83.84%
BM137749	7AL18-0.90-1.00	1	-	-	LOC_Os01g43851.1	1.10E-79	100.00%	80.72%
BG262960	7AL16-0.86-0.90	2	-	-	LOC_Os02g19130.1	2.50E-44	66.60%	80.12%
BE403423	7AL18-0.90-1.00	2	-	-	LOC_Os02g32009.1	1.30E-15	62.46%	71.56%
BM134450	7AL16-0.86-0.90	2	-	-	LOC_Os02g48870.1	5.20E-13	88.55%	63.33%
BE404737	7AL18-0.90-1.00	2	-	-	LOC_Os02g52430.1	2.90E-69	99.02%	80.75%
BF146165	7AL18-0.90-1.00	4	-	-	LOC_Os04g55660.1	9.50E-10	32.00%	71.78%
BE405648	7AL18-0.90-1.00	5	-	-	LOC_Os05g19270.1	1.90E-107	100.00%	87.97%
BF428868	7AL16-0.86-0.90	6	1459192	1464339	LOC_Os06g03700.1	2.50E-100	100.00%	85.49%
BF202806	7AL16-0.86-0.90	6	7924037	7920479	LOC_Os06g14190.1	1.10E-88	99.82%	86.29%
BF474379	7AL16-0.86-0.90	6	24817722	24814005	LOC_Os06g41390.1	1.20E-84	86.53%	82.56%
BE591637	7AL18-0.90-1.00	6	25967411	25963875	LOC_Os06g43190.1	5.80E-38	97.60%	68.49%
BE443877	7AL18-0.90-1.00	6	26187104	26183307	LOC_Os06g43550.1	2.40E-18	37.40%	70.04%
BE403180	7AL18-0.90-1.00	6	26204623	26199320	LOC_Os06g43570.1	8.70E-89	99.61%	89.47%
BE443357	7AL18-0.90-1.00	6	26379227	26375956	LOC_Os06g43800.1	4.40E-08	55.59%	68.05%
BE497838	7AL16-0.86-0.90	6	26379227	26375956	LOC_Os06g43800.1	1.90E-25	52.79%	81.34%
BE426274	7AL16-0.86-0.90	6	26414835	26411488	LOC_Os06g43860.1	2.20E-54	75.97%	85.59%

BE446809	7AL16-0.86-0.90	6	26427830	26421512	LOC_Os06g43870.2	1.40E-17	68.30%	68.12%
BE496850	7AL16-0.86-0.90	6	26461806	26456227	LOC_Os06g43930.1	3.70E-27	80.51%	71.60%
BE637838	7AL16-0.86-0.90	6	26529298	26538141	LOC_Os06g44030.2	2.70E-94	99.81%	90.84%
BF294002	7AL16-0.86-0.90	6	26579684	26575125	LOC_Os06g44060.1	1.50E-92	100.00%	86.82%
BE637853	7AL16-0.86-0.90	6	26680140	26690056	LOC_Os06g44230.1	9.10E-05	15.00%	96.08%
BE471156	7AL16-0.86-0.90	6	26781799	26778838	LOC_Os06g44370.1	6.10E-113	100.00%	88.94%
BE406505	7AL16-0.86-0.90	6	27219528	27223172	LOC_Os06g45000.1	2.90E-34	90.05%	74.49%
BG262287	7AL16-0.86-0.90	6	27292852	27286243	LOC_Os06g45120.1	4.90E-53	100.00%	84.31%
BE605194	7AL16-0.86-0.90	6	27369245	27363816	LOC_Os06g45280.1	4.00E-48	79.60%	84.70%
BE498985	7AL16-0.86-0.90	6	27384222	27386859	LOC_Os06g45300.1	6.40E-31	98.76%	81.25%
BG274853	7AL16-0.86-0.90	6	27728316	27724565	LOC_Os06g45820.1	1.70E-77	100.00%	90.41%
BF145815	7AL16-0.86-0.90	6	27760083	27756424	LOC_Os06g45870.1	7.30E-21	53.76%	65.80%
BF428699	7AL16-0.86-0.90	6	28203817	28204370	LOC_Os06g46460.1	2.80E-11	70.08%	59.90%
BG312585	7AL18-0.90-1.00	6	30231310	30225270	LOC_Os06g49930.1	4.70E-32	54.05%	66.17%
BG274625	7AL18-0.90-1.00	6	30423505	30422607	LOC_Os06g50250.1	1.80E-11	52.68%	64.94%
BE445527	7AL16-0.86-0.90	6	30830434	30828271	LOC_Os06g50940.1	5.20E-52	79.63%	72.99%
BF146129	7AL18-0.90-1.00	6	30913486	30907000	LOC_Os06g51100.1	1.50E-13	29.89%	72.62%
BE426802	7AL16-0.86-0.90	6	30918120	30915029	LOC_Os06g51110.2	7.80E-20	72.68%	62.87%

BE591469[a]	7AL18-0.90-1.00	6	30944196	30948366	LOC_Os06g51150.1	3.90E-113	98.16%	89.69%
BE637476[b]	7AL18-0.90-1.00	6	30944196	30948366	LOC_Os06g51150.1	5.10E-82	99.57%	90.50%
BE445506[c]	7AL18-0.90-1.00	6	30956664	30953028	LOC_Os06g51170.1	3.70E-55	59.43%	83.73%
BF483039[d]	7AL18-0.90-1.00	6	31029132	31025937	LOC_Os06g51260.1	1.70E-29	82.23%	67.60%
BF484041[e]	7AL18-0.90-1.00	6	31048512	31033381	LOC_Os06g51270.1	1.00E-56	100.00%	87.85%
BG607810	7AL18-0.90-1.00	6	31048512	31033381	LOC_Os06g51270.1	4.00E-11	18.75%	91.11%
BE445653	7AL18-0.90-1.00	6	31089543	31083106	LOC_Os06g51330.1	1.50E-32	94.33%	75.80%
BE591418	7AL18-0.90-1.00	6	31089543	31083106	LOC_Os06g51330.2	2.60E-31	78.55%	76.17%
BE406627	7AL18-0.90-1.00	6	31151345	31156634	LOC_Os06g51430.1	2.90E-33	100.00%	77.15%
BE637923	7AL16-0.86-0.90	7	-	-	LOC_Os07g07410.2	4.40E-39	89.46%	69.60%
BF146080	7AL16-0.86-0.90	7	-	-	LOC_Os07g29600.1	1.90E-67	93.37%	80.75%
BE442817	7AL16-0.86-0.90	8	-	-	LOC_Os08g09010.1	6.60E-68	85.99%	78.96%
BE494712	7AL18-0.90-1.00	8	-	-	LOC_Os08g12840.1	2.80E-53	94.39%	78.71%
BE499622	7AL18-0.90-1.00	8	-	-	LOC_Os08g43360.1	7.20E-28	83.78%	68.66%
BE606843	7AL18-0.90-1.00	9	-	-	LOC_Os09g11510.1	1.70E-62	99.82%	76.16%
BF293511	7AL18-0.90-1.00	9	-	-	LOC_Os09g38110.1	2.80E-23	70.19%	67.45%
BG313507	7AL18-0.90-1.00	11	-	-	LOC_Os11g05400.1	2.20E-84	100.00%	89.11%
BE590995	7AL18-0.90-1.00	11	-	-	LOC_Os11g11890.1	1.50E-22	52.92%	64.19%

BE444259	7AL16-0.86-0.90	11	-	-	LOC_Os11g41380.1	1.40E-05	79.22%	57.14%
BE405507	7AL18-0.90-1.00	11	-	-	LOC_Os11g41540.1	8.40E-64	99.33%	74.13%
BE405003	7AL16-0.86-0.90	11	-	-	LOC_Os11g47780.1	5.60E-36	85.43%	66.73%
BF483603	7AL16-0.86-0.90	12	-	-	LOC_Os12g01400.1	1.60E-51	82.21%	78.10%
BG606695	7AL18-0.90-1.00	12	-	-	LOC_Os12g06650.1	2.80E-61	100.00%	76.89%
BE518357	7AL16-0.86-0.90	12	-	-	LOC_Os12g10720.2	9.80E-56	81.29%	82.91%
BE446244	7AL18-0.90-1.00	12	-	-	LOC_Os12g27350.1	2.50E-33	86.97%	68.12%
BF293421	7AL16-0.86-0.90	12	-	-	LOC_Os12g34510.1	2.80E-25	59.17%	88.30%
BE405291	7AL18-0.90-1.00	-	-	-	no hits	-	-	-
BE424236	7AL18-0.90-1.00	-	-	-	no hits	-	-	-
BE591389	7AL18-0.90-1.00	-	-	-	no hits	-	-	-
BF483485	7AL18-0.90-1.00	-	-	-	no hits	-	-	-
BF474833	7AL18-0.90-1.00	-	-	-	no significant hits	-	-	-
BE444715	7AL18-0.90-1.00	-	-	-	no significant hits	-	-	-
BE495346	7AL18-0.90-1.00	-	-	-	no significant hits	-	-	-
BE497409	7AL18-0.90-1.00	-	-	-	no significant hits	-	-	-
BE591448	7AL18-0.90-1.00	-	-	-	no significant hits	-	-	-
BE606933	7AL18-0.90-1.00	-	-	-	no significant hits	-	-	-

BF429174	7AL18-0.90-1.00	-	-	-	no significant hits	-	-	-
BF483436	7AL18-0.90-1.00	-	-	-	no significant hits	-	-	-
BF484052	7AL18-0.90-1.00	-	-	-	no significant hits	-	-	-
BG604756	7AL18-0.90-1.00	-	-	-	no significant hits	-	-	-

Marker information: [a] PSR148 has homology to LOC_Os; [b] PSR148 has homology to LOC_Os; [c] *wri1*derived from gDNA homologous to TaEST sequence; [d] *wri5*derived from gDNA homologous to TaEST sequence; [e] CDO347 has homology to LOC_Os, wri3 and wri4 have homology to LOC_Os; [f] *wri2* derived from gDNA homologous to TaEST sequence; [g] *wri2* has homology to LOC_Os

Additional file S1.4

1. Full sequences of *wri2_F/R* amplicons from Excalibur and Kukri

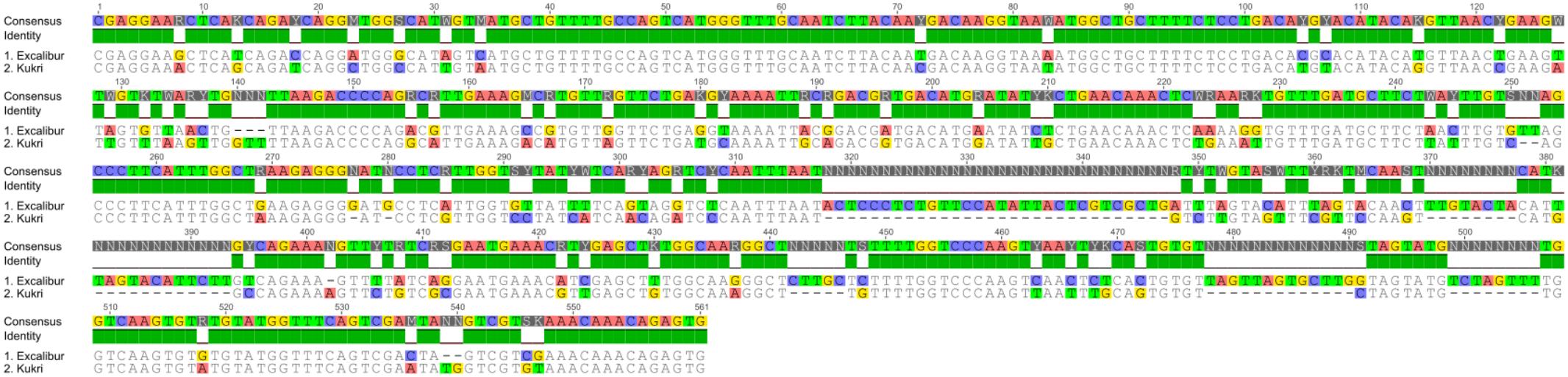

2. Partial sequences of *wri2_F/R* amplicons from Excalibur, Kukri and 10 other cultivars

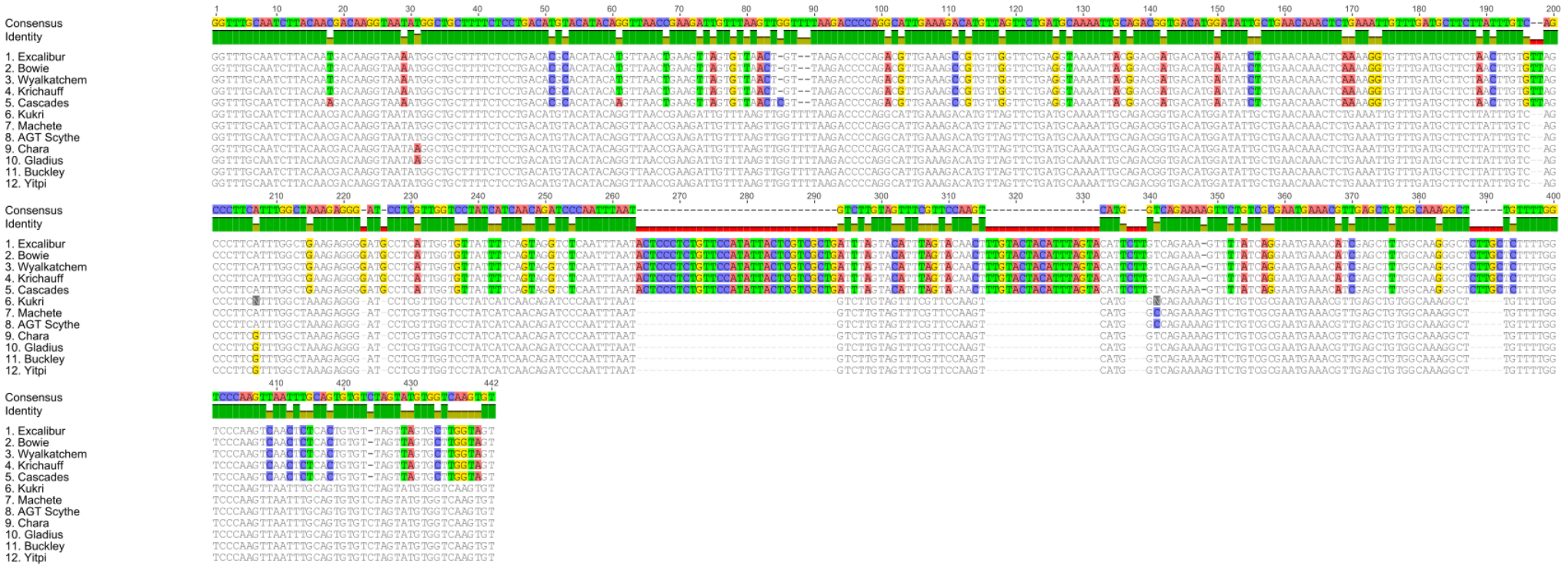

Figure S1.3: Alignment of sequences of *wri2_F/R* amplicons from Excalibur, Kukri and 10 other cultivars.

Additional file S1.5

1. Primer sequences

Table S1.2: Primer sequences of markers *schfc3*, *sts638*, *csPSY* and *PSY7A5*

Primer name	Forward primer sequence (5` - 3`)	Reverse primer sequence (5` - 3`)	Reference
schfc3	TGCAGACCACCTCGGCTG	TAACAGCGGATATGATGG	Personal communication (Meredith Carter)
sts638	GCGGTGACTACACAGCGATGA AGCAATGAAA	GCGGTGACTAGTCCAGTTGGTTGATGGAAT	Neu et al. (2002)
csPSY	GGCCTTCTAAGTTGACCAG GCCAAGCCGGTGTTCCGG	GTCATGTCTGTTCTTCAGAGG CCTCCTGCACCATACTGAAC	Howitt et al. (2009)
PSY7A5	GCGGAGTGGTGACTGGTG	GGCGGTCTGAACTCTGAAGTG	Crawford et al. (2011)

2. Primer sequences and conditions used for PCR and for separation of amplicons by gel electrophoresis and by high-resolution melting analysis

a) Methods for agarose gel electrophoresis based assays

PCR reaction mixtures

PCR reaction mixture 1: *sts638, wri4*

	Final concentration
Template DNA	15 ng/µl
Immolase	0.015 U/µl
Immolase buffer	1 ×
dNTPs	0.2 mM
$MgCl_2$	1.5 mM
Forward primer	0.5 µM
Reverse primer	0.5 µM

PCR reaction mixture 2: *schfc3, wri1, wri3*

	Final concentration
Template DNA	15 ng/µl
Immolase	0.015 U/µl
Immolase buffer	1 ×
dNTPs	0.2 mM
$MgCl_2$	2.5 mM
Forward primer	0.5 µM
Reverse primer	0.5 µM

PCR reaction mixture 3: *wri2*

	Final concentration
Template DNA	20 ng/µl
Immolase	0.015 U/µl
Immolase buffer	1 ×
dNTPs	0.2 mM
$MgCl_2$	2.5 mM
Bovine serum albumin (BSA)	0.1 mg/mL

Forward primer	0.5 µM
Reverse primer	0.5 µM

PCR reaction mixture 4: *wri5*

	Final concentration
Template DNA	15 ng/µl
Immolase	0.0375 U/µl
Immolase buffer	1 ×
dNTPs	0.2 mM
$MgCl_2$	1.0 mM
Bovine serum albumin (BSA)	0.1 mg/mL
Forward primer	0.3 µM
Reverse primer	0.3 µM

PCR reaction mixture 5: *csPSY*

	Final concentration
Template DNA	15 ng/µl
Immolase	0.015 U/µl
Immolase buffer	1 ×
dNTPs	0.2 mM
$MgCl_2$	2.5 mM
Forward primer	0.5 µM
Reverse primer	0.5 µM

Digestion of 5 µl of *csPSY* PCR product with *BstN1* (final reaction volume 10 µl)

	Final concentration
NEBuffer 2	1 ×
BstN1	0.5 U/µl
Bovine serum albumin (BSA)	1 mg/mL

PCR programs

PCR program 1: *schfc3 (Tm-55), sts638 (Tm-62), wri1(Tm-60), wri3(Tm-60)* and *wri5(Tm-60)*

Step 1 - 95 °C for 10 min

Step 2 - 94 °C for 30 s

Step 3 – *Tm* °C for 30s

Step 4 - 72 °C for 1 min

Step 5 - Step 2 for 34 cycles

Step 6 - 72 °C for 5 min

Step 7 - End

PCR program 2: *wri2*

Step 1 - 95 °C for 10 min

Step 2 - 94 °C for 30 s

Step 3 – 60 °C (-0.5 °C/cycle) for 30s

Step 4 - 72 °C for 1 min

Step 5 – step 2 for 19 cycles

Step 6 - 94 °C for 30 s

Step 7- 50 °C for 30s

Step 8 - 72 °C for 1 min

Step 9 – Step 6 for 24 cycles

Step 10 - 72 °C for 5 min

Step 11 – End

PCR program 3: *csPSY*

Step 1 - 95 °C for 10 min

Step 2 - 94 °C for 30 s

Step 3 - 65 °C (-0.5 °C/cycle) for 30s

Step 4 - 72 °C for 45 s

Step 5 - step 2 for 19 cycles

Step 6 - 94 °C for 30 s

Step 7- 55 °C for 30 s

Step 8 - 72 °C for 45 s

Step 9 - Step 6 for 24 cycles

Step 10 - 72 °C for 5 min

Step 11 – End

Digestion with *BstN1*

60 °C for 2 hours

PCR program 4: *wri4*

Step 1 - 95 °C for 10 min

Step 2 - 94 °C for 30 s

Step 3 – 58 °C for 30s

Step 4 - 72 °C for 1 min

Step 5 - step 2 for 14 cycles

Step 6 - 94 °C for 10 s

Step 7 - 45 °C for 30s

Step 8 - Step 6 for 4 cycles

Step 9 - 94 °C for 10 s

Step 10 - 53 °C for 30s

Step 11 - 72 °C for 5 s

Step 12 - step 9 for 14 cycles

Step 13 - End

Gel electrophoresis conditions

schfc3, sts638, wri1, wri4 and *wri5* – 2% agarose gel; 90V; 40 min

csPSY, wri2 and *wri3* – 2.5% agarose gel; 90V; 60 min

b) Methods for high-resolution melting based assays

PCR mixtures

PCR reaction mixture 5: *sts638*

	Final concentration
Template DNA	15 ng/µl
Immolase	0.015 U/µl
Immolase buffer	1 ×
dNTPs	0.2 mM
$MgCl_2$	1.5 mM
Forward primer	0.5 µM
Reverse primer	0.5 µM
Syto9 dye	2.0 µM

PCR reaction mixture 6: *wri1*, *wri3*

	Final concentration
Template DNA	15 ng/µl
Immolase	0.015 U/µl
Immolase buffer	1 ×
dNTPs	0.2 mM
$MgCl_2$	2.5 mM
Forward primer	0.5 µM
Reverse primer	0.5 µM
Syto9 dye	2.0 µM

PCR program

PCR program 1 (see above): *sts638*, *wri1*, *wri3*

HRM conditions

Step 1 - 95°C for 30 s

Step 2 - (*Tm* - 2) °C for 30 s; ramp to 95 °C (+ 0.02 °C/s; 25 acquisitions/ °C)

Step 3 – 37°C for 1 s

c) Methods for partial sequencing of *Psy-A1*

PCR mixture

PCR reaction mixture 7: *PSY7A5*

	Final concentration
Template DNA	15 ng/µl
Immolase	0.015 U/µl
Immolase buffer	1 ×
dNTPs	0.2 mM
$MgCl_2$	1.5 mM
Forward primer	0.4 µM
Reverse primer	0.4 µM
DMSO	6%

PCR program

PCR program 5: *PSY7A5*

Step 1 - 95 °C for 10 min

Step 2 - 95 °C for 15 s

Step 3 – 60 °C for 15 s

Step 4 - 72 °C for 30 s

Step 5 - Step 2 for 34 cycles

Step 6 - 72 °C for 7 min

Step 7 - End

Appendix 2: Supplementary material of Chapter 4

Additional file S2.1

1. Screening of Excalibur and Kukri with KASP™ marker assays

Table S2.1 Polymorphism of 53 KASP™ markers between Excalibur and Kukri

KASP™ assay	Polymorphic/Monomorphic
BS00000663	Polymorphic
BS00001450	Monomorphic
BS00002556	Monomorphic
BS00003621	Monomorphic
BS00003665	Polymorphic
BS00003720	Polymorphic
BS00003865	Polymorphic
BS00003894	Polymorphic
BS00004348	Polymorphic
BS00009404	Polymorphic
BS00009543	Polymorphic
BS00009550	Monomorphic
BS00009886	Polymorphic
BS00009975	Monomorphic

BS00009978	Polymorphic
BS00010006	Monomorphic
BS00010307	Polymorphic
BS00010605	Polymorphic
BS00014199	Monomorphic
BS00021962	Polymorphic
BS00021966	Polymorphic
BS00022119	Monomorphic
BS00022137	Polymorphic
BS00022170	Monomorphic
BS00022269	Polymorphic
BS00022284	Polymorphic
BS00022447	Polymorphic
BS00022811	Monomorphic
BS00023109	Polymorphic
BS00023178	Polymorphic
BS00023200	Polymorphic
BS00023207	Polymorphic
BS00009797	Monomorphic
BS00010748	Polymorphic
BS00010809	Monomorphic
BS00011350	Monomorphic
BS00011597	Monomorphic
BS00011622	Monomorphic
BS00011689	Monomorphic
BS00011926	Monomorphic

BS00013951	Monomorphic
BS00014246	Polymorphic
BS00021685	Polymorphic
BS00021744	Polymorphic
BS00110699	Polymorphic
BS00089844	Polymorphic
BS00021195	Polymorphic
BS00085421	Polymorphic
BS00076536	Polymorphic
BS00071736	Monomorphic
BS00023998	Monomorphic
BS00069019	Polymorphic
BS00089845	Polymorphic

2. Assay and polymorphism detection conditions

a) Published KASP™ markers

PCR mix

Reagent	Volume per reaction
Template DNA (15 ng/µl)	3 µl
KASPar 2× mix	3 µl
Primer mix	0.084 µl

PCR cycling

Step 1 - 94°C 15 min

Step 2 - 94°C 20 s

Step 3 - 61°C (- 0.6°C/per cycle) for 60 s

Step 4- Step 2 for 9 times

Step 5 - 94°C 10 s

Step 6 - 55°C for 60 s

Step 7 – Step 5 for 25

Polymorphism detection

Acquire fluorescence reading at 37°C

Re-cycling – up to 3 times

Step 1 - 94°C 10 s

Step 2 - 55°C for 60 s

Step 3 – Step 1 for 2 times

Acquire fluorescence reading at 37°C

b) Other marker assays

AWW5L7

PCR mix

Reagent	**Final concentration (12.5-µl reaction volume)**
Template DNA	150 ng
Immolase	0.625u
Immolase buffer	1 ×

dNTPs	0.2 mM
$MgCl_2$	2.5 mM
Forward primer 1	0.5 µM
Forward primer 2	0.5 µM
Reverse primer	0.5 µM
DMSO	5%

PCR cycling

Step 1 – 95 °C 10 min

Step 2 – 94 °C 10 s

Step 3 – 65 °C (- 0.5 °C/per cycle) for 30 s

Step 4- Step 2 for 9 times

Step 5 - 68 °C 1 min 30 s

Step 6 – 94 °C 10 s

Step 7 – 60 °C for 30 s

Step 8 – Step 6 for 25

Step 9 - 68 °C 1 min 30 s

Step 10 - 72 °C 10 min

Step 11 – End

Polymorphism detection

2% agarose gel; 90V; 40 min

AWW622

PCR mix

Reagent	**Final concentration (12-µl reaction volume)**
Template	150 ng
Immolase	0.3u
Immolase buffer	1×
dNTPs	0.2 mM
$Mgcl_2$	2.5 mM
Forward primer	0.25 µM
Reverse primer	0.25 µM
DMSO	5%

PCR cycling

Step 1 - 95 °C for 10 min

Step 2 - 94 °C for 10 s

Step 3 – 57 °C for 30 s

Step 4 - 68 °C for 1 min

Step 5 - Step 2 for 34 cycles

Step 6 - 72 °C for 10 min

Step 7 – End

Polymorphism detection

2% agarose gel; 90V; 40 min

Cat3A-1

PCR mix

Reagent	**Final concentration (10-µl reaction volume)**
Template	150 ng
Immolase	0.15u
Immolase buffer	1×
dNTPs	0.2mM
Mgcl2	1.5mM
Forward primer	0.4 µM
Reverse primer	0.4 µM
DMSO	6%

PCR cycling

Step 1 - 95 °C for 10 min

Step 2 - 95 °C for 15 s

Step 3 – 62 °C for 15 s

Step 4 - 72 °C for 1 min

Step 5 - Step 2 for 34 cycles

Step 6 - 72 °C for 7 min

Step 7 – End

Polymorphism detection

2% agarose gel; 90V; 40 min

c) Newly developed HRM-based markers

Codominant HRM-based markers

PCR mix

Reagent	Final concentration (10-µl reaction volume)
Template DNA	150 ng
Immolase	0.15u
Immolase buffer	1 ×
dNTPs	0.2 mM
$MgCl_2$	2.5 mM
Forward primer	0.5 µM
Reverse primer	0.5 µM
Syto9 dye	2.0 µM

PCR cycling

Step 1 - 95 °C for 10 min

Step 2 - 94 °C for 30 s

Step 3 – 60 °C for 30s

Step 4 - 72 °C for 1 min

Step 5 - Step 2 for 34 cycles

Step 6 - 72 °C for 5 min

Step 7 – End

Polymorphism detection

High resolution melting conditions

95 °C for 30 s

58 °C for 30 s: ramp to 95 °C (+ 0.02 °C/s; 25 acquisitions/ °C)

37 °C for 1 s

Dominant HRM-based markers

PCR mix

Reagent	Final concentration (10-µl reaction volume)
Template DNA	150 ng
Immolase	0.15u
Immolase buffer	1 ×
dNTPs	0.2 mM
$MgCl_2$	1.5 mM
Forward primer	0.5 µM
Reverse primer	0.5 µM
Syto9 dye	2.0 µM

PCR cycling

Step 1 - 95 °C for 10 min

Step 2 - 94 °C for 30 s

Step 3 – 62 °C for 30s

Step 4 - 72 °C for 1 min

Step 5 - Step 2 for 34 cycles

Step 6 - 72 °C for 5 min

Step 7 – End

Polymorphism detection

High resolution melting conditions

95 °C for 30 s

58 °C for 30 s: ramp to 95 °C (+ 0.02 °C/s; 25 acquisitions/ °C)

37 °C for 1 s

Additional file S2.2

Anchoring markers to the Chinese Spring chromosome-7 syntenic builds

Table S2.2: BLAST hit table of amplicon/EST/contig sequences representing molecular markers from the terminal cluster of Excalibur/Kukri chromosome 7A linkage map against chromosome 7A syntenic build

Marker name	Query size	Hits	E-value	Score	% Identity	Start	End
wri47	145	1	5.00E-78	287	100	17032382	17032526
BS00003720	534	1	e-105	381	100	17243684	17243493
BS00003720	534	2	2.00E-40	165	100	17244350	17244268
wri5	467	1	e-102	369	97	17385014	17384805
wri5	467	2	3.00E-51	200	99	17385185	17385081

wri4	684	1	0	1126	97	17464415	17463788
wri3	354	1	0.00E+00	638	97	17464458	17464105
Psy-A1	3651	6	4.00E-55	216	97	17486551	17486427
Psy-A1	3651	5	3.00E-65	250	100	17486773	17486648
Psy-A1	3651	1	0	3089	99	17488428	17486847
BS00003865	1398	3	9.00E-94	343	99	17522384	17522204
wri29	201	1	e-110	396	99	17523130	17522930
BS00003865	1398	1	0.00E+00	1428	99	17523277	17522533
BS00003865	1398	2	e-151	535	99	17523619	17523342
wri30	201	1	5.00E-53	205	99	17524653	17524549
BS00089844	331	1	e-147	518	99	17532044	17532306
wri2	1128	2	1.00E-40	167	97	17534390	17534299
wri27	201	1	e-110	396	99	17534827	17535027
BS00004348	348	2	2.00E-54	211	100	17621058	17620953
BS00021195	348	2	2.00E-54	211	100	17621058	17620953

BS00009886	888	5	1.00E-33	143	100	17621370	17621299
BS00004348	348	4	4.00E-34	143	100	17621370	17621299
BS00021195	348	4	4.00E-34	143	100	17621370	17621299
BS00004348	348	1	5.00E-67	252	99	17621839	17621711
BS00021195	348	1	3.00E-68	256	100	17621839	17621711
wri43	248	1	e-139	492	100	17741812	17742059
wri41	254	1	e-114	408	100	17780768	17780563
wri45	135	1	1.00E-44	176	97	17923002	17922906

Table S2.3: BLAST hit table of amplicon/EST/contig sequences representing molecular markers from the terminal cluster of Excalibur/ Kukri chromosome 7A linkage map against chromosome 7B syntenic build

Marker name	Query size	Hit number	E-value	Score	% Identity	Start	End
AWW5L7	809	3	4E-45	180	97	15069432	15069534
AWW622	4826	2	0	3293	99	15142890	15144554
AWW622	4826	1	0	5594	99	15144618	15147526
wri5	467	2	4.00E-84	309	97	15147526	15147355
wri5	467	1	e-151	533	98	15147880	15147592
wri4	684	1	0	1158	98	15210697	15210070
wri3	354	1	0.00E+00	694	99	15210740	15210387
BS00003865	1398	1	e-167	587	98	15261093	15260774

BS00003865	1398	2	e-165	579	97	15261485	15261165
wri29	201	1	1.00E-50	197	98	15261745	15261641
BS00003865	1398	3	e-138	490	99	15261895	15261641
BS00003865	1398	4	e-135	480	97	15262234	15261957
wri27	201	1	1.00E-98	356	97	15276666	15276466
wri2	1128	2	1.00E-46	186	100	15277103	15277196
BS00009886	888	2	1.00E-33	143	100	15374240	15374169
BS00004348	348	2	3.00E-34	143	100	15374240	15374169
BS00021195	348	2	3.00E-34	143	100	15374240	15374169
BS00009886	888	1	0.00E+00	671	99	15375072	15374733

Table S2.4: BLAST hit table of amplicon/EST/contig sequences representing molecular markers from the terminal cluster of Excalibur/Kukri chromosome 7A linkage map against chromosome 7D syntenic build

Marker name	Query size	Hit	E-value	Score	% Identity	Start	End
wri28	201	1	e-101	364	97	21065571	21065371
wri5	467	2	4.00E-51	200	99	23731433	23731329
wri5	467	1	0	656	99	23731856	23731518
wri4	684	1	0	1197	99	23821823	23821196
wri3	354	1	0	638	97	23821866	23821513
BS00003865	1398	1	0.00E+00	1608	97	23996311	23995424
wri29	201	1	9.00E-98	354	97	23996165	23995966
wri2	1128	2	6.00E-43	174	98	24004179	24004270

Additional file S2.3

Graphical representation of genotypes in informative Excalibur/Kukri recombinant inbred lines

Table S2.5: Graphical representation of the genotypes and estimated *P. neglectus* DNA/pot of Excalibur, Kukri and 14 informative Excalibur/Kukri recombinant inbred lines at the distal end of chromosome 7AL.

Excalibur/Kukri RI Line	424	1357	1248	1413	1488	1755	662	1026	1788	298	1105	419	1530	454	Excalibur	Kukri
wri36	B	B	B	B	B	B	B	A	A	A	A	A	A	A	A	B
wri34	B	B	B	B	B	B	B	A	A	A	A	A	A	A	A	B
wri38	B	B	B	B	B	B	B	A	A	A	A	A	A	A	A	B
BS00023178	B	B	B	B	B	B	B	A	A	A	A	A	A	A	A	B
BS00010748	B	B	B	B	B	B	B	A	A	A	A	A	A	A	A	B
wri22	B	B	B	B	B	B	B	A	A	A	A	A	A	A	A	B
wri48	B	B	B	B	B	B	B	A	A	A	A	A	A	A	A	B

wri49	B	B	B	B	B	B	B	A	A	A	A	A	A	A	A	B
wri50	B	B	B	B	B	B	B	A	A	A	A	A	A	A	A	B
wri39	B	B	B	B	B	B	B	A	A	A	A	A	A	A	A	B
wri35	B	B	B	B	B	B	B	A	A	A	A	A	A	A	A	B
BS00021966	B	-	B	B	B	B	B	A	A	A	A	A	A	A	A	B
BS00021962	B	B	B	B	B	B	B	A	A	A	A	A	A	A	A	B
BS00023207	B	B	B	B	B	B	B	A	A	A	A	A	A	B	A	B
wri23	B	B	B	B	B	B	B	A	A	A	A	A	A	B	A	B
wri24	A	B	B	B	B	B	B	A	A	A	A	B	B	B	A	B
wri25	A	B	B	B	B	B	B	A	A	A	A	B	B	B	A	B
wri26	A	B	B	B	B	B	B	A	A	A	A	B	B	B	A	B
BS00023109	A	A	B	B	B	B	B	A	B	B	B	B	B	B	A	B
BS00014246	A	A	B	B	B	B	B	A	B	B	B	B	B	B	A	B
wri40	A	A	B	B	B	B	B	A	B	B	B	B	B	B	A	B
BS00089844	A	A	A	A	A	A	A	B	B	B	B	B	B	B	A	B
BS00021195	A	A	A	A	A	A	A	B	B	B	B	B	B	B	A	B
BS00022447	A	A	A	A	A	A	A	B	B	B	B	B	B	B	A	B
BS00022269	A	A	A	A	A	A	A	B	B	B	B	B	B	B	A	B

wri46	A	A	A	A	A	A	A	B	B	B	B	B	B	B	A	B
wri44	A	A	A	A	A	A	A	B	B	B	B	B	B	B	A	B
wri47	A	A	A	A	A	A	A	B	B	B	B	B	B	B	A	B
BS00003865	A	A	A	A	A	A	A	B	B	B	B	B	B	B	A	B
BS00004348	A	A	A	A	A	A	A	B	B	B	B	B	B	B	A	B
BS00009886	A	A	A	A	A	A	A	B	B	B	B	B	B	B	A	B
wri41	A	A	A	A	A	A	A	B	B	B	B	B	B	B	A	B
wri42	A	A	A	A	A	A	A	B	B	B	B	B	B	B	A	B
BS00003720	A	A	A	A	A	A	A	B	B	B	B	B	-	B	A	B
BS00000663	A	A	A	A	A	A	A	B	B	B	B	B	B	B	A	B
wri1	A	A	A	A	A	A	A	B	B	B	B	B	B	B	A	B
wri30	A	A	A	A	A	A	A	B	B	B	B	B	B	B	A	B
wri29	A	A	A	A	A	A	A	B	B	B	B	B	B	B	A	B
wri2	A	A	A	A	A	A	A	B	B	B	B	B	B	B	A	B
sts638	A	A	A	A	A	A	A	B	B	B	B	B	B	B	A	B
wri3	A	A	A	A	A	A	A	B	B	B	B	B	B	B	A	B
wpt-0790	A	A	A	A	A	A	A	B	B	B	B	B	B	B	A	B
wri45	A	A	A	A	A	A	A	B	B	B	B	B	B	B	A	B

Psy-A1	A	A	A	A	A	A	A	B	B	B	B	B	B	B	A	B
wri31	A	A	A	A	A	A	A	B	B	B	B	B	B	B	A	B
wri43	A	A	A	A	A	A	A	B	B	B	B	B	B	B	A	B
schfc3	A	A	A	A	A	A	A	B	B	B	B	B	B	B	A	B
wri4	A	A	A	A	A	A	A	B	B	B	B	B	B	B	A	B
wri5	A	A	A	A	A	A	A	B	B	B	B	B	B	B	A	B
BS00085421	A	A	A	A	A	A	A	B	B	B	B	B	B	B	A	B
gwm344	A	A	A	A	A	A	A	B	B	B	B	B	B	B	A	B
wri27	A	A	A	A	A	A	A	B	B	B	B	B	B	B	A	B
wri28	A	A	A	A	A	A	A	B	B	B	B	B	B	B	A	B
cfa2240	A	A	A	A	A	A	A	B	B	B	B	B	B	B	A	B
AWW5L7	A	A	A	A	A	A	A	B	B	B	B	B	B	B	A	B
AWW622	A	A	A	A	A	A	A	B	B	B	B	B	B	B	A	B
Cat3-A1	A	A	A	A	A	A	A	B	B	B	B	B	B	B	A	B
P. neglectus DNA/pot (ng)	2352	2032	1645	2481	1813	1938	2395	4030	3217	3778	4013	3606	4021	2906	1875	3123
Standard deviation	296	296	296	297	297	296	297	296	297	296	296	297	297	296	304	304

Additional file S2.4

Phylogenetic analysis of *Psy1* alleles of wheat and related species

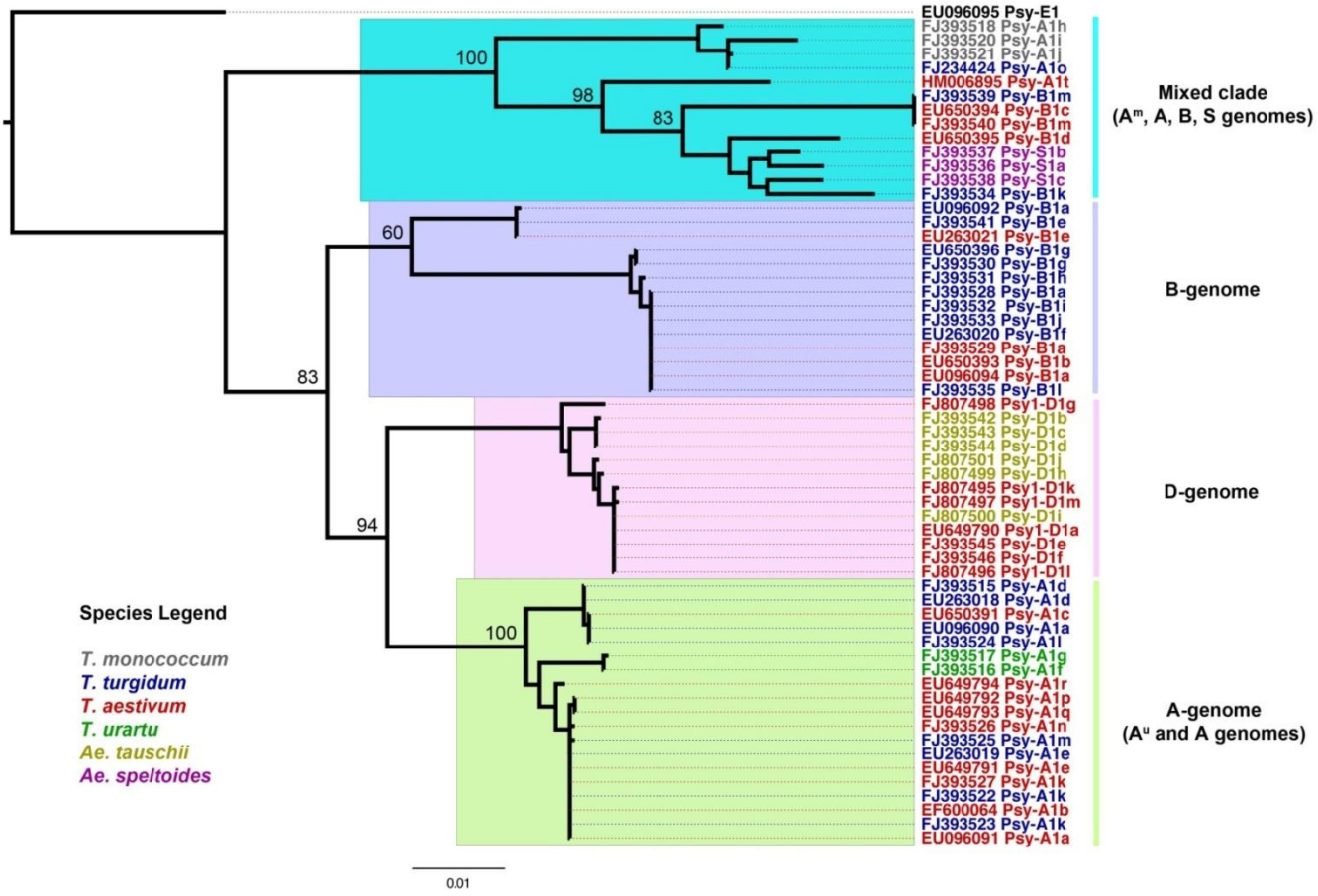

Figure S2.1: Phylogeny of *Psy1* alleles of wheat and close relatives

Table S2.6: Details about the Psy1 allele sequences used in the phylogenetic analysis

Genome	*Psy1* allele	Species	GenBank accession number
A	*a*	*T. aestivum* cv. Chinese Spring	EU096091
		T. turgidum ssp. *durum* cv. Kofa	EU096090
	b	*T. aestivum* cv. Shaan 9314	EF600064
	c	*T. aestivum* cv. M564	EU650391
	d	*T. turgidum* ssp. *dicoccon* iso. DM28	FJ393515
		T. turgidum ssp. *durum* cv. Langdon	EU263018
	e	*T. aestivum* cv. Sunco	EU649791
		T. turgidum ssp. *durum* cv. Dr8	EU263019
	k	*T. aestivum* ssp. *spelta* iso. Spelt167	FJ393527
		T. turgidum ssp. *dicoccoides* iso. DS3	FJ393522
		T. turgidum ssp. *dicoccon* iso. DM37	FJ393523
	l	*T. turgidum* ssp. *dicoccoides* iso. DS6	FJ393524
	m	*T. turgidum* ssp. *dicoccon* iso. DM26	FJ393525
	n	*T. aestivum* ssp. *spelta* iso. SP9	FJ393526
	o	*T. turgidum* ssp. *durum* cv. Commander	FJ234424
	p	*T. aestivum* cv. *Tasman*	EU649792
	q	*T. aestivum* cv. Cranbrook	EU649793
	r	*T. aestivum* cv. Halberd	EU649794
	t	*T. aestivum* cv. WAWHT2074	HM006895
A^u	*f*	*T. urartu* iso. UR1	FJ393516

	g	*T. urartu* iso. PI428326	FJ393517
A^m	*h*	*T. monococcum* ssp. *aegilopoides* iso. BO1	FJ393518
	i	*T. monococcum* iso. MO1	FJ393520
	j	*T. monococcum* iso. MO2	FJ393521
B	*a*	*T. aestivum* cv. Chinese Spring	EU096094
		T. aestivum ssp. *spelta* iso. SP9	FJ393529
		T. turgidum ssp. *dicoccoides* iso. DS4	FJ393528
		T. turgidum ssp. *durum* cv. Kofa	EU096092
	b	*T. aestivum* cv. Neixiang 188	EU650393
	c	*T. aestivum* cv. CA9648	EU650394
	d	*T. aestivum* cv. Ning 98084	EU650395
	e	*T. aestivum* ssp. *durum* cv. Dr8	EU263021
		T. turgidum ssp. *dicoccon* iso. DM28	FJ393541
	f	*T. turgidum* ssp. *durum* cv. Langdon	EU263020
	g	*T. turgidum* ssp. *dicoccoides* iso. DS6	FJ393530
		T. turgidum ssp. *durum* cv. DR1	EU650396
	h	*T. turgidum* ssp. *dicoccoides* iso. DS3	FJ393531
	i	*T. turgidum* ssp. *dicoccoides* iso. DS8	FJ393532
	j	*T. turgidum* ssp. *dicoccon* iso. DM26	FJ393533
	k	*T. turgidum* ssp. *dicoccon* iso. DM33	FJ393534
	l	*T. turgidum* ssp. *dicoccon* iso. DM37	FJ393535
	m	*T. aestivum* ssp. *spelta* iso. Spelt167	FJ393540
		T. turgidum ssp. *dicoccon* iso. DM47	FJ393539
D	*a*	*T. aestivum* cv. Chinese Spring	EU649790
	b	*Ae. tauschii* iso. Ae34	FJ393542
	c	*Ae. tauschii* iso. Ae46	FJ393543

	d	*Ae. tauschii* iso. Y99	FJ393544
	e	*T. aestivum* ssp. *spelta* iso. SP9	FJ393545
	f	*T. aestivum* ssp. *spelta* iso. Spelt217	FJ393546
	g	*T. aestivum* cv. Zhongliang88375	FJ807498
	h	*Ae. tauschii* strain Ae37	FJ807499
	i	*Ae. tauschii* strain Ae38	FJ807500
	j	*Ae. tauschii*	FJ807501
	k	*T. aestivum* cv. Nongda3291	FJ807495
	l	*T. aestivum* cv. E86642	FJ807496
	m	*T. aestivum* cv. Ning97-18	FJ807497
S	*a*	*Ae. speltoides* iso. Ae49	FJ393537
	b	*Ae. speltoides* iso. Ae48	FJ393536
	c	*Ae. speltoides* iso. Y162	FJ393538

Polymorphisms between the *Psy1* alleles in the 'mixed clade'

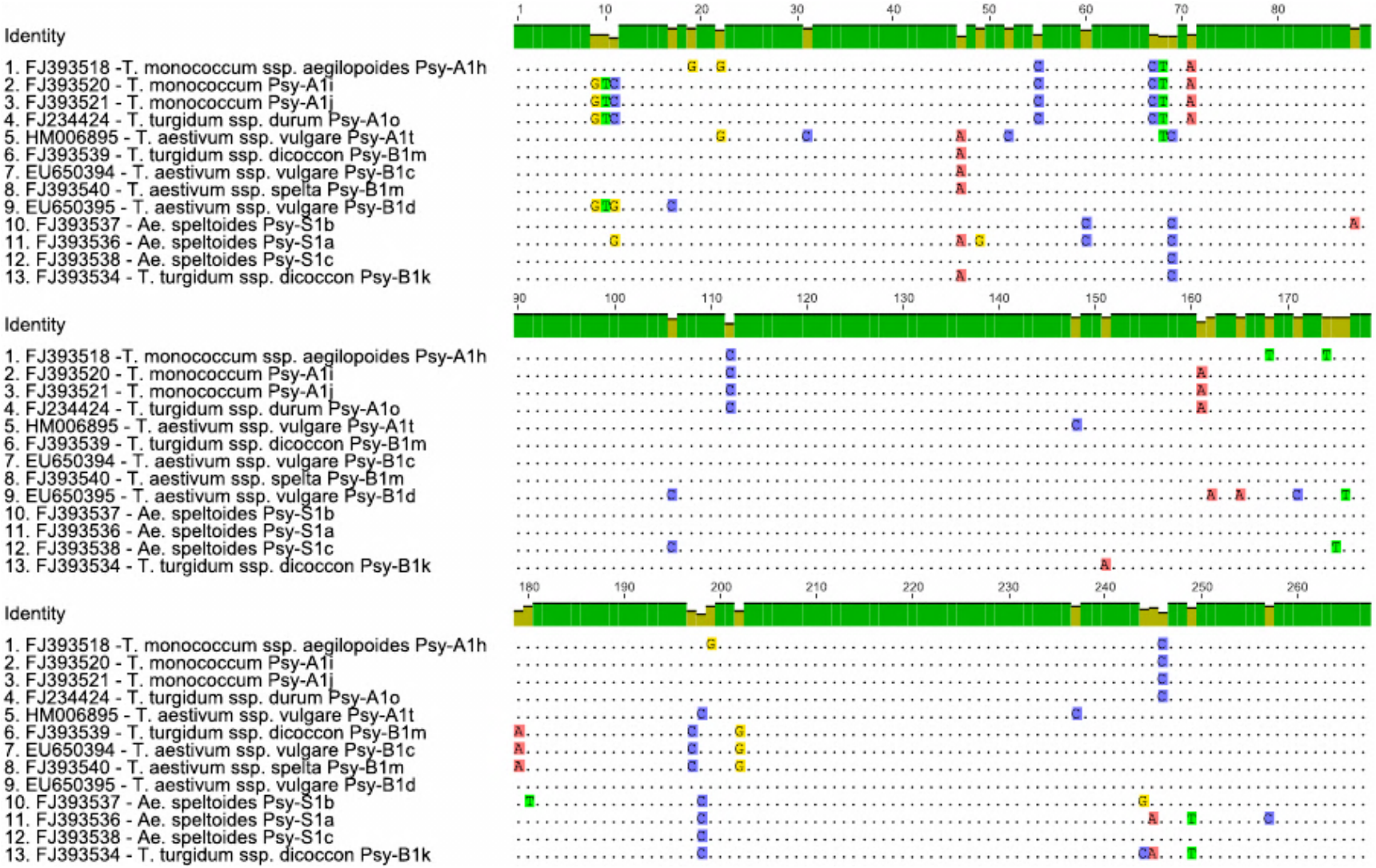

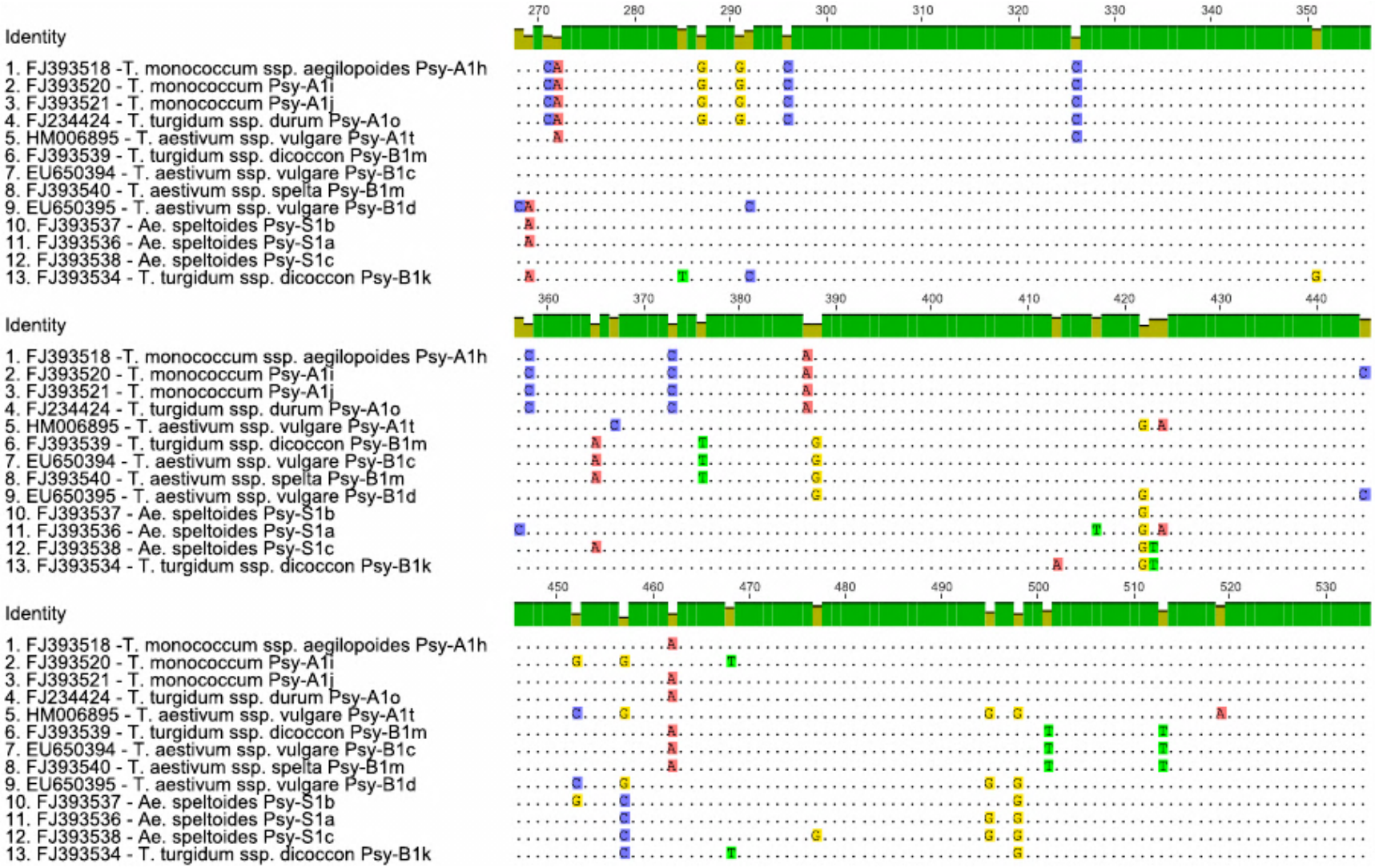
Identity
1. FJ393518 -T. monococcum ssp. aegilopoides Psy-A1h
2. FJ393520 - T. monococcum Psy-A1i
3. FJ393521 - T. monococcum Psy-A1j
4. FJ234424 - T. turgidum ssp. durum Psy-A1o
5. HM006895 - T. aestivum ssp. vulgare Psy-A1t
6. FJ393539 - T. turgidum ssp. dicoccon Psy-B1m
7. EU650394 - T. aestivum ssp. vulgare Psy-B1c
8. FJ393540 - T. aestivum ssp. spelta Psy-B1m
9. EU650395 - T. aestivum ssp. vulgare Psy-B1d
10. FJ393537 - Ae. speltoides Psy-S1b
11. FJ393536 - Ae. speltoides Psy-S1a
12. FJ393538 - Ae. speltoides Psy-S1c
13. FJ393534 - T. turgidum ssp. dicoccon Psy-B1k
270
280
290
300
310
320
330
340
350
360
370
380
390
400
410
420
430
440
450
460
470
480
490
500
510
520
530

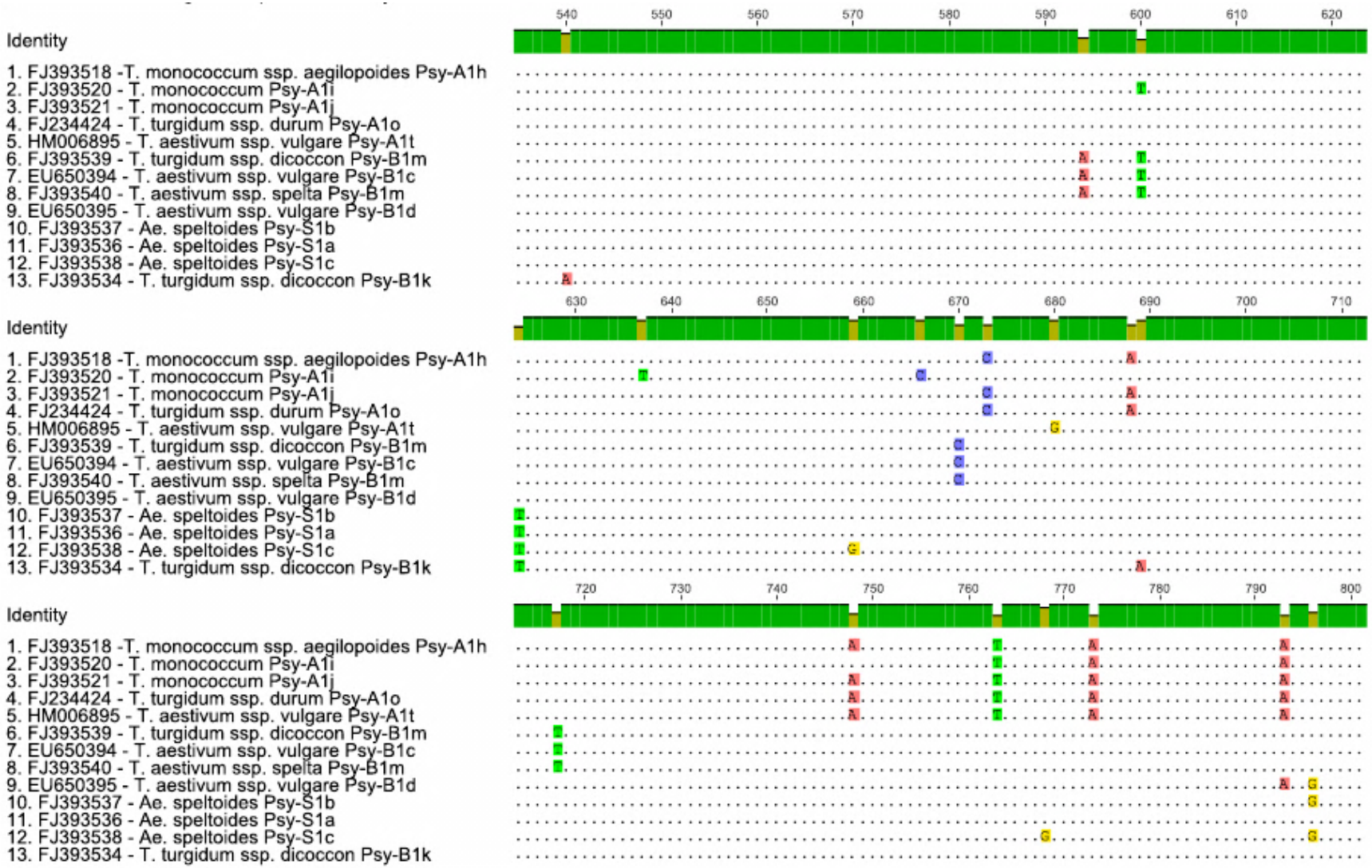
Identity
1. FJ393518 -T. monococcum ssp. aegilopoides Psy-A1h
2. FJ393520 - T. monococcum Psy-A1i
3. FJ393521 - T. monococcum Psy-A1j
4. FJ234424 - T. turgidum ssp. durum Psy-A1o
5. HM006895 - T. aestivum ssp. vulgare Psy-A1t
6. FJ393539 - T. turgidum ssp. dicoccon Psy-B1m
7. EU650394 - T. aestivum ssp. vulgare Psy-B1c
8. FJ393540 - T. aestivum ssp. spelta Psy-B1m
9. EU650395 - T. aestivum ssp. vulgare Psy-B1d
10. FJ393537 - Ae. speltoides Psy-S1b
11. FJ393536 - Ae. speltoides Psy-S1a
12. FJ393538 - Ae. speltoides Psy-S1c
13. FJ393534 - T. turgidum ssp. dicoccon Psy-B1k
540
550
560
570
580
590
600
610
620
630
640
650
660
670
680
690
700
710
720
730
740
750
760
770
780
790
800

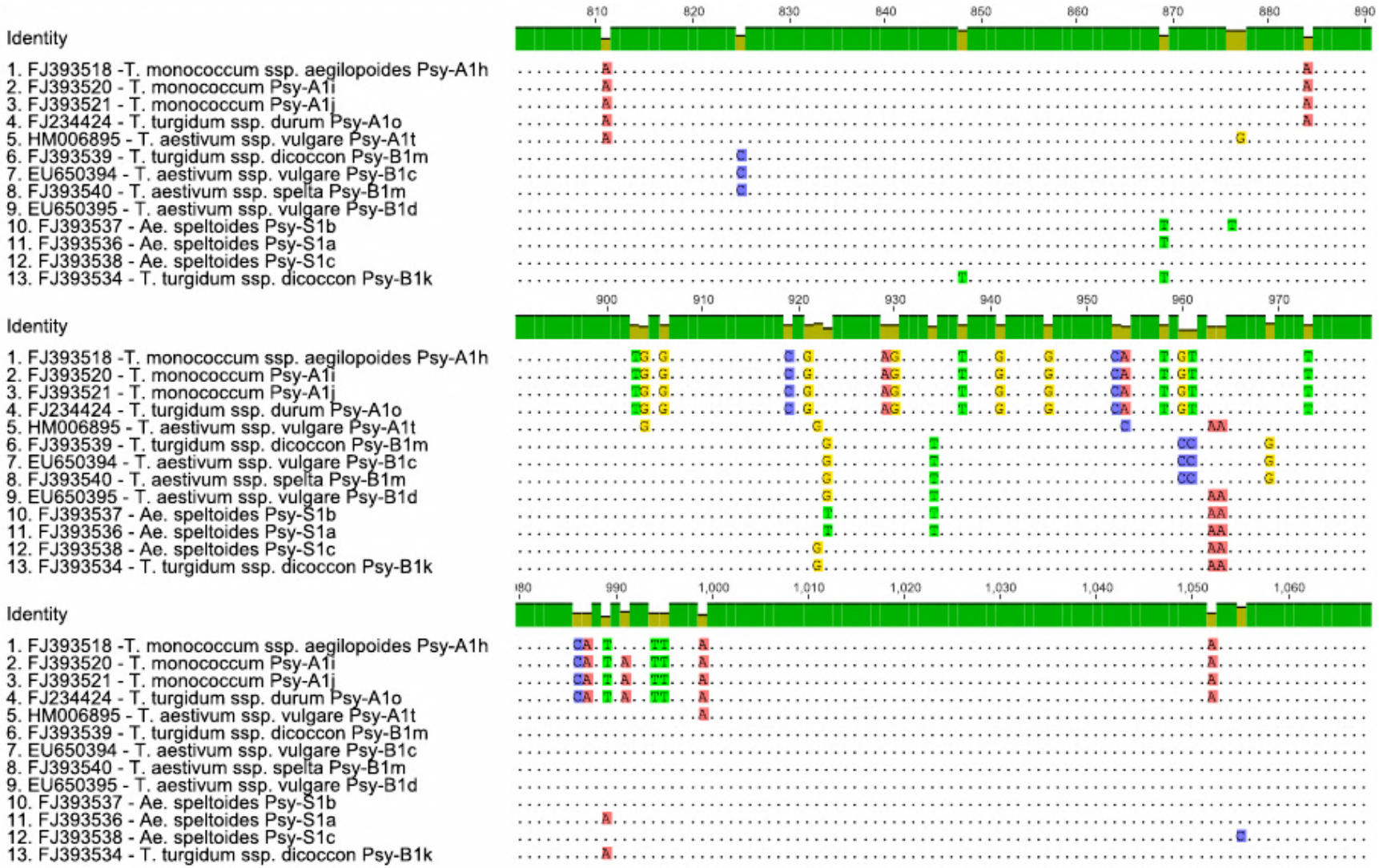
Identity
1. FJ393518 -T. monococcum ssp. aegilopoides Psy-A1h
2. FJ393520 - T. monococcum Psy-A1i
3. FJ393521 - T. monococcum Psy-A1j
4. FJ234424 - T. turgidum ssp. durum Psy-A1o
5. HM006895 - T. aestivum ssp. vulgare Psy-A1t
6. FJ393539 - T. turgidum ssp. dicoccon Psy-B1m
7. EU650394 - T. aestivum ssp. vulgare Psy-B1c
8. FJ393540 - T. aestivum ssp. spelta Psy-B1m
9. EU650395 - T. aestivum ssp. vulgare Psy-B1d
10. FJ393537 - Ae. speltoides Psy-S1b
11. FJ393536 - Ae. speltoides Psy-S1a
12. FJ393538 - Ae. speltoides Psy-S1c
13. FJ393534 - T. turgidum ssp. dicoccon Psy-B1k
810
820
830
840
850
860
870
880
890
900
910
920
930
940
950
960
970
990
1,000
1,010
1,020
1,030
1,040
1,050
1,060

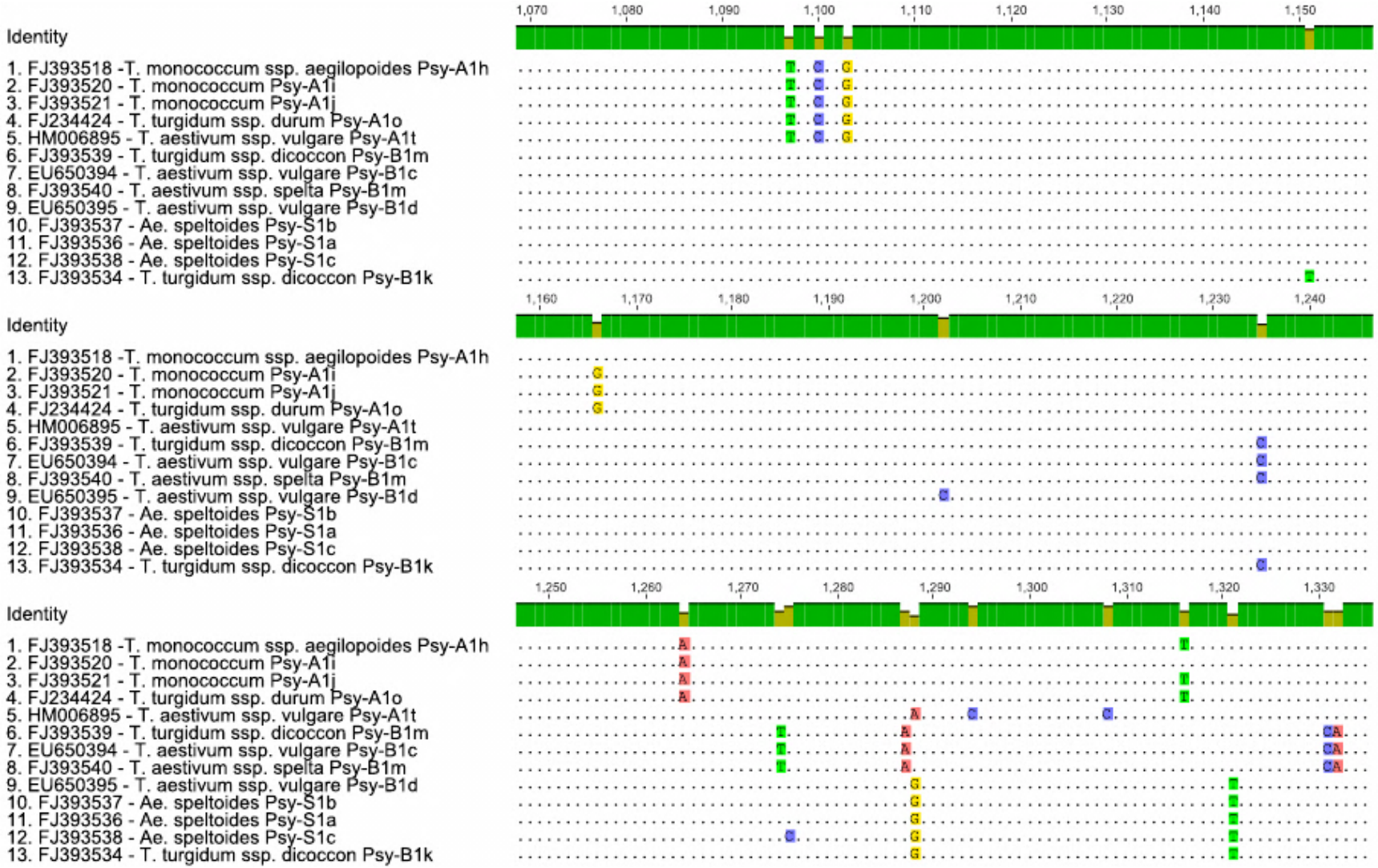
Identity
1. FJ393518 -T. monococcum ssp. aegilopoides Psy-A1h
2. FJ393520 - T. monococcum Psy-A1i
3. FJ393521 - T. monococcum Psy-A1j
4. FJ234424 - T. turgidum ssp. durum Psy-A1o
5. HM006895 - T. aestivum ssp. vulgare Psy-A1t
6. FJ393539 - T. turgidum ssp. dicoccon Psy-B1m
7. EU650394 - T. aestivum ssp. vulgare Psy-B1c
8. FJ393540 - T. aestivum ssp. spelta Psy-B1m
9. EU650395 - T. aestivum ssp. vulgare Psy-B1d
10. FJ393537 - Ae. speltoides Psy-S1b
11. FJ393536 - Ae. speltoides Psy-S1a
12. FJ393538 - Ae. speltoides Psy-S1c
13. FJ393534 - T. turgidum ssp. dicoccon Psy-B1k
1,070
1,080
1,090
1,100
1,110
1,120
1,130
1,140
1,150
Identity
1. FJ393518 -T. monococcum ssp. aegilopoides Psy-A1h
2. FJ393520 - T. monococcum Psy-A1i
3. FJ393521 - T. monococcum Psy-A1j
4. FJ234424 - T. turgidum ssp. durum Psy-A1o
5. HM006895 - T. aestivum ssp. vulgare Psy-A1t
6. FJ393539 - T. turgidum ssp. dicoccon Psy-B1m
7. EU650394 - T. aestivum ssp. vulgare Psy-B1c
8. FJ393540 - T. aestivum ssp. spelta Psy-B1m
9. EU650395 - T. aestivum ssp. vulgare Psy-B1d
10. FJ393537 - Ae. speltoides Psy-S1b
11. FJ393536 - Ae. speltoides Psy-S1a
12. FJ393538 - Ae. speltoides Psy-S1c
13. FJ393534 - T. turgidum ssp. dicoccon Psy-B1k
1,160
1,170
1,180
1,190
1,200
1,210
1,220
1,230
1,240
Identity
1. FJ393518 -T. monococcum ssp. aegilopoides Psy-A1h
2. FJ393520 - T. monococcum Psy-A1i
3. FJ393521 - T. monococcum Psy-A1j
4. FJ234424 - T. turgidum ssp. durum Psy-A1o
5. HM006895 - T. aestivum ssp. vulgare Psy-A1t
6. FJ393539 - T. turgidum ssp. dicoccon Psy-B1m
7. EU650394 - T. aestivum ssp. vulgare Psy-B1c
8. FJ393540 - T. aestivum ssp. spelta Psy-B1m
9. EU650395 - T. aestivum ssp. vulgare Psy-B1d
10. FJ393537 - Ae. speltoides Psy-S1b
11. FJ393536 - Ae. speltoides Psy-S1a
12. FJ393538 - Ae. speltoides Psy-S1c
13. FJ393534 - T. turgidum ssp. dicoccon Psy-B1k
1,250
1,260
1,270
1,280
1,290
1,300
1,310
1,320
1,330
Identity
1. FJ393518 -T. monococcum ssp. aegilopoides Psy-A1h
2. FJ393520 - T. monococcum Psy-A1i
3. FJ393521 - T. monococcum Psy-A1j
4. FJ234424 - T. turgidum ssp. durum Psy-A1o
5. HM006895 - T. aestivum ssp. vulgare Psy-A1t
6. FJ393539 - T. turgidum ssp. dicoccon Psy-B1m
7. EU650394 - T. aestivum ssp. vulgare Psy-B1c
8. FJ393540 - T. aestivum ssp. spelta Psy-B1m
9. EU650395 - T. aestivum ssp. vulgare Psy-B1d
10. FJ393537 - Ae. speltoides Psy-S1b
11. FJ393536 - Ae. speltoides Psy-S1a
12. FJ393538 - Ae. speltoides Psy-S1c
13. FJ393534 - T. turgidum ssp. dicoccon Psy-B1k

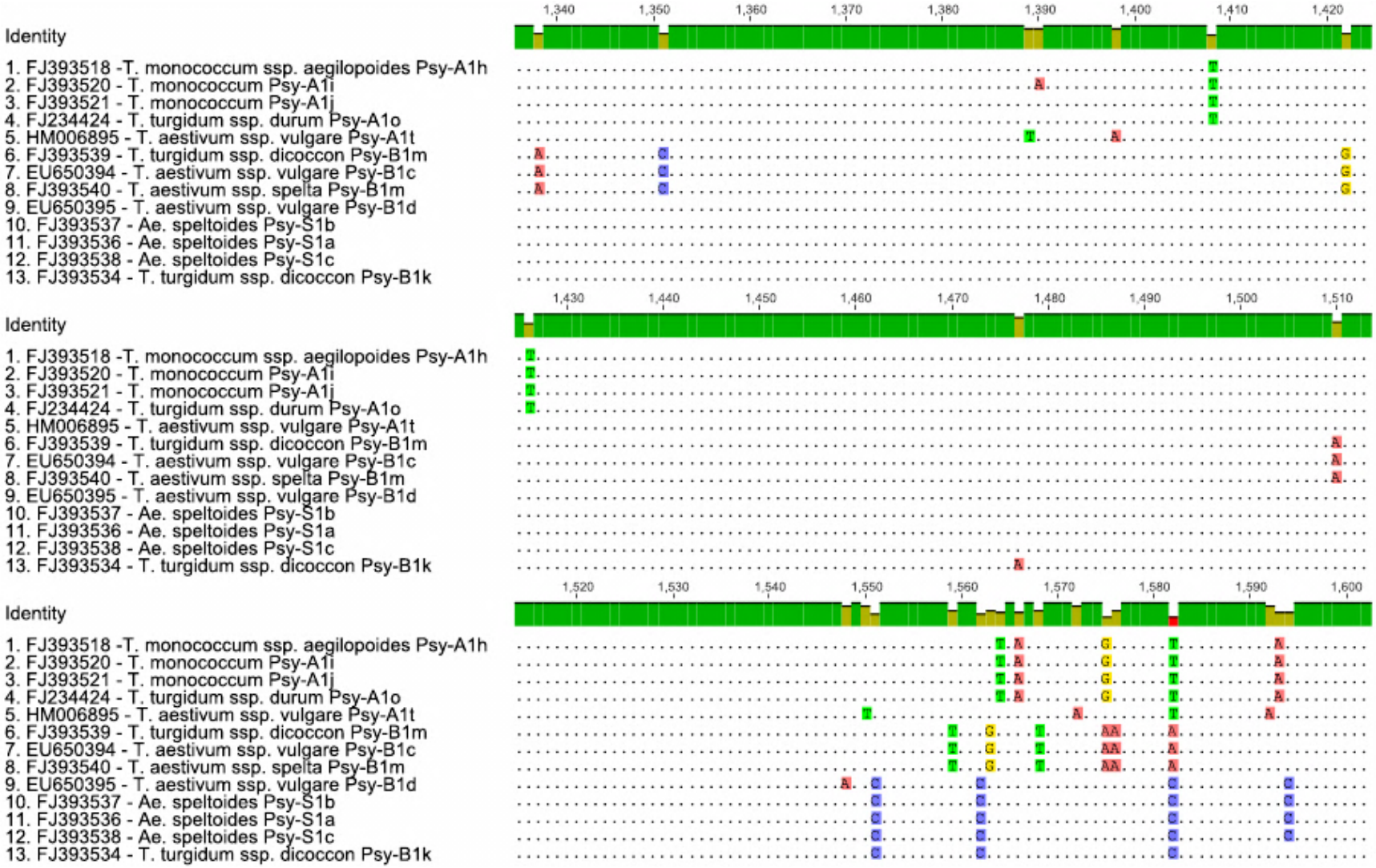
Identity
1. FJ393518 -T. monococcum ssp. aegilopoides Psy-A1h
2. FJ393520 - T. monococcum Psy-A1i
3. FJ393521 - T. monococcum Psy-A1j
4. FJ234424 - T. turgidum ssp. durum Psy-A1o
5. HM006895 - T. aestivum ssp. vulgare Psy-A1t
6. FJ393539 - T. turgidum ssp. dicoccon Psy-B1m
7. EU650394 - T. aestivum ssp. vulgare Psy-B1c
8. FJ393540 - T. aestivum ssp. spelta Psy-B1m
9. EU650395 - T. aestivum ssp. vulgare Psy-B1d
10. FJ393537 - Ae. speltoides Psy-S1b
11. FJ393536 - Ae. speltoides Psy-S1a
12. FJ393538 - Ae. speltoides Psy-S1c
13. FJ393534 - T. turgidum ssp. dicoccon Psy-B1k
1,340
1,350
1,360
1,370
1,380
1,390
1,400
1,410
1,420
1,430
1,440
1,450
1,460
1,470
1,480
1,490
1,500
1,510
1,520
1,530
1,540
1,550
1,560
1,570
1,580
1,590
1,600

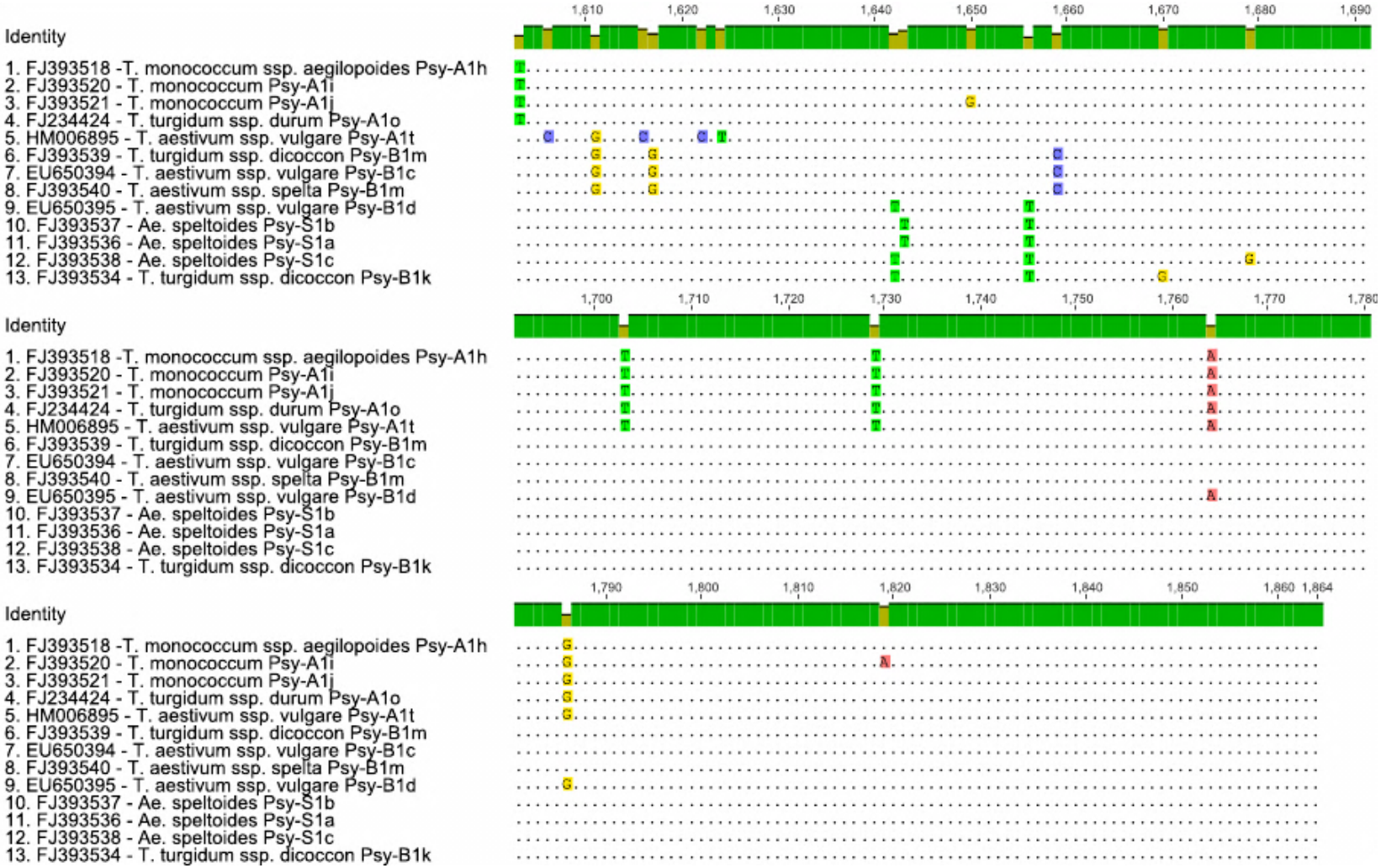

Figure S2.2: Sequence alignment of 13 *Psy1* alleles in the 'Mixed clade'

Additional file S2.5

Sequence of the longer product of Excalibur for the marker *AWW5L7*

>AWW5L7_Excalibur

CGCATCAACCCACCGCTGGAGGAAACGGTCTTGCCTGTGTTTTCATATAAGAT
ACAGTTTGGTTAGCAACGCTCCTTGATTTCTTCTATGGGCCTAAAGACTCGAAA
CAAATCAAACTGAGTTTGGGATGGAACCTGGCAGGGTCGAAGGATCGGTATCT
CTCGCCAGCCTGCTTGAAATTGTTCTCCTTCTCGATAATGCACTGCAGTTCCAA
AAGTACAAATGTAGCAAACAATTTGTCAAAACACATGGTAGGGGCTTAATTCA
CAGAGTATTTCAGTCATCATTAGCAAATAGCAATAAATAATAACTGGAAACAG
TTTGGCTACATGCAAAGGGACTGGCAGTAGTACGAATAGAATTAGAATTCTAA
CATTCCAATTTGCATACCTTTTCCCGGCAGCCAGACAGAACACGAGGAGGGAT
AGGGTACTGTTCAGCATGACGAGTAGGATCAAACCTTGAAGGGAAGTAGTTCA
CCTGAAAATCAAGCCAGATATATGTAACTGCAGTGAACTTGAGACATAACTAC
ATATTATTTCCGTCAACCGGAGGAAATACTGAATCATGCATGCAGAAGGGGAT
GAAATAGCTCTAAAGACCAATGTACCTCCTCATCCCTGTGCATGAAATTCATTA
GGCCATCATGATGGTTGTTGTGGTGAGCACATTTCGGGGCATTCACAGGAAGC
ATCAAGTAGTTTGGACCAAGACGGTGCCTTTGGGTATCAGCATAGGAGAAAAT
CCTTGTCTGGAGCAGCTTATCATCAGAGTAGTGGATTCCGGGGACAGTGACTG
CTGGGCAGAAA

Appendix 3: Supplementary material of Chapter 5

This appendix presents the contents of four online resources that have been submitted to the journal of Molecular Breeding as supplementary material.

Online Resource S3.1

1. Primer sequences

Table S3.1: Primer sequences of KASP™ assays

Marker name	iSelect SNP assay name/EST	Primer name	Primer sequence*
wri10	*iwa3224*	*wri10_F1*	GAAGGTGACCAAGTTCATGCTGGTCAATGAGGATGGTTCAATCAAAACC
		wri10_F2	GAAGGTCGGAGTCAACGGATTGGTCAATGAGGATGGTTCAATCAAAACT
		wri10_R	CACTTCAAGCACCATAGCCGGTT
wri11	*iwa3880*	*wri11_F1*	GAAGGTGACCAAGTTCATGCTTCACATTTAAACCCCAACTTCAGGTCTA

		wri11_F2	GAAGGTCGGAGTCAACGGATTTCACATTTAAACCCCAACTTCAGGTCTC
		wri11_R	ACATTTCTTGGCGAGACCTCTGTT
wri12	*iwa4246*	*wri12_F1*	GAAGGTGACCAAGTTCATGCTCAGAATCTCGTTCAGAGGAACATCACC
		wri12_F2	GAAGGTCGGAGTCAACGGATTCAGAATCTCGTTCAGAGGAACATCACT
		wri12_R	GGCATGGGCAGCTATGCTGA
wri13	*iwa8441*	*wri13_F1*	GAAGGTGACCAAGTTCATGCTCTTCAGCGTGTAAGGAAGTTTTGATCAAA
		wri13_F2	GAAGGTCGGAGTCAACGGATTCTTCAGCGTGTAAGGAAGTTTTGATCAAG
		wri13_R	GGCACCGCTTGAGCCACTAA
wri16	BE403950	*wri13_R1*	GAAGGTGACCAAGTTCATGCTTTGATTAGGATCAGGGCATTG
		wri13_R2	GAAGGTCGGAGTCAACGGATTGCTTTGATTAGGATCAGGGCATTC
		wri13_F	GAGAGATTATGTTATATTCGTCCAACGGTT

*KASP™ VIC/FAM fluorescence tail complementary to the FRET cassettes in the KASP™ Mastermix added to the 5`end is underlined

Table S3.2: Primer sequences of HRM and gel-based assays

Marker name	iSelect SNP assay name/EST	Assay type	Primer name	Primer sequence
wri6	*iwa2098*	HRM	*wri6_F*	CCGTCGACTGCAGCTACATA
			wri6_R	CTCGTACGTGTTCGCCTGTA
wri7	*iwa1495*	HRM	*wri7_F*	CAAGAGCTCTCGGCATTTTT
			wri7_R	GCAATCGACAGAGGAAGCAT
wri8	*iwa0824*	HRM	*wri8_F*	CTCCACGCTTCTCCTAATGC
			wri8_R	GGCTGACTGTGTATGCCAAG
wri9	*iwa4245*	HRM	*wri9_F*	GAACCCAGCATGTTTGTGAA
			wri9_R	CCAGAAGGATGAAGCAAAGG
wri14	GH723564	Gel-based	*wri14_LSPF*	CGAGCCCCTCAAATACTCCGGGAA
			wri14_LSPR	ACAGCCCCACGCTCATGATCGC
			wri14_ASP	CCAAATCACCTCATAGCAGGC

wri15	BE403950	Gel-based	*wri15_F*	TTTACTTTAAATGAACATTTCAGCAGCAATGTAGAC
			wri15_R1	CCGATTAGGATCAGGGCATTC
			wri15_R2	CCCATTAGGATCAGGGCATTG

2. Assay and polymorphism detection conditions

a) Markers: *wri10, wri11, wri12, wri13, wri16, BS00010627, BS00011795, BS00011603, BS00009548, BS00022529, BS00029210, BS00109879* and *BS00022444*

PCR mix

Reagent	Volume per reaction
Template DNA (15 ng/µl)	3 µl
KASPar 2x mix	3 µl
Primer mix	0.084 µl

PCR cycling

Step 1 - 94°C 15 min

Step 2 - 94°C 20 s

Step 3 - 61°C (- 0.6°C/per cycle) for 60 s

Step 4- Step 2 for 9 times

Step 5 - 94°C 10 s

Step 6 - 55°C for 60 s

Step 7 – Step 5 for 25

Polymorphism detection

Acquire fluorescence reading at 37°C

Re-cycling – up to 3 times

Step 1 - 94°C 10 s

Step 2 - 55°C for 60 s

Step 3 – Step 1 for 2 times

Acquire fluorescence reading at 37°C

b) Markers: *wri6, wri7, wri8* and *wri9*

PCR mix

Reagent	**Final concentration (10-µl reaction volume)**
Template DNA	150 ng
Immolase	0.15u
Immolase buffer	1 ×
dNTPs	0.2 mM
$MgCl_2$	2.5 mM
Forward primer	0.5 µM
Reverse primer	0.5 µM
Syto9 dye	2.0 µM

PCR cycling

Step 1 - 95 °C for 10 min

Step 2 - 94 °C for 30 s

Step 3 – 60 °C for 30s

Step 4 - 72 °C for 1 min

Step 5 - Step 2 for 34 cycles

Step 6 - 72 °C for 5 min

Step 7 – End

Polymorphism detection

High resolution melting conditions

95 °C for 30 s

58 °C for 30 s: ramp to 95 °C (+ 0.02 °C/s; 25 acquisitions/ °C)

37 °C for 1 s

c) Marker *wri14*

PCR mix

Reagent	**Final concentration (10-µl reaction volume)**
Template	150 ng
Immolase	0.15u
Immolse buffer	1×
dNTPs	0.2 mM
Mgcl2	1.5 mM
Locus specific primers (F and R)	0.5 µM
Allele specific primer	0.5 µM
BSA	10×

PCR cycling

Step 1 - 95º for 10min

Step 2 - 94º for 30s

Step 3 - 58º for 30s

Step 4 - 72º for 60s

Step 5 – Step 2 for 14 times

Step 6 - 94º for 10s

Step 7 - 45º for 30s

Step 8 – Step 6 for 4 times

Step 9 - 94º for 10s

Step 10 - 53º for 30s

Step 11 - 72º for 5s

Step 12 - Step 9 for 14 times

Step 13 – End

Polymorphism detection

Agarose gel electrophoresis

2.5 % agarose gel; 90V; 60 min

d) Marker *wri15*

PCR mix

Reagent	**Final concentration (10-µl reaction volume)**
Template DNA	150 ng
QIAgen Taq polymerase	0.25u
QIAgen buffer	1.25 ×
dNTPs	0.25 mM
$MgCl_2$	1.5 mM
Q solution	1.25 ×
Forward primer	0.5 µM
Reverse primer	0.5 µM

PCR 1: *wri15_F/R1*

PCR2: *wri15_F/R2*

PCR cycling

Step 1 - 95 °C for 10 min

Step 2 - 94 °C for 30 s

Step 3 – 58 °C for 30 s

Step 4 - 72 °C for 30 s

Step 5 - Step 2 for 34 cycles

Step 6 - 72 °C for 5 min

Step 7 – End

Polymorphism detection

Agarose gel electrophoresis

2.0 % agarose gel; 90V; 60 min

3. Allele calls of 'Trident' and 'Molineux' lines for KASP markers

Marker name	Trident allele	Molineux allele
wri10	C	T
wri11	A	C
wri12	T	C
wri13	A	G
wri16	C	G
BS00010627	T	C
BS00011795	C	A
BS00011603	C	T
BS00009548	G	T

BS00022529	C	G
BS00029210	G	C
BS00109879	G	T
BS00022444	C	G

4. Amplification and sequencing of genomic DNA to identify polymorphisms between Trident and Molineux

oET0041_F/R

PCR mix

Reagent	**Final concentration**
Template DNA (Trident or Molineux)	50 ng
Immolase polymerase	0.5u
Immolase buffer	1 ×
dNTPs	0.2 mM
$MgCl_2$	1.5 mM
Forward primer	0.2 µM
Reverse primer	0.2 µM

PCR cycling

Step 1 - 95 °C for 10 min

Step 2 - 94 °C for 30 s

Step 3 – 65 °C for 30 s (-0.5 º/cycle)

Step 4 - 72 °C for 60 s

Step 5 - Step 2 for 19 cycles

Step 6 – 94 °C for 30 s

Step 7 – 56 °C for 30 s

Step 8 - 72 °C for 60 s

Step 9 - Step 6 for 24 cycles

Step 10 - 72 °C for 5 min

Step 11 – End

BE403950A_F1_UCD / BE403950_cpR1_UCD

PCR mix

Reagent	**Final concentration**
Template DNA (Trident or Molineux)	100 ng
QIAgen Taq polymerase	0.5u
QIAgen PCR buffer	1 ×
dNTPs	0.2 mM
$MgCl_2$	1.5 mM
Forward primer	0.5 µM

Reverse primer	0.5 µM

PCR cycling

Step 1 - 94 °C for 3 min

Step 2 - 94 °C for 30 s

Step 3 – 62 °C for 30 s (-0.5 º/cycle)

Step 4 - 72 °C for 60 s

Step 5 - Step 2 for 19 cycles

Step 6 – 94 °C for 30 s

Step 7 – 52 °C for 30 s

Step 8 - 72 °C for 60 s

Step 9 - Step 6 for 24 cycles

Step 10 - 72 °C for 5 min

Step 11 - End

DNA purification

Ran 1.0 % agarose gel; 100V; 30min. Gel extracted PCR product from and purified using GE healthcare illustra GFX Gel band and PCR purification kit as per the manufacturers' instructions. Eluted in 30µl 10mM Tris pH8.

Sequencing

Sequenced purified products in both directions using the respective forward or reverse primer using Big Dye Terminator chemistry version 3.1 and the service provider the Australian Genome Research Facility.

Online Resource S3.2

High-resolution melting curves, end-point genotyping assay calls and gel-electrophoresis images of 11 newly developed markers

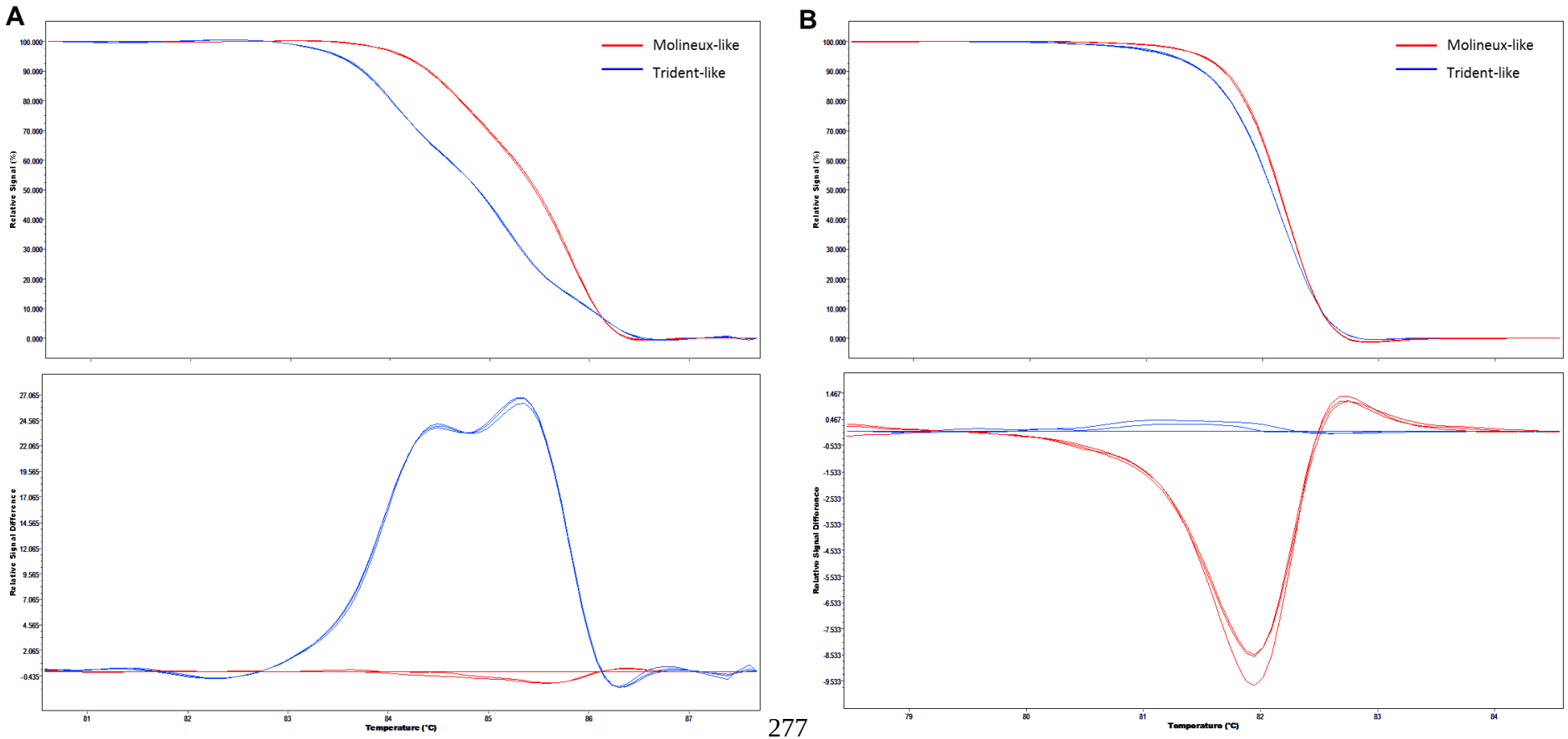

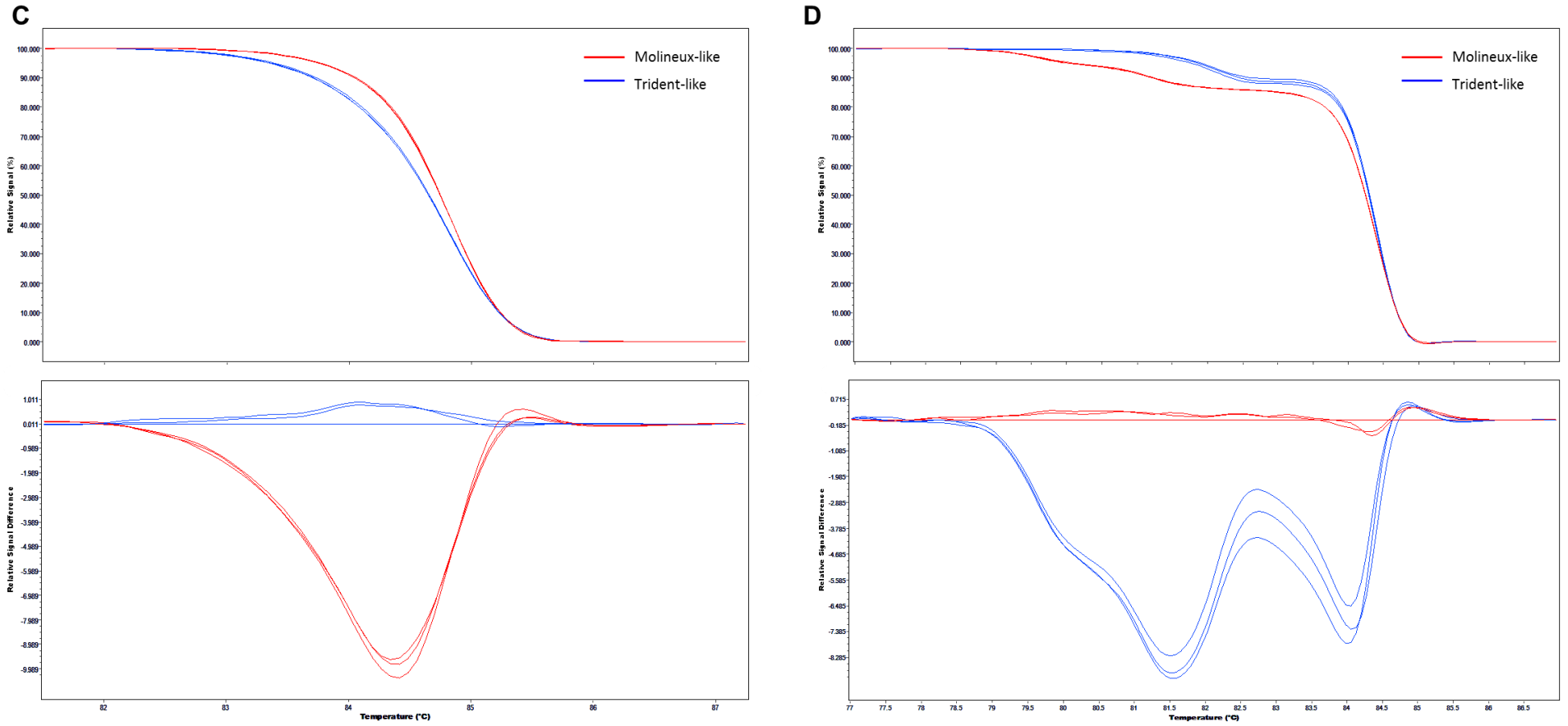

Figure S3.1 High-resolution melting curves for markers *wri6* (A), *wri7* (B), *wri8* (C) and *wri9* (D).

Upper panel: normalised and shifted melting curves; Lower panel: normalised and temperature-shifted difference plot. Curves are shown for products amplified in triplicate from genomic DNA of TMDH109 ("Trident-like") and TMDH150 ("Molineux-like").

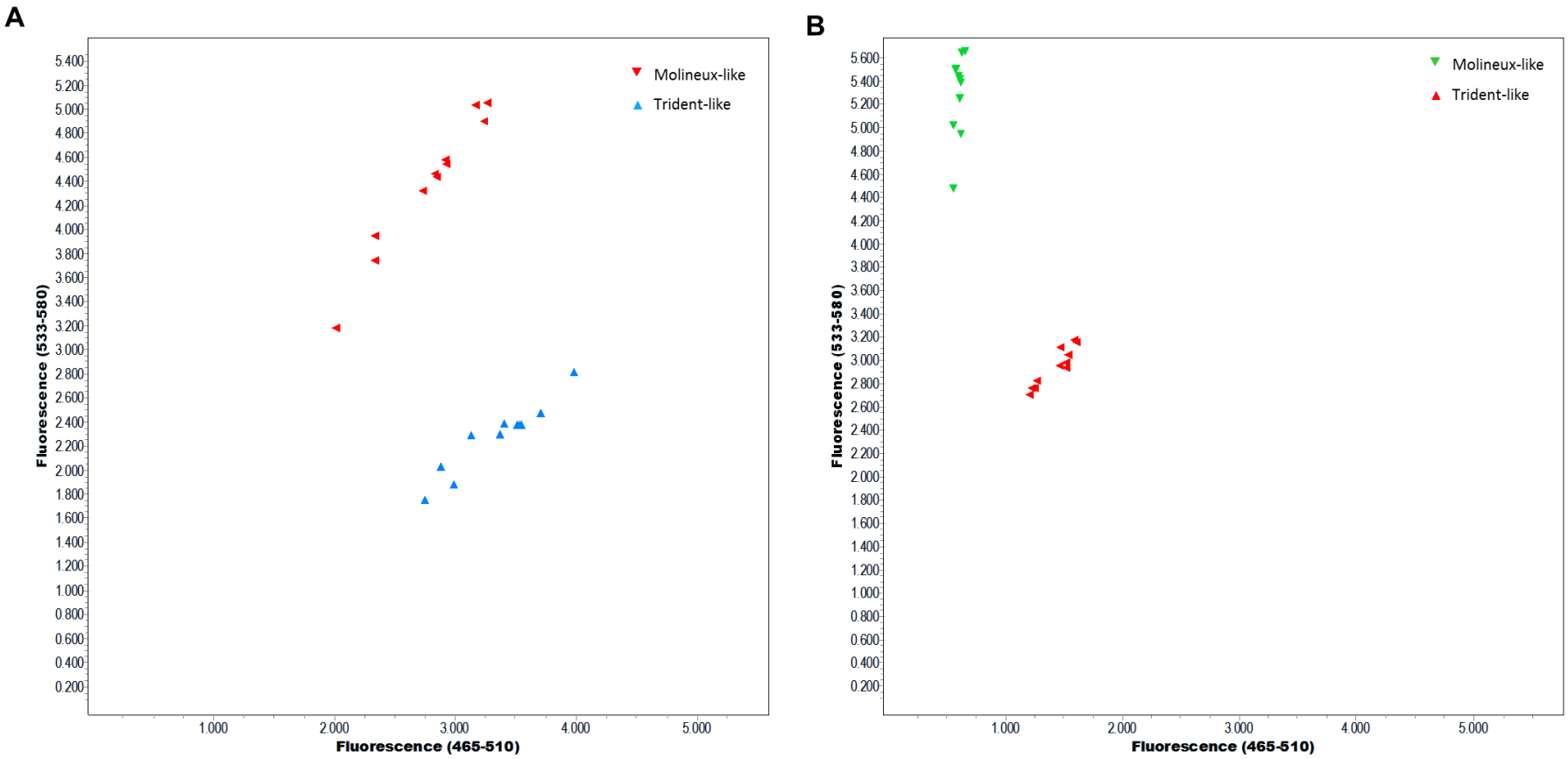
A
Molineux-like
Trident-like
Fluorescence (533-580)
Fluorescence (465-510)
B
Molineux-like
Trident-like
Fluorescence (533-580)
Fluorescence (465-510)

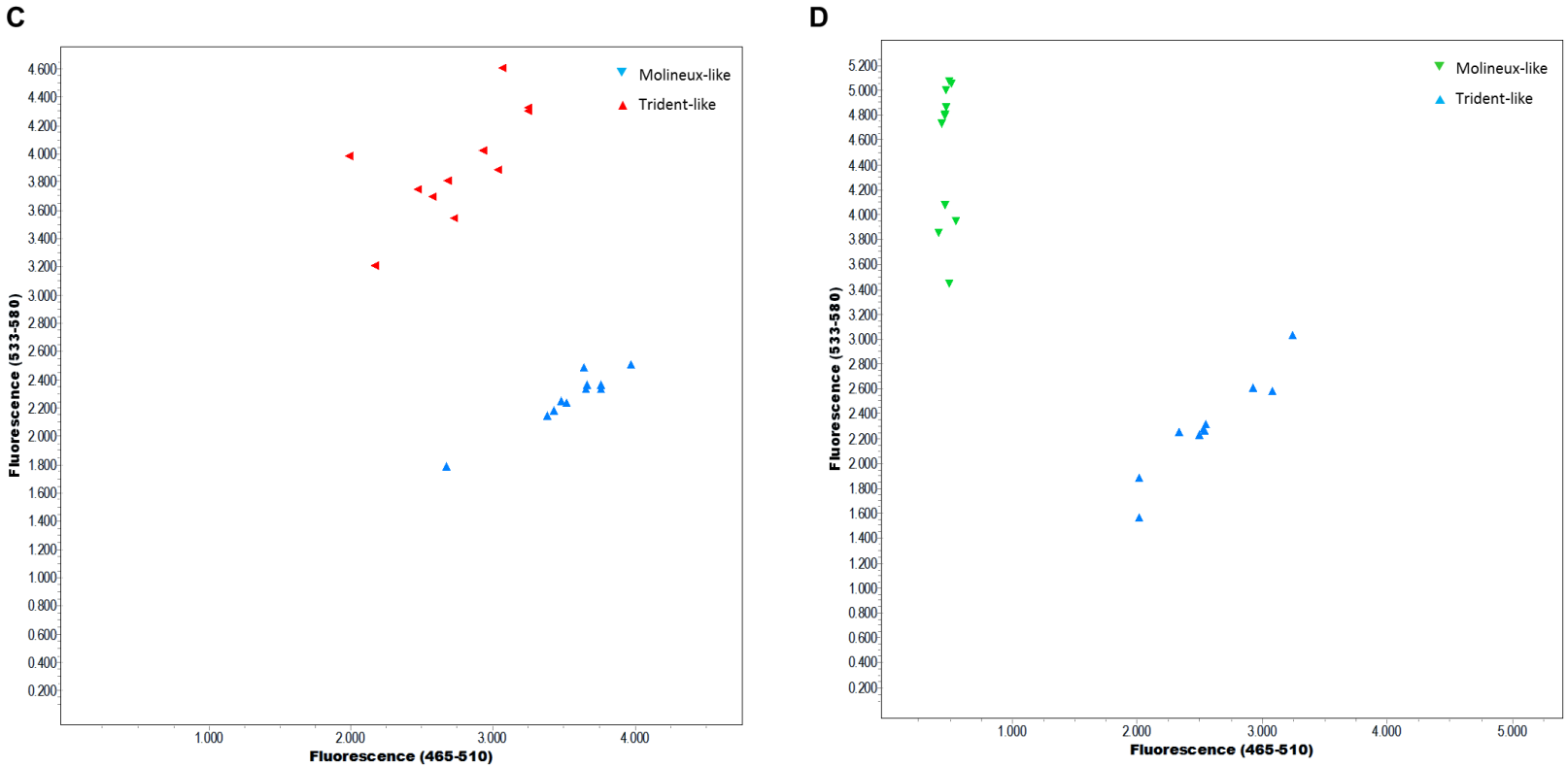

Figure S3.2: End-point genotyping clusters for markers *wri10* (A), *wri11* (B), *wri12* (C) and *wri13* (D).

Clusters are shown for products amplified from genomic DNA of TMDH109 ("Trident-like"), TMDH150 ("Molineux-like") and 20 Trident/Molineux doubled haploid lines.

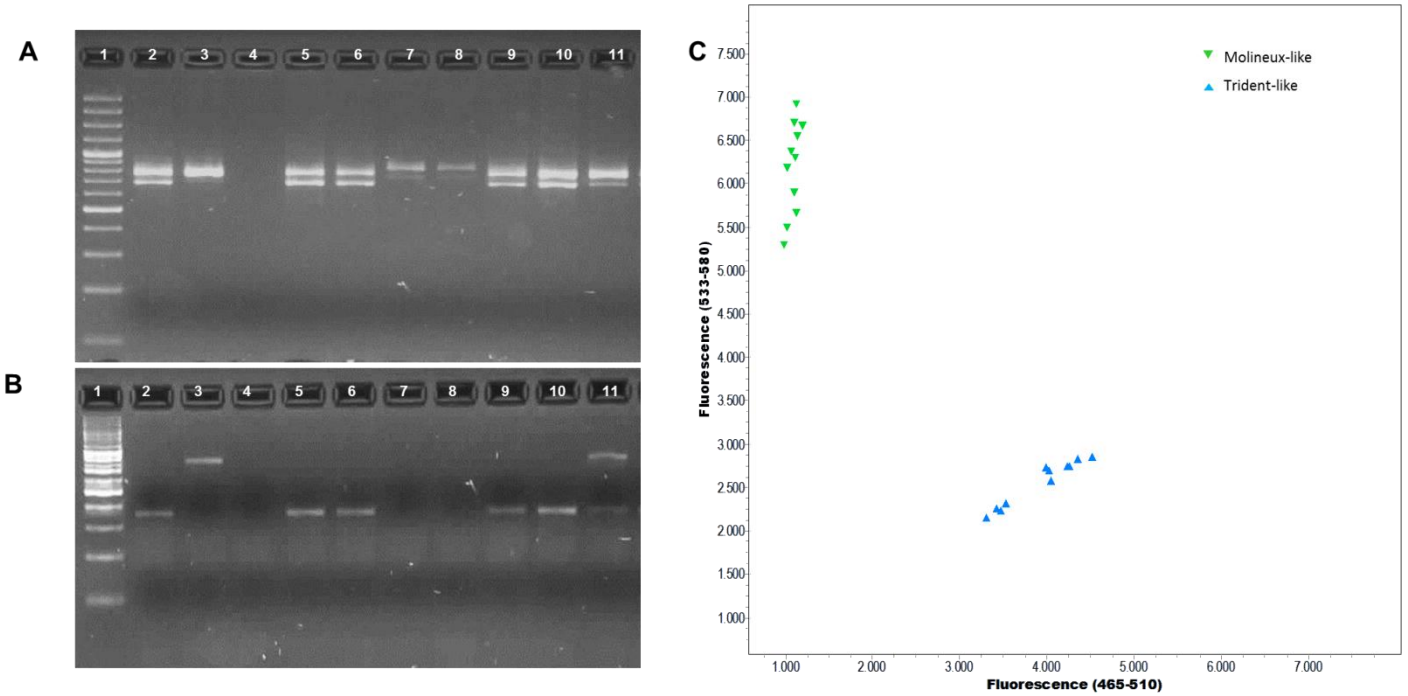

Figure S3.3: Agarose gel electrophoresis of amplicons of markers *wri14* (A), and *wri15* (B) and end-point genotyping scatter plot of amplicons of marker *wri16* (C).

For markers *wri14* and *wri15* from right to left: 1) GeneRuler® 100 bp DNA ladder (Thermo Fisher Scientific Inc.), 2) Molineux, 3) Trident, 4) water, 5) CS N6A-T6B, 6) CS N6A-T6D, 7) CS N6B-T6A, 8) CS N6B-T6D, 9) CS N6D-T6A, 10) CS N6D-T6B and 11) 1:1 mixture of Molineux and Trident DNA (artificial heterozygote). For marker *wri16* clusters are shown for products amplified from genomic DNA of TMDH109 (Trident-like), TMDH150 (Molineux-like) and 20 Trident/ Molineux doubled haploid lines.

Online Resource S3.3

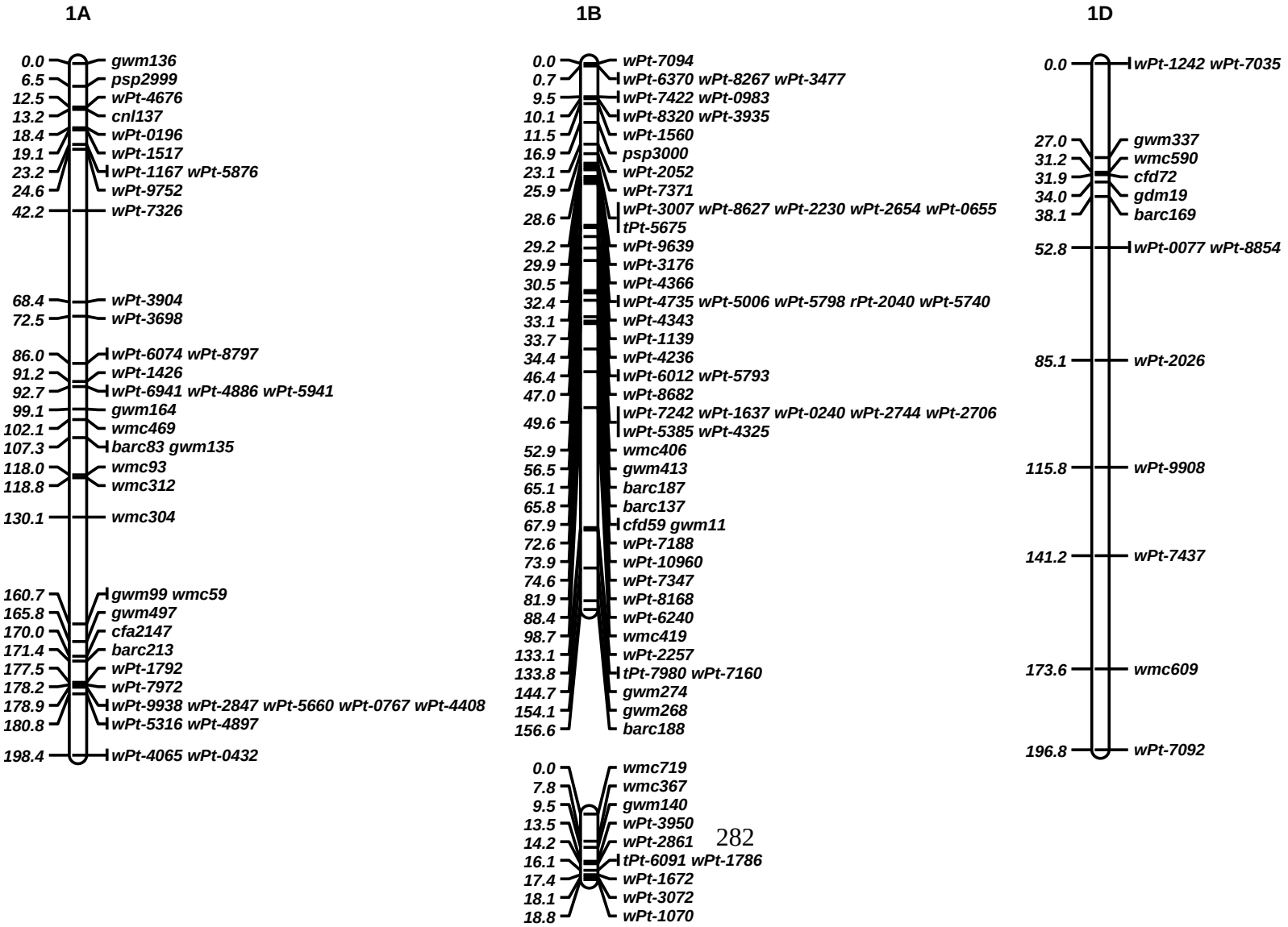

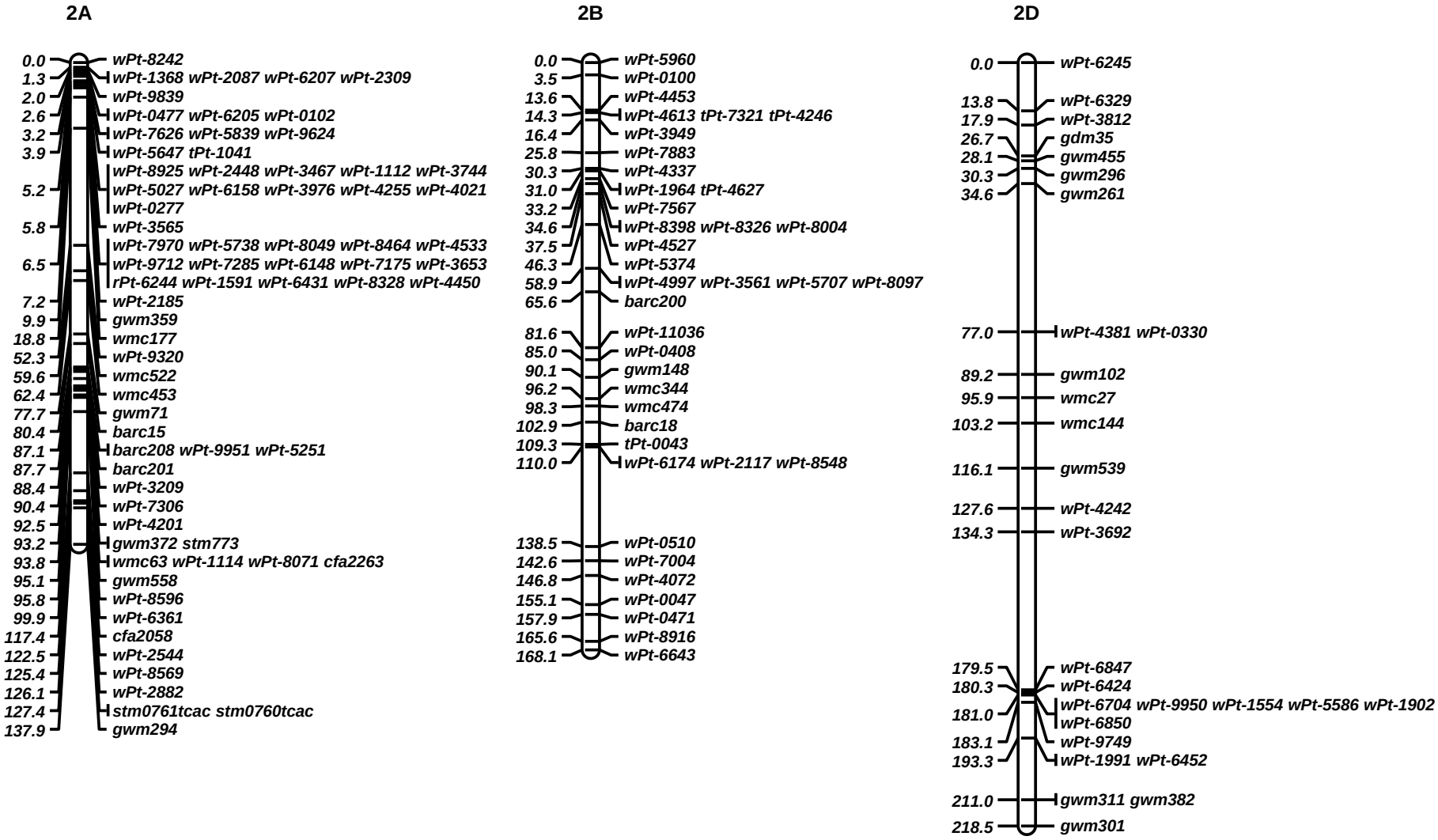
2A
0.0 wPt-8242
1.3 wPt-1368 wPt-2087 wPt-6207 wPt-2309
2.0 wPt-9839
2.6 wPt-0477 wPt-6205 wPt-0102
3.2 wPt-7626 wPt-5839 wPt-9624
3.9 wPt-5647 tPt-1041
wPt-8925 wPt-2448 wPt-3467 wPt-1112 wPt-3744
5.2 wPt-5027 wPt-6158 wPt-3976 wPt-4255 wPt-4021
wPt-0277
5.8 wPt-3565
wPt-7970 wPt-5738 wPt-8049 wPt-8464 wPt-4533
6.5 wPt-9712 wPt-7285 wPt-6148 wPt-7175 wPt-3653
rPt-6244 wPt-1591 wPt-6431 wPt-8328 wPt-4450
7.2 wPt-2185
9.9 gwm359
18.8 wmc177
52.3 wPt-9320
59.6 wmc522
62.4 wmc453
77.7 gwm71
80.4 barc15
87.1 barc208 wPt-9951 wPt-5251
87.7 barc201
88.4 wPt-3209
90.4 wPt-7306
92.5 wPt-4201
93.2 gwm372 stm773
93.8 wmc63 wPt-1114 wPt-8071 cfa2263
95.1 gwm558
95.8 wPt-8596
99.9 wPt-6361
117.4 cfa2058
122.5 wPt-2544
125.4 wPt-8569
126.1 wPt-2882
127.4 stm0761tcac stm0760tcac
137.9 gwm294
2B
0.0 wPt-5960
3.5 wPt-0100
13.6 wPt-4453
14.3 wPt-4613 tPt-7321 tPt-4246
16.4 wPt-3949
25.8 wPt-7883
30.3 wPt-4337
31.0 wPt-1964 tPt-4627
33.2 wPt-7567
34.6 wPt-8398 wPt-8326 wPt-8004
37.5 wPt-4527
46.3 wPt-5374
58.9 wPt-4997 wPt-3561 wPt-5707 wPt-8097
65.6 barc200
81.6 wPt-11036
85.0 wPt-0408
90.1 gwm148
96.2 wmc344
98.3 wmc474
102.9 barc18
109.3 tPt-0043
110.0 wPt-6174 wPt-2117 wPt-8548
138.5 wPt-0510
142.6 wPt-7004
146.8 wPt-4072
155.1 wPt-0047
157.9 wPt-0471
165.6 wPt-8916
168.1 wPt-6643
2D
0.0 wPt-6245
13.8 wPt-6329
17.9 wPt-3812
26.7 gdm35
28.1 gwm455
30.3 gwm296
34.6 gwm261
77.0 wPt-4381 wPt-0330
89.2 gwm102
95.9 wmc27
103.2 wmc144
116.1 gwm539
127.6 wPt-4242
134.3 wPt-3692
179.5 wPt-6847
180.3 wPt-6424
wPt-6704 wPt-9950 wPt-1554 wPt-5586 wPt-1902
181.0 wPt-6850
183.1 wPt-9749
193.3 wPt-1991 wPt-6452
211.0 gwm311 gwm382
218.5 gwm301

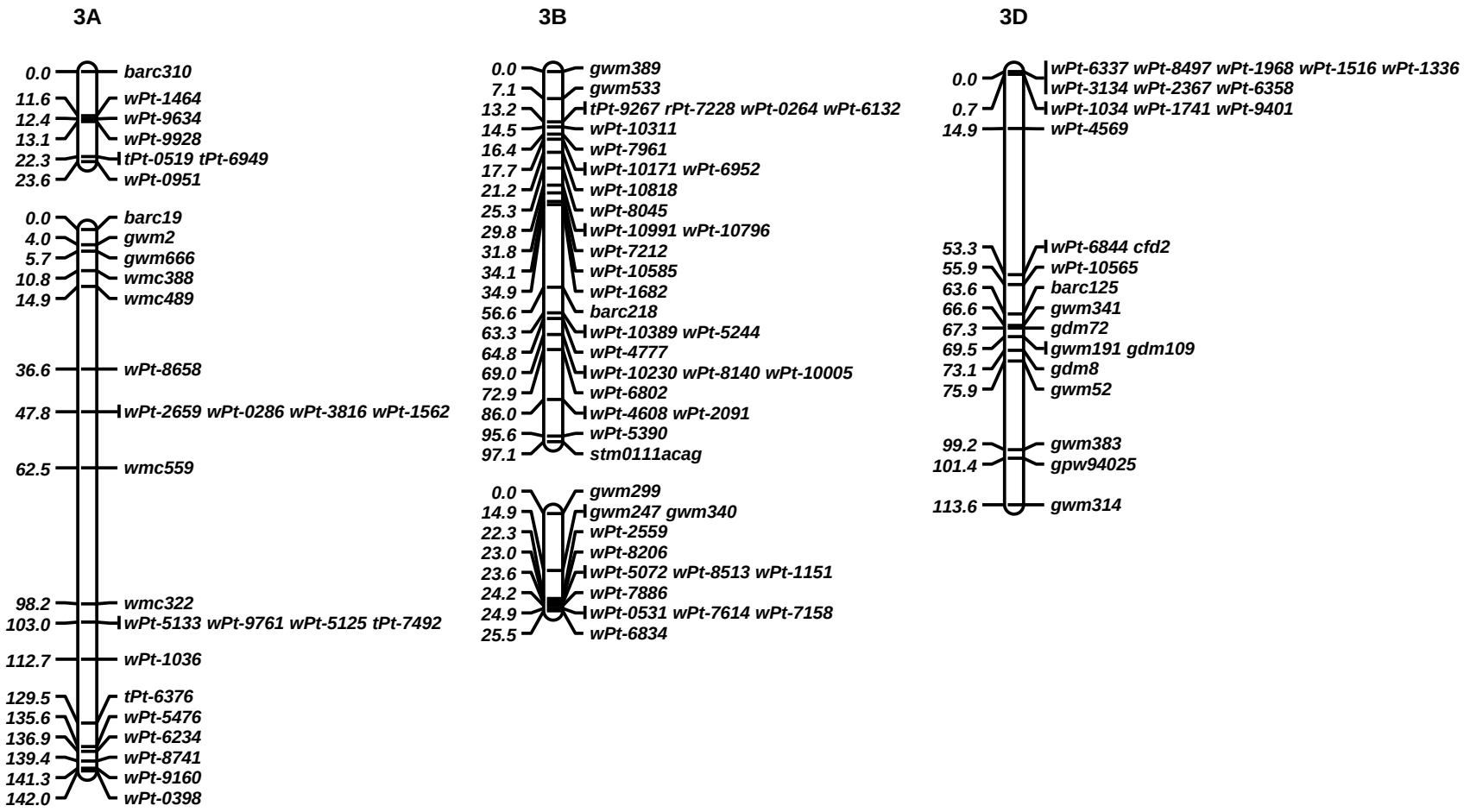
3A
0.0 barc310
11.6 wPt-1464
12.4 wPt-9634
13.1 wPt-9928
22.3 tPt-0519 tPt-6949
23.6 wPt-0951
0.0 barc19
4.0 gwm2
5.7 gwm666
10.8 wmc388
14.9 wmc489
36.6 wPt-8658
47.8 wPt-2659 wPt-0286 wPt-3816 wPt-1562
62.5 wmc559
98.2 wmc322
103.0 wPt-5133 wPt-9761 wPt-5125 tPt-7492
112.7 wPt-1036
129.5 tPt-6376
135.6 wPt-5476
136.9 wPt-6234
139.4 wPt-8741
141.3 wPt-9160
142.0 wPt-0398
3B
0.0 gwm389
7.1 gwm533
13.2 tPt-9267 rPt-7228 wPt-0264 wPt-6132
14.5 wPt-10311
16.4 wPt-7961
17.7 wPt-10171 wPt-6952
21.2 wPt-10818
25.3 wPt-8045
29.8 wPt-10991 wPt-10796
31.8 wPt-7212
34.1 wPt-10585
34.9 wPt-1682
56.6 barc218
63.3 wPt-10389 wPt-5244
64.8 wPt-4777
69.0 wPt-10230 wPt-8140 wPt-10005
72.9 wPt-6802
86.0 wPt-4608 wPt-2091
95.6 wPt-5390
97.1 stm0111acag
0.0 gwm299
14.9 gwm247 gwm340
22.3 wPt-2559
23.0 wPt-8206
23.6 wPt-5072 wPt-8513 wPt-1151
24.2 wPt-7886
24.9 wPt-0531 wPt-7614 wPt-7158
25.5 wPt-6834
3D
0.0 wPt-6337 wPt-8497 wPt-1968 wPt-1516 wPt-1336
wPt-3134 wPt-2367 wPt-6358
0.7 wPt-1034 wPt-1741 wPt-9401
14.9 wPt-4569
53.3 wPt-6844 cfd2
55.9 wPt-10565
63.6 barc125
66.6 gwm341
67.3 gdm72
69.5 gwm191 gdm109
73.1 gdm8
75.9 gwm52
99.2 gwm383
101.4 gpw94025
113.6 gwm314

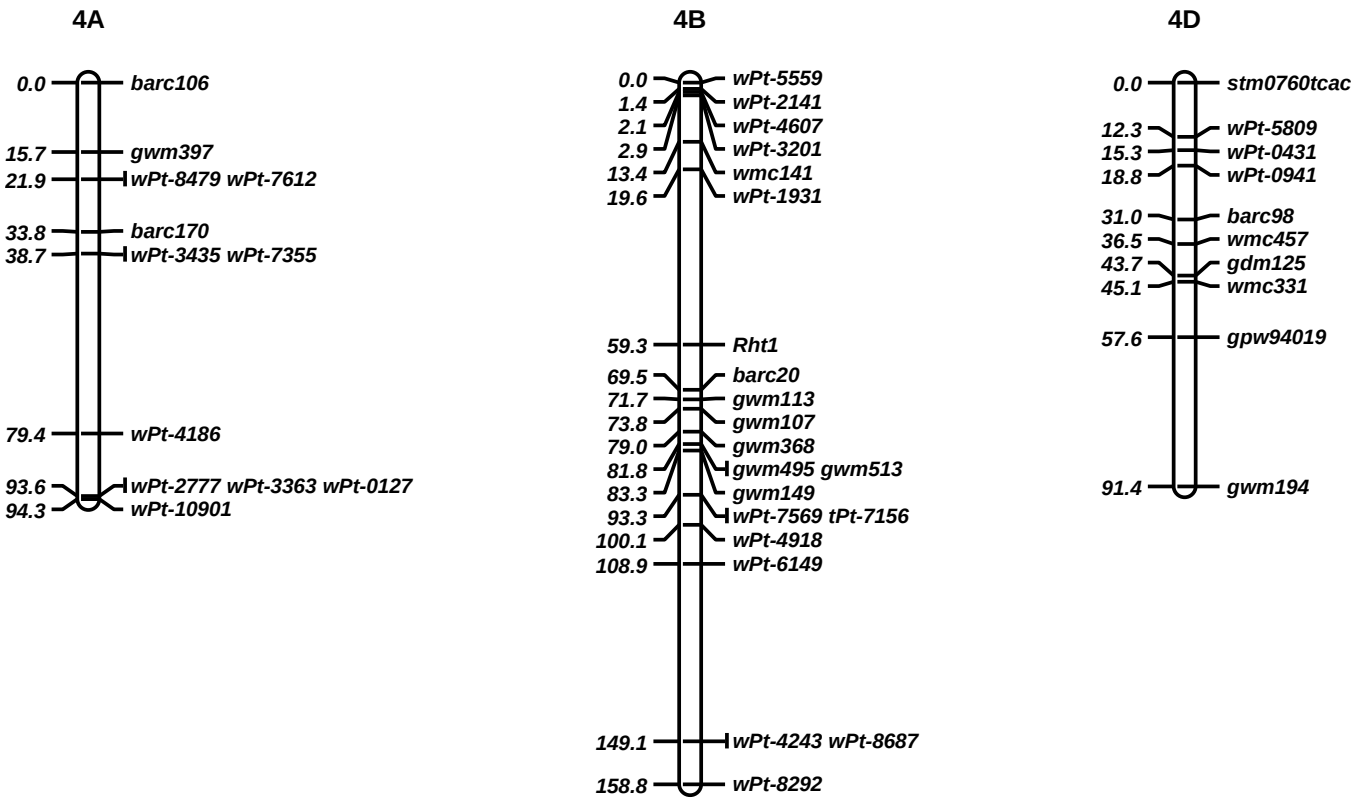
4A
0.0 barc106
15.7 gwm397
21.9 wPt-8479 wPt-7612
33.8 barc170
38.7 wPt-3435 wPt-7355
79.4 wPt-4186
93.6 wPt-2777 wPt-3363 wPt-0127
94.3 wPt-10901
4B
0.0 wPt-5559
1.4 wPt-2141
2.1 wPt-4607
2.9 wPt-3201
13.4 wmc141
19.6 wPt-1931
59.3 Rht1
69.5 barc20
71.7 gwm113
73.8 gwm107
79.0 gwm368
81.8 gwm495 gwm513
83.3 gwm149
93.3 wPt-7569 tPt-7156
100.1 wPt-4918
108.9 wPt-6149
149.1 wPt-4243 wPt-8687
158.8 wPt-8292
4D
0.0 stm0760tcac
12.3 wPt-5809
15.3 wPt-0431
18.8 wPt-0941
31.0 barc98
36.5 wmc457
43.7 gdm125
45.1 wmc331
57.6 gpw94019
91.4 gwm194

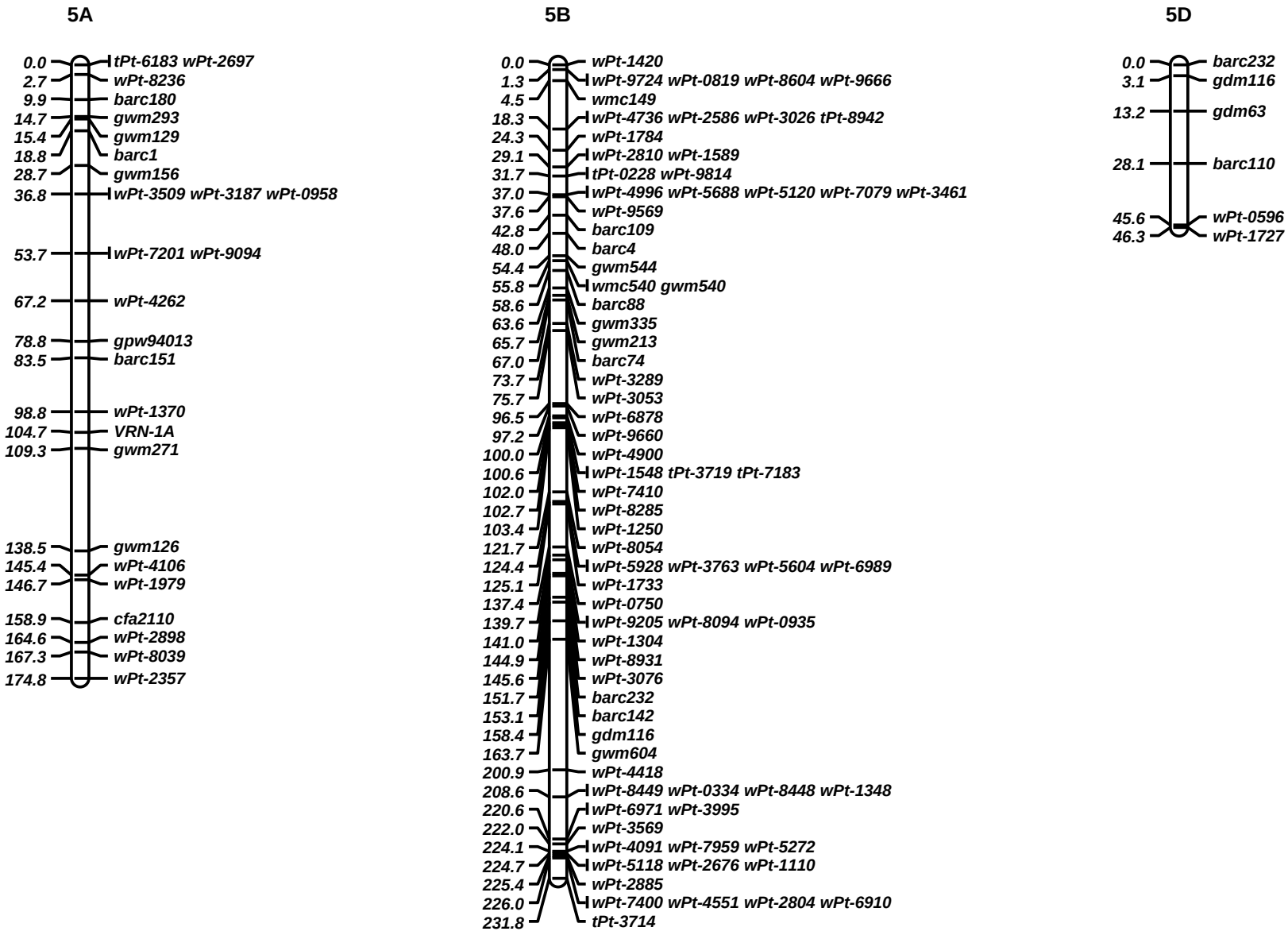
5A
0.0 tPt-6183 wPt-2697
2.7 wPt-8236
9.9 barc180
14.7 gwm293
15.4 gwm129
18.8 barc1
28.7 gwm156
36.8 wPt-3509 wPt-3187 wPt-0958
53.7 wPt-7201 wPt-9094
67.2 wPt-4262
78.8 gpw94013
83.5 barc151
98.8 wPt-1370
104.7 VRN-1A
109.3 gwm271
138.5 gwm126
145.4 wPt-4106
146.7 wPt-1979
158.9 cfa2110
164.6 wPt-2898
167.3 wPt-8039
174.8 wPt-2357
5B
0.0 wPt-1420
1.3 wPt-9724 wPt-0819 wPt-8604 wPt-9666
4.5 wmc149
18.3 wPt-4736 wPt-2586 wPt-3026 tPt-8942
24.3 wPt-1784
29.1 wPt-2810 wPt-1589
31.7 tPt-0228 wPt-9814
37.0 wPt-4996 wPt-5688 wPt-5120 wPt-7079 wPt-3461
37.6 wPt-9569
42.8 barc109
48.0 barc4
54.4 gwm544
55.8 wmc540 gwm540
58.6 barc88
63.6 gwm335
65.7 gwm213
67.0 barc74
73.7 wPt-3289
75.7 wPt-3053
96.5 wPt-6878
97.2 wPt-9660
100.0 wPt-4900
100.6 wPt-1548 tPt-3719 tPt-7183
102.0 wPt-7410
102.7 wPt-8285
103.4 wPt-1250
121.7 wPt-8054
124.4 wPt-5928 wPt-3763 wPt-5604 wPt-6989
125.1 wPt-1733
137.4 wPt-0750
139.7 wPt-9205 wPt-8094 wPt-0935
141.0 wPt-1304
144.9 wPt-8931
145.6 wPt-3076
151.7 barc232
153.1 barc142
158.4 gdm116
163.7 gwm604
200.9 wPt-4418
208.6 wPt-8449 wPt-0334 wPt-8448 wPt-1348
220.6 wPt-6971 wPt-3995
222.0 wPt-3569
224.1 wPt-4091 wPt-7959 wPt-5272
224.7 wPt-5118 wPt-2676 wPt-1110
225.4 wPt-2885
226.0 wPt-7400 wPt-4551 wPt-2804 wPt-6910
231.8 tPt-3714
5D
0.0 barc232
3.1 gdm116
13.2 gdm63
28.1 barc110
45.6 wPt-0596
46.3 wPt-1727

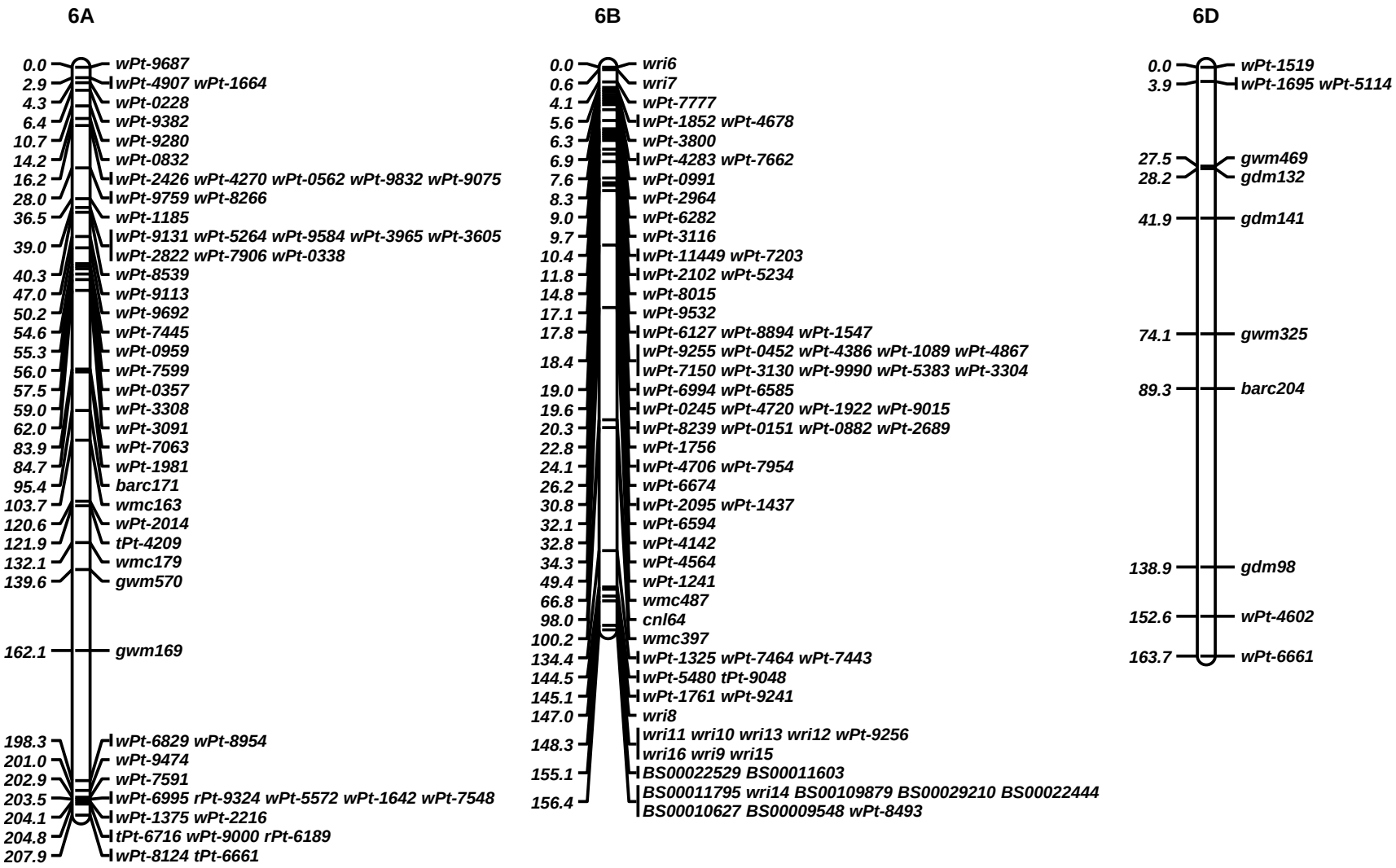
6A
0.0 wPt-9687
2.9 wPt-4907 wPt-1664
4.3 wPt-0228
6.4 wPt-9382
10.7 wPt-9280
14.2 wPt-0832
16.2 wPt-2426 wPt-4270 wPt-0562 wPt-9832 wPt-9075
28.0 wPt-9759 wPt-8266
36.5 wPt-1185
39.0 wPt-9131 wPt-5264 wPt-9584 wPt-3965 wPt-3605
wPt-2822 wPt-7906 wPt-0338
40.3 wPt-8539
47.0 wPt-9113
50.2 wPt-9692
54.6 wPt-7445
55.3 wPt-0959
56.0 wPt-7599
57.5 wPt-0357
59.0 wPt-3308
62.0 wPt-3091
83.9 wPt-7063
84.7 wPt-1981
95.4 barc171
103.7 wmc163
120.6 wPt-2014
121.9 tPt-4209
132.1 wmc179
139.6 gwm570
162.1 gwm169
198.3 wPt-6829 wPt-8954
201.0 wPt-9474
202.9 wPt-7591
203.5 wPt-6995 rPt-9324 wPt-5572 wPt-1642 wPt-7548
204.1 wPt-1375 wPt-2216
204.8 tPt-6716 wPt-9000 rPt-6189
207.9 wPt-8124 tPt-6661
6B
0.0 wri6
0.6 wri7
4.1 wPt-7777
5.6 wPt-1852 wPt-4678
6.3 wPt-3800
6.9 wPt-4283 wPt-7662
7.6 wPt-0991
8.3 wPt-2964
9.0 wPt-6282
9.7 wPt-3116
10.4 wPt-11449 wPt-7203
11.8 wPt-2102 wPt-5234
14.8 wPt-8015
17.1 wPt-9532
17.8 wPt-6127 wPt-8894 wPt-1547
18.4 wPt-9255 wPt-0452 wPt-4386 wPt-1089 wPt-4867
wPt-7150 wPt-3130 wPt-9990 wPt-5383 wPt-3304
19.0 wPt-6994 wPt-6585
19.6 wPt-0245 wPt-4720 wPt-1922 wPt-9015
20.3 wPt-8239 wPt-0151 wPt-0882 wPt-2689
22.8 wPt-1756
24.1 wPt-4706 wPt-7954
26.2 wPt-6674
30.8 wPt-2095 wPt-1437
32.1 wPt-6594
32.8 wPt-4142
34.3 wPt-4564
49.4 wPt-1241
66.8 wmc487
98.0 cnl64
100.2 wmc397
134.4 wPt-1325 wPt-7464 wPt-7443
144.5 wPt-5480 tPt-9048
145.1 wPt-1761 wPt-9241
147.0 wri8
148.3 wri11 wri10 wri13 wri12 wPt-9256
wri16 wri9 wri15
155.1 BS00022529 BS00011603
156.4 BS00011795 wri14 BS00109879 BS00029210 BS00022444
BS00010627 BS00009548 wPt-8493
6D
0.0 wPt-1519
3.9 wPt-1695 wPt-5114
27.5 gwm469
28.2 gdm132
41.9 gdm141
74.1 gwm325
89.3 barc204
138.9 gdm98
152.6 wPt-4602
163.7 wPt-6661

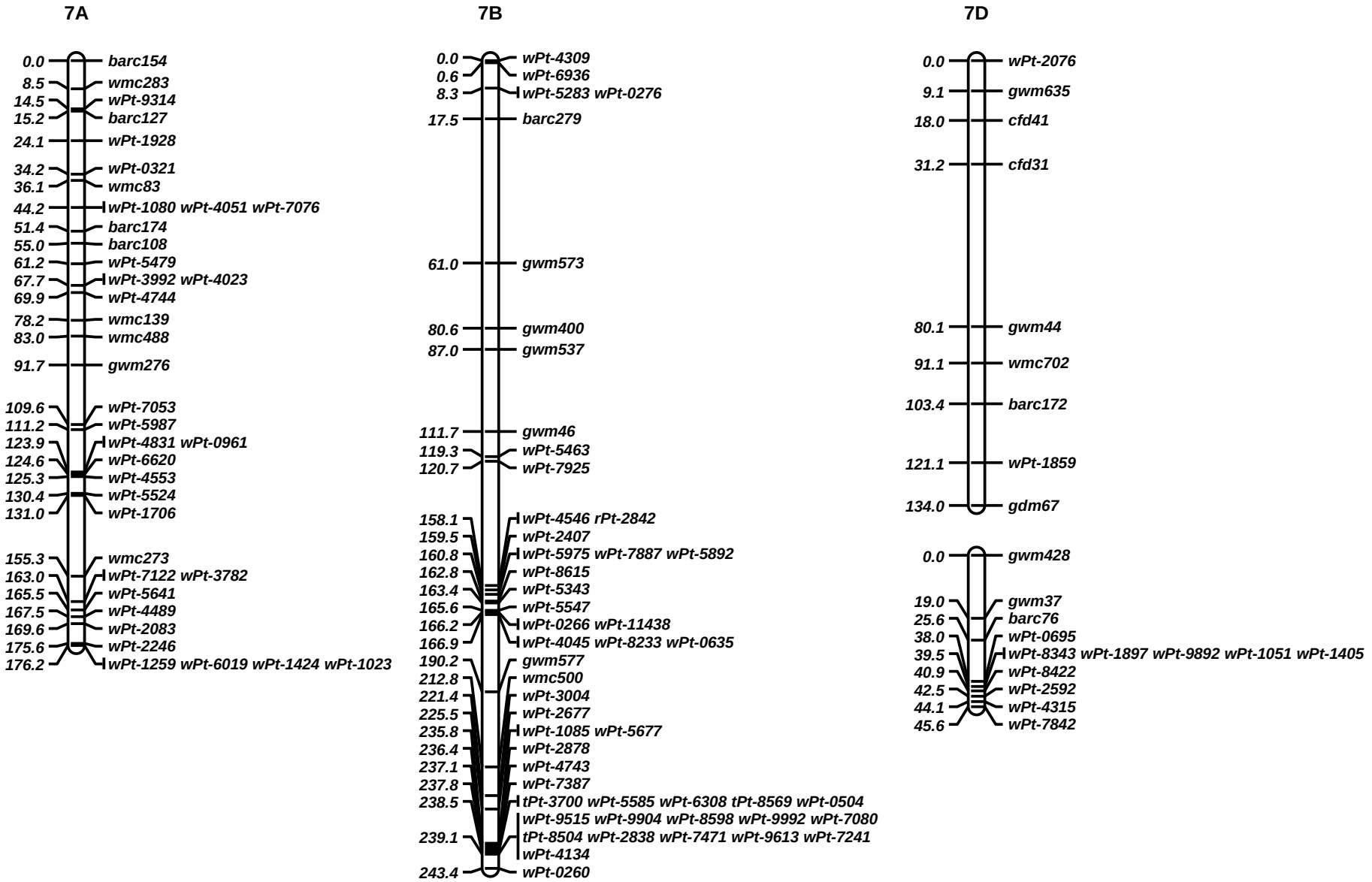

Figure S3.4: Trident/Molineux linkage map

Online Resource S3.4

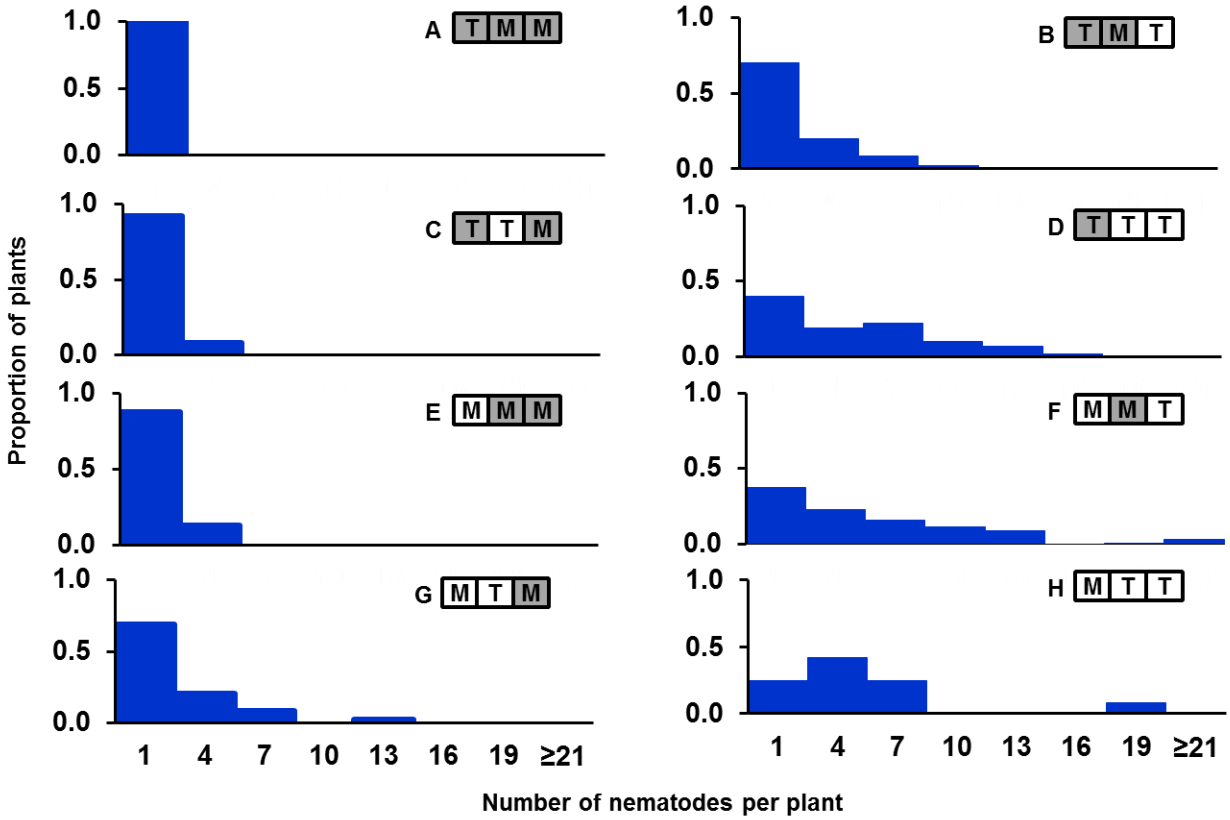

Figure S3.5 Distributions of *Heterodera avenae* nematode counts among 38 Trident/Molineux doubled haploid lines evaluated in pot tests.

Each pair of histograms (A and B, C and D, E and F, G and H) represents a group of lines classified according to the parental origin of their alleles at three loci. The allelic combination for each groups is shown using the letters T (for Trident) and M (for Molineux) with the Cre5, QCre.srd-1B and Cre8 shown from left to right and with the alleles that confer increased resistance shaded in grey. In each case, the values shown for the proportions of plants were calculated as the mean proportions across all lines within the genotypic class.

Appendix 4: A first look at the infection of cereal cyst nematode (*Heterodera avenae* Woll.) and establishment of syncytia in wheat carrying the *Cre8* resistance allele

S4.1 Introduction

In Chapters 5 and 6, the prospects of positional cloning of CCN *H. avenae* resistance locus *Cre8* were discussed. Other than positional cloning, it is also possible to isolate genes *via* a candidate gene approach. For either of these two approaches, knowledge about the resistance mechanisms and biological processes involved in delivering resistance responses could be useful to narrow down candidate genes.

The root responses of resistant lines carrying CCN *H. avenae* resistance loci *Cre1* (wheat), *Cre3* (*Ae. tauschii*), *Rha2* (barley) and *Rha4* (barley) have been compared to those from susceptible lines, in terms of nematode penetration and the histological changes associated with syncytia (designated nematode feeding sites formed by disintegrating the cell walls and fusion of the protoplasm of the adjacent parenchyma cells.) [51, 117, 154, 196] . None of the resistance loci (*Cre1*, *Cre3*, *Ha2* and *Ha4*) affected the initial penetration, the establishment and development of nematodes or the initiation and early development of syncytia, but at later stages the resistance loci seemed to affect the degradation of syncytia (extensive vacuolation and metabolically less active protoplasm), making it difficult for the female nematodes to get adequate nutrition to reach maturity [51, 117, 154, 196]. To my knowledge, no work has been done to understand the effects of the wheat *Cre8* resistance

locus, in terms of nematode penetration and/or the histological changes associated with the syncytium development. Here, I report the testing of the above concept, by comparing the responses of two Trident/Molineux DH lines carrying the opposite alleles at the *Cre8* resistance locus over four sampling time points.

S4.2 Methods

Plant materials

The plant materials used here were two Trident/Molineux F_1-derived DH lines (TMDH006 and TMDH082). As described in Chapter 6, TMDH006 carries the resistance allele at *Cre8*, but not at two other resistance QTL, while TMDH082 does not carry resistance alleles at any of the known CCN (*H. avenae*) resistance QTL (see Chapter 6 for further details on selection criteria).

Preparation of plant material

Seeds of TMDH006 and TMDH082 were sown in petri dishes lined with moistened Whatman filter paper, were kept in dark overnight at 5 °C and transferred to room temperature for another 2 d. The seedlings were then transplanted in 30 mm PVC tubes filled with sterilized moistened soil and kept in a growth room (15 °C / 12 h alternative dark/light cycle). Inoculum of *H. avenae* sourced from various fields in the Yorke Peninsula, South Australia (kindly provided by John Lewis, SARDI, Australia), was diluted in reverse osmosis purified water and juveniles (J_2 stage) were counted using a counting dish. The inoculum density was adjusted to100 nematodes/ml. Four-day-old seedlings were inoculated by pipetting 1 ml of well mixed inoculum close to the crown of

the seedling. Of 72 plants grown, 56 were inoculated and 16 were maintained as controls without inoculation.

Staining and counting of nematodes in roots

Acid fuchsin staining of nematodes was carried out at 11, 18, 21 and 25 DAI. For each time point, four inoculated plants from each DH line were picked randomly. The soil was washed off and the roots were treated with 2 % sodium hypochlorite for 10 min. The roots were carefully rinsed with water and pat dried to remove excess water. Roots were dipped in acid fusion staining solution (33 % glycerol, 33 % lactic acid and 0.5g/L of acid fuchsin) and heated up to boiling point. The stained roots were left to cool down for 20 min. Roots were transferred to destaining solution (50 % glycerol, 5 % lactic acid) and were reheated. The stained roots were observed through a dissection microscope and the total number of nematodes (stained in pink) in the root and the number of seminal roots were counted and recorded for each plant. Using the mean number of nematodes per seminal root as the variable, genotypic effects (TMDH006 *vs* TMDH082), DAI effects and the interaction between genotype and DAI were tested for significance by a two-way analysis of variance (ANOVA), performed using GenStat v15.3.0.9425 (VSN International limited, UK).

Microscopic examination of syncytia development

Root samples were collected on the 4, 7, 11 and 18 DAI with two control samples and three inoculated samples per line. Soil was washed off from the plants and the roots were fixed in a formalin acetic alcohol solution (50 % absolute ethanol, 5 % acetic acid and 4 % formaldehyde) overnight. The fixed root tissues were stored in 70 % ethanol at 4 °C. The root tissues were dehydrated using an ethanol concentration series of 70 %, 80 %, 90 %, 95

% and 100 % (dehydrated ethanol). At each concentration, three solution changes were done at 20 min intervals. Samples of swollen root tissue (2 to 5 mm in length) were cut from the inoculated plants. Samples of similar length were taken from the roots of control plants. The dehydrated tissues were transferred to a 50:50 mix of 100 % ethanol (dehydrated): LR white resin (London Resin Co., Berkshire, UK) and kept overnight to facilitate infiltration. Tissue specimens were infiltrated with 100 % LR white, by making three 100 % LR white changes at 8 h intervals. The root tissues were embedded flat on gelatine capsules and the capsules were filled with 100 % LR white. The embedded capsules were incubated in a 58 °C oven for 48 h to facilitate polymerisation of LR white.

Longitudinal serial sectioning (1-µm thickness) of the root tissues were carried out using a rotary microtome (Leica Microsystems Pty. Ltd. Germany) and the tissues were stained using toluidine blue stain (0.01 % toluidine blue in 0.1 % sodium tetraborate) and were examined under a light microscope (magnification 50×).

S4.3 Results

Nematode penetration and development

At all-time points, swollen root areas were observed in plants inoculated with *H. avenae,* but not on the roots of the non-inoculated controls. By 11 DAI, nematodes had successfully penetrated and established in the roots of both TMDH006 and TMDH082, and the lateral roots had emerged. Nematodes were seen predominantly colonising the swollen areas in the roots. At 11 DAI, nematodes had a vermiform body shape (Figure S4.1A) and could be identified as the J_2 juvenile stage, as described by Lilley et al. [91]. By the 18 DAI, both J_3 and J_4 stage nematodes with a plump body shape were observed (Figure S4.1B). At this stage a considerable increase in the root size was also noted, primarily due to the

development of bulky lateral roots. By the 21 and 25 DAI, J_4 stage nematodes predominated the swollen root areas (Figure S4.1C) and by the 25 DAI, it was observed that some swollen areas had been abandoned.

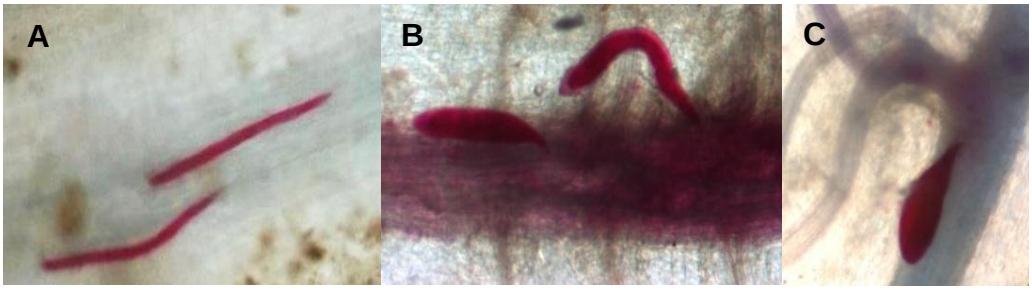

Figure S4.1: Cereal cyst nematode development in wheat roots.

J_2 stage at 11 day after inoculation (DAI) (A), J_3 (right) and J_4 (left) stages at 18 DAI (B), and J_4 stage at 25 DAI (C) (magnification factor 50)

The mean nematode count per seminal root had high variability (Table S4.1) and followed an increasing trend until 21 DAI and declined by 25 DAI, for both TMDH006 and TMDH082 (Figure S4.2). There was significant variation in the mean nematode counts among the sampling times (DAI in Table S4.1; $p < 0.05$), but not between TMDH006 and TMDH082 ($p > 0.05$) (Genotype in Table S4.1). There was no significant interaction ($p > 0.05$) between sampling times and lines.

Table S4.1: Analysis of variance (ANOVA) table.

A two-way ANOVA with days after inoculation (DAI) and the genotype (TMDH006 or TMDH082) as factors and the nematode count per seminal root as the variant.

Source of variation	Degrees of freedom	Sums of squares	Mean squares	Variance	F probability
DAI	3	51.851	17.284	3.65	0.028
Genotype	1	0.144	0.144	0.03	0.863
DAI × Genotype	3	8.425	2.808	0.59	0.627
Residual	22	104.305	4.741		
Total	29	164.725			

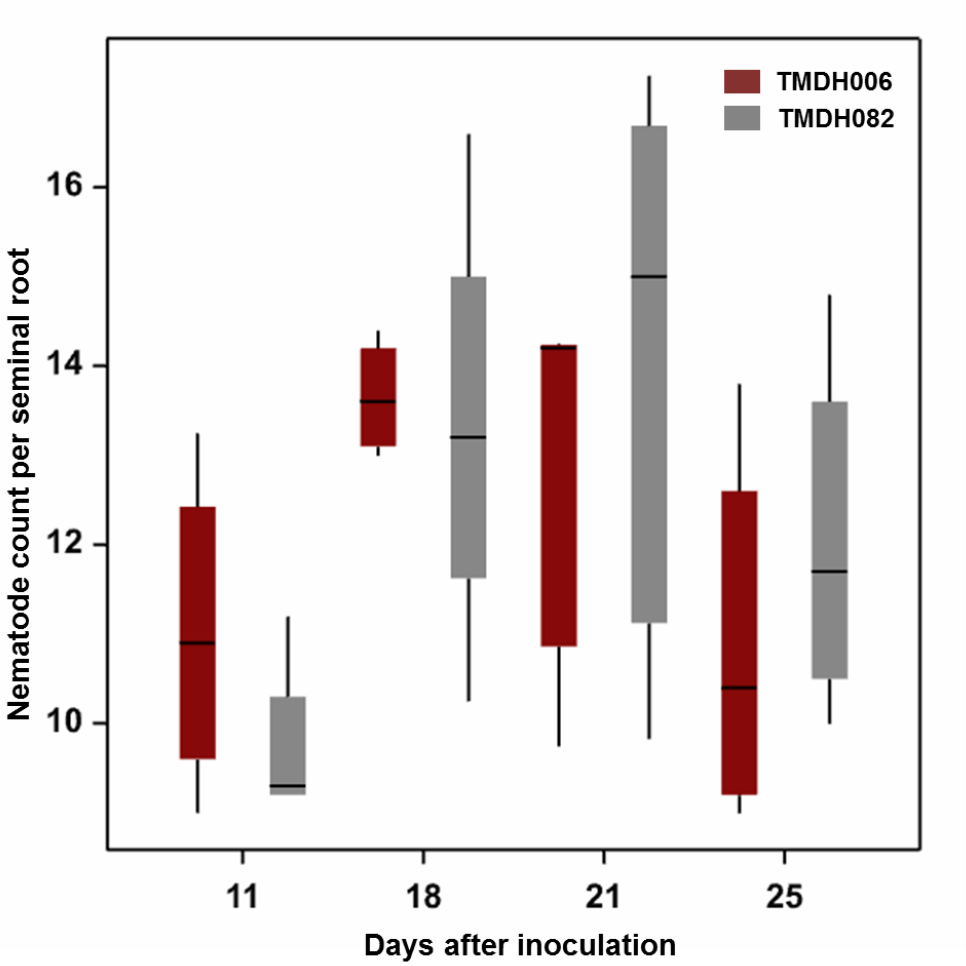

Figure S4.2: Nematode count per seminal root in TMDH006 and TMDH082 at 11, 18, 21 and 25 days after inoculation.

The box spans the interquartile range of the estimated nematode count per seminal root, the horizontal line within each box indicates the median. The whiskers extend to show the spread of data.

Syncytia development

As expected no syncytia were seen in the uninoculated controls. In the inoculated samples of both TMDH006 and TMDH082, initiation of syncytia occurred by 4 DAI. The only prominent difference observed between the TMDH006 and TMDH082 was at 4 DAI, where the cell walls of the syncytia of TMDH006 looked disintegrated compared to that of the TMDH082 (Figure S4.3A and B). There was no prominent difference between the

syncytia of TMDH006 and TMDH082 at 7, 11 and 18 DAI (Figure S4.3C to H). Further, a clear degradation of syncytia cell walls were observed between 4 and 7 DAI in TMDH082 (Figure S4.3B and D). Other than that no noticeable differences were observed either among the 7, 11 and 18 DAI sampling time points in TMDH006 or in TMDH082.

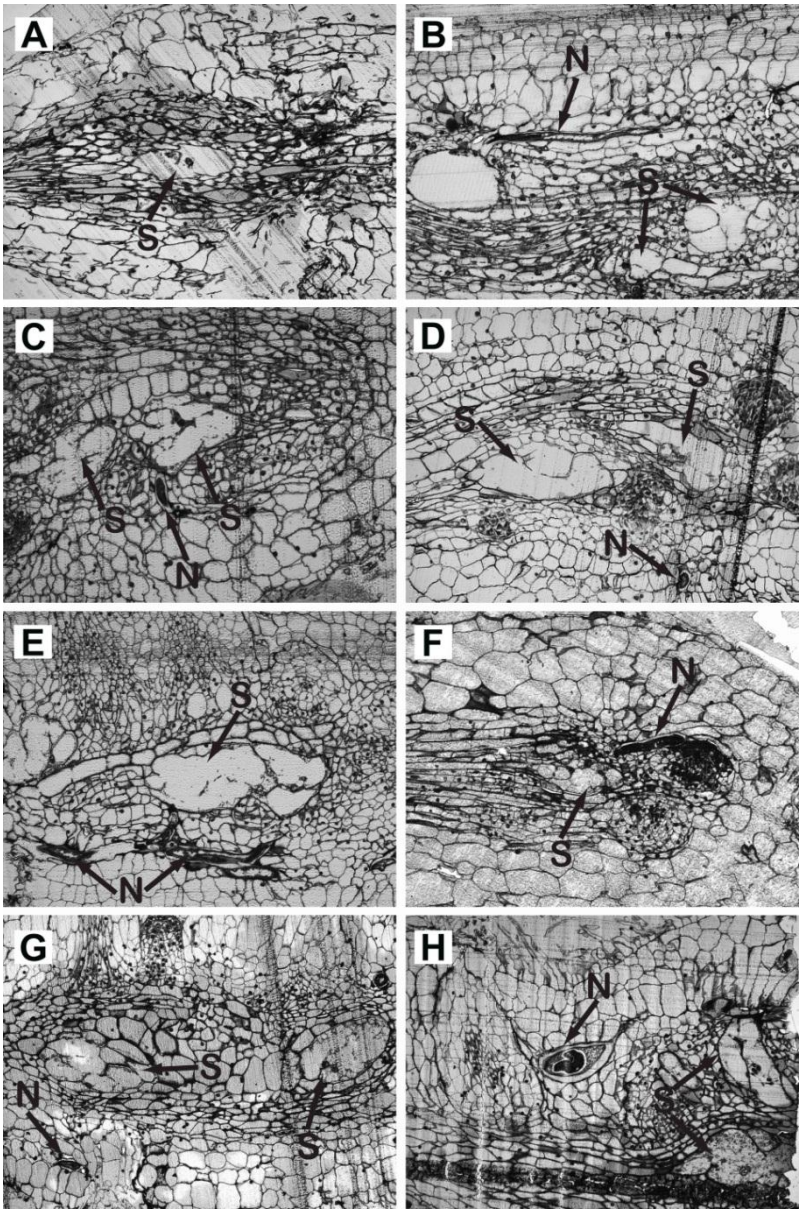

Figure S4.3: Development of syncytia in TMDH006 and TMDH082 in longitudinal root sections from 4, 7, 11 and 18 days after inoculation (DAI) with *H. avenae*.

TMDH006 at 4 DAI (A), TMDH082 at 4 DAI (A), TMDH006 at 7 DAI (C), TMDH082 at 7 DAI (D), TMDH006 at 11 DAI (E), TMDH082 at 11 DAI (F) TMDH006 at 18 DAI (G) TMDH082 at 18 DAI (H). N – nematode and S – syncytium (magnification factor 50).

S4.4 Discussion

Despite high variability in the nematode counts (Figure S4.2), statistically significant ($p < 0.05$) differences were detected among sampling times, with counts increasing in both lines between 11 and 21 DAI, then decreasing by 25 DAI. The increases in numbers of nematodes up until 21 DAI would have been due to continuing entry of nematodes from the soil during the experiment. Consistent with this, all three juvenile stages of the nematode life cycle (J_2, J_3 and J_4) were observed at each sampling date. While the non-synchronised infection that occurred in this experiment may reflect what actually happens in the field, it is not ideal for histology work. In future, clearer results could be obtained by transplanting seedlings to inoculum-free medium after the initial infection as was done by using methods described by Seah et al. [154] and by Williams and Fisher [196]. More precise results could be obtained by using more biological replicates.

Similar to what has been seen for other CCN resistance genes [51, 117, 154, 196], the *Cre8*-carrying line did not exhibit any resistance against the initial penetration by the nematodes. Syncytia were observed even at the first sampling date (4 DAI), consistent with previous observations for other resistant lines [154, 196], but in contrast to the observations of Grymaszewska and Golinowski [51], who reported that the syncytia were initiated much later (14 DAI) in a resistant line than in a susceptible line (4 DAI). Based on what had been observed for other resistant and susceptible lines, it was anticipated that by 18 DAI, there might be visible differences between the syncytia of the resistant and susceptible lines. No such differences were observed. In future, such differences might be observable at later stages and/or with improved techniques. Specifically, better sections might be obtained by using a diamond knife for sectioning. Here, very small particles of soil remained on the roots even after thorough washing. These damaged the glass knife and led to shearing of root sections.

The results of this experiment provide no direct observations of a resistance response in the *Cre8*-carrying line and thus little insight into the resistance mechanism. Nevertheless, the observation that juvenile nematodes infected the roots and established feeding sites as successfully in the *Cre8*-carrying line as in the susceptible line, indicates that future investigations should focus on later stages of syncytia development.